UNIVERSITY OF
BIRMINGHAM

A NEW APPROACH TO DEVELOP COST-EFFECTIVE LIGNOCELLULOSIC BIOETHANOL PRODUCTION

by

ARIELLE MUNIZ DE BARROS

A thesis submitted to the University of Birmingham

for the degree of

DOCTOR OF PHILOSOPHY

School of Chemical Engineering
College of Engineering and Physical Sciences
University of Birmingham
May 2016

Abstract

Second-generation bioethanol can be produced from cellulose fraction present in lignocellulosic biomass and has become a significant research focus due to its potential for replacing fossil fuels and decreasing greenhouse gases emissions. In order to produce 2nd-generation bioethanol, biomass must be processed in order to access cellulose within the lignocellulose matrix and convert it into glucose. However, an efficient cost-effective and environmental-friendly process has not been achieved. The aim of this work was to produce glucose from purified cellulose from *Miscanthus x giganteus*, a high yielding-biomass crop. The lignocellulosic biomass was selectively fractionated into its main components, hemicellulose, lignin and cellulose, after extractions using 'green' processes in a biorefinery approach. Hydrolysis of the cellulose-enriched fibres into glucose was evaluated using subcritical water (SBW) in a batch reactor at temperatures from 190-320^{o}C, residence times from 0-54min and biomass loading from 0.5-6.4% (w/v). The process used for cellulose purification had significant effect on glucose production by SBW, and higher glucose yields (~10%) were achieved at higher temperatures and shorter residence times. Glucose was used for bioethanol production by fermentation. Although the formation of fermentation inhibitors during SBW hydrolysis could not be prevented, fermentation could be performed in the presence of these compounds at some conditions, with ethanol yields up to 80% of the theoretical.

Dedicated to my family:
my mom,
my grandfather,
my uncle,
my stepfather,
and Flavio.

Acknowledgements

Firstly, I would like to thank my supervisors Dr. Regina Santos and Dr. Tim Overton for the opportunity and all the support throughout this work. My gratitude also goes to my industrial supervisor Dr. Steve Bowra, for his guidance and valuable experience.

I would like to thank my family for their unconditional love and for their every-day encouragement. I hope I have made you proud. I also would like to thank Flavio for his love, his help, and his support. I could not have accomplished it without you, my love.

I would like to thank my friends Janaina, Camila, and Lais, for all the help when I first arrived in the UK, for the support in the difficult moments, and for all the happy memories we have shared together (and I hope many more memories are still to come!). I would like to thank my lab friends, Dr. Fabio and Raitis for the company during the extensive lab work hours, for all our geek discussions, and all the support in the hard moments and all the fun in the good moments. I also would like to express my appreciation to all people who helped me during these 3 years of my PhD, particularly Dr. Luke, Dr. Iain, Dr. Luis, Dr. Ricardo, and Dr. Lu.

Finally, I would like to thank Capes and the University of Birmingham for the financial support.

Table of Contents

List of Figures

List of Tables

CHAPTER 1

LITERATURE REVIEW

1.1. Introduction

Biomass resources are both renewable and abundant (Demirbas, 2009a). Moreover, plants have the unique capability of converting CO_2 and water into biochemicals such as sugars, lignin, gums, resins, rubber, etc. (Naik et al., 2010).

The use of natural resources in industrial technologies is not a new concept, however, it is becoming more and more important particularly due to the oil crisis in the 70's and the increase in the concern regarding climate change. Consequently, the idea of using biomass for more than just food/feed has been intensified (Kamm et al., 2000).

Full utilization of biomass has the potential of drastically reduce fossil fuels use, reduce greenhouse gases (GHG) emissions, and support development of agricultural sector (Langeveld et al., 2010). Nevertheless, development of efficient as well as cost-effective technologies for biomass processing and use remains a significant challenge.

1.2. Bio-based economy and biorefinery

The First Industrial Revolution, in the 18^{th} century, stimulated the economy based on fossil fuels for the first time. The use of fossil fuels has greatly increased since then as well as the CO_2 released in atmosphere (Zhang, 2008). Climate change has become a global concern and the large scale use of fossils fuels is thought to be a major factor driving global warming (NASA, 2013).

A number of nations have already recognised the need to mitigate climate changes and have developed ambitious targets for reducing GHG emissions. For instance, the United States Department of Energy Office aims to substitute 30% of gasoline with biofuels by 2030; the European Union has the goal to use biofuel in at least 10% of its transportation fleet by 2020 (Viikari et al., 2012). The United Kingdom's Government intend to decrease at least 80% the net UK carbon account compared to 1990 by 2050, which could decrease the use of fuel from fossil origins as well as reduce the UK dependence on energy source importation (Parliament of the United Kingdom, 2008).

The shift from a petroleum based economy towards one supported by renewable resources is not only environmentally beneficial, but also it is believed to be a way of achieving a sustainable economy and energy independence (Ragauskas et al., 2006). Moreover, other potential benefits in a bio-based economy include minimization of waste through maximization of feedstock utilization, the reduction of industrial environmental impact, and technical development of agricultural sector (European Commission, 2011). On the other hand, potential risks of a bio-based economy expansion include the dilemma regarding food security and the over exploitation of natural resources and threats to biodiversity (European Commission, 2011).

The increased interest in the path towards a bio-based economy along with the technical advance of agriculture, biotechnology and chemistry as well as changing in society itself is leading the exploration of an integrated approach capable of utilising the entire biomass in a way to compete with existent technologies (Kamm et al., 2000). In this way, the concept of biorefinery has gain attention as an approach that integrates a number of biomass conversion processes in order to generate power, fuels and chemicals (Demirbas, 2009b) and contribute significantly to a bio-based economy (Wang and Sun, 2010).

The term biorefinary is an analogy to the petroleum refinery, in which the raw material is fractionated into multiple components that are utilised in further processing to generate a wide range of products (Ragauskas et al., 2006, Wang and Sun, 2010).

Biorefinery aims to utilise biomass in order to produce not only one product but several bio-based products from different biomass using distinct and/or combined processes (Menon and Rao, 2012). Furthermore, biorefinery can be seen as an integrated process that involves multiple steps to maximize the efficiency of all parts and minimize waste (Fitzpatrick et al., 2010) as shown in the scheme of Figure 1-1. Some of the sustainable principles that a biorefinery should follow are: 1) use of environment-friendly processes, also known as 'green' technologies; 2) minimization of waste throughout the efficient use of the complete biomass; and 3) minimization of overall environmental impact, i.e, energy consumption and GHG emission (Gullón et al., 2012). Moreover, the success of a biorefinery relies on the development of new/improved separation processes in order to fractionate biomass into its primary components (Ragauskas et al., 2006).

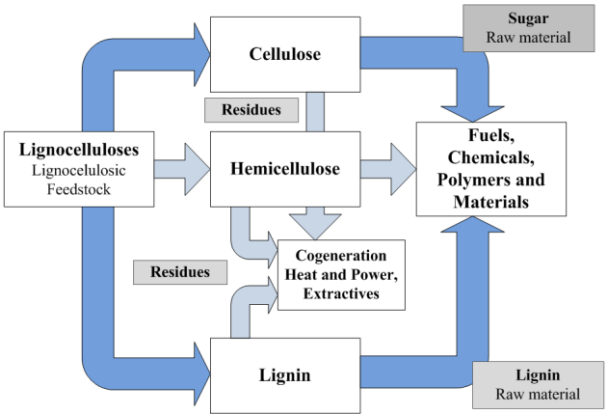

Figure 1-1 - Scheme of a lignocellulosic biorefinery. Source: modified from (Kamm et al., 2000).

Bioethanol is one of the products that is driving the pursuit of a biorefinery approach mostly because of availability and instability of oil prices and also due to environmental issues (Huang et al., 2008). However, 2nd-generation bioethanol production still holds major technical

and economic issues which prevents its effective commercialization (Spatari et al., 2010). The effective production of biofuels from renewable sources is deemed as a starting point for a wide platform that could lead towards a bio-based economy (Ragauskas et al., 2006).

1.3. Bioethanol

Bioethanol is one of the most common liquid biofuels and it is mainly produced nowadays from crops such as corn and sugarcane (Food and Agriculture Organization of the United Nations, 2008). Bioethanol is being recognized as a potential replacement of fossil fuels and presents several advantages compared to conventional fuels such as high octane number as well as low cetane number plus high heat of vaporization (Balat et al., 2008). Moreover, bioethanol can also be a precursor of a varied platform of chemicals including ethene, polyethylene and polyvinylacetate (Kamm and Kamm, 2004).

"1st-generation" and "2nd-generation" bioethanol are popular definitions and differ from each other based on the feedstock used (Larson, 2008). 1st-generation bioethanol production usually uses high cost feedstock such as grains plants (corn) and sugar cane which are high starch and sucrose contents plants, respectively (Limayem and Ricke, 2012). Both starch and sucrose are easily hydrolysed into fermentable sugars by specific enzymes. Although the process is well-developed and globally commercialized, the process cost-effectiveness is still a drawback as ethanol prices are not competitive with conventional fuels without subsidies (Larson, 2008).

2nd-generation bioethanol, also called cellulosic ethanol, is made from lignocellulosic biomass such as non-edible plants and agricultural residues. The concept of using lignocellulosic feedstocks to produce ethanol is very promising in many ways: the supply security, as a large variety of feedstock can be used; the minimization of food vs fuel debate

(Soccol et al., 2011); the use of perennial crops instead of annual crops; and a lower net GHG production and emission when compared to 1st-generation ethanol (Berndes et al., 2001).

The simplified scheme of the 2nd-generation bioethanol process is shown in Figure 1-2. The process can be divided into 4 steps: pretreatment of the lignocellulosic biomass in order to enable access to the polysaccharides (hemicellulose and cellulose); hydrolysis of the polysaccharides into fermentable monosaccharides; use the monosaccharides as carbon source for alcoholic fermentation; and separate the bioethanol by distillation (Limayem and Ricke, 2012).

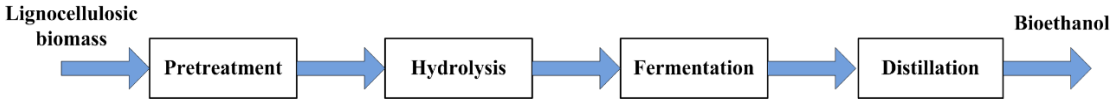

Figure 1-2 - Simplified scheme of 2nd-generation bioethanol production.

Nevertheless, in contrast to the 1st-generation bioethanol, the 2nd-generation is not yet being produced commercially in any country (Escobar et al., 2009, Larson, 2008, Spatari et al., 2010). There are, though, pilot plants already applying different processes using lignocellulosic material for bioethanol production and many more plants are being built around the world (Soccol et al., 2011). Iogen Corporation and Chemtex are two companies currently focused on development and testing of cellulosic ethanol processes. Companies such as the Danish Inbicon, the Brazilians Raizen and GranBio and the North American Poet already demonstrated 2nd-generation ethanol in pilot and/or industrial scale. These companies use a variety of agricultural waste feedstock (sawdust, wheat straw) (Soccol et al., 2011), and they utilize similar process pathway: a pretreatment (with or without addition of an acid/base catalyst), an enzymatic hydrolysis of cellulose, followed by fermentation of glucose into ethanol (Spatari et al., 2010). However, the ethanol produced is still not cost-effective for commercialization (Spatari et al., 2010).

The challenge to be overcome in 2nd-generation bioethanol is the development of an efficient economically competitive technology and, in this way, the concept of biorefinery can be applied (Kamm et al., 2000) as the potential of separating lignocellulosic biomass into its constituents could lead to a wide range of value-added products possibilities. Therefore, biorefinery is an interesting strategy for 2nd-generation bioethanol production as well as for waste management, power production and economic competitiveness (Hamelinck et al., 2005, Kamm and Kamm, 2004, Van Dyne et al., 1999).

1.4. Lignocellulosic biomass

Lignocellulosic biomass is an abundant natural material that contains 3 main components in its cell walls: cellulose (30-50% w/w), a homopolymer formed by glucoses; hemicellulose (20-40%), a heteropolymer formed by several sugars such as xylose, galactose, arabinose; and lignin (15-25%), a phenolic polymer (Cherubini, 2010, Menon and Rao, 2012). Lignocellulosic biomass composition also includes a small percentage of ash such as oxides and sulphur components (Lewandowski et al., 2000), and starch, proteins, pectin, aromatics, waxes, lipids and minerals (Pauly and Keegstra, 2008, Vassilev et al., 2012). Figure 1-3 shows a scheme of lignocellulosic biomass structure and main compounds.

Figure 1-3 shows that cellulose present in plant cell walls is linked in parallel fibres by hydrogen bonds (Klemm et al., 2005). Moreover, cellulose, hemicellulose and lignin are intimately associated and bonded by several linkages such as ether, ester, hydrogen and carbon-to-carbon bonds, which results in a complex cross-bonded matrix (Faulon et al., 1994).

The cell wall configuration provides cell shape, ensures resistance to microorganism attack, presents some flexibility and allows the entrance of selectively permeable components essential for cell survival (Levy et al., 2002). Moreover, lignocellulosic biomass is

predominantly recalcitrant to chemical and biological attack due to several features such as: 1) the complexity of cell wall structure (Himmel et al., 2007), 2) the degree of cellulose crystallinity (Kumar et al., 2009), 3) the crossed-bonds among the components (Harmsen et al., 2010), and 4) the amount of lignin (Himmel et al., 2007).

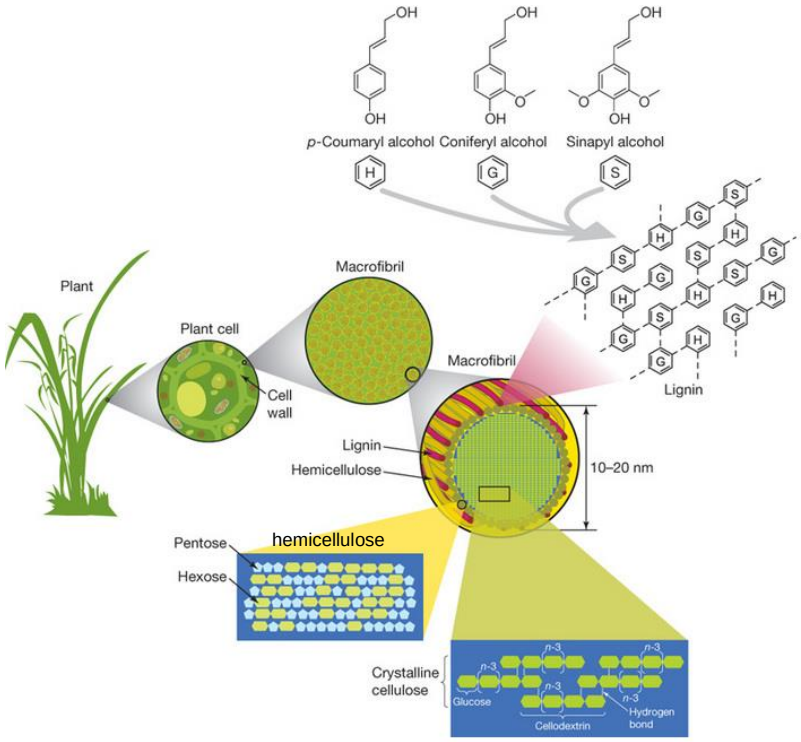

Figure 1-3 - Scheme of cell wall disposition and some of the constituents in a typical lignocellulose biomass. Source: (Rubin, 2008).

1.4.1. Cellulose

Cellulose was first discovered in 1838 and since then has achieved industrial importance and has been used in manufacturing processes for about 150 years (Klemm et al., 2005). Products such as thermoplastic polymer (made by cellulose nitrate) and Cellophane® have been produced since the beginning of 20th century (Simon et al., 1998). Cellulose is also an important material for textiles (cotton), furniture (wood), paper industry, and cellulose derivatives such

as cellulose ethers and esters are largely used in the pharmaceutical and food industry (Klemm et al., 2005, Olsson and Westman, 2013).

Cellulose is a homogenous linear polymer composed by glucose monomers linked by β-1,4-glycosidic bonds and have cellobiose (two glucose units) as its repeating unit (Moon et al., 2011). Cellulose degree of polymerization (DP) varies from 6000-16000 (Liu and Sun, 2010), depending on the source of fibres (Arato et al., 2005).

O´Sullivan (1997) described the seven polymorphs of cellulose that differ from each other by the location of hydrogen bonds outside and inside the strands: I_α, I_β, II, III_1, III_{11}, IV_1 and IV_{11}. Cellulose I is the native and predominant form of cellulose while all the other types are synthetically produced from the native form (O'Sullivan, 1997). From the two native polymorphs, I_β is the most abundant form. The alpha and beta form of cellulose I differ from each other in spatial conformation and it confers them with different reactivity, with I_α being more reactive than I_β (Poletto et al., 2013).

The cellulose polymer chain can be divided into three parts: 1) central glucose units, which are called anhydroglucose due to the loss of a molecule of water in the polymerization; 2) non-reducing end unit, which is the right side terminal glucose in a chain and has an anomeric carbon linked in a glycosidic bond, reducing its reactivity; and 3) reducing-end unit, which is the left side terminal unit which is an anomeric carbon free to react (Olsson and Westman, 2013). The scheme of the three glucose unit types is shown in Figure 1-4.

The glycosidic linkages enables the formation of long chains and, added to the fact that there are hydrogen bonds linked by hydroxides (presented on both side of the monomers), cellulose presents parallel chains arranged together as it can be observed in Figure 1-5 (Harmsen et al., 2010).

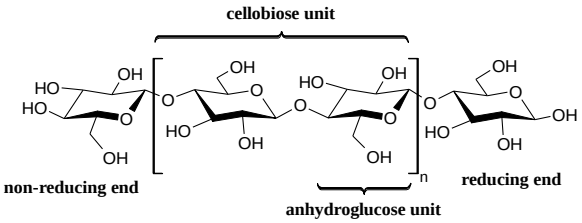

Figure 1-4 - Scheme of cellulose linear polymeric chain. Source: (Olsson and Westman, 2013).

Cellulose microfibril formation (shown in Figure 1-3) is the result of cross-linkage of hydroxyl groups between the planes (Liu and Sun, 2010). This complex and well organized structure confers cellulose compactness and strength (Carpita and Gibeaut, 1993). Moreover, although glucose units have three OH groups attached to its C-2, C-3 and C-6, which could provide a reasonable water affinity, due to strong intra- and intermolecular hydrogen bonds, cellulose assume a crystalline structure that makes it hard to solubilize in water or other common solvents (Sasaki et al., 2003a).

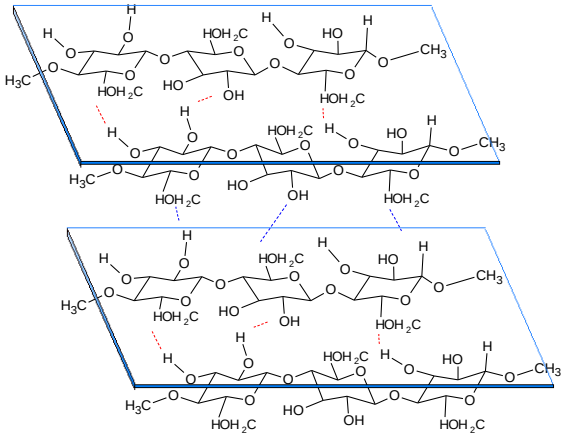

Figure 1-5 - Scheme of cellulose parallel structure of polymer chains. Source: modified from (Harmsen et al., 2010).

Cellulose structure presents both highly ordered (crystalline) and less ordered (amorphous) fractions (Klemm et al., 2005). Some authors also define a cellulosic structure that has a degree of organization in between of crystalline and amorphous portions, named para-crystalline (Foston and Ragauskas, 2012). The different structures present in cellulose have

different reactivity during hydrolysis and it is believed that amorphous structure is the most hydrolysable cellulose portion, followed by para-crystalline, cellulose I_α and, finally, cellulose I_β (Foston and Ragauskas, 2012).

Cellulose crystallinity is considered to be one of the major reasons for lignocellulosic recalcitrance to hydrolysis (Kumar et al., 2009). However, although it is common sense that the amorphous fraction of cellulose is more easily hydrolysed (Menon and Rao, 2012, Moon et al., 2011, Zhao et al., 2007), the real role of cellulose crystallinity is not well understood (Park et al., 2010, Zhao et al., 2012). Therefore, cellulose crystallinity and its relation with cellulose reactivity is currently an object of research (Klemm et al., 2005). These studies use analytical tools such as NMR, X-ray diffraction and FTIR to determine the degree of crystallinity of biomasses, often referred as crystallinity index (CI) (Park et al., 2010).

1.4.2. Hemicellulose

Contrary to cellulose, hemicellulose is a heterogeneous polymer composed by hexoses (mannose, galactose, glucose) and pentoses (xylose, arabinose) with varying amounts of side group substitutions. Both the composition and structure of hemicellulose varies depending on the source (Ebringerová, 2005).

Hemicellulose structure is formed by a backbone in an equatorial conformation, linked by β-1,4-glycosidic bonds as shown in Figure 1-6 (Scheller and Ulvskov, 2010). Hemicellulose DP varies between 80 and 200 (Ren and Sun, 2010). Hemicellulose is a branched structure in which the backbone have substituents that can include uronic, acetic and hydroxycinnamic (ferulic and p-coumaric) acids as well as 4-O-methyl ethers (Ren and Sun, 2010).

Hemicellulose is usually divided in 4 types that differ in structure: xylans, mannans, xyloglucans and mixed-linkage β-glucan and again is characteristic of a species (Ebringerová,

2005). The xylan type is the most abundant component of plants cell walls and it is present in 20-30% of dicotyledonous and 50% of grasses (Scheller and Ulvskov, 2010).

Within the lignocellulosic matrix, hemicellulose can be linked to both lignin, by α-benzyl ether linkages, and to cellulose, by hydrogen bonds (Ren and Sun, 2010). However, as a result of its highly branched structure as well as its non-crystalline structure and low DP, hemicellulose is more easily hydrolysed than cellulose (El Hage et al., 2010b, Palmqvist and Hahn-Hägerdal, 2000b).

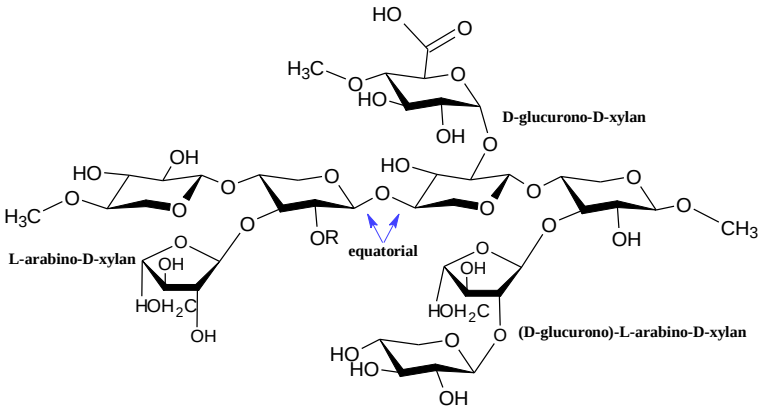

Figure 1-6 - Example of hemicellulose structures containing substituents groups: L-arabino-D-xylan, D-glucurono-D-xylan, and (D-glucurono)-L-arabino-D-xylan. Source: modified from (Ebringerová, 2005)

Hemicellulose can be used in the production of a variety of chemicals such as ethanol, acetone, butanol, xylitol, and furfural (Huang et al., 2008, Ren and Sun, 2010). More recently, xylo-oligosaccharides (XOS) have been attracting interest for their prebiotic properties that can be used in the production of high valuable products such as functional food beneficial to human and animal feed (Moure et al., 2006).

1.4.3. Lignin

Lignin is a 3-dimensional amorphous and highly branched aromatic polymer (Huber et al., 2006). Lignin is formed by the polymerization of three alcohol monomers: coniferyl, sinapyl

and coumaryl alcohol (Pandey and Kim, 2011) shown in Figure 1-7. Dehydrogenation of phenolic OH by plant enzymes generate free radicals that polymerises successively forming lignin polymer. The most abundant linkage in lignin structure is the β-O-4-aryl ether bond (Pandey and Kim, 2011). Lignin monomers combine to form three types of lignin units:1) p-hydroxyphenyl, formed by p-coumaryl alcohol, 2) guaicyl, formed by coniferyl alcohols, and 3) syringyl, formed by sinapyl alcohols (Lu and Ralph, 2010). Lignin monomers and units are shown in Figure 1-7.

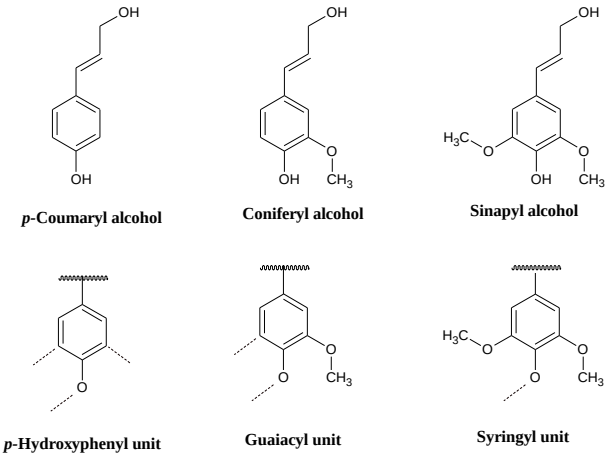

Figure 1-7 - Lignin monomers and units.Source: (Lu and Ralph, 2010).

Other common groups present in lignin are free phenolic hydroxyl, methoxyl, benzyl alcohols, carbonyls, and aldehyde groups (Santos et al., 2013). Although complete lignin structure is still unclear and it is believed to vary according to the biomass source (Saake and Lehnen, 2000), a well-accepted lignin scheme is presented in Figure 1-8.

Lignin is mainly produced as a residue of paper industry in the form of sulphur-content compounds, which limits its application (Saake and Lehnen, 2000). In biomass processing during 1st and 2nd-generation bioethanol, lignin is often underutilized and burned for power generation (Huber et al., 2006). However, sulphur-free lignin has the potential to be used in a

larger range of application such as asphalt, antioxidants, adhesives, coatings and chemicals such as vanillin, phenol and ethylene (Arato et al., 2005, Sannigrahi and Ragauskas, 2013).

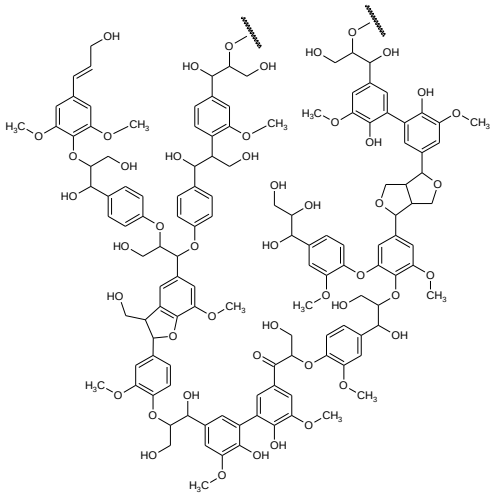

Figure 1-8 - Scheme of lignin structure. Source: modified from (Thielemans et al., 2002).

1.5. Miscanthus x giganteus

Current worlds largest ethanol producers, USA and Brazil, use corn and sugar cane as feedstock, respectively. These feedstocks can account for up to 40% of production costs (Balat et al., 2008) and are also food crops. The need for low cost feedstocks has increased the attention for the possibility of moving away from high sucrose/starch plants used in 1st-generation bioethanol towards energy crops and agriculture wastes for 2nd-generation bioethanol (Fitzpatrick et al., 2010, Ragauskas et al., 2006).

Miscanthus x giganteus (MxG) is a perennial energy crop currently being largely evaluated in the USA and Europe as a promising source of lignocellulosic feedstock (Le Ngoc Huyen et al., 2010).

Miscanthus is originally from Asia and Pacific islands, and have at least 20 known species worldwide and it belongs to the same taxonomic group as well-known feedstocks for bioethanol process as maize (*Z. mays*) and sugar cane (*Saccharum officinarum*) (Chou, 2009). *Miscanthus x giganteus* is a genetic hybrid obtained from the combination of two *Miscanthus*

species, *sacchariflorus* and *sinensis* (Brosse et al., 2012, Chou, 2009). As a result of being a sterile hybrid, MxG needs to be propagated vegetatively (Lewandowski et al., 2000).

In most plants such as wheat, barley and rice, the photosynthesis mechanism leads to C_3-compounds, whereas some plants such as *Miscanthus* and sugar cane have what is referred to as C_4 photosynthesis mechanism, which is more productive leading to an efficiency of the used of nitrogen, water and light (Rubin, 2008). Moreover, MxG rhizome system is a nutrients reserve for the annual formation of new shoots (Le Ngoc Huyen et al., 2010). In addition, while annual crops such as corn and sugar cane demand high cost for their maintenance, perennial crops are significantly less expensive (Fitzpatrick et al., 2010).

MxG productivity is higher than most of the similar plants, achieving 30tons per hectare of dry matter when it is irrigated and 20-25tons without irrigation (El Hage et al., 2009), while crops such as willow and poplar achieve 10-12tons per hectare per year (Lewandowski and Heinz, 2003). Moreover, MxG has demonstrated high capacity of carbon dioxide fixation (Yuan et al., 2008).

Although C_4 plants have low tolerance to cold climate (Rubin, 2008), MxG was found to be significant tolerant to temperatures as low as 14^{o}C with no negative effect in photosynthesis (Naidu et al., 2003). Furthermore, artificial freezing tests with MxG showed evidence of cold resistance in temperatures as low as -3.4^{o}C, which is an unique resistance for a lignocelluloses biomass (Clifton-Brown and Lewandowski, 2000).

Studies suggested that MxG crop could be viable for long periods of 15-20years (Clifton-Brown et al., 2007) particularly due to its rhizome system (Lewandowski and Heinz, 2003). Moreover, MxG also presents advantages in terms of reduced nitrogen inputs (Beale et al., 1996) and pesticide use is required only in the first year of cultivation for control of weeds (Lewandowski and Heinz, 2003).

In summary, MxG was chosen as an interesting lignocellulosic biomass with potential to be feedstock for ethanol production in this research work due its potential for high yields, low cost, and adaptability to low-quality land (Hamelinck et al., 2005).

1.6. Biomass processing - Pretreatment

The use of unprocessed lignoellulosic biomass for bioethanol production is not feasible due to its recalcitrant structure to chemical/biological attack. Therefore, the use of biomass processing, commonly called pretreatment, is usually a requirement in order to access cellulose and/or extract other biomass components (Sun and Cheng, 2002).

Although there have been significant improvements in biomass processing recently, 2nd-generation bioethanol production is still not cost-effective mainly due to high cost and/or low efficiency of pretreatment and hydrolysis steps (Mosier et al., 2005a).

Important features to consider in a pretreatment include: 1) cost and feasibility at large scale; 2) efficiency of cellulose, lignin and hemicellulose recovery and/or accessibility as well as decrease of these compounds degradation; 3) prevention of fermentation inhibitors formation; 4) applicability to a wide range of feedstock; and 5) environmental impact (Agbor et al., 2011, Kumar et al., 2009, Sun and Cheng, 2002). Pretreatments are often divided into categories: physical, chemical/physicochemical and biological and are often used in combination (Chandra et al., 2007).

1.6.1. Physical

Physical particle size reduction such as milling, grinding or chipping is often necessary prior to chemical pretreatment (Agbor et al., 2011). These treatments are aimed to increase biomass surface area as well as decrease DP of cellulose (Agbor et al., 2011). Moreover,

extensive particle size reduction is also thought to reduce cellulose crystallinity at some extent (Sun and Cheng, 2002).

The extent of particle size decrease require careful evaluation as the generation of small particle sizes demands high-energy use (Sun and Cheng, 2002). Moreover, below a certain particle size, that depends on feedstock source, particle size is thought not to be of extreme significance in hydrolysis (Agbor et al., 2011).

1.6.2. Biological

Biological treatments are less common, however, some fungi species such as brown, white and soft-rot fungi can degrade lignin and hemicellulose, making cellulose accessible to hydrolysis (Kumar et al., 2009). Although the environmental impact of biological treatments are minimal and the mild conditions needed require low energy inputs, the reactions are usually extremely slow (Menon and Rao, 2012). Moreover, biological treatments are rarely used for biomass processing mostly because the difficulties of scaling it up for industrial applications (Agbor et al., 2011).

1.6.3. Chemical/physicochemical

Chemical/physicochemical treatments include the use of acids, alkali, organic solvents, water and ionic liquids (Agbor et al., 2011). Some of the most common chemical/physicochemical are described below.

1.6.3.1. Steam explosion

Steam explosion is one of the most common pretreatments used at large-scale. Two of most important technologies for 2nd-generation ethanol currently being demonstrated, Proesa

and Iogen technologies, use steam explosion pretreatment to increase cellulose digestibility (Damaso et al., 2014).

Steam explosion treats biomass with high-pressure steam, which then is suddenly depressurized (Kumar et al., 2009). Temperatures and pressures are usually in the range 160-260ºC and 0.7-4.8 MPa, with residence times varying from seconds to few minutes (Sun and Cheng, 2002).

Although this treatment efficiently increases cellulose accessibility, recovery of lignin is ineffective and it is difficult to control formation of inhibitors (Agbor et al., 2011).

1.6.3.2. Ammonia fibres explosion (AFEX)

AFEX is a similar treatment to steam explosion, in which fibres are exposed to liquid ammonia at high pressures and then the system is rapidly depressurised (Kumar et al., 2009). Typical parameters used in this treatment are 1-2kg/kg biomass, temperatures from ambient to 190ºC and residence times ranging from hours to few days (Agbor et al., 2011). Contrarily to steam explosion, AFEX is not efficient solubilizing hemicellulose fraction (Kumar et al., 2009). Although AFEX potentially decreases the formation of fermentation inhibitors, the cost and environmental impact of the ammonia use is a significant drawback of this treatment (Sun and Cheng, 2002). Moreover, this treatment is not suitable for high lignin contents biomass (>25%) (Kumar et al., 2009).

1.6.3.3. Acid and alkali treatments

Concentrated mineral acids such as H_2SO_4 and HCl were largely evaluated for improving cellulosic enzymatic hydrolysis by hydrolysing hemicellulose and cellulose even at room temperatures through the cleavage of β-glycosidic linkages (Wyman et al., 2004).

However, due to mineral acids high toxicity, corrosion issues and waste management, they are becoming less common for lignocellulosic biomass pretreatment (Kumar et al., 2009).

Diluted acids (usually >1%), on the other hand, are still largely used as pretreatments (Hendriks and Zeeman, 2009). In this case, higher temperatures (130-230^{o}C) are usually applied in order to facilitate the hydrolysis (Menon and Rao, 2012). Although diluted acids pretreatment is highly efficient in hydrolysing polysaccharides, it is challenging to control the reactions in order to decrease the further decomposition of released monosaccharides (Chiaramonti et al., 2012). Moreover, although in less extent, this treatment also have the disadvantages encountered by concentrate acid treatments, inherent to the use of toxic/corrosive compounds.

Alkali compounds such as sodium hydroxide and calcium hydroxide (lime) are also the object of study of lignocellulosic treatments. Alkali substances disrupt ester and glycosidic linkages (Menon and Rao, 2012), partially removing lignin and solubilizing hemicellulose, which improve cellulose accessibility (Yang and Wyman, 2008).

Compared to acid treatment, alkali treatments have advantages such as less sugar degradation and easier reagent regeneration/reuse (Kumar et al., 2009). On the other hand, alkali treatments are much slower than acid treatment and require longer residence times, usually on the order of few hours to a day (Chiaramonti et al., 2012).

A significant disadvantage of both acid and alkali treatments is the need for a neutralization step prior to cellulose enzymatic hydrolysis and/or fermentation (Menon and Rao, 2012).

1.6.3.4. Ionic liquids

Ionic liquids are salts that are liquid at ambient temperatures (Yinghuai et al., 2013) such as 1-butyl-3-methylimidazolium chloride ([BMIM]Cl) and 1-butyl-3-methylimidazolium

bis(trifluoromethylsulfonyl)imide ([BMIM]NTf2) (Liu et al., 2012). In general, ionic liquids are formed by organic cations and organic/inorganic anions (Liu et al., 2012) that can bind to the lignocellulosic components and dissolve both carbohydrates and lignin with very little inhibitors formation (Yang and Wyman, 2008).

Ionic liquids are considered 'green' solvents and are non-flammable, non-volatile and can be recycled (Yang and Wyman, 2008). Moreover, treatments using ionic liquids require low energy, mild operation conditions and have low environmental impact (Menon and Rao, 2012).

The major drawback of this treatment is the difficult to recover solubilized biomass fractions (Xu et al., 2012). Moreover, the high cost of ionic liquids and the current lack of information about toxicity and suitability in large scale are disadvantages of this technology (Menon and Rao, 2012, Yinghuai et al., 2013).

1.6.4. Biomass fractionation

The cost of 2nd-generation bioethanol production is a limiting-factor affecting its commercialization. Therefore, a promising way of increasing the cost-effectiveness of the overall process is believed to be the co-production of valuable products from the lignocellulosic fractions (Demirbas, 2009a).

Selective biomass fractionation is a key point in order to generate purified streams that could be used for further processing in a biorefinery approach, resulting in significant increase in the 2nd-generation bioethanol overall value (Gullón et al., 2012).

Although some of the pretreatments previously presented are efficient techniques to obtain sugars from the lignocellulosic matrix, they do not allow the effective fractionation of biomass components and/or have a negative environmental impact. Therefore, two processes

that present the possibility of biomass fractionation considered promising technologies, particular in pursuit of a bioerefinery approach are subcritical water and the organosolv method.

1.6.4.1. Subcritical water

Subcritical water (SBW) treatment, also called hot compressed water, autohydrolysis or hydrothermal process, is water held under pressure so it can remain in the liquid phase under high temperatures (Kumar et al., 2009, Ruiz et al., 2013). The use of SBW for biomass treatment is gaining attention as a 'green' solvent that does not require additional catalyst, neutralization step or corrosion-resistant reactors (Rogalinski et al., 2008, Taherzadeh and Karimi, 2008).

SBW hydrolysis is used as a pretreatment mainly to remove hemicellulose and biomass extractives (starch, pectin) in order to make cellulose more accessible (Gullón et al., 2012). Reported hemicellulose recovery can be as high as 84% depending on biomass source and treatment conditions applied (Yu et al., 2012). Moreover, depending on the conditions used, some of low molecular fraction of lignin might also be solubilized during SBW treatment (Hendriks and Zeeman, 2009).

Hemicellulose solubilisation under SBW conditions is performed at temperatures in the range from 160-220^{o}C (Gullón et al., 2012). Under SBW conditions, the high availability of H^{+} due to water auto-ionization (Bröll et al., 1999) plus the in-situ generation of ions (acetic, uronic and/or phenolic acids) formed from groups present in hemicellulose structure, catalyses the hydrolysis reaction in a mechanism called autohydrolysis (Garrote et al., 1999). The solubilisation of hemicellulose makes cellulose more accessible to acid/enzymatic attack (Hendriks and Zeeman, 2009).

Yu et al. (2012) used SBW treatment prior to enzymatic hydrolysis for two biomasses: sweet sorghum bagasse and eucalyptus wood chips. The two biomasses were treated at 184^{o}C

with residence times from 8-18min. Hemicellulose recovery was dependent on biomass and reactor configuration and ranged from 56-84%. Moreover, they suggested that the best reactor configuration was dependent on biomass source as flow-type reactors are likely to work better for low lignin content biomasses; whereas batch reactors are more efficient for biomasses containing high lignin amounts as well as highly crystalline cellulose as they require harsher conditions to be hydrolysed (Yu et al., 2012).

The removal of biomass extracts prior to hemicellulose hydrolysis could also be interesting. It can easily be achieved using SBW temperatures lower than required for hemicellulose hydrolysis (>140^{o}C). As there is no clear market for biomass extractives, it is still in question if extractive removal is worth the additional step required for it (Gullón et al., 2012). However, the removal of extractives prior to hemicellulose extraction generates a more purified hemicellulose fraction, which could be interesting if the application of this fraction requires high purity. Therefore, extractives removal should be considered in a biorefinery approach.

The major challenge of SBW treatment is to prevent the decomposition of released sugars into fermentation inhibitors, such as 5-hydroxymethylfurfural (HMF), furfural and organic acids (acetic, formic) (Mosier et al., 2005a), which decreases sugar recovery and difficult fermentation.

1.6.4.2. Organosolv method

The method described as Organosolv combines water, organic solvents and acid catalysts under high temperatures for hemicellulose and lignin solubilisation. Several kinds of organic solvents can be applied in organosolv method such as the short chains aliphatic alcohols (methanol and ethanol) and other alcohols (ethylene glycol and glycerol), and also other classes

or organics have been reported such as ethers and ketones (Zhao et al., 2009a). Ethanol is widely used as the organic solvent due to advantages such as low cost, low toxicity, miscibility in water and it is considered an environment-friendly solvent (Zhao et al., 2009a). Moreover, the possibility of recovering ethanol is essential to decrease the processing cost and it has been reported that ethanol can be recovered from organosolv liquor in percentages as high as 98% (Botello et al., 1999).

The addition of an acid catalyst often improves the efficiency of organosolv methods. H_2SO_4 and HCl are commonly employed to increase delignification (lignin extraction) percentage (Brosse et al., 2009). However, the use of acids leads to disadvantages such as the need for a neutralisation step afterwards, corrosion and the need for waste treatments (van Walsum, 2001). Moreover, although the use of mineral acid increases delignification, it also degrades lignin structure, which decreases its potential for high valuable applications (Sannigrahi and Ragauskas, 2013).

In a biorefinery perspective, the use of mineral acid should be avoided due to the environment impact. The replacement of acid by carbon dioxide has been investigated to increase system acidity without the drawbacks resulting from the use of mineral acids (Kim and Hong, 2001). Under pressure, CO_2 generates carbonic acid that acts as a catalyst for hydrolysis. The partial pressure of CO_2 in water determines the system pH, nevertheless, the system is neutralised once pressure is released (van Walsum and Shi, 2004). Advantages of the use of carbon dioxide when compared to mineral or organic acid include non-toxicity, low cost and low environmental impact (Kim and Hong, 2001).

The effect of each component of water/ethanol/CO_2 mixture in the organosolv treatment of corn stover was studied by Lü et al. (2013). They reported that the effect of carbonic acid generated by water and CO_2 increased both hemicellulose hydrolysis and cleavage of hydrogen

bonds between lignin, cellulose and hemicellulose. However, the formation of a black solid fraction suggested that water-CO_2 did not solubilise lignin fragments. Therefore, ethanol addition to the mixture was essential for lignin solubilisation as well as to increase treatment efficiency (Lü et al., 2013).

Ingram et al. (2011) compared SBW and organosol treatments in order to produce accessible cellulosic fibres from rye straw. In the SBW treatment, they used a fixed-bed reactor at 200^{o}C, 50bar and 10min of residence time. For the organosolv treatment, they used the same reactor at 167^{o}C and 35bar for 35min using a water and ethanol (1:1) solution and 0.5N H_2SO_4 as catalyst. Cellulose fibres obtained from these two treatments were hydrolysed by enzymes and reported that both pretreatments could achieve high glucose yields (Ingram et al., 2011). However, each process only allows the recovery of one major lignocellulosic component: SBW was efficient for hemicellulose recovery, whereas organosolv recovered lignin fraction.

The combination of SBW hydrolysis for hemicellulose recovery followed by organosolv method for lignin recovery have also been investigated. Huijgen et al. (2012) used SBW followed by organosolv method to treat wheat straw. They performed SBW treatment using H_2SO_4 as catalyst in a batch reactor and temperatures from 160-190^{o}C with residence times from 30-120min. The organosol method was performed in the same reactor at 190-220^{o}C for 60min using water:ethanol (6:4 v/v) solution. The enriched-cellulose fibres obtained after this sequential treatment were then enzymatically converted into glucose (Huijgen et al., 2012).

1.7. Cellulose hydrolysis into glucose

The most common microorganisms used in fermentation for bioethanol production are not capable of metabolising oligosaccharides (Carvalheiro et al., 2008). Therefore, after cellulose is purified, there is the need to hydrolyse cellulose fibres into its monomers, glucose.

Hydrolysis is a common reaction in biochemistry in which water reacts to break linkages as those found in polymers, nucleic acids, etc. (Nelson and Cox, 2004). Lignocellulosic biomass hydrolysis is usually performed after an adequate pretreatment, which increases significantly hydrolysis efficiency (Hamelinck et al., 2005).

The conversion of cellulose into glucose can be catalysed by acid or enzymes and the most common and studied processes are enzymatic hydrolysis and acid (concentrated or diluted) hydrolysis (Kumar et al., 2009). More recently, subcritical water hydrolysis has been gaining attention as an alternative process (Yu et al., 2007).

1.7.1.1. Enzymatic hydrolysis

Enzymatic hydrolysis is the most common process to convert cellulose into glucose (Van Dyk and Pletschke, 2012). During enzymatic hydrolysis, the enzymes act as catalyst in the hydrolysis process and they are very specific, which leads to high efficiency and no generation of degradation products from glucose. Moreover, due to moderate operating conditions, the utility costs in this process are usually low (Duff and Murray, 1996).

The enzyme used in this process, cellulase, is a mixture formed by three enzyme types: endoglucanase, which breaks β-1,4-glycosidic linkages randomly; exoglucanase, which acts in the termini β-1,4-glycosidic linkages liberating cellobiose or glucose; and β-D-glucosidase which breaks β-1,4-glycosidic of small oligosaccharides (cellobiose, cellotriose) (Wyman et al., 2004). These enzymes can be obtained from fungi (*Orpinomyces* sp., *Piromyces* sp.) or bacteria sources (*Thermobifida fusca*) (Wyman et al., 2004). Under optimal conditions, enzymatic hydrolysis was reported to yield up to 95% of glucose (Hamelinck et al., 2005).

The cost of the enzymes used to be a significant drawback for large-scale process. However, with the recent increase in the interest of a cost-effective cellulosic bioethanol

process, significant progress has been achieved in terms of both efficiency and cost of enzymes (Maris et al., 2006). Moreover, the two already mentioned large-scaled existent technologies, Proesa and Iogen, use enzymatic hydrolysis for cellulose conversion into glucose (Damaso et al., 2014).

Challenges faced during enzymatic hydrolysis process are the high sensitivity of enzymes to pH and temperatures, thus, control of these parameters is mandatory in order to obtain high efficiency and prevent enzyme damage (Van Dyk and Pletschke, 2012). Moreover, enzyme efficiency can be severely compromised by inhibitory substances generated during previous pretreatments such as organic acids and furans (Van Dyk and Pletschke, 2012) and products of enzymatic hydrolysis such as glucose and cellobiose have also an inhibitory effect in the enzymes (García-Aparicio et al., 2006). Finally, although the process is usually performed in mild conditions such as pH 5 and 45-50ºC, it takes a long period, usually in the range of hours to few days (Yu et al., 2007).

1.7.1.2. Acid hydrolysis

Acid hydrolysis is largely used in lignocellulosic biomass pretreatment in order to make cellulose more accessible. Nevertheless, it can also be used to hydrolyse cellulose into glucose.

During acid hydrolysis, the addition of H^+ acts as catalyst in the cleavage of glycosidic bonds. In general, 50-60% sugars yield can be obtained using dilute acid hydrolysis at temperatures about 220ºC (Wyman et al., 2004) and yields as high as 90% have been reported using concentrated acid (30-70%) at mild temperatures (40ºC) (Hamelinck et al., 2005). Furthermore, this method is effective in a wide range of different feedstocks, particularly residues such as municipal waste that presents large variability in the composition (Harmsen et al., 2010).

The advantages of acid hydrolysis, compared to enzymatic process, is the faster rate and non-requirement for a previous treatment (Lenihan et al., 2010). However, due to the drawbacks (mentioned in acid pretreatments), large scale acid hydrolysis has not been evaluated.

1.7.1.3. Subcritical water (SBW) hydrolysis

Subcritical water is referred to water at high temperatures and under sufficiently pressure to maintain a liquid state, however, below the critical point (T_c=374^{o}C, P_c=22.1MPa) (Kruse and Dinjus, 2007).

SBW water is commonly investigated as an environment-friendly pretreatment in which hemicellulose is removed. Moreover, the common approach after the SBW treatment is to submit the solid fraction, composed of cellulose and lignin, to enzymatic hydrolysis for glucose production (Ingram et al., 2011). Nevertheless, at increased temperatures, SBW can also hydrolyse the cellulose fraction into glucose.

Water properties such as dielectric constant (ε), density and ionic product (K_w) change according to temperature and pressure. Figure 1-9 shows these water properties changing according to the temperature.

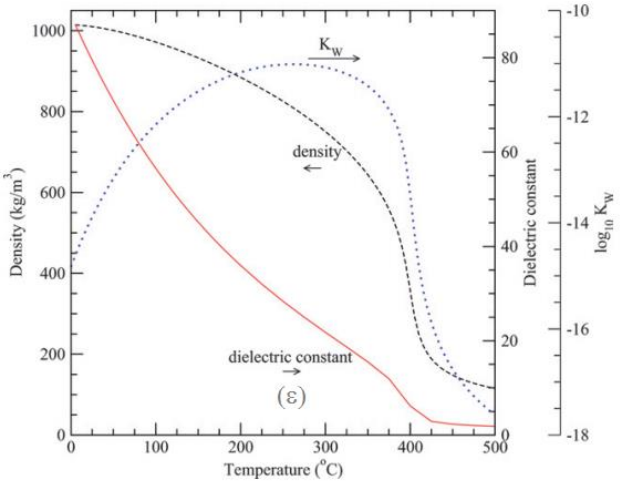

Figure 1-9 - Water properties. Source:(Peterson et al., 2008).

An increase in temperature causes an increase in K_w due to auto-ionization, which creates hydronium ions (H_3O^+), depending on water temperature and pressure conditions (Ruiz et al., 2013). This leads to increase in autohydrolysis as the produced H_3O^+ ions catalyse hydrolysis of bonds in a similar way as diluted acid hydrolysis, by attacking glycosidic linkages in both cellulose and hemicellulose and also acetyl groups in hemicellulose (Carvalheiro et al., 2008).

The dielectric constant is a property of solvents relateing the electrical fields around particles and it affects reactions and equilibrium rates (Mohsen-Nia et al., 2010). The decrease in ε due to the increase in temperature is related to the degree of hydrogen bonds (Kruse and Dinjus, 2007). The decrease of both ε and density change water properties as a solvent, improving solubility of non-polar substances (Bröll et al., 1999).

There have been many studies of SBW hydrolysis of pure cellulose (Abdullah et al., 2014, Kumar and Gupta, 2008). On the other hand, there are only few studies using SBW for hydrolysis of the complex lignocellulosic biomass. Cheng et al. (2008) used SBW to hydrolyse switchgrass in a batch reactor at temperatures from 250-350^{o}C and residence times from 0-5min. (Cheng et al., 2009). Prado et al. (2013) hydrolysed sugarcane bagasse using SBW at temperatures from 213-290^{o}C in a flow reactor with flow rates ranging between 11-55mL/min (Prado et al., 2014). Nevertheless, these studies focus on cellulose hydrolysis, not in the recovery of hemicellulose and lignin, which results in degradation of theses fractions.

There are also studies using supercritical water for biomass hydrolysis (Lü and Saka, 2010, Zhao et al., 2009c), however, at these harsh conditions, corrosion problems are more significant and equipment costs are considerably higher (Bröll et al., 1999).

Comparing SBW hydrolysis with acid and enzymatic hydrolysis, SBW is non-toxic reagent, has a much faster reaction rate and also it is not inhibited by intermediate and end-products formed during the hydrolysis (Zhao et al., 2009c). On the other hand, monosaccharides yield achieved by SBW from lignocellulosic biomass is low when compared to acid and enzymatic hydrolysis (Yu et al., 2007). Moreover, one of the key factors of SBW hydrolysis is the balance between the severity needed for cellulose hydrolysis and the formation of fermentation inhibitors generated to great extents at harsh conditions (Rogalinski et al., 2008).

1.8. Glucose Fermentation for bioethanol production

Glucose can be anaerobically metabolised by microorganism such as yeast and fungi to produce ethanol (and energy) (Nelson and Cox, 2004). A simplified scheme of ethanol production by fermentation is shown in Figure 1-10.

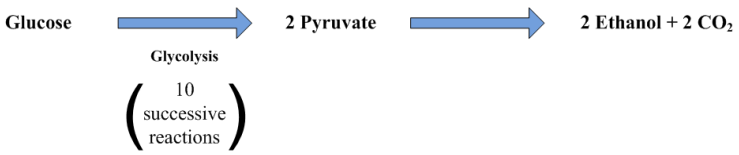

Figure 1-10 - Simplified scheme of ethanol production in anaerobic conditions. Source: modified from (Nelson and Cox, 2004).

Fermentation of glucose obtained by cellulose fibres, i.e., 2nd-generation process, is in theory similar to the well-established fermentation of sucrose (sugarcane) and starch (corn) (Lin and Tanaka, 2006). However, in practice fermentation of glucose produced from lignocellulose is more challenging due to the presence of non-fermentable compounds such as C-5 sugars (xylose), lignin and inhibitors, and also due to low glucose concentrations (Wang and Sun, 2010).

It is well established that inhibitors of fermentation are formed during pretreatments/hydrolysis and comprised of three main groups: weak acids (acetic, formic), furan derivatives (furfural, HMF) and phenolic compounds (Palmqvist and Hahn-Hägerdal, 2000a). The anion of weak acids can diffuse in organism membrane, which results in a decrease of intracellular pH (Palmqvist and Hahn-Hägerdal, 2000b). Furan compounds are believed to inhibit essential metabolic enzymes (Taherzadeh and Karimi, 2011), while phenolic inhibitors has been related to loss of cells membrane integrity (Palmqvist and Hahn-Hägerdal, 2000a). Moreover, the synergetic effect of the presence of several inhibitors is reported to be higher than the effect of each of these compounds separately (Palmqvist and Hahn-Hägerdal, 2000a). In addition, high glucose and ethanol concentrations can also inhibit microorganism growth and ethanol production (Taherzadeh and Karimi, 2011).

Although there are many microorganism capable of producing ethanol, *Saccharomyces cerevisiae* is well-established organism and is widely used in laboratory research (Ostergaard et al., 2000). Moreover, some *S. cerevisiae* strains have demonstrated significant tolerance to some inhibitors such as HMF (Rosatella et al., 2011).

In the case that cellulose hydrolysis is performed enzymatically, fermentation can be performed simultaneously in a process known as Simultaneous Saccharification and Fermentation (SSF). SSF has some advantages such as preventing glucose inhibition due its rapid consume by the microorganism and the use of a single step for two processes (Wang and Sun, 2010). However, the conditions required to run both processes at the same time are not optimal for either of them (Wyman, 1996).

The use of SBW for cellulose hydrolysis makes it unfeasible to perform SSF, thus a separate hydrolysis and fermentation (SHF) process can be conducted. Moreover, to date the fermentation of glucose obtained by SBW hydrolysis of MxG has not been reported.

1.9. Aims and objectives

The aim of this project was to evaluate the utility of subcritical water as a 'green solvent' with and without modifiers, to support an environment-friendly process of: (a) cellulose purification from lignocellulosic biomass; (b) conversion of cellulose into glucose; and (c) bioethanol production via glucose fermentation.

A biorefinery approach was applied to fractionate *Miscanthus x giganteus* into its main components by extraction of hemicellulose in SBW followed by lignin extraction using organosolv method. Subsequently, cellulose-enriched fibres were hydrolysed using SBW to obtain glucose, which was then used for bioethanol production by fermentation using *S. cerevisiae*.

In order to achieve the project aim, this work was divided into the following specific objectives:

- Promote hemicellulose and lignin extractions from MxG using SBW and organosolv methods evaluating direct extraction and sequential extractions in a biorefinery approach (Chapter 3);
- Investigate physicochemical modification on enriched-cellulose fibres after biomass processing to understand the relation between cellulose structure and cellulose hydrolysis (Chapter 3);
- Develop an understanding of SBW mediated hydrolysis of cellulose-enriched fibres for glucose production (Chapter 4) and;
- Evaluate the efficacy of glucose obtained from cellulose by SBW hydrolysis on bioethanol production by fermentation. (Chapter 5)

CHAPTER 2

MATERIALS AND METHODS

2.1. Introduction

This section describes the material, procedures and equipment used throughout this research project for characterization and quantification analysis.

2.2. Feedstock

Feedstock used in this work was *Miscanthus x giganteus* (MxG), kindly provided by Phytatec Ldt (UK). *Miscanthus* was cultivated in Aberystwyth (Wales), harvested in 2013 and air-dried. The biomass was kept in a dry black bag inside a closed box during all the work.

Table 2-1 shows MxG composition (lignin, hemicellulose, cellulose and extractives) in percentage of dry weight.

Table 2-1 - MxG composition.

Component	% (dry weight)
Lignin (Klason)	22.6
Xylan	17.1
Arabinan	1.0
Galactan	0.2
Hemicellulose (xylan+arabinan+galactan)	18.3
Extractives	11.0
Cellulose (estimative by difference)	48.1

Lignin was quantified by Klason Lignin procedure; hemicellulose was determined by High Performance Anion Exchange Chromatograph (HPAEC); extractives were quantified

according to the National Renewable Energy Laboratory (NREL) procedure for determination of extractives in biomass (Sluiter et al., 2005); and cellulose was estimated by difference. The methods used for the quantitative analysis of components are described in detail throughout this chapter.

2.3. Klason lignin method

2.3.1. Background

There are a number of methods used to quantify lignin such as non-invasive methods for instance infrared spectroscopy (IR) and nuclear magnetic resonance (NMR) and chemical modification such as lignin solubilisation by thioglycolic acid or acetyl bromide. Nevertheless, the most common used are gravimetric methods such as Klason lignin and detergent insoluble lignin (Hatfield and Fukushima, 2005, Tuomela et al., 2000).

The non-invasive methods do not require an extensive sample preparation, however, the overlapping of peaks due to other compounds and the lack of a proper standard make these methods more appropriate for qualitative than quantitative analyses (Hatfield and Fukushima, 2005). Thioglycolic acid and acetyl bromide are used to solubilise the lignin from cell walls. Thioglycolic acid reacts with benzyl alcohol while acetyl reacts with unsubstituted OH, both making lignin soluble. Solution containing soluble lignin is then quantified by absorbance changes (Hatfield and Fukushima, 2005). Although these methods can have less interference from other compounds present in lignocellulose matrix, complete lignin solubilisation and lack of standard make these method less reliable (Dence, 1992).

Klason lignin method consists in acid hydrolyse biomass carbohydrates (hemicellulose and cellulose) in two steps (72% acid at mild temperature (30^{o}C); then 4% acid at boiling

temperature) and weigh the acid insoluble lignin (AIL) which remains in solid phase (Sluiter et al., 2008).

Acid detergent lignin (ADL) can be quantified by a detergent method that uses a similar principle as Klason, the difference being the order in which higher temperature and acid concentration are applied (Hatfield et al., 1994). In the procedure to quantify ADL, first reported by Van Soest and Wine (1967), low concentrated acid (4%) is mixed with a detergent solution at high temperatures to hydrolyse mostly hemicellulose. Then, the solid left (cellulose+lignin) is hydrolysed in concentrated acid (72%) detergent solution at mild temperatures (25-30^{o}C) (Van Soest and Wine, 1967). After both hemicellulose and cellulose are removed in the 1st- and 2nd-step, respectively, remaining solid lignin can be weighed. However, it has been suggested that ADL procedure underestimates lignin quantity significantly, particularly for grasses, due to lignin solubilisation (Kondo et al., 1987, Lowry et al., 1994). Therefore, Klason lignin was chosen as analytical method for quantification of lignin in *Miscanthus*.

Prior to Klason procedure, biomass needs to be ground and biomass extractives needs to be removed. These procedures are detailed below.

2.3.2. Grinding biomass using liquid nitrogen

MxG was ground using liquid nitrogen in order to obtain a small particle size (<1.4mm) needed for Klason analysis. 5g of MxG was weighed and placed in a blender (Philips, 400W, 1.5L). Liquid nitrogen was added until biomass was completely covered and frozen. Frozen biomass was then ground for 15s.

Ground MxG was passed through a 1.4mm sieve and portion retained in 1.4mm sieves (d>1.4mm) was ground again and placed once more in the sieves. This step was repeated three times in total.

2.3.3. Removal of extractives

Biomass extractives, composed mostly by non-structural carbohydrates (starch), proteins and waxes (Hatfield and Fukushima, 2005), are important interfering in Klason lignin method, therefore they need to be removed prior the procedure. Solvents used for extraction were water followed by ethanol, according to the National Renewable Energy Laboratory (NREL) procedure for determination of extractives in biomass (Sluiter et al., 2005).

2.3.3.1. Material

Cellulose thimbles (Whatman®, 26×60mm, thickness 1.5mm) were used for the extraction. Extraction solvents were HPLC grade water (Sigma) followed by ethanol absolute (Fisher Scientific). The Soxhlet apparatus was composed by a heating mantle, a glass extractor, a glass condenser and a 250mL glass flask.

2.3.3.2. Method

The thimble was weighed (E_1) and used for extraction of about 6g of nitrogen ground MxG. Thimble+MxG were weighed (E_2) and thimble was closed by folding its top to avoid MxG to spread once submersed in the solvent.

Thimble was then placed into a Soxhlet apparatus and HPLC grade water was added until the thimble was completely submersed. Soxhlet extraction works by boiling the solvent, which accumulates in the extractor and extracts the soluble components from the biomass; when the extractor is full of solvent, a siphon empties the extractor, returning the solvent to the flask to boil again. The cycle is then repeated. Water extraction was carried for two consecutive days during 8h per day.

Water containing the extractives was removed from the apparatus and replaced by ethanol. Ethanol extraction was also carried for two consecutive days during 8h per day. The objective of this step was to remove extractives, therefore, volume of water and ethanol were not measured. Instead, solvents were added until the thimble was completely submersed.

At the end of ethanol extraction, the thimble containing the extractives-free *Miscanthus* was removed from the Soxhlet apparatus and then dried at 65ºC for 48h and weighed (E_3). Extractives percentage was calculated as shown in Equation 2-1:

$$Extractives\ (\%) = \frac{E_3 - E_1}{E_2 - E_1} \qquad \text{Equation 2-1}$$

2.3.4. Lignin determination by Klason method

2.3.4.1. Method

Klason lignin was quantified in this work using a standard procedure adapted from the NREL for lignin quantification in biomass (Sluiter et al., 2008).

Glass filtering crucibles (Pyrex, Gooch borosilicate, porosity grade 4, 30mL) were placed in a muffle furnace at 575ºC for four hours for drying and cleaning organic residues that might be left in the crucibles. Then, they were transferred to a desiccator until room temperature and weighed (K_1).

0.3 ± 0.01g of biomass (B) to be analysed was weighed into a glass test tube and 3mL of 72% sulphuric acid (Fluka) was added to the tube. Mixture was homogenised using a glass stir rod and placed into a pre-heated water bath at 30ºC for 60min. Mixture was stirred every 10-15min without taking the tube out of the water bath to maximise carbohydrate hydrolysis.

The tube was removed from the bath after 60min and mixture was transferred to a 100mL glass Duran® bottle and diluted to 4% acid (that was done by adding 84mL of distilled

water). The bottle was closed with plastic lid and placed in an oven for the 2nd-step acid hydrolysis at 121ºC for 60min.

After the 2nd-step acid hydrolysis, samples were cooled for 30min and vacuum filtered in the pre-weighed crucibles. Liquid fraction was stored (-20ºC) for carbohydrate analysis. 50mL of warm distilled water (~50ºC) was used to rinse the solid left in the crucibles. Crucibles were dried at 105ºC for 6h and placed into a desiccator until room temperature before being weighed again (K_2).

Crucibles were placed into a muffle furnace at 575ºC for 4h and then placed to cool down in a desiccator and re-weighed (K_3). This stage was used for quantification of ashes present in the samples.

In order to calculate Klason lignin, the oven dry weight (ODW, in grams) was calculated using Equation 2-2:

$$ODW = \frac{B * \%total\ solids}{100} \qquad \text{Equation 2-2}$$

Total solids percentage was obtained by weighing a small amount (~1g) of biomass (T_1) that will be analysed by Klason procedure into a pre-weighted Eppendorf tube (T_2). The tube was then dried for 48h at 65ºC and re-weighed (T_3). Total solids and moisture contents were determined by Equation 2-3 and Equation 2-4.

$$Total\ Solids\ (\%) = \frac{T_3 - T_2}{T_1 - T_2} * 100 \qquad \text{Equation 2-3}$$

$$Moisture\ (\%) = 100 - Total\ solids \qquad \text{Equation 2-4}$$

Klason lignin was calculated by Equation 2-5:

$$Klason\ lignin\ (\%) = \frac{(K_2 - K_1) - (K_3 - K_1)}{ODW} \qquad \text{Equation 2-5}$$

2.3.4.2. Limitations

Klason procedure might overestimate lignin in high protein content biomasses as part of protein might remain solid after acid hydrolysis (Hatfield and Fukushima, 2005). There is also the possibility of incomplete acid hydrolysis of carbohydrates (Kondo et al., 1987, Sluiter et al., 2008).

Lower molecular weight lignin (known as acid soluble lignin (ASL)) might be solubilised in acid during the process, (Sluiter et al., 2010). According to the NREL protocol for Klason lignin, ASL should be estimated by UV-absorbance of the liquid fraction after 2nd-step acid hydrolysis (Sluiter et al., 2008). However, the difficulty of this procedure is to choose the correct wavenumber to read absorbance, because of the potential inferences such as furans and carbohydrates (Hatfield and Fukushima, 2005). Moreover, as ASL only represents up to 0.5-1.5% (w/w) of *Miscanthus* (Brosse et al., 2009, Visser et al., 2001), it was not quantified in this work.

2.4. Fourier-transform infrared spectroscopy (FTIR)

2.4.1. Background

FTIR is a method commonly used for structural analysis of lignocellulosic biomass particularly because of its simplicity in sample preparation, fast analysis, non-destruction of samples and the possibility of investigating more than one compound at time using the same spectra (Xu et al., 2013a).

The principle of FTIR is the detection of absorbed radiation due to the interaction of IR radiation with vibrating bonds. Different bonds interact to different components of the IR spectrum (Xu et al., 2013a).

FTIR spectra can be used to identify/evaluate biomass structure, composition, and modifications during different processing (Park et al., 2010). There are several attempts to generate calibration curves in order to predict lignocellulose composition using FTIR spectra, however the lack of standards make quantification challenging (Xu et al., 2013a).

2.4.2. Limitations

Although FTIR can provide fast analysis and comparison among samples, this method usually only generates qualitative results unless calibrated with known standards (Park et al., 2010). Also, the interpretation of spectra is challenging, particularly in biomass due to overlapping of peaks due to different compounds (Barnette et al., 2012).

2.4.3. Principal Component Analysis (PCA) on FTIR data

Principal Component Analysis is a statistical multivariate technique, which decomposes the original data into orthogonal components to investigate possible data correlations. PCA is a powerful tool to analyse large amounts of data by decreasing the number of variables into few principal components (uncorrelated variables) (Xu et al., 2013a).

The principle of PCA is to 'plot' a matrix of X variables and Y samples in a multidimensional space, called variable space, and find 'hidden correlation'. This variable space is composed by z variable axis, i.e., x_1 = variable1, x_2 = variable2 and so on. Although it is only possible to visualise z<=3, the number of variables are usually much higher in multivariate data analysis (Esbensen, 2002).

After 'hidden correlations' are found in the variable space, a central axis can be created in the direction of the maximum variance. This central axis is obtained by minimizing the distance between each variable to the axis using the principle of least squares. This axis will be

a new variable, called PC1, which partially describes the data (Esbensen, 2002). An illustration of data plot and PC1 determination is shown in Figure 2-1.

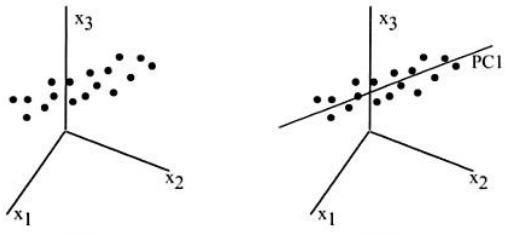

Figure 2-1 - The creation of PC1 in data plotted in space.Source: (Esbensen, 2002).

PC2 can be determined using the same technique of finding a new axis, orthogonal to PC1, that minimizes the distance of each data point to the axis. Then, PC3 is determined in the same way and so on (Esbensen, 2002). The number of possible PCs is the smallest between variable or sample number, however, usually only the first few PCs (PC1-PC3) are needed for data interpretation as they describe most of the data variance (Hori and Sugiyama, 2003, Sim et al., 2012).

The projection of each data point into a coordinate formed by a pair of any 2 PCs is called scores plot (Figure 2-2).

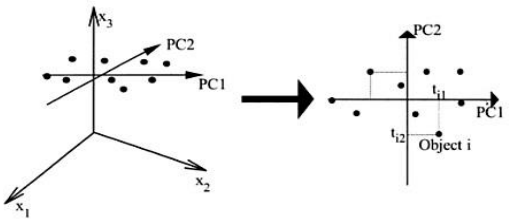

Figure 2-2 - Scores plot for PC1 and PC2. Source: (Esbensen, 2002).

The scores plot is widely used to find relations among the samples, identify sample grouping (clusters), recognise possible outliers, etc. (Esbensen, 2002) and that is the tool that was mostly used in this work.

The loading plot in PCA is related to the scores plots and provide some further sample analysis (Plácido and Capareda, 2014). Figure 2-3 shows an example of the loading plot for PC1 and PC2 from FTIR data.

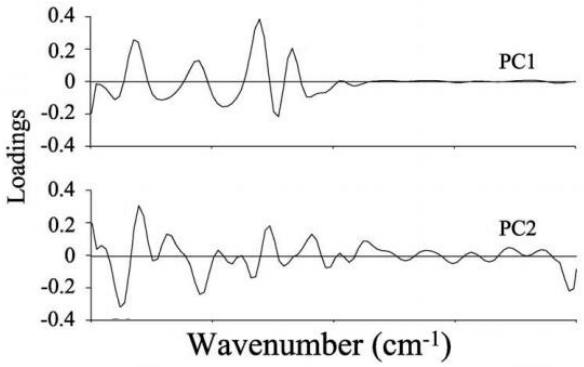

Figure 2-3 - Loading plot for PC1 and PC2 from FTIR data. Source: modified from (Hori and Sugiyama, 2003)

In the loading plot, the highest peaks (positive and negative) are the ones that contribute the most for the variability that affects the position of the samples and, therefore, the clusters observed in the scores plot (Kline et al., 2010). In this work, the analysis of loadings plots was focused on PC1, as this is the PC that explains the highest data variability.

2.4.3.1. PCA for FTIR analysis and FTIR data manipulation

FTIR spectra can easily generate thousands of variables and visual comparison among samples is unlikely to result in definitive conclusions (Sim et al., 2012). Therefore, the use of multivariate analysis is increasing especially for biomass analysis in order to obtain more conclusive results (Xu et al., 2013a).

Prior to PCA analysis, one or more data treatment such as smoothing, normalisation, 2^{nd}-derivative and baseline correction, is commonly applied with the purpose of decreasing noise and increasing spectra resolution (Hori and Sugiyama, 2003, Michell, 1990, Xu et al., 2013a).

Normalisation of FTIR data is commonly applied before PCA. Moreover, this tool can be applied using a variability of peaks (height and area) such as 1162, 1800 and 2900cm^{-1} (Chen et al., 2015, Monrroy et al., 2015, Ryden et al., 2014). In this work, normalisation was applied using the highest peak of each spectrum (which varies for each spectrum). Hence, the wavenumber values used for PCA are a relation between absorbance in each spectrum, not an absolute absorbance value. Hence, comparison among spectra is easier.

Finally, although PCA can be used for a variety of purposes, including prediction and calibration curves (Monrroy et al., 2015), the focus of this work was mostly try to understand the FTIR data and to answer simple questions such as if the spectra represent significant differences. Therefore, the scores and loading plots were the main tools used in the PCA study and analysis was focused on PC1 and PC2.

2.4.4. Material and method

FTIR was performed in a Jasco FTIR 6300 spectrometer. Samples (few milligrams) were analysed with no previous preparation. Parameters used were resolution of 4cm^{-1} and 32 scans in a range between 4000-600cm^{-1}. Background scans, without samples, were performed before each sample using the same parameters.

2.5. Scanning Electron Microscopy (SEM)

Scanning electron microscopy was performed in order to obtain images of biomass fibres. Prior the analysis, samples were coated with platinum for 120s using an Emscope Sc500 sputter coater. Samples were then kept in a desiccator until the analysis. Images were obtained using a Philips XL30 FEG Environmental scanning electron microscopy operating at 10kV at several amplification magnitudes.

2.6. High-Performance Anion-Exchange Chromatography with Pulsed Amperometric Detection (HPAEC-PAD)

2.6.1. Background

Carbohydrates can be analysed by several methods and the most common include high performance liquid chromatography (HPLC), gas chromatography (GC) and more recently, high performance anion exchange chromatography coupled with pulse amperometric detection (HPAEC-PAD) (Zhang et al., 2012b).

Among these techniques, HPLC coupled with refractive index (RI) detector is the most used, however, although HPLC can be used with no or little sample preparation, the method lacks sensitivity and the separation efficiency for similar sugars is poor (Corradini et al., 2012). Moreover, changes in eluent composition affect significantly the RI detector signal which excludes gradient methods for elution, which makes detection of di-, tri- and oligosaccharides very challenging (Raessler, 2011).

GC with flame ionization (GC-FID) or GC with mass spectrometry (GC-MS) detectors offer good accuracy for monomers, particularly for low concentrated samples, nevertheless sample preparation needed is very time consuming as sugars need to be derivatized to be volatile (Agblevor et al., 2007).

In the specific case of complex mixtures containing mono- and oligosaccharides, HPAEC-PAD separation and detection efficiency is superior to both HPLC and GC (Cataldi et al., 2000).

2.6.2. HPAEC-PAD

Carbohydrates have pK_a values in the in the range from 12-14, hence, in a highly alkaline system they can be converted into their oxyanions which offers the possibility of

separation by anion-exchange chromatography (Xu et al., 2013b). In this method, they are eluted according to their pK_a value: the higher the pK_a, the lower is their interaction with an ion exchange surface resulting in lower retention times (Corradini et al., 2012).

Sodium hydroxide is commonly used as mobile phase to provide the high pH needed in the system (Zhang and Lee, 2002). Lower concentrations are used for monosaccharides elution and higher concentrations (>80mM) for oligomers elution (Cataldi et al., 2000).

Sodium acetate (NaOAc) is frequently used when analysis of larger molecules, i.e., oligosaccharides, is needed. NaOAc works as a pushing agent that increases the ionic strength of the mobile phase, therefore larger molecules can be eluted faster, otherwise retention time of large molecules would be excessively long (Xu et al., 2013b). Sodium nitrate can also be used as a more powerful eluting agent than NaOAc, with reported separation of polysaccharides with degree of polymerisation (DP) up to 80. However, column regeneration becomes more challenging when nitrate is used (Zhang and Lee, 2002). This work was focused in molecules with low DP (<10), therefore, NaOAc was selected to facilitate elution.

There is a range of columns specifically designed for carbohydrate separation using HPAEC-PAD, known as CarboPac™. Instead of common silica resin columns, which would not be suitable at highly alkaline systems, CarboPac™ are made of modified pellicular resin composed by microporous divinylbenzene containing quaternary amine groups for high ion exchange capacity and latex resin that are chemically and mechanically stable and offers a fast exchange process (Raessler, 2011, Rohrer et al., 2013). The column used in this work, CarboPac® PA1, was selected for the suitability of monosaccharides, disaccharides and low degree of polymerisation oligosaccharides analysis. The stationary phase of this column is a mixture of polystyrene (2%) and divinylbenzene substrate agglomerated with “Microbed” quaternary ammonium and 5% crosslinked latex (Dionex).

Temperature has an impact on the elution in HPAEC-PAD as higher temperatures result in lower retention times. Moreover, this effect is more pronounced in higher DP molecules compared to monosaccharides (Cataldi et al., 2000). However, temperatures above 45^{o}C can intensify carbohydrate undesirable reactions, that are insignificant at room temperature, and can also degrade column resin (Dionex, Zhang and Lee, 2002). Thus, mild temperatures are preferred in HPAEC analysis

A pulse amperometric detector (PAD) coupled to HPAEC provides excellent resolution of carbohydrates. A gold working electrode is used in the detector to oxidize carbohydrates under high pH and generate a current that can be measured and is proportional to carbohydrate concentration (Rohrer et al., 2013). However, the constant oxidation generates residues that accumulate in the electrode, resulting in a fast decrease of sensitivity. This is corrected by applying a pulse of potentials (waveforms) which oxidize the carbohydrate first and, subsequently, cleans and restore the gold working electrode (Rohrer et al., 2013).

2.6.2.1. Equipment and materials

The Ion Chromatography System (ICS-3000) from Dionex/Thermo was composed of: an autosampler; a single pump; an oven compartment with a guard CarboPac^{TM} PA1 column (4x50mm) and analytical CarboPac^{TM} PA1 column (4x250mm); and a detector compartment with a PAD using a disposable working gold electrode and an Ag/AgCl reference electrode.

Solvents used were Milli-Q® water (18.2MΩ/cm), 50% sodium hydroxide solution and sodium azide (analytical grade, Fisher Scientific), and anhydrous NaOAc (electrochemical grade, Thermo Scientific). Milli-Q® water was degassed for 10min prior to eluent preparation.

Special attention needs to be taken during manual preparation of hydroxide eluent to prevent formation of carbonates as they can bind to the column and decrease significantly

column sensitivity and interfere in resolution and retention times (Corradini et al., 2012). Stock NaOH solution cannot be shaken by any means and eluent can only be gently stirred during preparation. New NaOH solution was prepared every day for analysis while NaOAc was used for a maximum of 7 days.

Glucose (99.5%), arabinose (98%), xylose (99%), fructose (99%), cellobiose (98%), 5-hydroxymethyl-2-furaldehyde (HMF) (99%), and erythrose (75%) were purchased from Sigma Aldrich. Cellotetraose (95%) and cellohexaose (90%) were purchased from Megazyme and galactose (99%) was purchased from Acros Organics.

2.6.2.2. Method

The method used was modified from two works, Zhang et al. (2012) and Xu at al. (2013), in which hydroxide is injected isocratically in low concentration to elute monosaccharides followed by an increase in hydroxide concentration and introduction of a gradient step of NaOAc solution to elute oligosaccharides (Xu et al., 2013b, Zhang et al., 2012b). Preliminary tests (not presented) evaluated hydroxide concentration from 15 to 25mM for isocratic step and 21mM was chosen as it resulted in the most efficient monomers separation. Similarly, several gradient profiles for NaOAc were tested before choosing the best condition.

Milli-Q® water was used as solvent A and also in the preparation of the other solvents. 200mM NaOH and 1M NaOAc were used as solvent B and C. Sodium Azide solution (20ppm) was used to wash the syringe once a day.

Oven and detector compartments were kept at 30^{o}C and 25^{o}C, respectively. Flow rate was 1mL/min and sample volume injected was 10μL. Waveform used for the PAD was the pre-

programmed by the ICS unit for Ag/AgCl reference electrode and gold working electrode: Quadruple Potential Waveform for Carbohydrate Analysis.

The method started with an isocratic step using 21mM of B during 20min. At 20min, B was increased to 80mM. Then, from 20 to 60min, solvent C was introduced from 0-20mM and B was kept at 80mM. A washing step was performed from 60min in which B and C were increased to 120mM and 40mM, respectively, and kept constant for 10min. At 70min, C was set to 0 and B was set to 21mM for 20min for column reconditioning. Total run time was 90min per sample.

All the increasing/decreasing in solvent concentrations were linear (curve 5). Except for solvent C increasing from 0-20mM (20-60min) that was made in curve 6, what, by trial and error, was proven to help pushing out higher molecular weight molecules (oligosaccharides).

2.6.2.1. Limitations

Although HPAEC is widely accepted as one of the most efficient techniques for carbohydrate quantification (Zhang and Lee, 2002), some very similar monomers might be challenging to separate, for instance mannose-xylose and glucose-mannose (Panagiotopoulos and Sempéré, 2005).

Carbonate formation from hydroxide solutions is very difficult to avoid and it might eventually bind in the column resin and affect retention time of carbohydrates. A regularly column regeneration with high concentrated hydroxide (200mM) is advised to restore columns performance (Raessler, 2011).

2.6.2.2. Calibration curves

Calibration curves were made in order to calculate concentration of detected compounds. Fructose, glucose, cellobiose, cellotetraose and cellohexaose calibration curves were performed together using the following standard concentrations: 0.006, 0.013, 0.02, 0.05 and 0.1g/L. Xylose, arabinose and galactose calibration curves were performed together using the same concentrations. HMF calibration curve was made using: 0.005, 0.01, 0.05, 0.1 and 0.2g/L.

Figure 2-4 shows separation of a mixture containing 0.02g/L of each of the following: fructose, glucose, cellobiose, cellotetraose and cellohexaose. All standard peaks were identified by their retention times after running each compound separately (not shown).

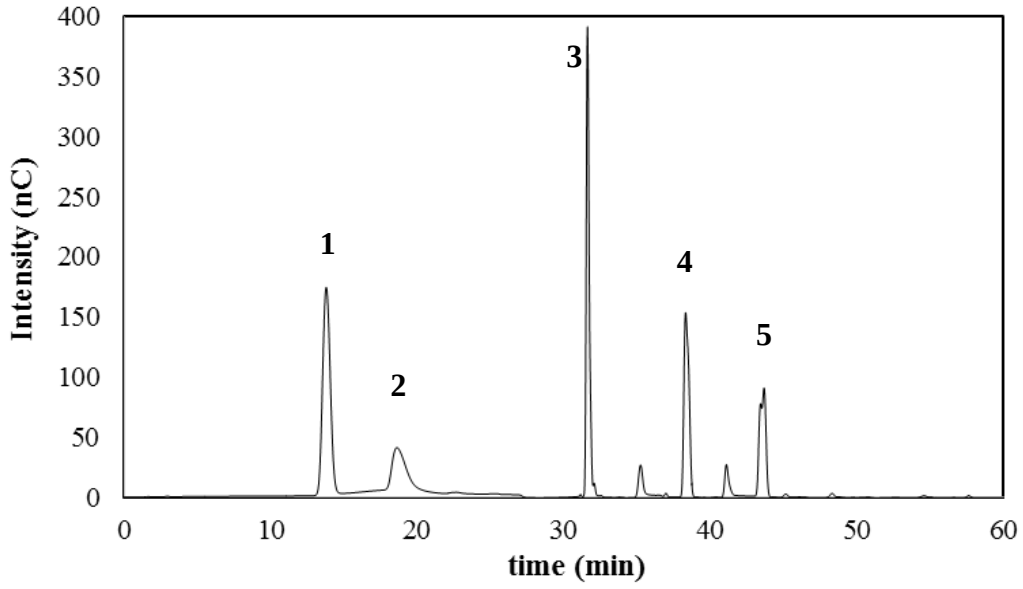

Figure 2-4 - Chromatogram of carbohydrate separation by HPAEC-PAD.Elution order: 1) glucose, 2) fructose, 3) cellobiose, 4) cellotetraose and 5) cellohexaose.

The parameters were obtained using the software Chromeleon 7®. Apart from the five identified peaks, two more peaks are shown in Figure 2-4. They are most likely impurities

presented mainly in cellotetraose and cellohexaose as these two standards have lower purity than the other standard used.

Table 2-2 shows the slope and R^2 for all the compounds analysed by HPAEC-PAD.

Table 2-2 - Standard calibration curves parameters obtained by HPAEC-PAD for carbohydrates and HMF.

Compound	R^2	Slope
HMF	0.9982	668.50
Arabinose	0.9780	676.18
Galactose	0.9708	839.79
Glucose	0.9915	1036.71
Xylose	0.9716	1069.26
Fructose	0.9960	539.20
Cellobiose	0.9940	935.97
Cellotetraose	0.9948	613.28
Cellohexaose	0.9929	442.20

Samples obtained during this work were in general very concentrated. Therefore, due to the sensitivity of the equipment, dilutions were often necessary. These dilutions (from 2-200 times, depending on the sample) were made using Milli-Q® water.

2.7. High Performance Liquid Chromatography (HPLC) for furfural analysis

Furfural is a dehydration product from sugars, therefore, it is expected to be present in biomass extracts. HPAEC was not able to resolve furfural, hence, HPLC combined with UV detector was used instead.

2.7.1. Background

High performance liquid chromatography is a widely known separation technique comprised of a mobile phase (eluent) and stationary phase (column) wherein solute interaction with these two phases provides separation (El Rassi, 2002).

Many separation methods can be applied in HPLC such as size exclusion, ion exchange, and the most common used, adsorption (Corradini, 2010). Reversed-phase liquid

chromatography (RPC) is an adsorption/desorption method in which the mobile phase is more polar than the stationary phase (the opposite of normal-phase chromatography). RPC is used in separation of a wide range of compounds including carbohydrate, phenolic, etc. (Doyle and Dorsey, 1998).

Columns used in RPC are commonly made using silica as support because of its properties such as stability at high pressures, mechanical strength and variability of pore/particle size (Doyle and Dorsey, 1998). Nevertheless, silica does not support high pH systems (El Rassi, 2002). The silica is modified by attaching hydrophobic alkyl groups such as octyl (C_8) or octadecyl (C_{18}) to the silica throughout silyl ester bonds (-Si-O-Si-) to provide different surface properties (Doyle and Dorsey, 1998).

The most common HPLC detectors, used in 80% of HPLC applications, are RI, ultraviolet absorbance (UV), fluorescence and conductivity detectors (Corradini, 2010). Although fluorescence is highly sensitive, the majority of compounds do not present natural florescence, which makes this detector less used (Kok, 1998). Conductivity detectors can be used for ionised solute and difference in conductivity between the sample and the mobile phase is detected. This type of detector is almost exclusively used in ion chromatography (Corradini, 2010). RI detection have disadvantages such as low sensitivity and stability issues, however it simple to work and it is still widely used for sugars determination (Kok, 1998). UV has a general applicability particularly when the maximum absorbance of the compound of interested is known, therefore, it is commonly used, even though it lacks sensitivity (Kok, 1998).

Mobile phase in RPC is a mixture of water and an organic modifier such as methanol, acetonitrile, and isopropanol (El Rassi, 2002). Acetonitrile was chosen because the mixture acetonitrile-water results in a less viscous solvent then other water-organic solvent mixtures, which leads to lower back pressure in the system (Doyle and Dorsey, 1998).

Temperature needs to be controlled as changes in temperature affect retention time negatively, i.e., an increase in temperature will decrease retention times (El Rassi, 2002).

2.7.2. Materials and method

The method used for furfural detection was adapted from Carapetudo Antas (2015) in which a shorter procedure was adopted as furfural was the only compound of interest (Carapetudo Antas, 2015).

The analysis was performed in a Shimadzu equipment consisting of an autosampler (SIL-10AD), a dual pump (LC 10AD), a vacuum degasser (DGU – 14A), an oven (CTO-10AS), and a UV detector (SPD – 10A, VP) set to 280nm.

Solvents were prepared using HPLC grade water (Chromasolv®Plus), acetic acid (99.8-100.5%, Fisher Scientific) and HPLC grade Acetonitrile (Chromasolv®Plus). Solvents used as mobile phase were (v/v): (A) water with 2% acetic acid; (B) 1:1 water / acetonitrile with 0.5% acetic acid, and; (C) acetonitrile. Solvent A concentration (%) is always 100 - B(%) - C(%). Acetic acid is added to solvents A and B to work as a buffer and improve separation when ionic compounds are presented in solution (Carapetudo Antas, 2015).

The column used was a Prodigy 5µ ODS3 100A (250x4.6mm) from Phenomenex coupled to a guard column with a cartridge. Column temperature and flow rate were kept constant at 40^{o}C and 1mL/min, respectively. Injection volume was 10µL per sample. Furfural (99%) was purchased from Sigma.

The method was a gradient step in which B starts from 10-55% from 0-20min. Then, from 20 to 30 min, B increases to 100%. A washing step is then performed to wash out any residues and recondicionate the column. At 30min, B is set to 0 and C is set to 100%. This

washing step lasts for 10min. At 40 min, B is set back to 10% and C is set to 0% until 50min to equilibrate the column for next run. Total run time is 50min.

2.7.3. Calibration curve

Figure 2-5 shows furfural calibration curve performed using concentrations at 0.01, 0.10, 0.25 and 0.625g/L.

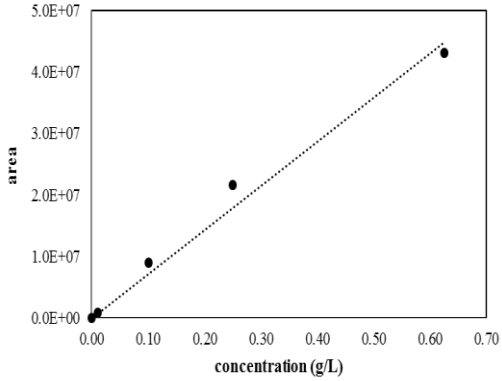

Figure 2-5 - Furfural calibration curve by HPLC.

Furfural presented a retention time of 9.9min as it can be seen in Figure 2-6. Slope and R^2 were calculated using Excel and values obtained were $6.9x10^7$ and 0.984, respectively.

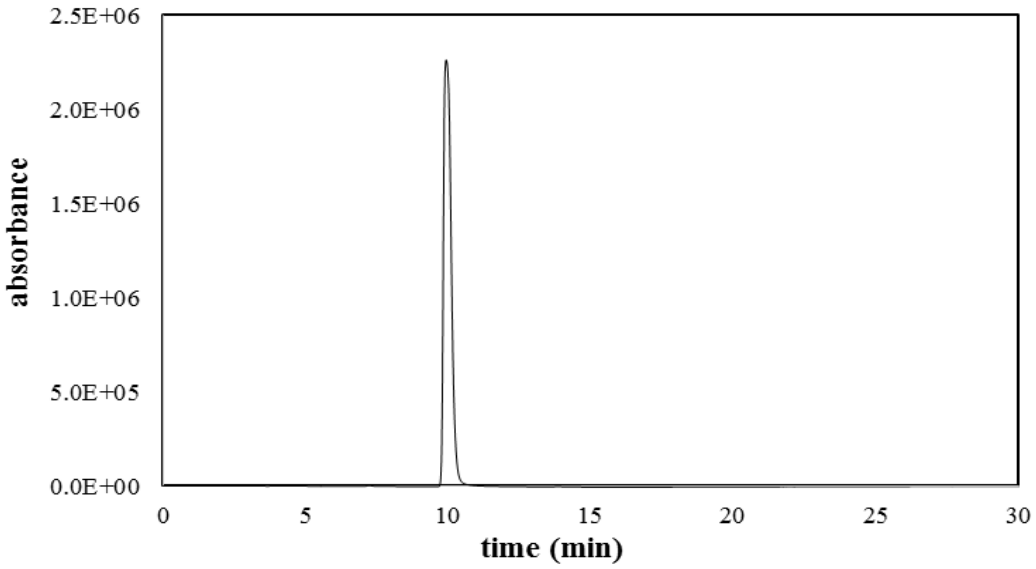

Figure 2-6 - Furfural at 0.625 g/L by HPLC.

2.8. UV absorbance method for glucose quantification

2.8.1. Background

The HPAEC-PAD system was not available in the first year of this work. Hence, glucose concentrations in the first experiments, i.e., the scoping experiments, were analysed using an UV-method based on an enzyme reaction provided by Megazyme (D-Glucose HK Assay Kit). Afterwards, all samples were run in HPAEC and results of these two techniques were compared.

According to Megazyme (2013), glucose presented in solution reacts with adenosine-5'-triphosphate (ATP) in the presence of enzyme hexokinase (HK) to generate glucose-6-phosphate (G6P) as described in Equation 2-6 (Megazyme International, 2013).

$$Glucose + ATP \xrightarrow{HK} G6P + ADP \qquad \text{Equation 2-6}$$

G6P is then oxidised by nicotinamide-adenine dinucleotide phosphate ($NADP^+$) in the presence of gluconate-6-phosphate (G6P-DH). The products of this reaction are gluconate-6-phosphate and reduced nicotine-adenine dinucleotide phosphate (NADPH) as shown in Equation 2-7.

$$G6P + NADP^+ \xrightarrow{G6P-DH} gluconate - 6 - phosphate + NADPH + H \qquad \text{Equation 2-7}$$

The amount of NADPH produced is proportional to glucose in solution and can be measured by changes in absorbance at 340nm (Zhao et al., 2010).

2.8.2. Limitations

Detection limitation is from 0.04-0.8g/L and the assay is linear in this range. Also, strongly coloured samples might affect absorption readings (Megazyme International, 2013).

Bondar and Mead (1974) also describe an inhibition effect during the enzymatic reactions caused by mannose and fructose due to competition for HK (Bondar and Mead, 1974).

Therefore, this method was used for a preliminary glucose estimation and all the quantification was relied on HPAEC analysis.

2.8.3. Materials and Method

D-glucose HK Assay Kit contained four solutions: 1) buffer (pH 7.6); 2) ATP+$NADP^+$ mixture; 3) enzyme solution (HK+ G6P-DH); 4) glucose standard (0.4g/L). All bottles were stored as instructed in the assay manual.

The spectrophotometer used was a Cecil Aquarius CE 7500 set at 340nm. Prior to each analysis, the equipment was switched on and wavenumber was set and left for equilibration for at least 30min.

Plastic UV micro-cuvettes of 10mm pathlength (Brand®) were used to prepare three classes of solutions: blank, samples and standard solutions.

Blank was prepared by filling the cuvette with 0.42mL of distilled water and then adding 0.02mL of buffer and 0.02mL of ATP+$NADP^+$ using micropipettes (2-20μL, Discovery Comfort and 100-1000μL, Biohit). Samples were prepared using 0.40mL of distilled water plus sample, buffer and ATP+$NADP^+$ (0.02mL of each). Standards were prepared using the same volumes as in samples solution, replacing the sample volume by standard solutions.

After preparing all three classes of solutions, cuvettes were closed using a plastic cap and stirred gently. After 5min, all the solutions were read in spectrophotometer and absorbance were recorded (A_1).

After reading the first absorbance value, 4μL of enzyme solutions (HK+ G6P-DH) were added to each cuvette. Thus, all cuvettes (blank, sample and standard) had a total volume of 4.64mL. Cuvettes were once again closed with plastic caps and stirred. The enzymatic reaction

was complete in about 5 min and then the second absorbance of each cuvette was recorded (A_2). Samples that presented high A_2 absorbance (> 1.8) were prepared again after 2 times dilution.

Glucose absorbance ($\Delta A_{glucose}$) was calculate as described in Equation 2-8.

$$\Delta A_{glucose} = (A_2 - A_1)_{sample/standard} - (A_2 - A_1)_{blank} \quad \text{Equation 2-8}$$

Figure 2-7 shows glucose calibration curve that was made using glucose standard provided in the enzyme kit and diluting it to the following concentrations: 0.025, 0.05, 0.1, 0.2 and 0.4g/L. Slope and R^2, 1.579 and 0.999 respectively, were calculated using Excel.

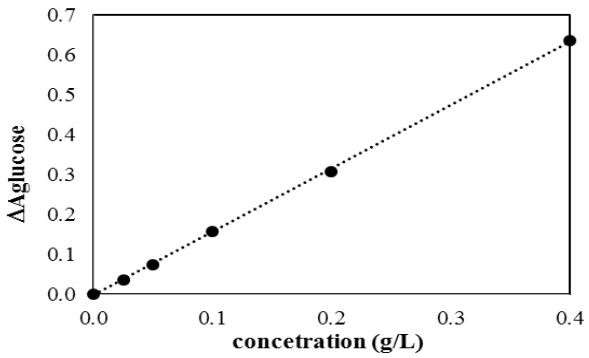

Figure 2-7 - Glucose calibration curve by glucose enzymatic assay.

CHAPTER 3

CELLULOSE PURIFICATION BY BIOMASS FRACTIONATION IN A BIOREFINERY APPROACH

3.1. Introduction

Lignocellulose biomass is a complex matrix found in plants cell wall (Kumar et al., 2009) and composed mainly by cellulose, hemicellulose and lignin (Mosier et al., 2005a) as well as minor quantities of other compounds such as extractives and ash (Jørgensen et al., 2007).

Cellulose, hemicellulose and lignin are linked in lignocellulosic biomass by both covalent (ether, ester, glycoside) and hydrogen bonds, in a complex matrix, which results in a structure recalcitrant to hydrolysis (Fitzpatrick et al., 2010, Gírio et al., 2010). Cellulose accessibility from the lignocellulosic matrix and its further conversion into glucose monomers is considered to be a major technical bottleneck of the production and commercialization of 2nd-generation bioethanol (Pan et al., 2005). Therefore, the cost of 2nd-generation bioethanol is still a substantial drawback for its global commercialization (Demirbas, 2009a, Kaylen et al., 2000).

Therefore, it is increasing the interest in an integrated concept, known as biorefinery, predicted to be capable of generating fuels, power and multiple value added chemicals and materials (Demirbas, 2009a). Moreover, it is believed that the successful implementation of an

integrated biorefinery platform with the co-production of valuable products can make 2nd-generation bioethanol cost-effective (Huang et al., 2008, Kaylen et al., 2000).

Thus, fractionating lignocellulosic biomass into its main components in a biorefinery approach is gaining attention as a promising concept that supports cost effective biomass processing (Pan et al., 2005). In a biorefinary approach, biomass polymers such as lignin and carbohydrates are selectively purified with the aim of opening a wide range of possibilities for generation of high value compounds as well as bioethanol (Fitzpatrick et al., 2010, Huang et al., 2008).

Cellulose fibres contribute to lignocellulose recalcitrance due to cellulosic crystalline structure which is a result of inter- and intramolecular hydrogen bonds (Viikari et al., 2012). Cellulose recovery/purification from the matrix is essential prior to its conversion into glucose for bioethanol production as with no biomass processing cellulose is inaccessible (Hamelinck et al., 2005, Kamm et al., 2000).

Among the three main compounds in lignocellulose biomass, hemicellulose is the most easily extractable polymer (El Hage et al., 2010b). Common temperatures used in hydrothermal treatments for hemicellulose recovery vary from 140ºC-200ºC (Chen et al., 2014). At this range of temperature, lignin and cellulose are left in the insoluble phase, resulting in a hemicellulose liquor composed mostly of xylo-oligosaccharides (XOS) of degree of polymerisation (DP) from 2-20, xylose, decomposed products such as furfural and also biomass extractives (Moure et al., 2006). To increase purity of XOS in the liquor, a hydrothermal step with mild conditions (T<140ºC) can be introduced to separate the extractives prior to hemicellulose solubilisation (Moure et al., 2006).

After hemicellulose is extracted from lignocellulosic biomass, lignin can be recovered from the solid fraction, resulting in purified cellulose fibres. Lignin extraction by organosolv

methods is an alternative to the common paper Kraft and sulphite technologies that lead to a sulphur-lignin product (Arato et al., 2005). Processes using organic solvents to solubilise lignin result in sulphur-free lignin which increases the range of applicability of the purified polymer (Carvalheiro et al., 2008) as currently lignin is often burned for energy production (Mansouri and Salvadó, 2006). Moreover, solvents such as ethanol can be recovered and re-used in the process (Botello et al., 1999). Mineral acids are often used to improve lignin extraction, however the use of acid leads to the need of a neutralisation step and creates waste. Pressurised carbon dioxide was used as a replacement for mineral acid, generating carbonic acid to act as a catalyst and enhance delignification (Pasquini et al., 2005).

The use of a sequential biomass extraction process has the potential to increase the purity of fractions generated during the process, thereby enhancing their utility in down stream applications. Moreover, the selective removal of the hemicellulose and lignin prior to conversion of cellulose into glucose could help avoid the formation of fermentation inhibitors such as furfural and phenolic compounds, that are thought to be originated mostly from hemicellulose and lignin fraction, respectively. In addition, extractions of hemicellulose and lignin might also have an effect in cellulose crystalline structure, therefore having an impact on subsequent conversion of cellulose into glucose.

The first aim of this chapter was to evaluate the impact of processing *Miscanthus x giganteus* (MxG) in two different ways on cellulose purification for further conversion into glucose. In the first proposed route, MxG was directly delignified using a modified organosolv method for lignin and hemicellulose extraction. In the second route, MxG was subjected to a 3-step extraction (removal of biomass extractives by subcritical water (SBW), removal of hemicellulose by SBW hydrolysis, and then delignification using the modified organosolv method).

In addition, the second aim of this chapter was to evaluate and understand the impact of hemicellulose and lignin extraction on the remaining cellulose fibres to assess the role of fibres processing in cellulose crystallinity and in subsequently cellulose hydrolysis.

3.2. Material and Methods

3.2.1. Direct delignification

Delignification of MxG with no prior treatment, in this work called direct delignification, was performed applying a modified organosolv method. In his work, Roque (2013) optimised lignin extraction from MxG using water/ethanol under subcritical conditions and applying CO_2 as modifier to acidify the media (Roque, 2013). The process extracts lignin as well as hemicellulose and extractives from the lignocellulose matrix, leaving a solid cellulose-enriched fibre.

250mL of 50% (v/v) ethanol and distilled water was prepared and pre-heated to 50^{o}C. 5g of MxG was then soaked in the solution for 20min. As biomass is not soluble in water, the soaking stage prior to the reaction is performed in order to increase the wettability, i.e., facilitate the interaction between water and biomass (Matsunaga et al., 2008). The biomass and solution mixture was ground in a blender (Philips, 400W, 1.5L) for 3min.

The rig used for reaction (Figure 3-1) was composed of a 500mL high-pressure reactor (Parr, alloy C276), a heating jacket, an automatic stirrer, inlet and outlet valves, a cooling loop, and a controller (Parr, model 4836). The same rig was used for sequential extraction described in section 3.2.2.

Ground biomass suspension was placed inside the reactor and the reactor was sealed. Vapour withdrawal CO_2 (BOC UK, 99.8%) was used to purge the air inside the reactor and pressurise the reactor to ~50bar. The reactor heating jacket was then turned on and temperature

was set to 200ºC. The reaction lasted for 1h after the temperature achieved the set point. Temperature was kept constant during the reaction time. After that, the reactor temperature was decreased by inserting the reactor in an ice bath and turning on the cooling line.

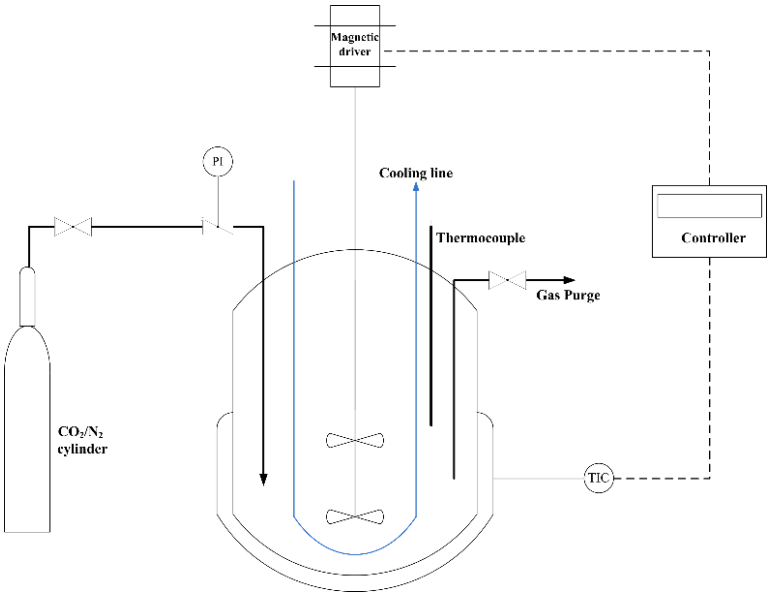

Figure 3-1 - Scheme of the rig used for direct delignification and for the three steps of sequential extraction.

When the temperature cooled to ~60ºC, the reactor was depressurised and opened. Cooling time was usually between 5-10min. The solid fraction (fibres) were vacuum filtered with a porcelain sintered disc (porosity 1) and rinsed three times with 50mL (each time) of water/ethanol solution (1:1) heated to about 50ºC. The liquid fraction was stored in a freezer for analysis in High Performance Anion Exchange Chromatography (HPAEC). Fibres were completely dried at 65ºC and then placed into a desiccator until room temperature. Dried fibres were weighed and recovery of solid fraction was calculated by Equation 3-1:

$$Recovery\ (\%) = \frac{m_f}{m_i} * 100 \qquad \text{Equation 3-1}$$

In which:

m_i = initial mass of *Miscanthus* used for delignification (~ 5g)

m_f = final solid fibres after delignification.

After the delignification, percentage of lignin remaining in the recovered fibres was quantified by Klason lignin procedure. Delignification percentage was calculated by Equation 3-2.

$$Delignification\ (\%) = \frac{lignin_i - lignin_f}{lignin_i} * 100 \qquad \text{Equation 3-2}$$

In which $lignin_{i/f}$ are the amount of initial/final lignin in grams calculated by multiplying m_i and m_f by the percentage of Klason lignin.

The fibres remaining from direct delignification were named 'DEL' fibres in this work.

It is possible to recover lignin from the liquid fraction after modified organosolv delignification method by decreasing the ethanol concentration of the liquid fraction followed by centrifugation. However, this step was not performed in this work.

3.2.2. Sequential extraction

Sequential MxG extraction was performed in three steps described below.

1. Extraction of non-bounded compounds

200mL of distilled water was pre-heated at 50^{o}C and used to soak 10g of MxG for 20min. The suspension was then ground in a blender for 3min. The same reactor rig used for direct delignification was used for all 3 steps of sequential extraction. Ground biomass was transferred to the reactor. After sealing the reactor, the air was purged and the reactor was pressurised to ~50bar using nitrogen. Temperature was set to 120^{o}C. Once this temperature was achieved, the reaction lasted for 30min at constant temperature.

At the end of 30min, the reactor was inserted into an ice bath and the cooling line was opened. When temperature was ~60^{o}C, the reactor was depressurised and opened. The solid fraction (fibres) was sieved in a 45-mesh sieve and dried at room temperature for 48h. These

fibres were named '120ºC' fibres throughout this work and the liquid fraction was stored at -20ºC until analysis by HPAEC.

2. Extraction of hemicellulose

Hemicellulose extraction was performed after removal of biomass extractives in the first step. 10g of 120ºC fibres were soaked in 200mL of distilled water (50ºC) for 20min and then transferred to the reactor.

After sealing and purging the reactor, pressure was increased to ~50bar using nitrogen. Temperature was set to 180ºC and the reaction lasted for 30min at constant temperature. After the reaction time, the reactor was cooled to ~60ºC using an ice bath and the cooling line, and then opened. Fibres were once again sieved using the 45-mesh sieve and dried at room temperature for 48h. These fibres were named '180ºC' fibres and liquid fraction was kept in -20ºC until analysis by HPAEC.

Xylan, arabinan and galactan extraction were calculated by Equation 3-3:

$$carb\ extraction\ (\%) = \frac{(carb_i - carb_f)}{carb_i} * 100\% \qquad \text{Equation 3-3}$$

In which $carb_{i/f}$ is the initial/final mass (in grams) of the carbohydrate (xylan, arabinan and galactan). Carbohydrates initial/final mass was calculated by using their percentage in initial/final fibres obtained using HPAEC and multiplying it by initial/final mass.

3. Extraction of lignin

The exactly same procedure for direct extraction of lignin was used in this step. However, instead of using raw MxG, 180ºC fibres were used in this third step and no additional grinding was performed (because these fibres were ground in the 1st-step extraction). After delignification, the fibres were named 'SEQ' fibres. The liquid fraction was kept at -20ºC until analysis by HPAEC.

3.2.3. Qualitative analysis of liquid fractions

Liquid fractions resulting from each step of sequential extraction and also after direct delignification were analysed using HPAEC for carbohydrates quantification. HPAEC method is described in section 2.6. Prior to analysis, samples were hydrolysed using the 2-step acid hydrolysis of Klason lignin procedure (section 2.3) in order to obtain monosaccharides, which are more easily quantified by HPAEC.

3.2.4. Qualitative analysis of solid fractions (fibres)

After the extractions performed (sequential and direct), resulting fibres (120ºC, 180ºC, SEQ and DEL) were analysed using SEM and FTIR as well as evaluated by PCA. The methods used are described in sections 2.4 and 2.5. For the FTIR and PCA analysis, commercial cellulose (Avicel PH 101, Sigma, UK) was also evaluated for comparison with fibres obtained from MxG.

Klason lignin contents of MxG and each fibre obtained after biomass processing (120ºC, 180ºC, SEQ and DEL) was quantified according to Klason lignin procedure. Hemicellulose fraction (xylan, arabinan and galactan), was quantified by HPAEC after 2-step acid hydrolysis.

3.3. Results and Discussion

3.3.1. Reactor heating time

Table 3-1 shows the average time needed to achieve the target temperature for each of the extractions performed in the 500mL reactor. Variability of up to 2min could be observed.

The reaction times (residence times) described in section 3.2 started as soon as the reactor achieve the target temperature for each extraction. Therefore, the heating time was not considered in the results.

Table 3-1 - Average of heating time for 500mL reactor.

T(°C)	120	180	200
t (min)	12	18	27

3.3.2. Processing routes: direct vs sequential extractions

During the organosolv process of delignification, lignin and hemicellulose are hydrolysed and can be recovered from the liquid fraction, while cellulose remains almost entirely in the solid fraction with non-extracted fractions of hemicellulose and lignin (Sannigrahi and Ragauskas, 2013).

Figure 3-2 shows the scheme of the two processing routes performed: direct delignification and sequential extraction followed by delignification.

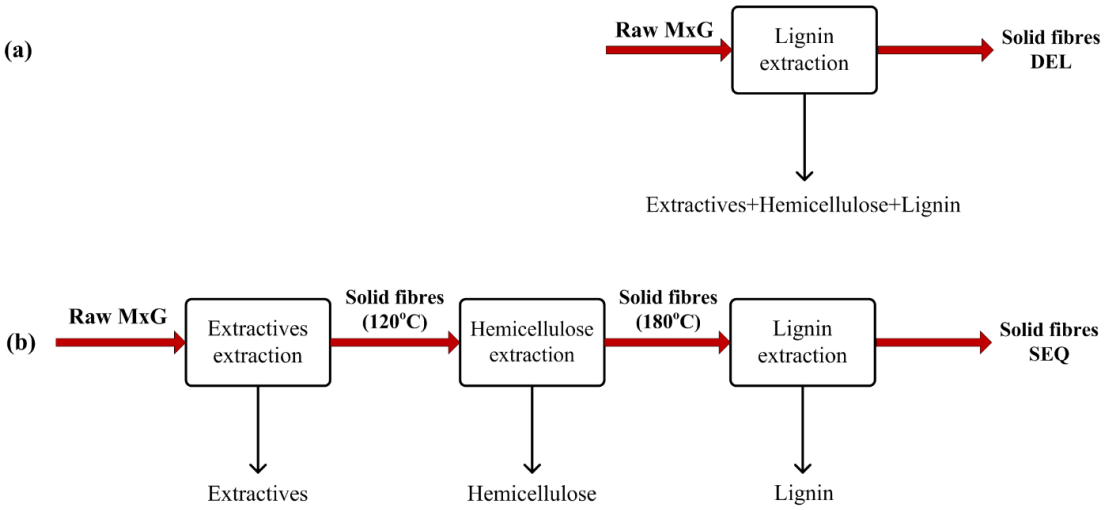

Figure 3-2 - Scheme of direct delignification (a) and sequential extraction followed by delignification (b).

Direct delignification generates a liquid fraction rich in solubilized lignin, hemicellulose (XOS and xylose) and its decomposition products such as acetic acid and furfural as well as biomass extractives. Although lignin can be recovered from this liquor by decreasing ethanol concentration followed by centrifugation (Arato et al., 2005), separation of hemicellulose from the other components becomes challenging. Moreover, temperatures used for organosolv

method potentially increase the amount hemicellulose decomposition because hemicellulose can be extracted in lower severity conditions than lignin extraction requires. Therefore, sequential extraction with an increase in severity was also performed in a biorefinery approach in an attempt to improve both hemicellulose and lignin extractions and to obtain cellulose fibres that are more susceptible to hydrolysis.

Hence, purified cellulose fibres from MxG were obtained after organosolv extraction in two different routes of processing: direct delignification (DEL fibres) and sequential extraction followed by delignification (SEQ fibres). In this work, the focus of the proposed routes was recovering the cellulose fibres from the lignocellulosic matrix. Therefore, no optimisation was performed in each extraction step.

3.3.3. Extraction of non-bonded compounds (extractives)

Non-structural polysaccharides such as starch and pectin, as well as proteins and waxes compose what is called the extractives fraction of lignocellulosic biomass (Le Ngoc Huyen et al., 2010). These are non-bounded compounds and, therefore, they are easily soluble in water and/or ethanol. In the first step of the sequential extraction performed in this work (Figure 3-3), biomass extractives were removed using subcritical water under mild temperature (120ºC) for 30min.

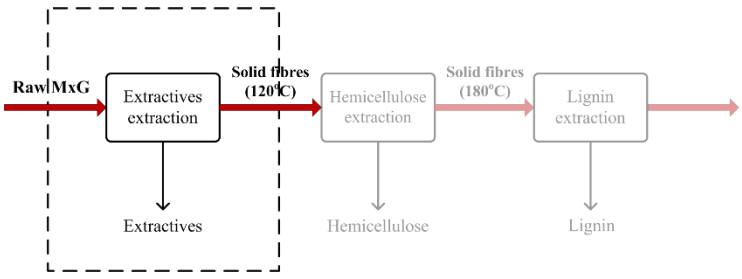

Figure 3-3 - Scheme of biomass processing in sequential extractions: removal of biomass extractives step.

Ideally, this step should aim only for solubilisation of biomass extractives and avoid hemicellulose hydrolysis. Vázquez at al. (2005) proposed that extractives removal from wood (*Eucalyptus*) could be performed using water at temperatures up to 130ºC with little hemicellulose extraction (Vázquez et al., 2005). González-Muñoz et al. (2012) also reported the use of water at 130ºC for extractives removal from wood (*Pinus*) and no hemicellulose solubilisation was observed (González-Muñoz et al., 2012).

Using the procedure described in the section 3.2.2 for extractives removal, two fractions were obtained: a liquid fraction containing primarily biomass extractives and a solid fraction named 120ºC fibres (i.e., extractives-free fibres). From the initial dry weight of MxG, 11.0 ± 0.5% was solubilised in the liquid fraction.

The most common way to quantify biomass extractives cited in the literature is using a Soxhlet extraction by water and ethanol described by the National Renewable Energy Laboratory (NREL) (Sluiter et al., 2005). Using this technique, 11.5% of the dry mass of MxG was extracted. Therefore, it was considered that the extraction of MxG at 120ºC for 30min and 50bar was able to extract 100% of biomass extractives.

The amount of extractives of MxG can vary significantly. Extractives reported in literature are usually quantified only for composition analysis purposes using the NREL procedure for biomass extractives quantification (Sluiter et al., 2005). Frias and Feng (2013) specified a value of 7.7% for water/ethanol extractives from MxG (Frias and Feng, 2013), while Zhang et al. (2012) described a value of 9% (Zhang et al., 2012a) and Chen et al. (2014) reported 11.3% of extractives (Chen et al., 2014). Chen et al. (2016) attested that extractives percentages decreased from 14.7 to 8% for the same MxG crop but harvested in two consecutive years, 2011 and 2012, respectively (Chen et al., 2016). Furthermore, Le Ngoc Huyen et al. (2010) suggested that the variable percentage of extractives in MxG is closely related to its leaves, which contains

the highest level of these soluble compounds. Therefore, the harvesting time would affect extractives percentage due to leaves being lost (Le Ngoc Huyen et al., 2010).

3.3.3.1. Qualitative analysis of MxG extractives by HPAEC

The extractives obtained after the 120ºC step were analysed in the HPAEC for qualitative analysis of carbohydrates. Figure 3-4 shows the chromatogram obtained from the analysis of the extractives. Very little monosaccharide contents were extracted, as expected.

Glucose was the main compound found, generated mostly likely from the starch present in MxG as energy storage (Purdy et al., 2014) because at this temperature cellulose disruption is very unlikely to happen (Vázquez et al., 2005). Negligible quantities of arabinose and xylose were detected, suggesting that hemicellulose was almost intact.

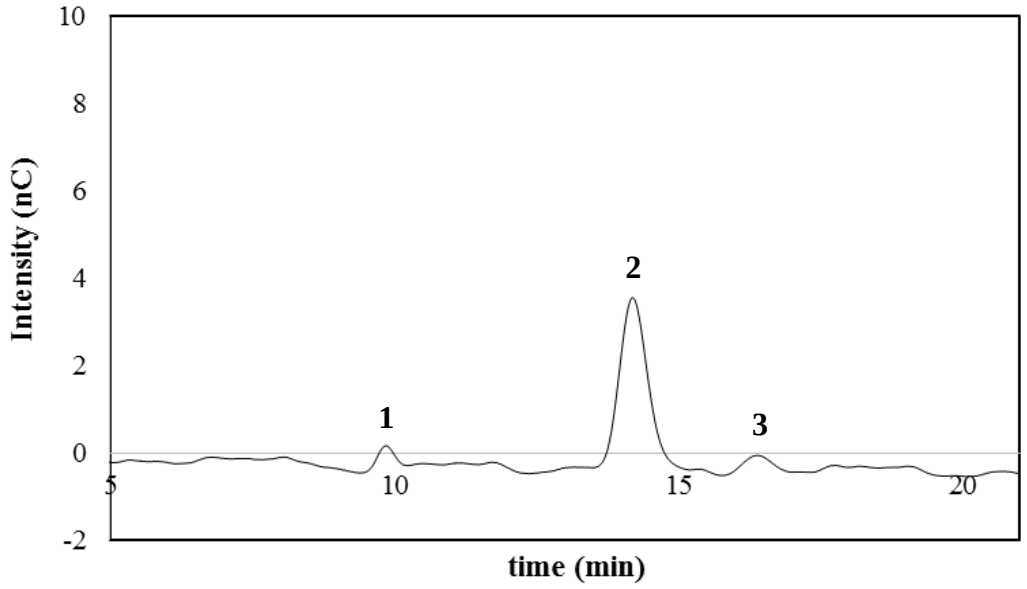

Figure 3-4 - Chromatogram by HPAEC of liquid fraction after extractives extraction of MxG at 120ºC.Compounds: 1-arabinose; 2-glucose; 3-xylose.

The advantage of using the procedure described for extractives removal at 120ºC compared to Soxhlet extraction is the short time required, as it takes only 30min reaction, and

the need for only water as solvent. In contrast, Soxhlet extraction performed during Klason lignin takes four days and two solvents, water and ethanol (Sluiter et al., 2005).

In previous work from this group, the same procedure was evaluated using 140ºC instead of 120ºC for the same 30min of reaction time (data not shown). Compared to results obtained at 120ºC, extraction was slightly higher (about 13%) when using 140ºC, and both arabinose and xylose were produced in higher concentration, suggesting that hemicellulose was partially hydrolysed. Therefore, the temperature chosen for this step was 120ºC to minimise hemicellulose hydrolysis.

Subsequently to MxG extractives removal, 120ºC fibres obtained from this step were used for the next hemicellulose recovery step.

3.3.4. Extraction of hemicellulose

Hemicellulose is a heterogeneous branched polymer composed mainly by 5-carbon (C-5) sugars such as xylose, and arabinose and also 6-carbon (C-6) sugars as glucose, mannose and galactose. Composition of these sugars in hemicellulose vary according to each plant species (Vázquez et al., 2000)

In MxG, hemicellulose is formed mainly by a xylan backbone with arabinose ramifications and small amounts of galactose (El Hage et al., 2010b, Ligero et al., 2011). Other groups commonly connected to xylan and arabinan branches are uronic acid and acetyl groups (Le Ngoc Huyen et al., 2010, Ligero et al., 2011).

The hemicellulose fraction of the raw MxG used in this work was extracted using acid hydrolysis and quantified by HPAEC analysis. Total hemicellulose contents was 18.3% of dry biomass. Figure 3-5 shows the contents of hemicellulose fraction, in which xylan is the main component and accounts for 17.1% of the dry biomass weight, while arabinan and galactan

represent 1.0 and 0.2%, respectively. Mannose was not detected. Uronic acid and acetyl groups were not quantified.

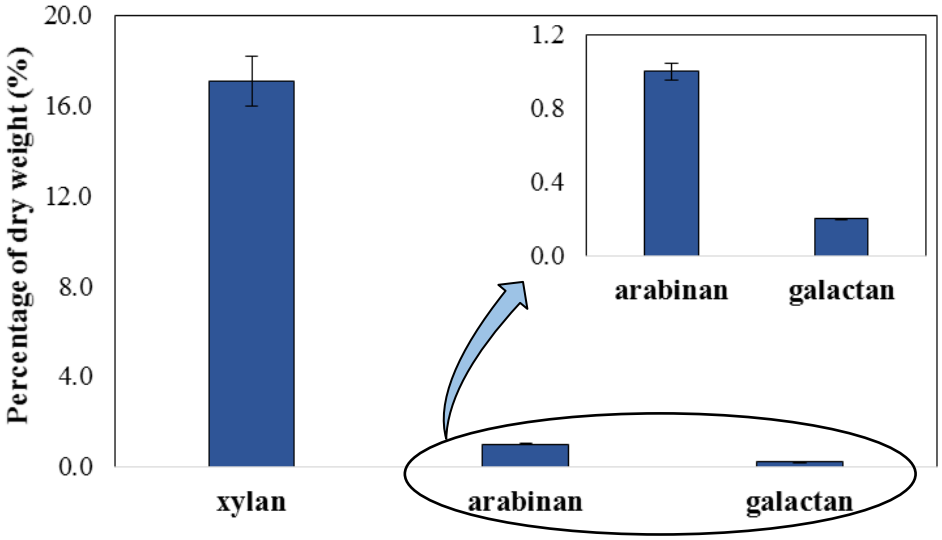

Figure 3-5 - Hemicellulose contents in MxG obtained by HPAEC analysis.

At this stage, extractives-free biomass (120ºC fibres) were processed for hemicellulose extraction as shown in Figure 3-6.

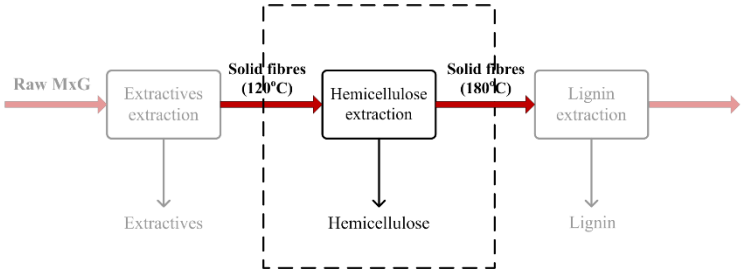

Figure 3-6 - Scheme of biomass processing in sequential extractions: removal of hemicellulose step.

Hemicellulose is easier to extract from lignocellulosic matrix than lignin and cellulose due to its amorphous and highly branched structure (Otieno and Ahring, 2012). The main challenge when extracting hemicellulose from lignocellulosic matrix is the yield of products of interest (XOS and xyloses) as undesirable products generated from the decomposition of xylose are very difficult to prevent. Temperature, reaction residence time and addition or not of an acid

catalyst and its concentration are the parameters considered keys to optimise hemicellulose extraction and increase efficiency of obtaining XOS and xylose (Otieno and Ahring, 2012).

3.3.4.1. Efficiency of extraction

All the efficiencies were calculated in percentage (wt%) based on the initial mass of xylan, arabinan and galactan available in MxG, as determined by 2-step acid hydrolysis followed by HPAEC analysis.

The procedure described for hemicellulose extraction was capable of solubilising 70.8±1.3% of the total xylan available. Percentages of arabinan and galactan solubilised were 80.2±1.9% and 79.5%±1.7%, respectively. Glucose was not detected at this condition, suggesting that cellulose remained intact, as expected. Figure 3-7 shows the percentage in mass of xylan in the fibres before and after hemicellulose extraction.

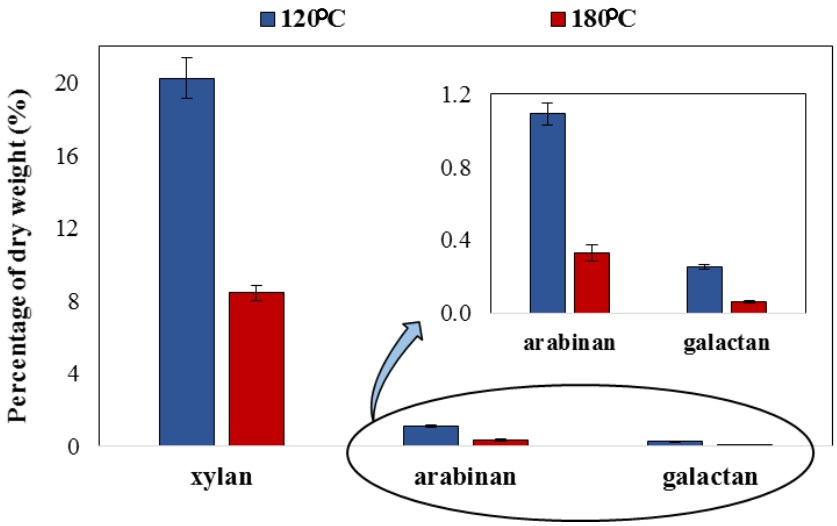

Figure 3-7 - Percentage of xylan, arabinan and galactan present in biomass before (120ºC fibres) and after (180ºC fibres) hemicellulose extraction.

There are some recent studies about XOS and xylose extraction from MxG reported in literature (Chen et al., 2014, El Hage et al., 2010b, Ligero et al., 2011) and in all of them,

evaluation of temperature and residence time is the key for optimisation of hemicellulose extraction and XOS/xylose production.

Chen et al. (2014) tried to optimise XOS extraction from MxG using a small batch reactor (20mL) using SBW from 160-200ºC for up to 70min. They reported that best xylan extractions reached about 79.5% at 200ºC for 5min. After 5min, produced XOS was quickly decomposed and it was completely degraded by 20min (Chen et al., 2014).

El Hage et al. (2010) evaluated MxG SBW hydrolysis using a 0.6L batch reactor in a range from 130-150ºC and very high residence times (up to 43h). They reported that from the initially available xylan they could achieve 54% extraction at 150ºC and 8h with only traces of furan generated. Also, 100% of arabinan was extracted in these conditions (El Hage et al., 2010b).

Ligero et al. (2011) achieved 65% of xylan extraction from MxG after SBW hydrolysis in a 0.1L batch reactor. They evaluated temperature from 160-200ºC and times up to 60min. The optimal condition in this range was at 160ºC for 60min (Ligero et al., 2011).

Therefore, results obtained at this step were comparable to the literature reports. Differences can be attributed to the feedstock itself (period of harvesting, age of harvesting, growth conditions) and extraction conditions (reactor size, heating time differences, etc.).

Fibres obtained after the 2-step sequential extraction (180ºC fibres), were delignified by the organosolv method.

3.3.4.2. Overview of hemicellulose extraction mechanism

There are two main reactions in hydrothermal conditions during hemicellulose depolymerisation: xylan degradation into XOS and xylose (Figure 3-8) and deacetylation (Garrote et al., 2001). These two reactions are catalysed by hydronium ions (H^+) generated from

water auto-ionization in subcritical water condition and acetic acid produced by deacetylation (Garrote et al., 2001). The generation of acetic acid in hydrothermal extraction increases availability of catalyst and therefore this process is called autohydrolysis. Because the acetic acid plays such an important role in this process, the natural feedstock ability of neutralisation, which depends on each feedstock, also affects hemicellulose disruption by autohydrolysis (Garrote et al., 2001). For instance, mineral salts present naturally in biomass can react with the hydronium ions, decreasing its availability as a catalyst (Parajo et al., 1995).

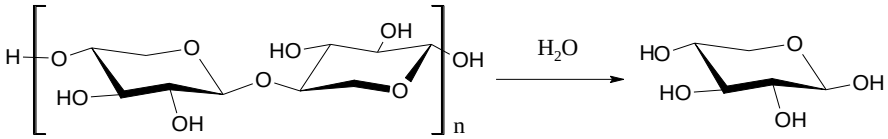

Hemicellulose Xylose

Figure 3-8 - Scheme of hemicellulose (xylan type) hydrolysis into xylose.

Vázquez (2005) proposed that biomass exposed to a first step of hydrothermal treatment for extractives removal would require more severe conditions at a second step for hemicellulose solubilisation. That would be due to partial deacetylation in the first step resulting in a decrease in acetic acid during hemicellulose extraction, which could lead to a decrease in autohydrolysis (Vázquez et al., 2005).

The kinetics of xylan depolymerisation are described as being in two different rates: a fast stage at the beginning followed by a slower stage, which decreases gradually (Chen et al., 2014, Garrote et al., 2001). Most authors also agree that arabinose and acetic acid attached to xylan backbone will be hydrolysed first as their lateral chains are more accessible and easily breakable compared to xylan linear bonds (Chen et al., 2014, Garrote et al., 2001, Nabarlatz et al., 2004).

Garrote et al. (2001) first suggested the existence of a fast reaction rate in a first stage, followed by a slow rate reaction. They theorised that the first and faster stage is due to rapid increase in concentration of hydronium ions due to increase in acetic acid production. The availability of hydronium ions to catalyse the cleavage was believed to be the limiting in the reaction rate at this stage. Furthermore, in a second stage, the factor limiting the reaction rate was suggested to be the substrate concentration as significant part of xylan has already been degraded and acetyl groups are less available (Garrote et al., 2001).

However, several authors believe that these two rate steps are a result of differences in xylan structure. In a first stage, a less resistant portion of xylan would react, followed by a decrease in reaction rate due to a more resistant portion (Nabarlatz et al., 2004, Otieno and Ahring, 2012). The resistance of xylan to cleavage could be due to the concentration of ramification as well as the molecular weight of hemicellulose fractions. Therefore, fractions of xylan containing lower molecular weight and higher levels of arabinan and acetic acid substitutions would break more easily (Chen et al., 2014). The degree of association between fractions of xylan to lignin and cellulose could also affect the resistance of different hemicellulose fractions (Nabarlatz et al., 2004).

The concept of xylan fractions with different reactivity is more widely accepted among the literature (Chen et al., 2014, Otieno and Ahring, 2012). Nabarlatz et al. (2004) studied autohydrolysis kinetics in corn and they hypothesized that about 81% of the xylan was very reactive and easy to break, while the 19% left was a more difficult to access and depolymerise. Moreover, they estimated that reactive part was formed of 78% of xylan in mass and 22% of arabinan and acetyl groups whereas in the less reactive fraction xylan accounted for 90% of the total mass and the ramifications were only 10% (Nabarlatz et al., 2004).

During hemicellulose extraction, fractions of xylan are broken into oligosaccharides of different DPs. Subsequently, these oligosaccharides are further degraded into lower DP and xylose units (El Hage et al., 2010b). Therefore, theoretically, xylose is not formed directly from xylan backbone, but instead it is exclusively a product of XOS depolymerisation (Nabarlatz et al., 2004). If not recovered from the liquid, xylose, galactose and arabinose can further decompose into degradation products such as furfural, HMF and organic acids.

One of the main decomposition product of xylose during hydrothermal extractions is furfural. As furfural is not a stable product under hot water, it will generate degradation products such as carboxylic acids and/or condensation products (Nabarlatz et al., 2004).

Xylose is degraded into furfural by dehydration as shown in the scheme in Figure 3-9 (Jing and Lü, 2007). Furfural can be generated from any C-5 sugar, therefore, arabinose units can also be a source of furfural during hemicellulose extraction from MxG.

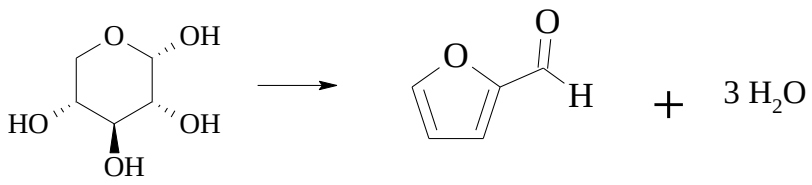

Figure 3-9 - Scheme of xylose dehydration to furfural.

The mechanism of xylose dehydration into furfural is still not completely understood. There are evidences in literature of mechanisms in which xylose undergoes to a ring opening before the dehydration, and others propose direct cyclic mechanisms in which the ring remains during the reaction (Ahmad et al., 1995, Rasmussen et al., 2014). This suggests that more than one mechanism might exist and it is not very clear whether or not there is a preferred route (Rasmussen et al., 2014).

Some authors have proposed that there is an intermediate species in the decomposition of xylose in water at high temperatures, although its detection has been a challenge (Aida et al., 2010). Aida et al. (2010) were able to detect xylulose and confirm that this is an intermediate of xylose decomposition (Aida et al., 2010). Moreover, formation of xylulose can be compared to the isomerisation between glucose and fructose (Paksung and Matsumura, 2015). However, the detection of xylulose was only possible at high temperatures (>300^{o}C), and, although xylulose presence in lower temperatures has been hypothesized, it has not been proved (Rasmussen et al., 2014).

Under hydrothermal treatment, furfural can further decompose into formic acid (Jing and Lü, 2007). The mechanism of furfural breakdown into formic acid, although not confirmed, is thought to be a hydrolytic break of furfural aldehyde group (Williams and Dunlop, 1948). Additionally, after decomposition of furfural into organic acids, gasification of these products into hydrogen and carbon monoxide is possible (Paksung and Matsumura, 2015).

Retro-aldol reaction (cleavage of C-C bonds) is also a possible route for xylose decomposition under sub- and supercritical water conditions (with or without the presence of catalyst (Sasaki et al., 2003b). Figure 3-10 shows the scheme of xylose decomposition by retro-aldol condensation in which glyceraldehyde and glycoaldehyde are the products.

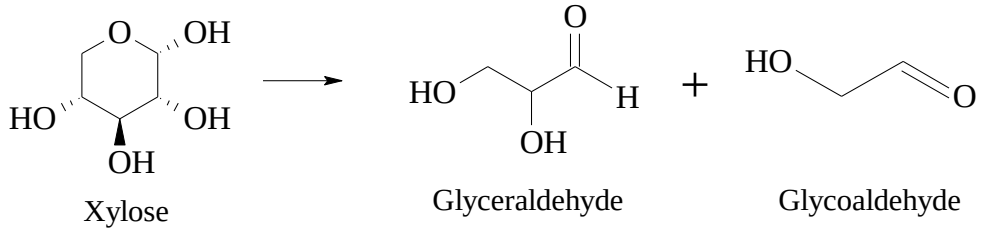

Figure 3-10 - Scheme of retro-aldol reaction of xylose to glyceraldehyde and glycolaldehyde.

Sasaki et al. (2003) studied xylose decomposition under sub- and supercritical water (360-420^{o}C) using a flow micro-reactor and very short residence times (0.02-1s). Their results

showed that the main reaction products under these conditions were glyceraldehyde and glycoaldehyde, while only traces of furfural were obtained. This suggested that at these high temperatures, xylose degradation by retro-aldol reaction is preferred compared to dehydration to furfural. In their study, they also proposed that glyceraldehyde can further decompose to dihydroxyacetone via keto-enol tautomerism (chemical equilibrium between a ketone and an enol) or dehydrate into pyruvaldehyde (Sasaki et al., 2003b). Pyruvaldehyde can then generate latic acid as shown in Figure 3-11 (Aida et al., 2010).

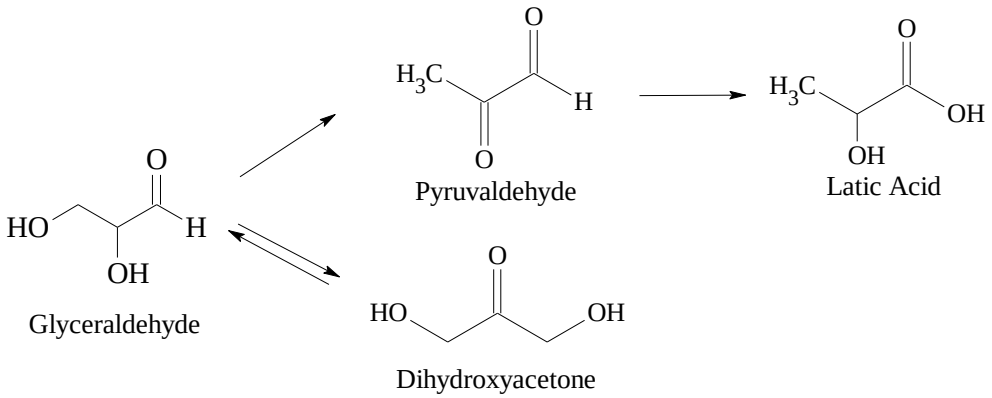

Figure 3-11 - Scheme of glyceraldehyde decomposition in sub- and supercritical water.

Jing and Lü (2007) evaluated xylose decomposition in water using a batch reactor at temperatures from 180-220ºC and reported that in this range no glyceraldehyde or glycoaldehyde was detected and furfural and formic acid were the main products. Therefore, they confirmed that dehydration is favoured compared to retro-aldol reaction at mild temperatures (Jing and Lü, 2007).

Glyceraldehyde and glycoaldehyde were not evaluated in this study, however, it can be concluded that their generation during hemicellulose extraction will be only minimal or absent at the temperature used for this step (180ºC). Therefore, it is expected that furfural and its decomposition products were the main compounds generated in this step.

3.3.5. Delignification by modified organosolv method

The use of organosolv treatments for lignin extraction (delignification) have been considered a good alternative for industrial processes and present advantages such as the use of more environment-friendly solvents and generation of sulphur-free lignin (Botello et al., 1999).

In summary, the organosolv method promotes the cleavage of hemicellulose (if still present) and lignin intra- and intermolecular linkages and generates products (XOS, xylose, low molecular lignin) that are soluble in water-organic solvents mixtures (Zhao et al., 2009a). In this work, a modified organosolv method was applied using CO_2 as modifier. Figure 3-12 shows the delignification step from the two processing routes proposed in this work.

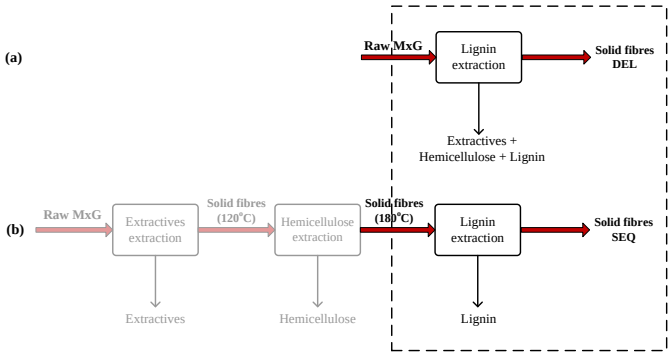

Figure 3-12 - Scheme of biomass processing in two routes: direct delignification (a) and sequential extraction followed by delignification (b): removal of lignin step.

3.3.5.1. Lignin contents in MxG

Klason lignin in the MxG used throughout this study represents 22.6± 0.7% of its dry weight. Lignin contents for *Miscanthus x giganteus* in the range from 18-28% have been reported in literature (Brosse et al., 2009, El Hage et al., 2010b, Le Ngoc Huyen et al., 2010, Lygin et al., 2011) and the value differences are attributed to several factors such as weather conditions, availability of nutrients during growth, harvesting period and age of the crop (Domon et al., 2013, Le Ngoc Huyen et al., 2010).

Acid soluble lignin (ASL) was not quantified in this study primarily because of the lack of an accurate method (Hatfield and Fukushima, 2005). Moreover, the choice for not quantifying ASL is also due to the fact that ASL is hardly recovered because of its high solubility and it accounts for very small percentage of *Miscanthus* dry weight (0.5-1.5%) (Brosse et al., 2009, El Hage et al., 2010b).

3.3.5.2. Overview of kinetics of lignin extraction during organosolv method

The kinetics of delignification are strongly dependent on the nature of the biomass, process conditions and lignin composition, for example, lignin is easier to extract in hardwoods than in softwoods, which might be due to different quantities of α- and β-aryl ether linkages, lignin contents and susceptibility to condensation reactions (McDonough, 1992).

The way lignin depolymerises is not entirely understood and two hypotheses have been presented, nevertheless in both of them it is consensual that the delignification reaction occurs in more than one phase (Shatalov and Pereira, 2005).

The first theory assumes one general type of lignin and two different phases: a faster initial stage in which lignin is mostly depolymerised following a pseudo-first order reaction; followed by a second slow stage in which lignin undergoes condensation reactions in a first-order model (Parajo et al., 1995). Vázquez et al. (1997) postulated that under organosolv process, lignin is extracted to a maximum percentage and then, if the reaction is not stopped, the condensation reaction will become predominant (Vázquez et al., 1997).

The second idea is more recent and widely accepted and theorizes about the existence of three kinds of lignin, named initial, bulk and residual lignin (Oliet et al., 2000, Zhao et al., 2009a). These three lignin types were proposed due to a possible decrease in reactivity during delignification observed by a deceleration of reaction rates in three steps (Shatalov and Pereira,

2005). Although physical differences leading to different lignin reactivity is not proved, some authors believe that initial lignin might correspond to the easiest extractable portion due to its structure, which would be of lower complexity compared to other portions, and due to its localisation at the middle lamella and cell corner, which is likely to be more accessible (Oliet et al., 2000). Residual lignin, on the other hand, is thought to be hardly extractable because of its highly cross-linked structure and its location in the cell wall (Oliet et al., 2000).

Assuming that lignin consists of the three described fractions (initial, bulk and residual), two kinetic models have been proposed: simultaneous reactions, in which all three fractions start to decompose since the beginning of reaction; and the most commonly used model of consecutive reactions, in which initial lignin reacts first, followed by bulk and residual lignin, respectively (Shatalov and Pereira, 2005). Moreover, the amount of each lignin portion and, thus, the rate of delignification, is closely dependent on the feedstock (Shatalov and Pereira, 2005).

3.3.5.3. Overview of mechanims of lignin extraction during organosolv method

The mechanisms and cleavage of lignin linkages are not well understood. Furthermore, mechanism differ significantly according to the extraction conditions (Santos et al., 2013). The aim of this section is to provide an overview of mechanism focusing on the conditions used in this work: presence of an organic solvent in mild acidic conditions.

The primary reaction of lignin depolymerisation in organosolv method under mild acidic condition is thought to be a solvolytic cleavage (reaction in which the solvent, in this work ethanol, is a reagent in excess) of the α-aryl ether linkages (Figure 3-13) (McDonough, 1992, Santos et al., 2013). Nevertheless, the cleavage of β-aryl ether bonds (Figure 3-13) becomes more and more important as the severity of processing conditions increase (McDonough, 1992).

Mild acid hydrolysis of both α- and β-aryl ether can generate vanillin and vanillic acid (Santos et al., 2013).

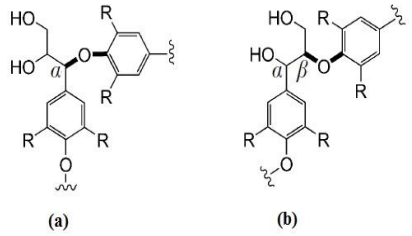

Figure 3-13 - α–(a) and β–(b) aryl ether linkages present in lignin structure Source: (Pandey and Kim, 2011)

Hemicellulose (and, in less extent, glucose) glycosidic linkages and lignin-carbohydrates ether, ester and glycoside bonds (Figure 3-14) are also broken during organosolv, particularly in acidic medium (Li et al., 2007, Sannigrahi and Ragauskas, 2013). El Hage et al. (2009) reported that ester linkages were hydrolysed in significant quantities when MxG was subjected to organosolv method (El Hage et al., 2009).

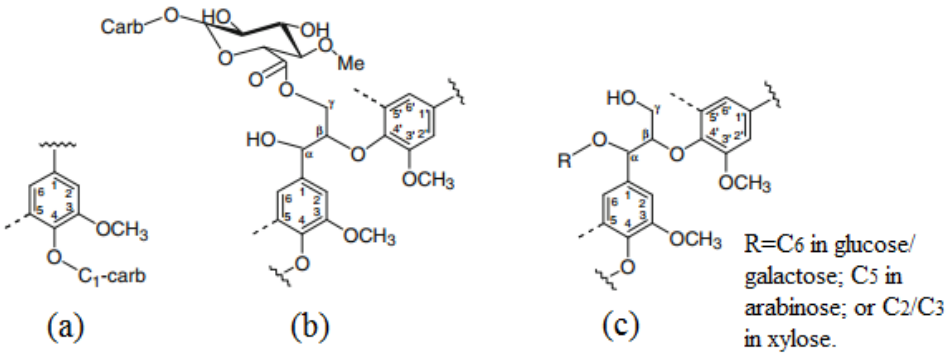

Figure 3-14 - Linkages presented in lignin-carbohydrate matrix commonly cleavage during ethanol organosolv method: (a) phenyl glycoside; (b) ester; and (c) benzyl ether. Source: modified from (Balakshin et al., 2011).

Condensation reactions (formation of C-C bonds) can also take place and reflect the treatment conditions. These condensations reactions form higher molecular weight compounds that are not soluble in water-ethanol and decrease the recovery of lignin (Sannigrahi and Ragauskas, 2013). Lignin re-polymerisation due to condensation reactions is believed to be a

result of the generation of carbonium ions (CH_5^+) during cleavage of α-aryl bonds (Li et al., 2007). Both inter- and intramolecular lignin condensation might occur during the organosolv method (McDonough, 1992).

3.3.5.4. Parameters affecting lignin extraction

Although several parameters can affect the extent of lignin extraction, two are believed to have the greatest influence on the process: 1) lignin composition; and 2) operation conditions (temperature, residence time, H^+ availability, etc.). How these two classes are thought to affect lignin extraction are detailed below.

1) Lignin composition

The efficiency of delignification by any method applied is closely related to biomass composition. For instance, the quantity of biomass extractives might have some influence on lignin extraction as higher quantities of extractives might increase the accessibility of lignin (Shatalov and Pereira, 2005).

However, it is the lignin composition, i.e., proportion of each of the three main structural elements presented in lignin: syringyl (S), guaiacyl (G) and p-hydroxyphenyl (H), that plays the key role in delignification processes (Timilsena et al., 2013). In general, guayacyl units are highly branched, which decrease accessibility to the linkages and, additionally, guayacyl is also believed to be related to increases in condensation reactions (Timilsena et al., 2013). Therefore, a high G/S ratio in biomass could represent a drawback in delignification.

Miscantthus x giganteus, as a grass, has high guayacyl contents (Timilsena et al., 2013). El Hage et al. (2009) presented one of the first guaycyl/syringyl/hydroxyphenyl quantifications for MxG reported in literature. Using NMR analysis, they proposed a ratio of 52/44/4 for G/S/H, respectively (El Hage et al., 2009).

2) Operational conditions

Although the increase of H^+ availability promotes greater delignification, highly acidic systems can lead to opposite effect, increasing condensation reactions (McDonough, 1992). The increase in other key parameters of lignin extraction such as residence time and temperature was also reported to have the same pattern: an increase in delignification until a maximum, followed by a decrease in efficiency due to lignin re-polymerisation (Li et al., 2007).

Figure 3-15 shows a schematic pattern for two possible reactions when lignin is treated under acidic conditions: 1) depolymerisation due to acid catalysed cleavage of α-aryl-ether bonds; and 2) acid catalysed condensation between the carbonium ion located in a side chain and the carbon (5 or 6) of aromatic rings (Li et al., 2007).

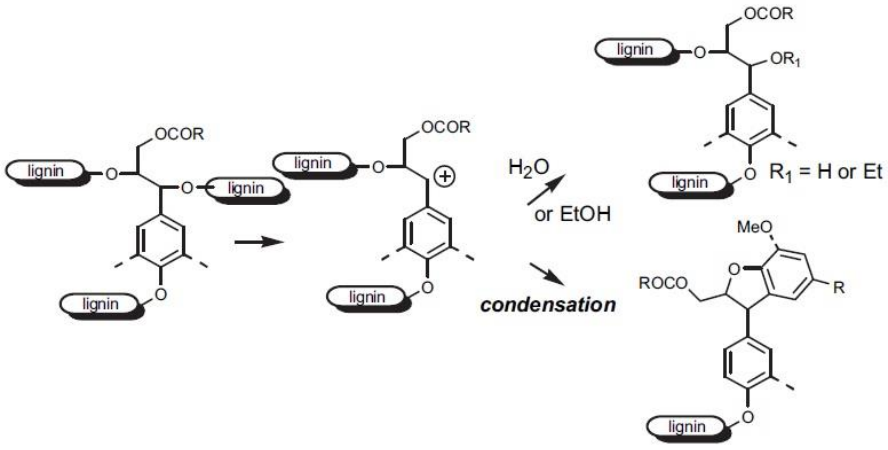

Figure 3-15 - Scheme of two possible paths when α-aryl lignin bonds are broken under acidic conditions: depolymerisation and condensation (re-polymerisation). Source: (El Hage et al., 2010a).

As it can be seen, the formation of carbonium ions is believed to be an intermediate specie of both depolymerisation and condensation reactions (Li et al., 2007, McDonough, 1992). Therefore, the conditions (pH, temperature, residence time) applied during lignin extraction conditions are decisive for the extraction products generated and, thus, need to be optimised in order to maximise lignin fragmentation as well as minimise its re-polymerisation.

In addition, the efficiency of organosolv treatment is not only related to the ability of accessing and cleaving lignin ether bonds and preventing lignin re-polymerisation, but also to the capability of solubilising lignin fragments in the aqueous phase (Xu et al., 2007).

Therefore, ethanol concentration in organosolv method is decisive for lignin extraction efficiency. Low ethanol concentration lead to higher availability of nucleophilic species, which are catalyst of lignin depolymerisation, however, high ethanol concentration will facilitate lignin fragments solubilisation (Pan et al., 2006). Roque (2013) evaluated ethanol concentrations from 0-70% in organosolv method for delignification of MxG using CO_2 as modifier. He proposed that 50% was the best condition to provide the highest delignification and solubilisation of lignin fragments (Roque, 2013).

Finally, the use of carbon dioxide generates an acidic medium as CO_2 reacts with water to form carbonic acid (Kim and Hong, 2001). However, even though water-CO_2 improves lignocellulosic bond cleavage, Lü et al. (2013) reported the need for the addition of an organic solvent to solubilise lignin fragment and improve overall treatment (Lü et al., 2013). Moreover, Pasquini et al. (2005) studied the effect of carbon dioxide pressure in the ethanol organosolv delignification of wood and sugar cane bagasse and concluded that the pressure has little influence on delignification (Pasquini et al., 2005).

Therefore, the synergy generated by water-ethanol-CO_2 makes this mixture is a complex solvent capable of generate an interesting medium of non-toxic, acidic and partially soluble system for lignocellulose bonds cleavage and lignin extraction (Lü et al., 2013).

3.3.5.5. Delignification of MxG

In this work, recovered fibres are the solid portion (not hydrolysed) after delignification step. Figure 3-16 shows the delignification and recovered fibres percentage (%) for the two

processing routes evaluated: direct delignification (DEL) and sequential extraction prior to delignification (SEQ).

In the beginning of this chapter, it was hypothesised that the sequential extraction of biomass extractives and hemicellulose could improve the lignin extraction in delignification step, compared to direct delignification, by leaving lignin more accessible due to the prior steps performed. Nevertheless, the results showed a different outcome: direct delignification resulted in the removal of 71.7% lignin present in MxG; whereas delignification after sequential extraction only removed 60.9% of the lignin presented in 180ºC fibres.

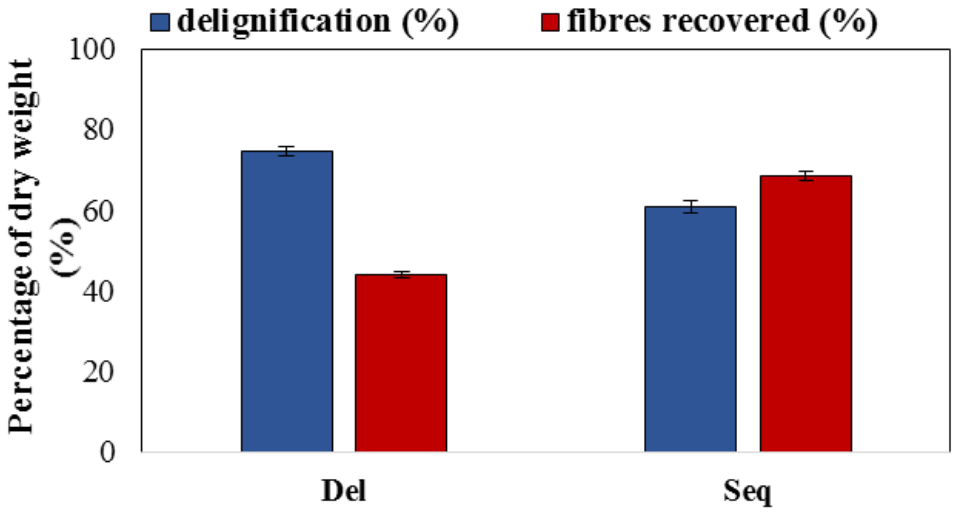

Figure 3-16 - Direct and Sequential delignification percentages and fibres recovering in MxG after processing method (n=3).

Table 3-2 shows the mass balance of lignin (in grams) for each route of extractions. It can be seen that delignification was more efficient in direct route in terms of percentage, but the mass of lignin extracted during the organosol method was similar for both direct and sequential routes.

Table 3-2 - Average of lignin mass balance for the two delignification routes (direct and sequential).

Fibres	initial lignin (g)	final lignin (g)	extracted lignin (g)
MxG	1.14 ± 0.02	0.28 ± 0.01	0.86 ± 0.02
180°C	1.44 ± 0.01	0.56 ± 0.01	0.88 ± 0.01

The percentage of recovered fibres, i.e., fraction that remained solid after delignification, was higher for the organosolv step in sequential extraction, as expected. In direct delignification, from 5g of initial MxG, 2.2g was remained as solid fibres (recovery =44.0%). In sequential extraction followed by delignification, from the 5g of 180ºC fibres, 3.4g is recovered as solid fibres (recovery=68.4%). This difference is due to the composition difference between the start materials. When using MxG in direct delignification, not only lignin is extracted in this step, but also hemicellulose and extractives. On the other hand, 180ºC fibres used for delignification after sequential extractions are already a lignin/cellulose-enriched fibre. Therefore, delignification step extracts mainly lignin and a residual fraction of hemicellulose that remained from previous steps.

The reasons why sequential extraction resulted in less percentage of lignin removal after delignification step when compared to direct delignification could be several, including carbohydrate degradation, increasing in condensation reactions, formation of pseudo-lignin, and/or re-precipitation of lignin into the remaining fibres. All these processes were described to happen in acidic ethanol organosolv method (El Hage et al., 2010a, Sannigrahi et al., 2011, Sannigrahi and Ragauskas, 2013, Xu et al., 2007) and they could contribute to decreasing in lignin removal efficiency in different degrees, depending on organosolv conditions applied. Each process is explained in more detail below.

1) Carbohydrate degradation

It has been suggested that autohydrolysis treatment prior to delignification would not only remove hemicellulose from biomass but also deconstruct lignin structure by breaking aryl-ether bonds, facilitating lignin fragmentation (El Hage et al., 2010b). However, several studies presented an increase in Klason lignin contents when biomass was subjected to autohydrolysis prior to organosolv method (El Hage et al., 2010a, Timilsena et al., 2013).

El Hage et al. (2010a) suggested that the increase in severity for ethanol organosolv in lignin extraction of MxG increased delignification until a maximum. From this point on, further increase in severity resulted in higher Klason lignin values. They attribute this increase to the degradation of carbohydrates due to the severity of the process, i.e., if glucose is being decomposed along with lignin (or even in a higher rate), lignin percentage calculated by Klason lignin will be higher (El Hage et al., 2010a).

Therefore, due to the extraction steps prior to delignification, it is possible that cellulose in 180ºC fibres might have become more susceptible to degradation compared to the intact cellulose presented in MxG used in direct delignification. Hence, the increase in Klason lignin could be due to glucose release during delignification. Moreover, glucose release in direct delignification is most likely insignificant as its accessibility should be hard because of the presence of hemicellulose and lignin.

2) Lignin condensation reactions.

The possibility of lignin condensation reactions could also be a reason for the increase in Klason lignin after sequential biomass processing. It is well documented that severe parameter condition could lead to re-polymerisation of lignin fragments (Sannigrahi and Ragauskas, 2013).

Vázquez et al. (1997) promoted lignin extraction of wood using acetone organosolv at temperatures up to 180ºC. They investigated the effect of HCl addition (0-0.2%) and observed a significant increase in condensation reactions when wood was treated with the highest HCl concentration tested (0.2% w/w) (Vázquez et al., 1997). El Hage et al. (2010a) also reported an increase in Klason lignin for more severe conditions after treating MxG with SBW followed by ethanol organosolv (El Hage et al., 2010a).

Sannigrahi and Ragauskas (2013) suggested that the presence of an electrophilic species could inhibit lignin condensation reactions after an autohydrolysis treatment. This species would react with the carbonium ions generated during lignin de-polymerisation and avoid condensation reactions (Sannigrahi and Ragauskas, 2013). Li et al. (2007) suggested the use of 2-naphtol as a 'carbonium ion scavenger'. Prior to wood chips steam treatment, they inserted the wood into an aqueous acetone solution containing about 4% (w/w) of 2-naphtol. Then, the modified wood was treated with steam in temperature ranging from 152-170^{o}C and times from 20min to 7h. They reported that 2-naphtol was capable of supressing lignin re-polymerisation by reacting with carbonium ions (Li et al., 2007). Similar results of inhibition of lignin condensation by using 2-naphtol during lignin extraction from MxG under ethanol organosolv methods were presented by Timilsena et al. (2013) and El Hage et al. (2010b) (El Hage et al., 2010b, Timilsena et al., 2013). However, 2-naphtol is extremely toxic and its use is a major drawback particularly in terms of post residues treatment and environmental issues.

3) Generation of pseudo-lignin

In addition to carbohydrate degradation and lignin re-polymerasation, another factor that might contribute to increase in Klason lignin is the generation of the compound called 'pseudo-lignin' (Sannigrahi et al., 2011). This compound is recognised to be formed mainly in steam explosion and diluted acid treatments, however, although no direct confirmation was reported, it is believed that pseudo-lignin could be generated in any low pH treatment (Sannigrahi et al., 2011).

Pseudo-lignin is described as being an aromatic compound having hydroxyl and carbonyl groups and generated exclusively by the condensation reactions of sugars dehydration products such as furfural and HMF (Rasmussen et al., 2014). Therefore, even though pseudo-lignin is not a lignin derivative compound, they are not solubilised in the 2-step acid hydrolysis

procedure to determine Klason lignin and, therefore, they will result in overestimation of lignin during lignin quantification analysis by Klason lignin procedure.

Sannigrahi et al. (2011) proposed a test to confirm that pseudo-lignin origins was solely from polysaccharides: they extract the holocellulose (hemicellulose+cellulose fraction) from hybrid poplar and processed this fraction using sulphuric acid at different temperatures and residence times. They attested that even after lignin had been extracted almost entirely (residual Klason lignin in holocellulose was 1.6%), Klason lignin contents increased after holocellulose acid treatment for most of the conditions used. Moreover, they observed that the Klason lignin increased as the severity of treatment applied increased (Sannigrahi et al., 2011).

Hu and Ragauskas (2014) were able to decrease the formation of pseudo-lignin using dimethyl sulphoxide (DMSO) during 2-step hydrothermal treatment of hydrid poplar under acidic conditions (H_2SO_4). The first step was performed at room temperature for 4h and 1% (w/w) acid; followed by a second step at 180ºC for 40min and 1% acid. They suggested that DMSO reacts with HMF in a preferred path, which avoids HMF condensation with other compounds to generate pseudo-lignin (Hu and Ragauskas, 2014).

Although it has been suggested that pseudo-lignin could affect cellulose digestibility by enzymes (Hu and Ragauskas, 2014, Kumar et al., 2013), whether or not cellulose accessibility and glycosidic bonds cleavage are reduced by the formation of pseudo-lignin in non-biological systems such as sub- and supercritical water, remains unclear.

4) Lignin re-precipitation

Lastly, even after de-polymerisation and solubilisation by ethanol organosolv method, lignin can re-precipitate onto the remaining fibres. The main cause of lignin re-deposition is the change in temperature and, therefore, in lignin solubility. When the organosolv reaction is

stopped by decreasing reactor temperature, lignin solubility in the system decreases, causing lignin to re-precipitate into the surface of the fibres (Xu et al., 2007).

Although some lignin re-precipitation is possible, it can be considered that the same extent of re-precipitation might have happened for both DEL and SEQ fibres. Therefore, lignin re-precipitation in the fibres do not account significantly when comparing direct and sequential delignification processes.

In conclusion, the sequential SBW treatment applied before delignification did not increase lignin removal when compared to direct delignification as first expected. Results observed open a range of opportunities for improvement. For instance, the modified ethanol organosolv method used in this work was optimised for raw MxG. However, it seems that the conditions applied were too severe for pre-processed fibres (180^{o}C fibres), leading to undesirable side reactions. Further investigation is needed to optimise this step in order to increase lignin de-polymerisation after a sequence of SBW treatments.

Nevertheless, the resultant fibres from sequential extraction (SEQ) still have the potential to present a more accessible cellulose due to the sequential treatment and, therefore, the potential to increase efficiency of glucose production.

Moreover, the streams of extractives, hemicellulose and lignin generated in the sequential extraction are more promising regarding to future application compared to the one stream (extractives+hemicellulose+lignin) generated in direct delignification. Although each extraction step performed in this work could be further optimised depending on the products of interest, it was demonstrated that SBW with no acid addition was efficient to extract MxG extractives entirely and presented a high hemicellulose extraction efficiency.

Finally, the use of a modified ethanol organosolv using CO_2 as catalyst instead of a mineral or organic acid also showed a great potential of delignification with values of lignin

extraction compared to results using H_2SO_4 or formic/acetic acid (Brosse et al., 2009, Vanderghem et al., 2012). Therefore, CO_2/water/ethanol organosolv method suggests a promising technique for lignin extraction from biomass.

3.3.6. Analysis of fibres composition

3.3.6.1. Klason lignin and carbohydrates 2-step acid hydrolysis

Klason lignin determination was performed on MxG and fibres after processing (120ºC, 180ºC, SEQ and DEL) for lignin quantification. In summary, this procedure consists of acid hydrolysing the carbohydrates (in 2-step acid hydrolysis) and weighing the remaining acid insoluble lignin (Klason lignin). Moreover, acid hydrolysed carbohydrates that were present in the fibres can be quantified by HPAEC.

One of the principles of Klason lignin is to hydrolyse all carbohydrates into their monomeric soluble forms, e.g., cellulose into glucose, xylan into xylose, etc. (Sluiter et al., 2008). Moreover, by quantifying the monomeric sugars in a sample, it is possible to calculate the polysaccharide concentration (cellulose, xylan, arabinan) in the solid sample. Figure 3-17 shows the chromatogram obtained by HPAEC after 2-step acid hydrolysis of MxG.

The presence of a significant amount of cello-oligosaccharide (COS) compounds can be seen in Figure 3-17. Moreover, no XOS were identified in samples after 2-step acid hydrolysis, which suggested that all xylan was converted into xylose. In addition, as arabinan and galactan presented in xylan backbone are branches and easily hydrolysed (Otieno and Ahring, 2012), it was assumed that they were 100% hydrolysed into arabinose and galactose. Therefore, these three sugars were easily quantified in all fibres.

Peaks named I_1 and I_2 in Figure 3-17 were not identified by standards. However, their position right in between the other identified oligosaccharides (cellobiose (C_2), cellotetraose

(C_4) and cellohexaose (C_6)) suggests I_1 and I_2 to be cellotriose and cellopentose, respectively. Moreover, the fact that no XOS were identified in the samples after 2-step acid hydrolysis also indicates that I_1 and I_2 are probably cellulose derived, confirming the hypothesis of these peaks to be cellotriose and cellopentose.

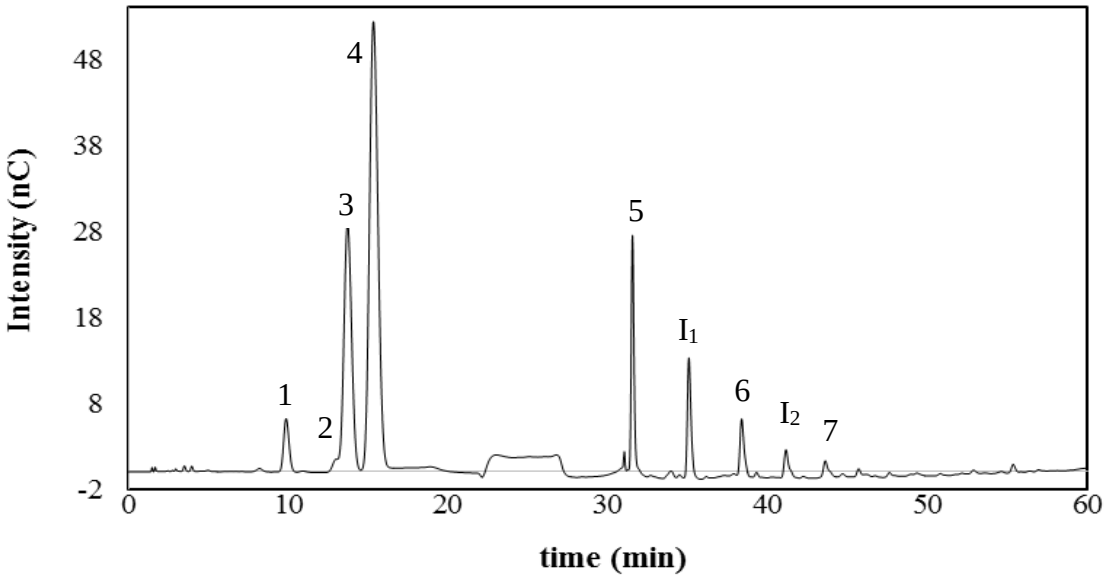

Figure 3-17 - Chromatogram of MxG (raw Misc) after 2-step acid hydrolysis by HPAEC. (1-arabinose; 2-galactose; 3-glucose; 4-xylose; 5-cellobiose; 6-cellotetraose; and 7-cellohexaose. I_1 and I_2 are suggested to be cellotriose and cellopentose, respectively).

The change in baseline that can be observed between 20-30min is due to the introduction of sodium acetate in the elution method.

As a result of the high contents of cello-oligosaccharides present after 2-step acid hydrolysis, cellulose could not be quantified properly in MxG. Nevertheless, after processing MxG, it can be assumed that only cellulose, lignin and hemicellulose are presented in the remaining fibres. Therefore, for 120ºC, 180ºC, SEQ and DEL fibres, cellulose can be quantified by difference: cellulose (%) = 100 – lignin (%) – hemicellulose (%), in which hemicellulose is the sum of xylan, arabinan and galactan.

Throughout this work, it was also assumed that even though cellulose was not entirely hydrolysed, it did not affect results of Klason lignin quantification. Figure 3-17 shows that COS with high DP were present in very small amounts. Therefore, even in the unlikely possibility of a portion of insoluble COS of high DP is still intact, which could account for Klason lignin, this portion can be considered insignificant.

3.3.6.2. Lignin and xylan contents in fibres after processing of MxG

Figure 3-18 shows the percentage of Klason lignin and xylan in MxG, in remaining fibres after direct delignification (DEL), as well as in the fibres after each of the three steps for sequential extraction: extraction of biomass extractives (120^{o}C), hemicellulose extraction (180^{o}C), and delignification after sequential extractions (SEQ). Klason lignin values were quantified by Klason lignin procedure, while xylan was quantified by HPAEC after 2-step acid hydrolysis.

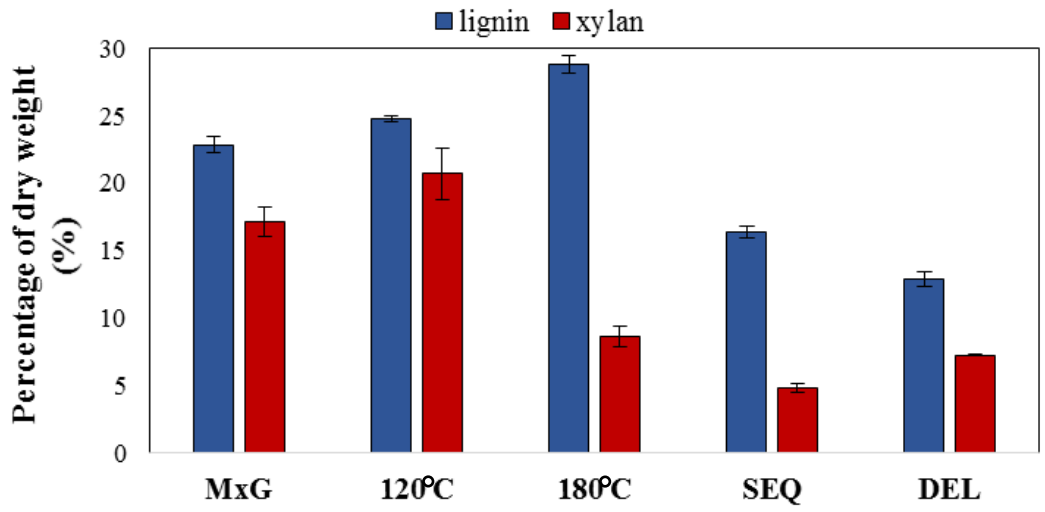

Figure 3-18 - Percentage of Klason lignin and xylan (%) in MxG and after processing steps (n=3).

After the delignification step, lignin percentage decreased significantly. Moreover, there was also a decrease in hemicellulose contents in this step. Therefore, not only lignin is extracted

in the modified organosolv method as some hemicellulose is also hydrolysed during this procedure.

Lignin and xylan contents increased in percentage of dry matter in 120ºC fibres compared to MxG because of the extraction of extractives.

After hemicellulose removal at 180ºC, fibres presented higher Klason lignin contents. As lignin and cellulose contents are the same, in grams, before and after hemicellulose removal, if assumed that no lignin and cellulose extraction took place in this step, the increase in Klason lignin percentage is due the decrease in hemicellulose contents. Lignin and cellulose contents in 180ºC fibres were calculated as 28.9 and 62.5%, respectively. Therefore, the result of this step is an enriched cellulose and lignin fibre resulting from decreasing hemicellulose percentage from 20.7 to 8.6%.

3.3.6.3. Mass Balance

DEL fibres obtained after ethanol organosolv contained 7.2% hemicellulose, 12.9% lignin and 79.9% cellulose, whereas fibres obtained from sequential delignification (SEQ) contained 4.8% hemicellulose, 16.3% lignin and 78.9% cellulose. Cellulose quantification by HPAEC was not possible due to incomplete acid-hydrolysis. Therefore, cellulose values for DEL and SEQ were calculated by difference as these fibres are composed only by lignin, hemicellulose and cellulose. No arabinan or galactan were identified after organosolv treatment either in DEL or in SEQ fibres. Therefore, the resultant fibres from the two processing routes proposed, SEQ and DEL, presented a reasonably similar composition and the MxG processing was successful in producing cellulose-enriched fibres when compared to the raw material. Table 3-3 shows lignin/hemicellulose and total mass balance for the direct and sequential extractions from an initial mass of 10g of MxG.

Table 3-3 - Mass balance for direct and sequential extraction of MxG to produce cellulose-enriched fibres (DEL and SEQ).

Route	Fraction	MxG m_i (g)	120°C m_f (g)	180°C m_f (g)	Delignification m_f (g)
Direct	MxG	10.00	-	-	4.40
	Lignin	2.00	-	-	0.57
	Hemicellulose	1.67	-	-	0.32
	Loss (%)	-	-	-	7.8
Sequential	MxG	10.00	7.71	6.00	4.02
	Lignin	2.00	1.91	1.73	0.66
	Hemicellulose	1.67	1.57	0.53	0.19
	Loss (%)	-	2.5	4.5	8.0

The fibres and compositions obtained in this work are in agreement with other published studies using SBW/ethanol organosolv extractions in MxG. Timilsena et al. (2013) reported comparable results for MxG after a similar sequential extraction using SBW (150ºC for 8h) followed by ethanol organosolv method (ethanol:water 8:2 + 0.5% w/w H_2SO_4 at 170ºC for 60min). In their study, the solid fibres after the sequential treatment presented mainly glucose (76.6%), lignin (17.3%) and residual xylan (5.8%) and only traces of other sugars such as arabinose and galactose (Timilsena et al., 2013).

El Hage et al. (2010) presented fibres containing 14.1% of Klason lignin after treating MxG with ethanol/water (8:2) organosolv acid catalysed by 0.5% sulphuric acid at 170ºC for 60min (El Hage et al., 2010b).

Physical analysis of DEL and SEQ cellulose-enriched fibres are presented and discussed in the following sections.

3.3.7. Impact of direct and sequential extraction on cellulose fibres

The direct and sequential extraction performed in this work aimed not only to recover lignocellulosic components (extractives, hemicellulose, lignin), but also to obtain cellulose enriched fibres and modify the structure of the cellulose in order to make it more accessible to

hydrolysis. Lignin extraction methods, for instance, are thought to create pores in the lignocellulosic matrix, facilitating cellulose disruption (Santos et al., 2013).

Composition analysis of SEQ and DEL fibres through Klason lignin determination and HPAEC did not show significant differences between these fibres. However, whether or not the fibres are physically different and as a result impact on the efficiency of SBW mediated hydrolysis of cellulose into conversion of cellulose into glucose remains unclear. Therefore, in order to try to characterize the fibres obtained from MxG processing via the two proposed routes (direct and sequential extraction), two physical analysis were performed: scanning electron microscope (SEM) and Fourier transform infrared spectroscopy (FTIR).

3.3.7.1. Scanning electron microscopy of cellulose fibres

Scanning electron microscopy (SEM) is a tool that can be used to generate images of lignocellulosic biomass surface and help understanding biomass physical characteristics. For comparison reasons, commercial cellulose (Avicel) was analysed as a standard cellulose fibre and compared to DEL and SEQ fibres. Figure 3-19 shows SEM images for Avicel, DEL and SEQ fibres.

Figure 3-19-a,c,e shows that Avicel fibres have a diameter of about 20μm. DEL and SEQ fibres, on the other hand, have significantly larger fibre diameters of about 150μm and 100μm, respectively. Several other images were taken to assure that images in Figure 3-19 representative, however, they are not shown.

Comparing Avicel to DEL and SEQ fibres, it can be noticed that Avicel presents a smoother surface. Moreover, the horizontal pattern of fibres observed in both SEQ and DEL is not detected in Avicel fibres, suggesting that the pure cellulose has differences in structure compared to cellulose in lignocellulosic biomass.

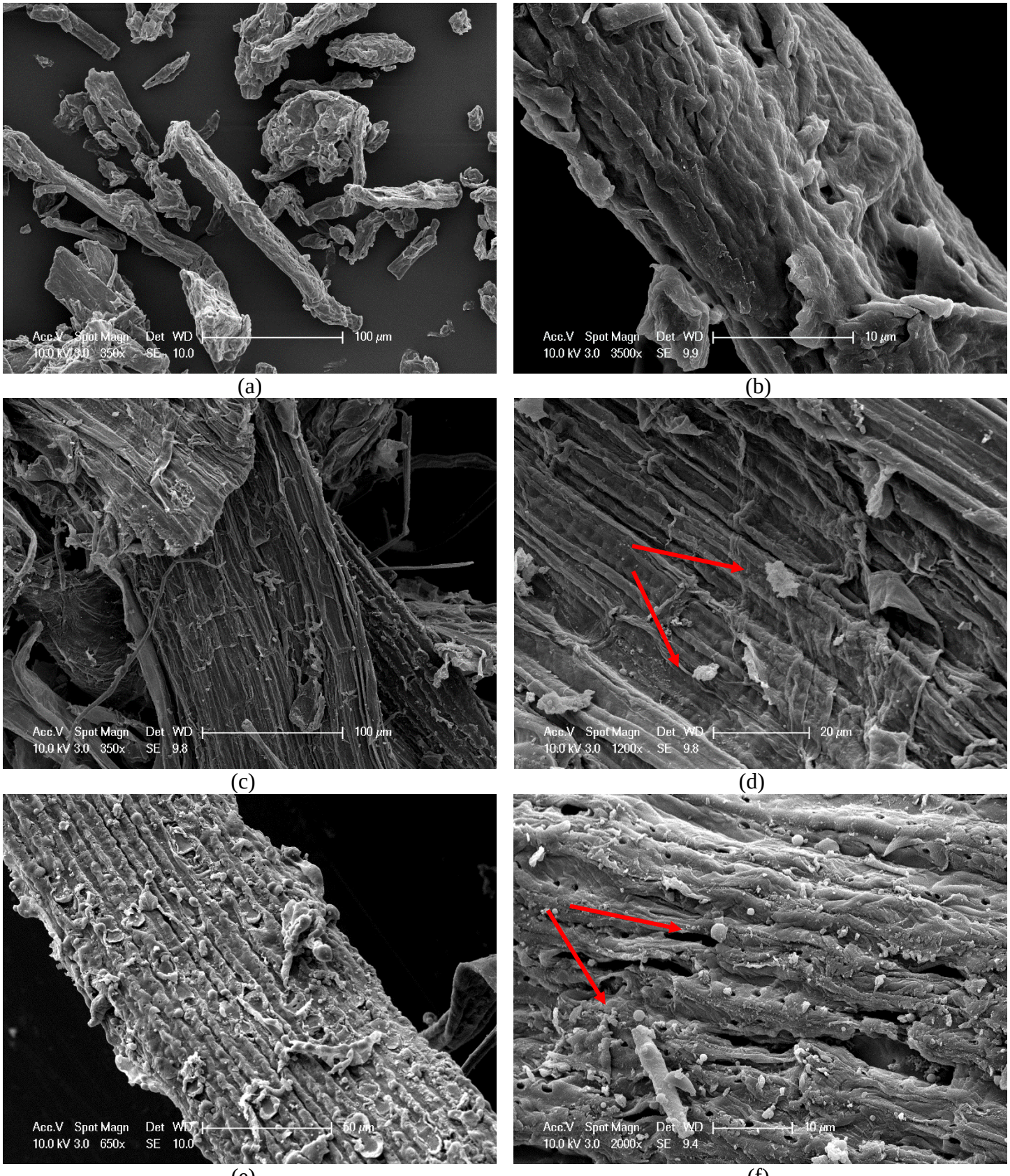

Figure 3-19 - SEM images for cellulose fibres of: Avicel (a-b); DEL (c-d); and SEQ (e-f). Images magnification: (a) 350x, (b) 3500x, (c) 350x, (d) 1200x, (e) 650x, and (f) 2000x.

Figure 3-19-b,d,f shows a magnified image of the fibres in which it is possible to observe lignin particles in DEL (d) and SEQ (e) as they stand out as little droplets in the fibres surface (Donohoe et al., 2008).

Figure 3-20 shows a closer image of the lignin droplets in DEL (a) and SEQ (b) fibres. It is very clear that the lignin particles are substantially different between these two fibres. In terms of surface, lignin droplets in SEQ fibres are smoother than in DEL fibres. It seems that lignin in DEL fibres is a result of several small particles agglomerated together in an elongated shape.

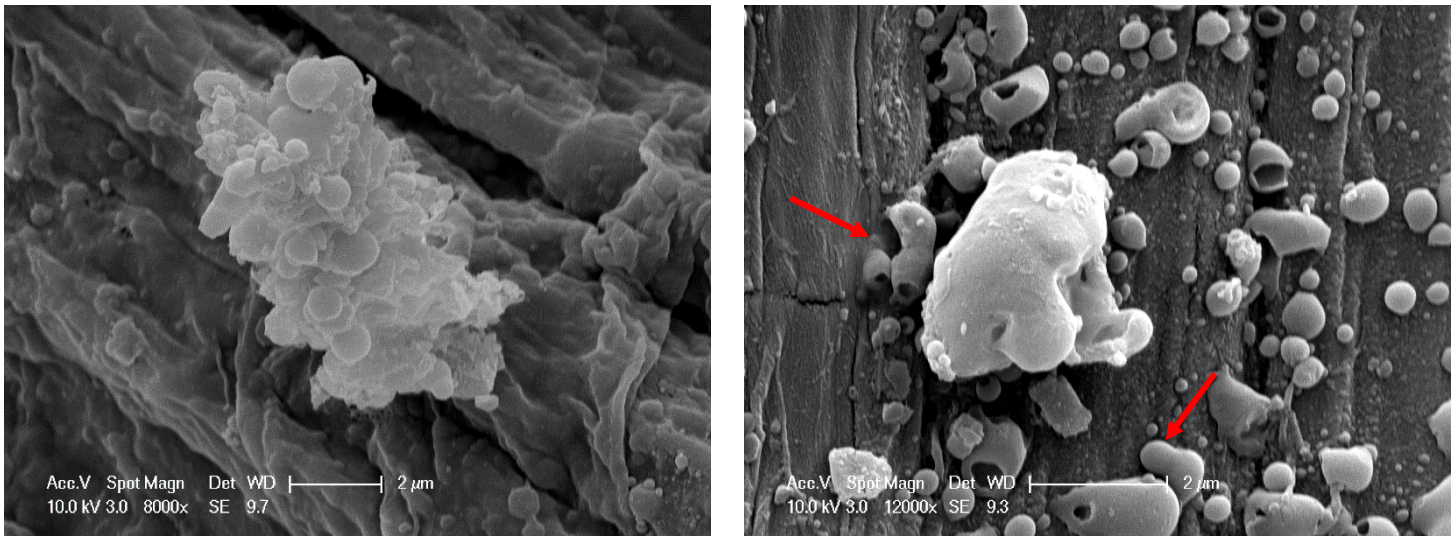

(a) (b)

Figure 3-20 - SEM imagines of lignin droplets present in DEL (a) and SEQ (b) fibres using magnifications of 8000x and 12000x, respectively.

On the other hand, lignin droplets in SEQ fibres look like a single spherical shaped particle. These lignin droplets are significantly different in size as well: lignin droplet in DEL fibres are at least 3 times larger in length compared to those in SEQ fibres. In addition to the shape and size difference, the quantity of droplets seems to be much higher for SEQ compared to DEL fibres.

Xiao at al. (2011) evaluated the lignin droplets produced after SBW treatment of wood from 140-200ºC and observed that the density of lignin droplets onto cellulose fibres surface increased with the increase in temperature (Xiao et al., 2011). This result is similar to what observed for *Miscanthus* fibres as SEQ fibres was treated in harsher conditions as a result of sequential treatment and this led to a higher density of lignin droplets compared to DEL fibres.

Donohoe et al. (2008) studied the lignin drops generated after treating corn stover with dilute acid (0.8% H_2SO_4) at 150ºC for 20min. The structure presented in their SEM images resembles the lignin of SEQ fibres (Figure 3-20-b) as most of the droplets were spherical shaped and presented a flat surface and large size variability. They also notice a 'fusion' of small droplets as highlighted by the arrows in Figure 3-20-b, which might as well be a result of droplets fragmentation. Although they did not observe elongated particles as shown in Figure 3-20-a, they detected particles with rough surface and attributed this structure as being due to carbohydrate shells and, therefore, these structures could be non-disrupted lignin-carbohydrate complexes (Donohoe et al., 2008).

Therefore, although SEQ fibres present a larger amount of lignin droplets, their shape and size could indicate that the lignin has been more extensively fragmented when comparing with lignin presented in DEL fibres. Hence, in theory, cellulose from SEQ fibres are potentially more exposed than in DEL fibres.

3.3.7.2. FTIR analysis

Infrared spectroscopy is commonly used for structural analysis of lignocellulosic biomass particularly because of its simplicity in sample preparation, fast analysis, and the possibility of investigating more than one compound at time using the same spectra (Xu et al., 2013a).

Figure 3-21 shows the spectra obtained by FTIR of Avicel, DEL and SEQ fibres. Avicel stands out from the other two mostly due to higher intensity peaks as apart from few exceptions (peak at 1510cm^{-1}, for instance), most of the peaks are presented in the spectra of all three fibres.

Cellulose and hemicellulose may present a peak around 1160cm^{-1} due to C-O-C stretching and at about 1310cm^{-1} due to CH_2 wagging, i.e., out of plane vibration (Adel et al., 2010, Liu and Chen, 2006). These peaks can be seen in all three spectra. Both cellulose and hemicellulose also present peaks at 1200cm^{-1} due to O-H bending (Hulleman et al., 1994) and peaks at 1030cm^{-1} also addressed to C-O-C bonds (Sun et al., 2007). The peak at about 1055cm^{-1} is related to vibration of C-O-C in pyranose ring (Lan et al., 2011). Symmetric glycosidic stretch and/or ring stretching (C-O-C) is seen at 1100cm^{-1} (Bessadok et al., 2007).

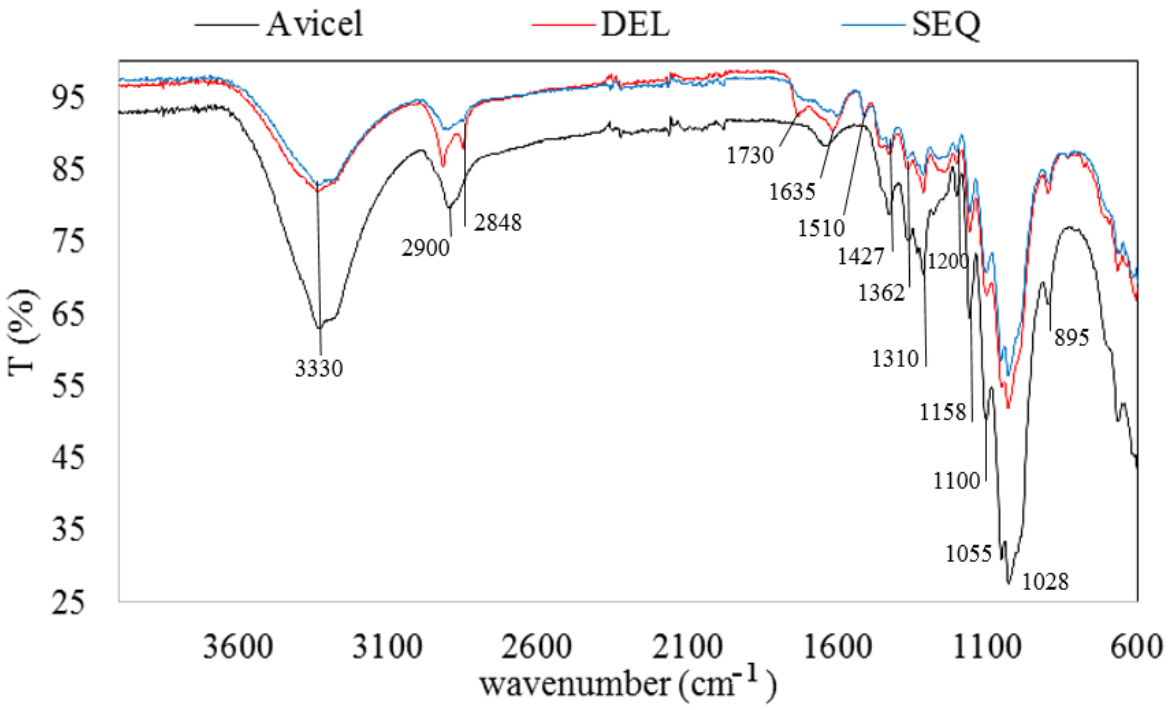

Figure 3-21 - FTIR spectra of Avicel, DEL and SEQ fibres

Cellulose fibres present peaks at 1360cm^{-1} due to OH deformation of alcohol groups (Bessadok et al., 2007). C-H stretching is presented at about 2900cm^{-1} (Adel et al., 2010) and C-

H_2 is presented at 2850cm^{-1} (Bessadok et al., 2007) and it is interesting to notice that pure cellulose (Avicel) only presents the first. Characteristic peaks presented in cellulose due to crystalline and amorphous structures are 1427 and 895cm^{-1}, respectively (Nelson and O'Connor, 1964) and they can be seen in all three fibres.

Peak at about 1730cm^{-1} are assigned to carboxyl presented in uronic acid and ester in hemicellulose or to hemicellulose-lignin complexes (Adel et al., 2010, Peng et al., 2009). DEL fibres present a more pronounced peak while SEQ fibres shows only a shoulder at this band. That could be related to the higher xylan quantity presented in DEL fibres (7.2%) compared to SEQ fibres (4.8%). Avicel has no peaks in this region.

Lignin presents several unique peaks such as at 1330 and 1263cm^{-1} that are due to syringyl and guaiacyl respectively (Villaverde et al., 2009). Figure 3-21 shows that none of these peaks is presented in any of the spectra.

One of the most characteristic peaks presented in lignin is at 1510cm^{-1}, due to aromatic skeletal vibration, and it is suggested that this peak can be used for lignin quantification as this peak appears exclusively for lignin (Barnette et al., 2012). This peak is presented in both DEL and SEQ at almost the same low intensity. Moreover, this peak is completely absent in Avicel, as expected.

Absorbance between 4000 and 3000cm^{-1} is thought to be due to stretching vibration of intramolecular hydrogen bonds (Bessadok et al., 2007, Lan et al., 2011). Hydrogen bonds due to absorbed water appears at 1635cm^{-1} (Lan et al., 2011).

The difficulty of using FTIR in analysis of lignocellulosic biomass is the overlapping of peaks due to different linkages. For instance, the absorbance at 1427cm^{-1} is due to not only cellulose C-H bonds, but also appears in lignin and hemicellulose (xylan) structures (Barnette et al., 2012). The peak around 1035cm^{-1} is due to C-O, C=C and C-O-C and it is presented in

cellulose, lignin and hemicellulose (Sills and Gossett, 2012). Moreover, it can also be rather difficult to differentiate which peaks are due to cellulose or hemicellulose as these polymers present similar linkages such as β-glycosidic which appears at 895cm^{-1} (Kačuráková et al., 2000).

In conclusion, the FTIR is a fast analysis and can indicate some differences among the spectra of the different fibres. However, for a deeper comprehension of the significance of the physical differences presented by the FTIR results, a more complete analysis must be implemented. Therefore, in order to analyse the cellulose crystallinity/amorphous structure and PCA was performed and results are presented in the next sections.

3.3.7.3. Cellulose crystallinity and Crystallinity Index (CI)

Cellulose is a well-organized polymer composed of crystalline and amorphous (less-organized) portions. Although it is well accepted that amorphous regions of cellulose are more susceptible to hydrolysis (Zhao et al., 2012), the relation between degree of crystallinity and cellulose hydrolysis is still not well-understood (Hu and Ragauskas, 2012).

The IR crystallinity index (CI) of cellulose is a measurement that indicates crystalline portion related to the amorphous portion in a cellulosic sample and can be empirically calculated by the ratio of IR absorptions at 1427cm^{-1} (A_{1427}) and 895cm^{-1} (A_{895}) (Kataoka and Kondo, 1998). A_{1427} is addressed to C-H_2 scissoring motion (Nelson and O'Connor, 1964) and A_{895} is related to β-glycosidic linkage (Kačuráková et al., 2000) and they correspond to the crystalline and amorphous portions in cellulose structure (Nelson and O'Connor, 1964).

Figure 3-22 shows the CI values calculated by A_{1427}/A_{895} for Avicel, MxG, 120ºC, 180ºC, DEL and SEQ fibres. CI values calculated for Avicel and MxG were very similar, even though they are very different materials in terms of composition (Avicel is pure microcrystalline cellulose) and particle size. The results led to questions related the validity of the technique and

suggest that it might not be accurate for lignocellulose biomass because of the interferences caused by other components present in the matrix along with cellulose (Barnette et al., 2012).

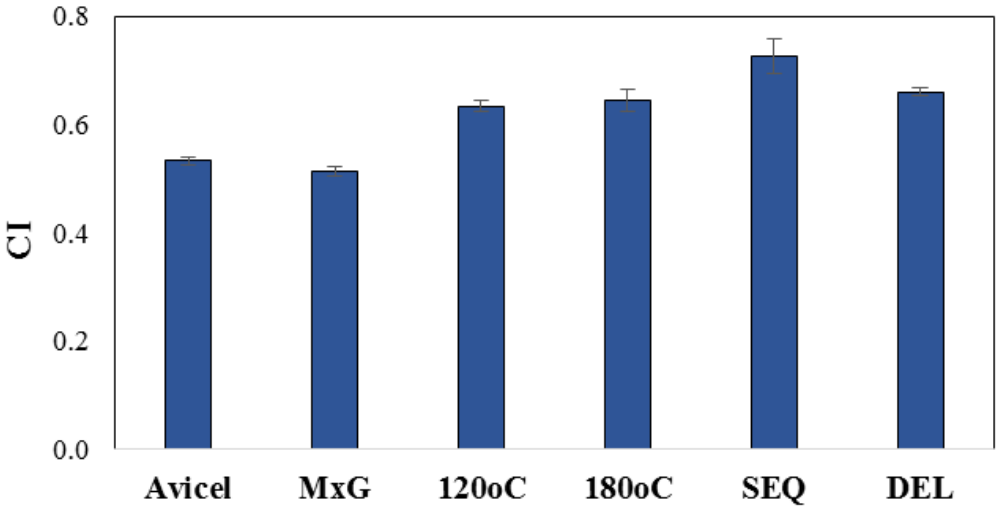

Figure 3-22 - Crystallinity index (CI) values calculated by FTIR absorbance (A_{1427}/A_{895}) for Avicel, MxG, DEL and SEQ fibres (n=3).

Barnette et al. (2012) suggested that for pure cellulose (commercial), calculation of CI through the ratio of A_{1427} and A_{895} has a good correlation with other methods used to evaluate crystallinity in cellulose, X-ray diffraction for instance. However, complex lignocellulosic structure might present inaccurate results due to overlapping of the peak 1427cm^{-1} that is also presented in lignin and hemicellulose/xylan spectra (Barnette et al., 2012). Moreover, the peak at 895cm^{-1} can be due to β-glycosidic linkages between glucose or also between xylan units (Kačuráková et al., 2000). Additionally, the particle size may also affect the intensity of absorbance, making comparisons among different samples challenging (Zhao et al., 2012).

However Figure 3-22 shows that the CI of MxG increased after treatment. Moreover, for SEQ fibres, each treatment stage led to a further increase in CI values, resulting in higher CI than DEL fibres presented. As CI is, by definition, the ratio between the crystalline and the amorphous portions of a sample, the treatments increased CI values not because of an increase in crystalline

portion, but as a result of a decrease in amorphous polymers quantities. Therefore, it is theorized that the increase in CI values after treatments is most likely due to the extraction of non-crystalline compounds as hemicellulose and lignin (Kim and Holtzapple, 2006).

Kim and Holtzapple (2006) demonstrated that the degree of crystallinity in pulp from corn stover measured by X-ray diffraction increased from 43 to 60% after delignification using calcium hydroxide using temperatures from 35-55^{o}C for up to 16 weeks of treatment (Kim and Holtzapple, 2006).

Haverty et al. (2012) treated MxG with H_2O_2 (2.5-7.5%) + formic acid + NaOH. They calculated CI for raw MxG and pulp after H_2O_2 treatment by X-ray diffraction and CI values were in the range from 0.81-0.86. However, although CI did not change significantly after the treatment, they reported glucose release during enzymatic hydrolysis to be 20 times higher for treated MxG compared to raw MxG (Haverty et al., 2012). Moreover, several treatments such as alkaline and acids can lead to an increase in crystallinity in biomass due to extraction of amorphous fractions (Vandenbrink et al., 2011).

Furthermore, the studies that evaluate the relation between crystallinity and hydrolysis often decrease cellulose crystallinity by applying a physical (ball milling) or chemical (acid, alkaline) treatment and compare the results of digestibility with crystalline cellulose. However, in addition to the decrease of cellulose CI, these treatments result in a significant decrease in particle size and, consequently, in an increase in surface area. Therefore, the increase in digestibility observed by some authors (Zhao et al., 2006) is presumably not only due to decrease in CI but also due to other modifications achieved by the treatment such as decreasing in DP and increasing in surface area, which are often not elucidated (Zhao et al., 2012). Consequently, an increase in crystallinity does not necessarily means a decrease in digestibility and vice-versa (Taherzadeh and Karimi, 2008).

Moreover, although CI calculated by IR data can give some information about the samples, the use of this technique in complex lignocellulosic biomass is challenging (Barnette et al., 2012). Oh et al. (2005) demonstrated a good correlation between CI values obtained by X-ray diffraction and by IR absorbance bands (A_{1427}/A_{895}). However, in their study only commercial cellulose was evaluated (Oh et al., 2005). On the other hand, Stevulova et al. (2014) reported significant values difference between CI for hemp hurds calculated by X-ray and IR (Stevulova et al., 2014).

Therefore, other analytical techniques that allow the level of crystalline/amorphous cellulose structure to be determined such as NMR and X-ray diffraction might be preferred for lignocellulosic biomass due to less interference (Kim et al., 2013). Moreover, calculation of CI from IR data was usable to understand differences caused by the treatments in MxG and compare the fibres obtained, however, CI as a value is most likely not enough to explain cellulose digestibility in complex lignocellulosic structures and should not be seen as an independent factor (Viikari et al., 2012, Zhao et al., 2012).

3.3.7.4. FTIR data analysed by Principal Component Analysis (PCA)

Although the FTIR analysis and CI calculation can give an insight about cellulose fibres produced by the performed treatment, it is hard to obtain results from these analysis that clearly differentiate DEL and SEQ fibres in physical terms.

Therefore, in order to try to establish a better better understanding of the physical characteristics of MxG and the potential for change during treatment, the FTIR data was analysed by applying principal component analysis (PCA) using the Unscrambler X version 10.3 software (CAMO).

The FTIR data used for PCA analysis consisted of five biological replicates of each fibre: 120ºC, 180ºC, DEL, SEQ and Avicel (AV). The range of wavenumbers analysed was from 600 to 4000cm^{-1}, resulting in 1764 wavenumber (variables) for each spectrum.

3.3.7.5. FTIR data Manipulation

Several data manipulations such as smoothing, normalisation and 2nd-derivative are used prior to PCA in order to decrease noise/increase resolution (Hori and Sugiyama, 2003, Michell, 1990, Xu et al., 2013a). However, there is no consensus about which tool/tools would work best for all cases of FTIR data. Therefore, with the purpose of evaluate which manipulations of FTIR data would increase the resolution of spectra and lead to an easier interpretation of the data, smoothing, normalisation and 2nd-derivative were performed in different sequences and analysed one by one in order to select the one which suits the most the FTIR data in this work.

Table 3-4 shows the sequences of data manipulation applied to FTIR data prior to PCA.

Table 3-4 - FTIR data manipulation performed in samples spectra prior to PCA.

Manipulation	**1st**	**2nd**	**3rd**
M1	smoothing	-	-
M2	smoothing	normalisation	-
M3	smoothing	2nd-derivative	-
M4	smoothing	2nd-derivative	normalisation

3.3.7.6. Data manipulations M1 and M2 - Smoothing and normalisation

3.3.7.6.1. Scores plot

The scores plots of PCA present the samples grouped by their variability. The differences among the samples presented in the scores plot are thought to be chemical (composition) and/or structural (Kline et al., 2010), therefore, samples in the same cluster present similar features among them.

Figure 3-23 shows the scores plots for PC1 and PC2 after applying only smoothing (M1) (a) and smoothing followed by normalisation (M2) (b) in the FTIR data. The ellipse in every scores plot represents the confidence interval (95%).

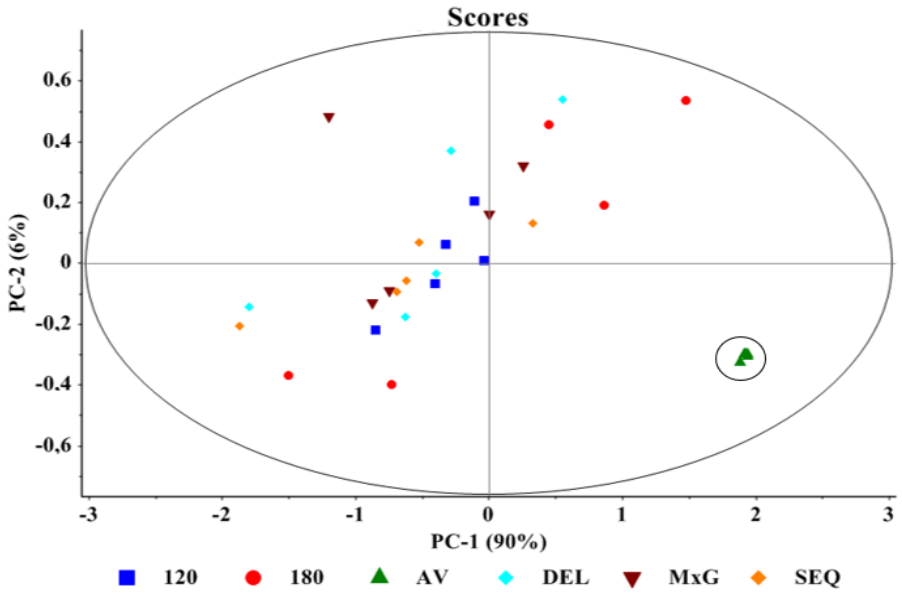

(a)

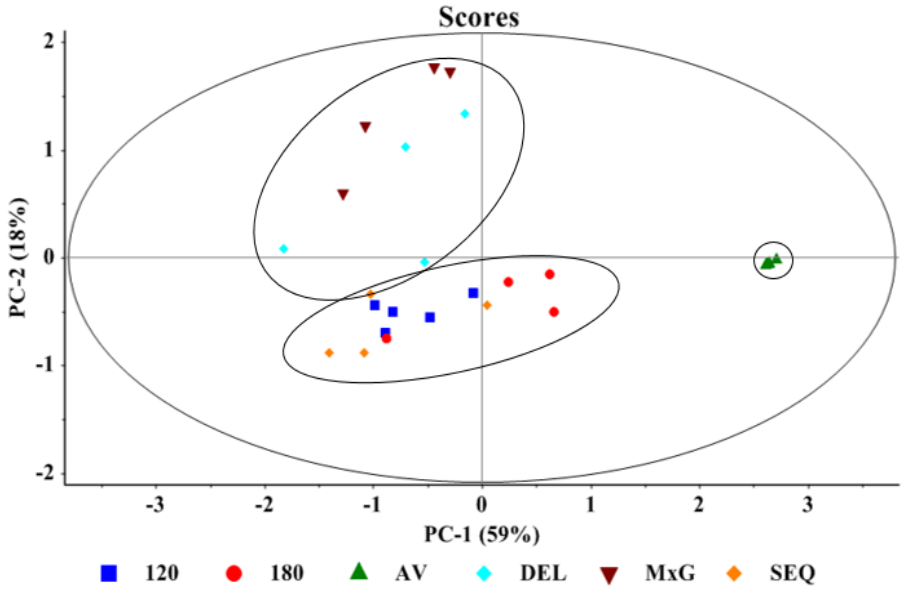

(b)

Figure 3-23 - PCA scores plots for FTIR data after smoothing (a) and smoothing followed by normalisation (b) manipulation.

Figure 3-23-a shows that Avicel is clearly distinctive from the other samples. This is an insight that PCA was able to distinguish FTIR spectra of Avicel from those of the other samples. Moreover, as the scores plot is a representation of data variability, it can be concluded that samples less spread through this plot are less variable, i.e., more homogeneous. Hence, it is indeed expected that Avicel, as commercial pure cellulose, is the most homogeneous samples among the fibres evaluated, as indicated in Figure 3-23. However, as this is the only evident cluster when using only smoothing prior data analysis, other data manipulation might be needed to increase spectra resolution and improve samples differentiation.

When normalisation is applied after the smoothing tool (M2), a different scores plot is generated (Figure 3-23-b). Even though samples still present a large variability, two more clusters might be suggested, apart from the already observed cluster of Avicel samples: a cluster positive in PC2 containing MxG and DEL fibres; and a negative PC2 cluster for the remaining fibres (120ºC, 180ºC and SEQ).

In some cases, the evaluation of samples position along the PCs in the scores plots can infer which characteristics each principal component most describes. For instance, from the way different extracted lignin were presented in the scores plots of PCA, Leskinen et al. (2015) were able to suggest that their PC1 was directed related to crystallinity and PC2 was strongly related to hydroxyl functionalities (Leskinen et al., 2015).

However, in most of the cases, the interpretation of the PCs is not straightforward (Hori and Sugiyama, 2003). Moreover, although the new arrangement provided by M2 through data normalisation improved the representation of the data by possible decreasing noise, it is still hard to suggest a single feature/characteristic that would explain PC1 or PC2.

3.3.7.6.2. Loading plot

The loading plot is a visual representation of the degree to which variables affect the sample variability. In the loading plot, the wavenumbers with highest peaks (both negative and positive) are the wavenumbers that contribute the most to differences in PC1, as observed in the scores plot (Kline et al., 2010).

Figure 3-24 shows the loading plot for FTIR data after manipulations M1 (a) and M2 (b). Only the loading plot for PC1 was evaluated because PC1 explains the highest percentage of data variability (90 and 59% for M1 and M2, respectively).

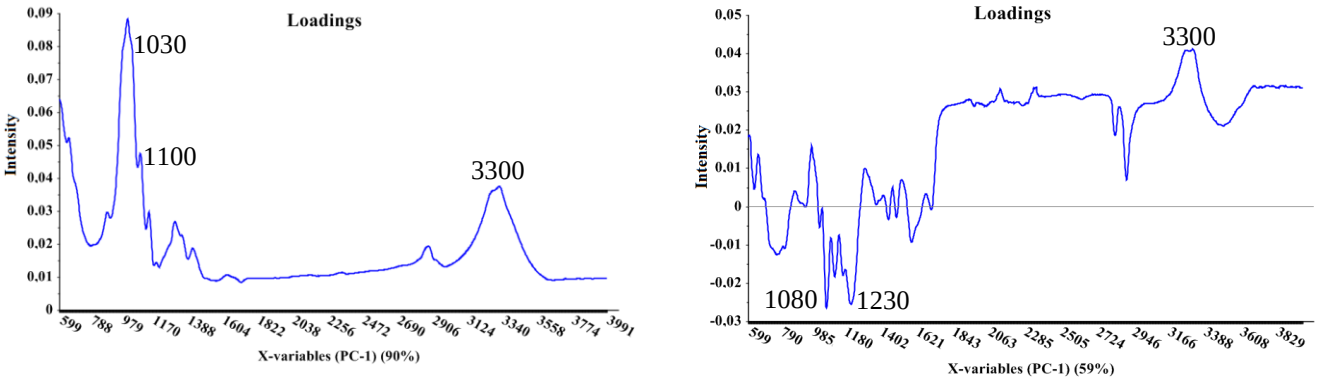

(a) (b)

Figure 3-24 - Loading plot for FTIR data after applying smoothing (a) and smoothing followed by normalisation (b) for PC1.

For the analysis performed on data after smoothing (Figure 3-24-a), all the loading were positive and wavenumbers at 1030, 1100 and 3300cm^{-1} had the highest influence on PC1. After normalisation was also applied on the data (M2), the loading changed significantly and the bands at 1080, 1230 and 3300cm^{-1} presented the most influence on the variability.

The band from 4000 to 3000cm^{-1} is due to OH stretching and it commonly present in lignocellulose materials, therefore, it is not usually used to characterize the biomass (Bessadok et al., 2007, Lan et al., 2011). The band at 1080cm^{-1} is due to cellulose C-C/C-OH (Kačuráková et al., 2000) and at 1024cm^{-1} is assigned to C-OH (Garside and Wyeth, 2003), respectively;

1100cm^{-1} is attributed to ring or glycosidic stretching (Bessadok et al., 2007); and 1230cm^{-1} are due to aryl alkyl ether (C-O-C) in cellulose and lignin (Morán et al., 2008). Therefore, it can be suggested that cellulose plays an important role in data variability.

As the samples were not well separated in the scores plot using these approaches (smoothing and normalisation), next section will present the attempt to improve resolution of the FTIR data.

3.3.7.7. Data manipulations M3 and M4 - Smoothing and 2nd-derivative followed by normalisation

The use of the 2nd-derivative in FTIR data prior to PCA can improve peak resolution and help to overcome peak overlapping (Chen et al., 2015). Therefore, in this section, smoothing and 2nd-derivative (M3) were applied to the data and compared to the same method followed by data normalisation (M4).

3.3.7.7.1. Scores plot

Figure 3-25 shows the scores plot for manipulation M3 (a; smoothing + 2nd-derivative) and M4 (b; smoothing + 2nd-derivative + normalisation).

The difference between these two plots in Figure 3-25 strongly suggests that normalisation of the data was in fact able to decrease whatever noises/peak overlapping were affecting the analysis and preventing the spectra from being clearly separated among the samples. The use of 2nd-derivative of FTIR spectra in PCA have been reported to increase resolution of the data analysed (Michell, 1990). However, Figure 3-25-a shows that the 2nd-derivative by itself did not improve the visualisation and normalisation was essential to improve the analysis.

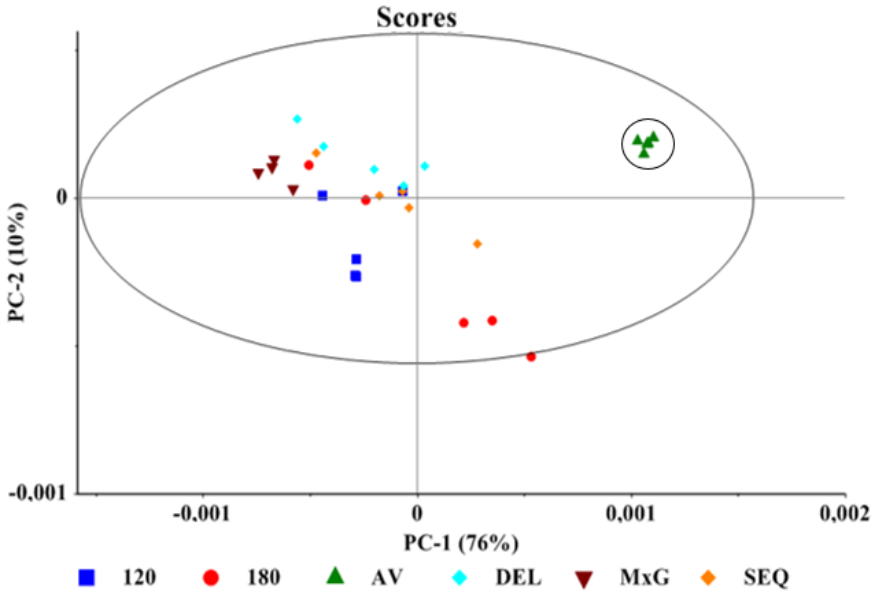

(a)

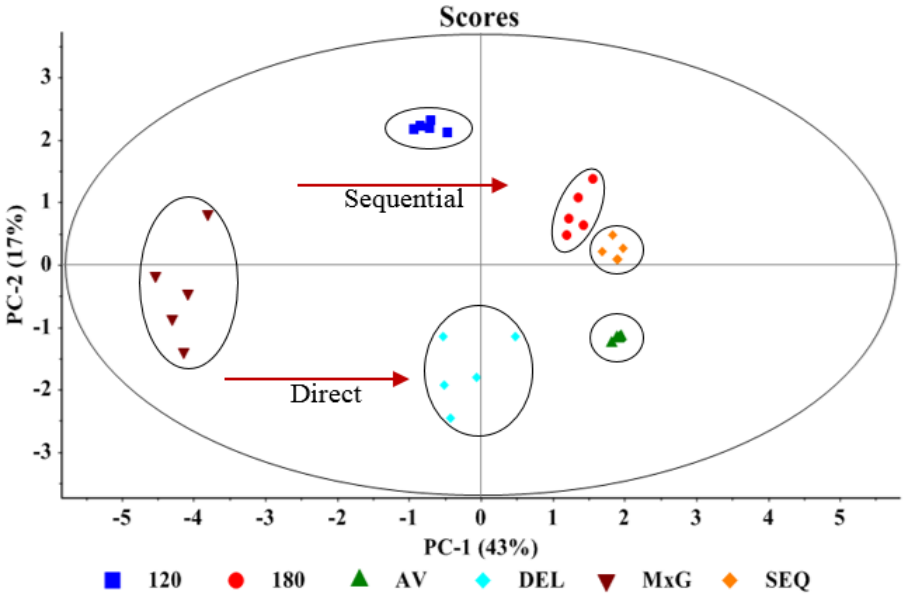

(b)

Figure 3-25 - PCA scores plots for FTIR data after smoothing+2nd-derivative (a) and smoothing+2nd-derivative+normalisation (b).

Apart from the clear cluster of each of the samples obtained in Figure 3-25-b, it is also possible to suggest a pattern: from the raw material (MxG) in the left side, every treatment

performed led to a fibre that moved from the left to the right side (from PC1 negative to positive). It is known that each of the treatments performed resulted into an increase in cellulose percentage in the fibres, therefore, PC1 could have a direct relation to the cellulose contents and/or cellulose purity. Moreover, the position of Avicel in the positive region of PC1 supports this suggestion.

However, SEQ and DEL have very similar contents (79.9 and 78.9%, respectively) and do not have the same PC1 value. Moreover, each treatment performed on MxG led to an increase of CI, which could also be correlated to PC1 from negative (lowest CI) to positive (highest CI). In this case, Avicel does not fit in the theory, as MXG and Avicel presented similar CI values. Therefore, it is clear that cellulose contents is not the only feature that PC1 describes.

In addition, the presence of hemicellulose and lignin is believed to increase amorphous contents in lignocellulosic biomass. Therefore, PC1 could also be related to amorphous/crystalline contents. MxG is the sample that present the highest content of amorphous compounds (hemicellulose/lignin/extractives) and it is placed at the negative portion of PC1. Then, at each treatment performed, amorphous compounds are being extracted and it resulted in samples moving along PC1 from the negative to the positive portion. Therefore, crystallinity might be increasing along PC1 from negative to positive portions as a result of extraction of amorphous compounds.

In addition, the sequential and direct treatment generated samples that present opposite values along PC2. However, the feature described by PC2 is not easily determined. It could be related to hemicellulose contents, as the fibre that has the highest PC2 value (120^{o}C) is also the one that presents the highest percentage of hemicellulose among all samples. Moreover, after losing a significant amount of hemicellulose, 180^{o}C fibres presented a significant decrease of PC2 values compared to 120^{o}C. Nevertheless, it is clear that hemicellulose is not the only

feature described by PC2 as DEL fibres have higher hemicellulose contents than SEQ, but present lower PC2 values. These results indicate that PC2 describe not one single characteristic, but a group of not straightforward features.

Although the analysis of features described by PC1 and PC2 is coherent with what can be observed by the scores plots and what is known about each fibre composition, evaluation of PCs are generally speculative and qualitative if further evidence is not presented (Hori and Sugiyama, 2003).

Finally, the variability of each group of samples shows that the sequential treatment (SEQ fibres) result in more homogeneous samples when compared to direct treatment (DEL fibres).

3.3.7.7.2. Loading plot

From the data manipulations evaluated, M4 (smoothing+2nd-derivative+normalisation) generated the best results in terms of spectra separation and resolution. Therefore, only the loading plot of this manipulation is shown in Figure 3-26.

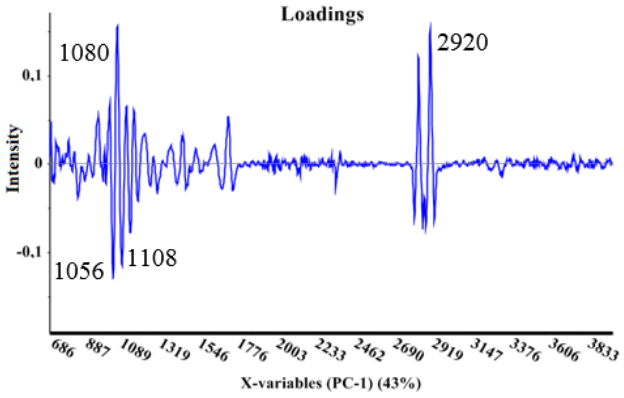

Figure 3-26 - Loading plot for PC1 after manipulation of FTIR data (M4).

The variables loading are closely related to the position of each sample in the scores plot. When using M4 as data manipulation route, the wavenumbers that most affected PC1 positively were 1080cm^{-1} that is attributed to pyranose ring (Morán et al., 2008) and 2920cm^{-1},

which is assigned to CH_2 in cellulose (Sun et al., 2007). On the other hand, bands at 1056cm^{-1}, due to asymmetric C-C (Garside and Wyeth, 2003) and 1108cm^{-1} due to C-OH (Morán et al., 2008) had a negative effect on the loading plot.

Therefore, although these wavenumbers are different from the ones obtained by the loading plot of M1 and M2, they are also mainly due to cellulose linkages. Moreover, once again wavenumbers related to infrared CI values (895 and 1427 cm^{-1}) did not affect the analysis significantly.

From both scores and loading plots it can be concluded that the 2nd-derivative and data normalisation revealed the wavenumbers that define the features of the spectra and therefore separate them efficiently as can be seen in the scores plot in Figure 3-25.

3.3.7.7.3. Explained data variability by the principal components

Each principal component (PC) explains a portion of data variability in a decreasing order, i.e., variability explained by PC1>PC2>PC3 and so on (Esbensen, 2002). Both scores and loading plot shows the percentage of explained variability by each PC in between brackets. For instance, the first scores plot (Figure 3-23) shows that PC1 explains 90% of the data variability, while PC2 explains 6%. Therefore, the scores plot represents 96% of total data variability.

Comparing the plots shown in Figure 3-25, it can be observed that the sum of percentage of data variance explained by PC1 and PC2 was decreased when normalisation was introduced. Data explained by PC1+PC2 decreased from 86 to 60% when M3 and M4 are applied, respectively. The same decrease was observed for M1 (96%) compared to M2 (77%) (Figure 3-23). That might indicate that although normalisation was effective in resolving both pair of data (M1/M2 and M3/M4), its use resulted in the need of more variables (PCs) to explain the data, suggesting the high complexity of the samples.

However, in this work, the decreasing in explained variability did not compromise the overall analysis. Moreover, analysis focused on only PC1 and PC2 was still enough to provide useful samples information.

3.3.7.8. CI investigation by PCA analysis

In a last attempt of further investigating cellulose crystallinity and CI values, PCA was performed using only the wavenumbers that are thought to describe crystalline and amorphous cellulose portions: 1427 and 895cm^{-1}. Therefore, for this analysis, two ranges of wavenumbers were used only: 1425-1430cm^{-1} and 890-900cm^{-1}.

In addition, PCA was also performed using the spectra with the exception of CI related bands to evaluate if the absence of these bands would cause any difference in the results. Then, the results of PCA using CI wavenumbers were compared to PCA performed on the whole FTIR spectra. All the analysis of this section were performed after transformation M4 was applied to the FTIR data.

Figure 3-27 shows the scores plot for PC1 and PC2 for the FTIR spectra without CI wavenumbers (a), and for CI wavenumbers only (b). Figure 3-27-a confirms that the analysis of FTIR spectra after removing the CI wavenumber is the same as the whole spectra analysis (Figure 3-25-b) as they are superimposable. That suggests that CI wavenumbers are not crucial in the PCA of the biomass analysed (MxG, 120^{o}C, 180 ^{o}C, DEL, SEQ and Avicel).

However, when analysing the PCA results only for CI wavenumbers only (Figure 3-27-b), there is a clear difference compared to the whole spectra. PC1 apparently differentiates pure cellulose (negative PC1) from MxG (positive PC1). Furthermore, it can be suggested that along PC2: 180^{o}C, SEQ and Avicel are preferentially negative, while 120^{o}C and DEL are positive.

However, as PC2 only accounts for 2% of samples variability, no conclusion on fibre composition/structure could be made based on only CI wavenumber data.

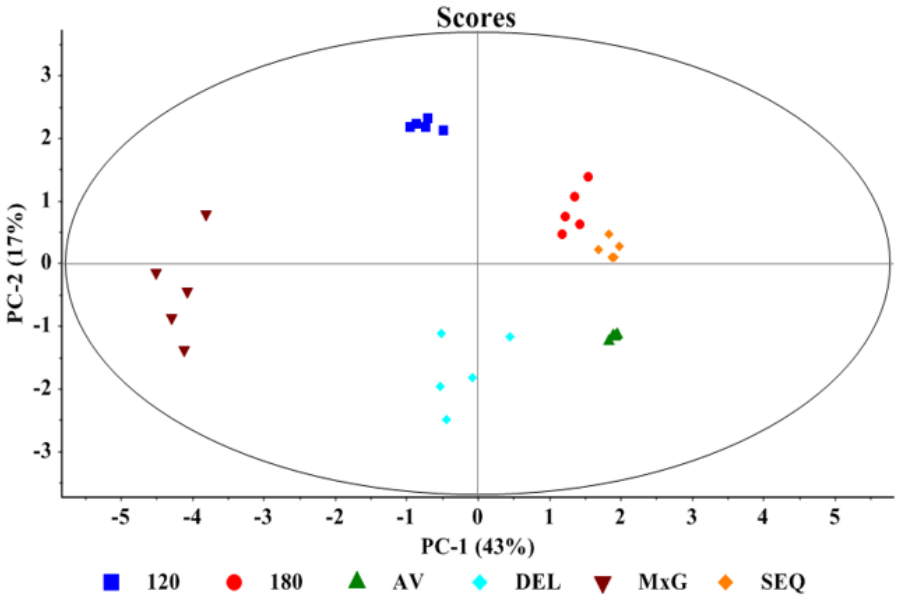

(a)

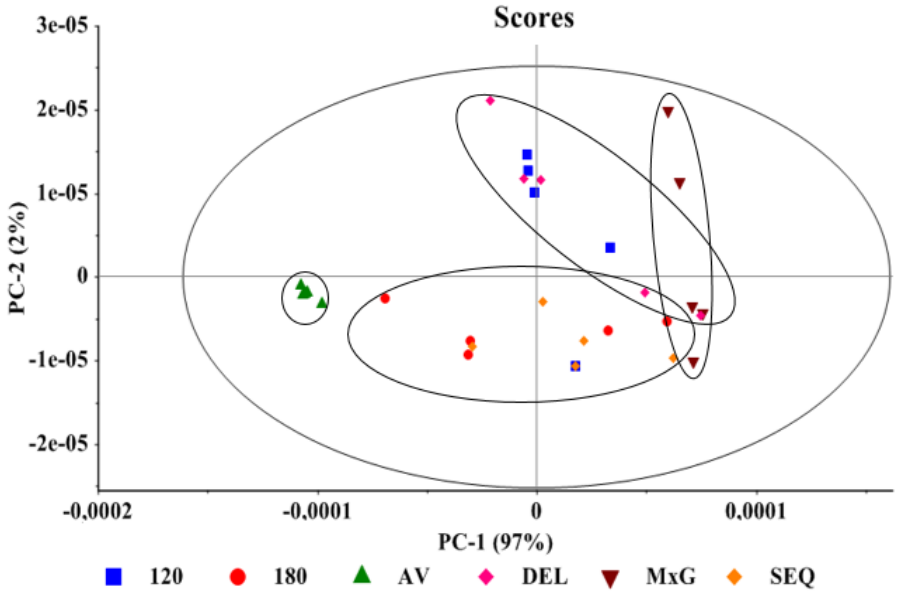

(b)

Figure 3-27 - PCA scores plot after applying M4 using: the spectra with the exception of CI wavenumbers (a); and only CI wavenumbers (b).

The analysis of the same set of data shown in Figure 3-27-b was also performed using other data manipulation (M1, M2 and M3). Although some clustering differences were observed compared to manipulation M4, they did not change the overall analysis and, therefore, this data is not shown.

The results suggest that CI values obtained from FTIR data did not demonstrate significance among the samples analysed. The reason for that is most likely due to the complex nature of lignocellulosic structure and its compounds that can affect FTIR analysis (Barnette et al., 2012).

3.4. Conclusion

Using the biorefinery approach, cellulose-enriched fibres were successfully obtained from MxG in two routes: 1) direct delignification; and 2) sequential extraction followed by delignification.

Differently from what was expected, after the modified organosolv method step, DEL fibres presented lower percentage of lignin compared to SEQ fibres, suggesting that the delignification process was more efficient in direct route compared to sequential extraction route. That could be due to several non-target reactions (condensation, pseudo-lignin formation) resultant from the increased process severity applied during sequential extraction. In addition, direct route resulted in fibres with higher hemicellulose contents when compared to the sequential route. Cellulose contents in both fibres were very similar.

However, different from the purified liquid streams generated during sequential extraction, direct delignification originated a liquid stream containing a mixture of several components (biomass extractives, hemicellulose, and lignin). This complex mixture decreases

its potential use for further processing, particularly for hemicellulose fraction that is highly soluble in this stream and difficult to be recovered.

Although sequential extraction is still preferred because of the potential of using liquid streams for high-valuable products generation, the fibres composition achieved by these two routes was very similar. Moreover, the first aim of this chapter was achieved by successfully removing biomass fractions using SBW and a modified organosolv method to produce cellulose-enriched fibres.

In order to understand structural characteristics of fibres produced, physical evaluation was performed using SEM, FTIR and PCA. SEM showed significant differences in the surface of biomass. PCA demonstrated to be a powerful tool for FTIR data analysis. While FTIR spectra and infra-red crystallinity index (CI) values only provided limited information about fibres structures and differences among the samples, PCA was able to provide more definitive results about the structural differences present in the fibres. PCA efficiency proved to be closely dependent on data manipulation, therefore the evaluation of several data manipulations was performed to determine which one would be most suitable for the particular set of samples of this work. Data normalisation demonstrated to have a significant effect on data analysis. The use of data 2nd-derivative by itself did not display a significant improvement. However, the combined effect of 2nd-derivative and normalisation achieved the best data resolution providing useful information about the samples.

Therefore, the use of physical analysis combined with statistical tools achieved the second aim of this chapter that was to evaluate/differentiate fibres produced by SBW and modified organosolv extractions. Hence, PCA successfully proved qualitatively that different treatments led to a production of two distinct cellulose-enriched fibres: DEL and SEQ.

These fibres were used as starting materials to assess the efficiency of using SBW as media/catalyst in the conversion of cellulose fibres into glucose monomers following the biorefinery approach and this process is discussed in Chapter 4.

CHAPTER 4

AN ASSESSMENT OF SUBCRITICAL WATER FOR CELLULOSE HYDROLYSIS AND GLUCOSE PRODUCTION

4.1. Introduction

Cellulose is a water insoluble linear polymer composed of glucose units bonded by β-1,4-glycosidic linkages (O'Sullivan, 1997) and present both highly organized (crystalline) and less ordered (amorphous) fractions (Klemm et al., 2005) and degrees of polymerisation (DP) that varies from 6000 to 16000 (Liu and Sun, 2010). Cellulose is a substantial natural polymer and it is the most abundant compound presented in lignocellulosic biomass (Vanholme et al., 2013). Cellulose is currently largely used in industry of paper and chemicals (Liu and Sun, 2010) and its interest as an important carbon source for a bio-based economy is increasing significantly as glucose can be converted into a variety of fuels and chemicals (Vanholme et al., 2013).

The current global energy economy based on fossil fuel reserves lacks sustainability and it is leading to a series of environmental, economic and geopolitical implications regarding to its future (Demirbas, 2009a). Therefore, issues such as the increase of fuel demands, climate changes, and the instability of fossil fuel prices are driving an economic transition towards a bio-based economy (Langeveld et al., 2010). A bio-based economy is believed to be the most

promising way to achieve energy independence as well as a sustainable development and management of environmental issues (Demirbas, 2009a, Fitzpatrick et al., 2010).

In order to utilize cellulose for production of fuels, chemicals and/or materials, cellulose needs to be recovered/accessible from lignocellulosic matrix. However, whereas high sugar/starch contents feedstocks such as sugar cane and corn are easily hydrolysed, cellulose requires a more extensive treatment in order to disrupt its linkages and release glucose units (Demirbas, 2009a).

The use of water in subcritical conditions for lignocellulose biomass fractionation is gaining attention as an environment-friendly process due to the non-requirement for additional catalysts, fast processing and operational simplicity, and limited corrosion a problem commonly encountered by supercritical and acid treatments (Ruiz et al., 2013, Toor et al., 2011).

Water in subcritical conditions has interesting properties that differ from ambient conditions such as higher ionic constant, lower viscosity and higher solubility of organic species (Toor et al., 2011). In addition, subcritical water (SBW) acts simultaneously as solvent and catalyst for hydrolysis reaction as its auto-ionization creates hydronium ions (H_3O^+) that catalyse hydrolysis (Ruiz et al., 2013). Moreover, a neutralisation step is not necessary as the H^+ ions are a function of temperature and, therefore, will naturally decrease when temperature decreases (Tolonen et al., 2011).

SBW has and continues to be widely studied as potential solvent to support pretreatment of biomass fractionation but and also to modify cellulose in order to make it more accessible to hydrolysis (Taherzadeh and Karimi, 2008). Subsequent cellulose hydrolysis, however, is usually performed by mineral acids or enzymes (Demirbas, 2009a) in processes that have significant drawbacks such as long time required for the reaction, problems with corrosion and

acid disposal/recycling, cost of enzymes, and enzymatic inhibition by co-products generated during pretreatments (Carvalheiro et al., 2008, Vanholme et al., 2013).

The aim of this chapter is to assess the use of SBW as a 'green' solvent for cellulose hydrolysis into glucose using pre-processed MxG fibres (DEL and SEQ) in a biorefinery concept. Moreover, the objective is to develop an understanding of chemical reactions taking place during cellulose hydrolysis under SBW conditions as well as to evaluate the role of cellulose structure during hydrolysis in addition to develop an understanding of the impact of MxG direct and sequential extraction on glucose release and formation of fermentation inhibitors (HMF, furfural, etc.).

4.2. Material and methods

4.2.1. Subcritical water (SBW) hydrolysis

The reactors used throughout this chapter were built using stainless steel tubes (thickness 0.3cm) and stainless steel caps (Swagelok, UK). Reactors dimensions were 1.5cm of internal diameter and 11.4cm length, totally 20mL volume.

Distilled water (15mL) was pre-heated to 50^{o}C prior to the reaction. Pre-heated distilled water was mixed with the biomass from 0.5-6.4% (w/v), depending on the loading condition, and placed into the reactor.

A GC oven (Hewlett Packard HP, 5890 series II) was used to perform the reactions because of the rapid rate of temperature increase and easier temperature control compared to common ovens. In order to decrease the heating time, once the reactors were placed inside the oven, the oven was set to its maximum temperature (325^{o}C). Then, once the target temperature (190-320^{o}C) was about to be achieved, the oven was set back to target temperature. In this way,

the ramp of temperature increase was considered to be the same for all experiments regardless of the target temperature.

During every experiment performed, a reactor containing only distilled water was placed together in the oven and connected to a thermocouple (type K, 310 stainless steel sheath, 1.5mm) for temperature profile and control. As the biomass loading in this study was low (up to 6.4%), it was considered that the reactor containing only water and the reactors containing biomass suspension followed the same temperature profile.

Reaction retention time zero was taken as soon as the target temperature was achieved in the reactor (t=0). Therefore, heating time was not taken into consideration when analysing residence time. After the residence time was completed, reactors were placed in an ice bath to stop the reaction. Reactor cooling time was fast and took less than a minute to achieve 50-60ºC. After cooling the reactor, it was opened and samples were centrifuged at 2900g for 20min.

4.2.1.1. Solid fraction

The solid fraction was dried completely in a drying cabinet at 65ºC and weighed. Hydrolysis percentage was calculated by the mass balance of solids according to Equation 4-1:

$$hydrolysis\ (\%) = \left(\frac{m_i - m_f}{m_i}\right) * 100 \qquad \text{Equation 4-1}$$

In which m_i is the initial mass (in grams) placed in the reactor and it is dependent on the condition, and m_f is the mass (in grams) remaining in the reactor after the reaction, separated from the liquid fraction by centrifugation and dried.

After weighing the solid fraction for hydrolysis percentage calculation, samples were analysed by FTIR (see section 2.4).

4.2.1.2. Liquid fraction

4.2.1.2.1. Compounds concentrations

After centrifugation, the liquid fraction was stored at -20ºC until further analysis. Glucose, fructose, xylose, arabinose, galactose and HMF were quantified by HPAEC (section 2.6). Glucose was also quantified by glucose enzyme kits (section 2.8) for the samples of the scoping experiments when HPAEC was not available. Furfural was analysed by HPLC (section 2.7).

4.2.1.2.2. Glucose yield

After glucose quantification by HPAEC, glucose yield (Y_{glu}) was calculated according to Equation 4-2:

$$Y_{glu}(\%) = \frac{[Glu]}{1.11 * f * [biomass]} * 100 \qquad \text{Equation 4-2}$$

In which $[Glu]$ is the glucose concentration (g/L) obtained by HPAEC after each reaction; $[biomass]$ is the concentration of biomass (g/L) in the beginning of the reaction; 1.11 is the conversion factor of cellulose into glucose conversion; and f is the fraction of cellulose in each biomass, i.e., Avicel=1, DEL=0.80 and SEQ=0.79. Cellulose fraction of DEL and SEQ fibres were obtained in the previous chapter.

4.2.1.2.3. Dry weight (DW) in liquid fraction

In order to analyse the dry weight in the liquid fraction, samples were evaporated and the residual solid (mostly non-volatile carbohydrate) was weighed.

1mL of each sample was placed into a pre-weighed 1.5mL Eppendorf (D_1) using a micropipette (Biohit, 100-1000µL). Eppendorf with sample was placed into a drying cabinet at 65ºC with the lid opened until constant weight was achieved. Dried Eppendorf was placed into

a desiccator until room temperature and re-weighed (D_2). Dry weight was then calculated according to Equation 4-3.

$$DW(g) = (D_2 - D_1) * V \quad \text{Equation 4-3}$$

As the DW was calculated for 1mL, it was then multiplied by the reaction volume (15mL) to obtain the total grams in the liquid fraction. This procedure was repeated 3 times for each sample and the results showed are an average of the values.

4.2.1.3. Mass balance

The mass balance of the reaction was calculated considering the hydrolysis and DW measurements and it is showed in Equation 4-4.

$$Mass\ balance\ (\%) = \frac{(m_f + DW)}{m_i} * 100\% \quad \text{Equation 4-4}$$

In which m_i is the initial weight (g) placed in the reactor; $m_f$is the solid weight (g) remained in the reactor after SBW hydrolysis, and DW is the dry weight in the liquid fraction after SBW hydrolysis. Therefore, using Equation 4-4 it is possible to estimate the losses of the process, as this equation should be as close as possible of 100% for an ideal process (no losses).

4.2.2. Scoping of experiments

Although several parameters are believed to affect subcritical water hydrolysis of cellulose, three parameters are considered to play key roles in this process: temperature (T), residence time (res. time) and biomass load (w/v%) (Goh et al., 2010). Therefore, these three parameters were chosen to be evaluated in this chapter.

In order to choose a range of each of these parameters, scoping experiments were used. Three biomasses were evaluated in this scoping: pure cellulose (Avicel, used as a standard), SEQ and DEL fibres. The summary of experimental conditions performed is shown in Table

4-1. Each condition was repeated at least 3 times for each biomass. For each condition, hydrolysis percentage (%) was calculated and resulting glucose, fructose and HMF were analysed by HPAEC.

Table 4-1 - Parameters evaluated in the scoping experiments: temperature (ºC), residence time (min) and biomass load (%).

Run	T (ºC)	Residence time (min)	Loading (%)
1	250	0	1
2		10	
3		20	
4		30	
5		40	
6	220	10	1
7	280		
8	310		
9	250	10	2.5
10			5

4.2.3. Design of Experiments (DoE)

A Response Surface Methodology (RSM) was performed using the Central Composite Design (CCD) of experiments in order to evaluate the effect of independent variables and optimize SBW hydrolysis of cellulose into glucose. DoE is a common mathematical and statistical way to analyse a processes that are dependent on several factors (and possibly the combination of them) and optimize the process (Tan et al., 2011).

CCD is one of the most used design of experiments because of its high efficiency for fitting second-order models (Montgomery, 2000). Figure 4-1 shows a 3-dimension representation of a 3-factors CCD, including the factorial, centre and axial points.

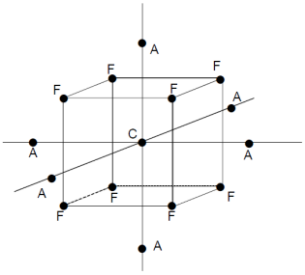

Figure 4-1 - Scheme of a Central Composite Design including its factorial (F), centre (C) and axial (A) points. Source: (Oehlert, 2000).

The DoE model used consisted of 3 factors (variables), 2 levels, 6 repetitions in the central point and axial points (α = ±1.68). The software Design Expert 7.0.0 (Stat-Ease) was used for statistical analysis and modelling. Factors evaluated (F1, F2 and F3) were the same as in the scoping and levels used are shown in Table 4-2.

Table 4-2 - Factors (variables) and levels used for the DoE.

Factor	Code	Unit	(-) α	-1	0	+ 1	(+) α
Temperature	F1	^{o}C	190	220	265	310	340
Res. time	F2	min	-13	0	20	40	54
Load	F3	%	-0.36	1	3	5	6.4

Due to the physical impossibility of performing conditions, i.e. -0.36 % of biomass loading and -13min of residence time, and also due to oven maximum temperature (325^{o}C), some of the α points were changed. Res. time of -13min was changed to 0min; temperature of 340^{o}C was changed to 320^{o}C; and loading of -0.36% was changed to 0.5%.

The experimental results obtained by the DoE were analysed using a polynomial quadratic equation as described in Equation 4-5 (Dejaegher and Vander Heyden, 2011). The effect of each variable and their interaction was evaluated and the significance of the model was tested by ANOVA.

$$y = \beta_o + \sum_{i=1}^{3} \beta_i x_i + \sum_{i=1}^{3} \beta_{ii} x_i^2 + \sum_{i=1}^{3} \sum_{j=i+1}^{3} \beta_{ii} x_i x_j \qquad \text{Equation 4-5}$$

In which y is the response, β_o is the intercept, β_i, $\beta_{ii}$and β_{ij} are the main, two-factors interactions and quadratic coefficients, respectively, and x_i and x_j are independent variables.

The model was evaluated by the determined R-squared and adjusted R-squared coefficient, as well as its significance and lack of fit according to variance analysis (ANOVA).

The responses analysed by the DoE were produced glucose and HMF (g/L) as well as and the amount of solid that was hydrolysed into soluble products, here named hydrolysis

percentage (%). Moreover, concentration of fructose, furfural (g/L) and glucose yield (%) were also analysed for each run of the DoE.

Once this first DoE was finished and analysed, the range of parameters chosen was established to be incorrect, particularly for temperature. Therefore, a second design of experiments (DoE-2) was performed using the same variables as before and different levels for temperature as presented in Table 4-3. Once again, some of the conditions were changed: res. time of -13min was changed to 0min and loading of -0.36% was changed to 0.5%.

Table 4-3 - Factors and levels used for the second DoE (DoE-2) performed.

Factor	Code	Unit	(-) α	-1	0	+ 1	(+) α
Temperature	F1	^{o}C	200	220	250	280	300
Res. time	F2	min	-13	0	20	40	54
Load	F3	%	-0.36	1	3	5	6.4

Table 4-4 shows the 20 conditions that were performed in the two DoE including eight factorial and six axial conditions and six repetition in the centre point.

Table 4-4 - Experimental conditions For DoE (a) and DoE-2 (b) for CCD using 3-factors (T, res. time and load). Conditions marked by * were modified to feasible values.

(a)

Run	F1-T (^{o}C)	F2-res. time (min)	F3- Load (%)
1	265	20	6.4
2	310	0	1.0
3	265	20	3.0
4	310	0	5.0
5	265	20	3.0
6	220	0	5.0
7	220	40	5.0
8	310	40	5.0
9	220	40	1.0
10	265	20	0.5*
11	265	0*	3.0
12	265	20	3.0
13	265	54	3.0
14	265	20	3.0
15	190	20	3.0
16	320*	20	3.0
17	265	20	3.0
18	310	40	1.0
19	265	20	3.0
20	220	0	1.0

(b)

Run	F1-T (^{o}C)	F2-res. time (min)	F3- Load (%)
1	220	40	5.0
2	280	0	5.0
3	220	0	1.0
4	250	20	3.0
5	250	20	3.0
6	250	54	3.0
7	220	40	1.0
8	250	0*	3.0
9	280	0	1.0
10	250	20	3.0
11	250	20	3.0
12	200	20	3.0
13	250	20	3.0
14	250	20	3.0
15	250	20	6.4
16	220	0	5.0
17	250	20	0.5*
18	280	40	5.0
19	280	40	1.0
20	300	20	3.0

Marked parameter values (*) were the ones changed. Both DoE and DOE-2 were performed for the three fibres: Avicel, SEQ and DEL. The experiments were performed in a random order in both DoE.

4.3. Results and Discussion

4.3.1. Heating time in small batch reactors

The average of heating times for 20mL batch reactors in the range of temperatures studied in this work (190-320^{o}C) is shown in Table 4-5. Values were measured with a thermocouple connected to the reactor and variations of up to 1 minute could be observed in each set temperature.

One of the drawbacks of using a batch reactor is the heating time (Taherzadeh and Karimi, 2008). Therefore, small reactors (20mL) were used in this chapter to decrease the influence of heating time on the results.

Table 4-5 - Average of heating time for 20mL reactors for each of the target temperature used.

T(^{o}C)	190	220	250	265	280	300	310	320
t (min)	5	7	10	11	14	17	20	24

Comparing the results from Table 4-5 with results presented in Table 3-1 (heating times needed for the 500mL reactor used for previous biomass extraction), it can be seen that the heating time is substantially smaller for the 20mL reactors. For instance, the time needed to achieve 200^{o}C dropped from 27 minutes in the 500mL to 7min when using 20mL reactors. Therefore, the total time that the biomass remains inside the reactor (heating + residence time) is decreased, which could potentially decrease further decomposition of glucose (Sasaki et al., 2000).

4.3.2. Glucose determination: HPAEC vs glucose enzyme assay

The HPAEC was not available until the second half of this research project. Therefore, in order to evaluate SBW hydrolysis during the scoping experiments, an enzyme assay was used for glucose determination. Afterwards, all samples were analysed by HPAEC for comparison. The evaluation of the conditions and results presented in Figure 4-2 is presented in section 4.3.3. In this section, the aim is to evaluate and discuss the validity of the enzyme assay used for glucose quantification.

Figure 4-2 shows glucose contents analysed by HPAEC and enzyme assay after SBW hydrolysis at 250ºC using 1% biomass load and residence times from 0-40min for Avicel (a), DEL (b) and SEQ fibres (c). It can be seen that glucose contents results from enzyme kits and HPAEC are in a good correlation in some cases, mostly, when glucose concentration is less than 0.3g/L. For higher concentration values, the enzymatic procedure seems to underestimate glucose contents in the samples.

Analysis of variance (ANOVA) was applied in order to define if the values difference obtained by HPAEC and enzyme assay were significantly different. Calculated p-values for Avicel, DEL and SEQ samples were $1.2.10^{-5}$, $3.8.10^{-2}$ and 7.10^{-3}, respectively. Therefore, using 95% of confidence interval, differences presented by the two quantification methods are significant for all three biomasses.

Glucose quantification from enzyme assay is a result of glucose reaction using two enzymes, hexokinase and glucose-6-phosphate dehydrogenase (HK/G-6-PDH) to generate NADPH, which will be proportional to glucose contents and can be quantified by absorbance (more detailed reaction can be found in section 2.8).

Samples having up to 0.8 g/L of glucose could be analysed with no dilution. Hence, samples that presented higher glucose contents were re-analysed using necessary dilution

factors. In this way, it was assured that underestimated values were not a result of over-concentrated samples.

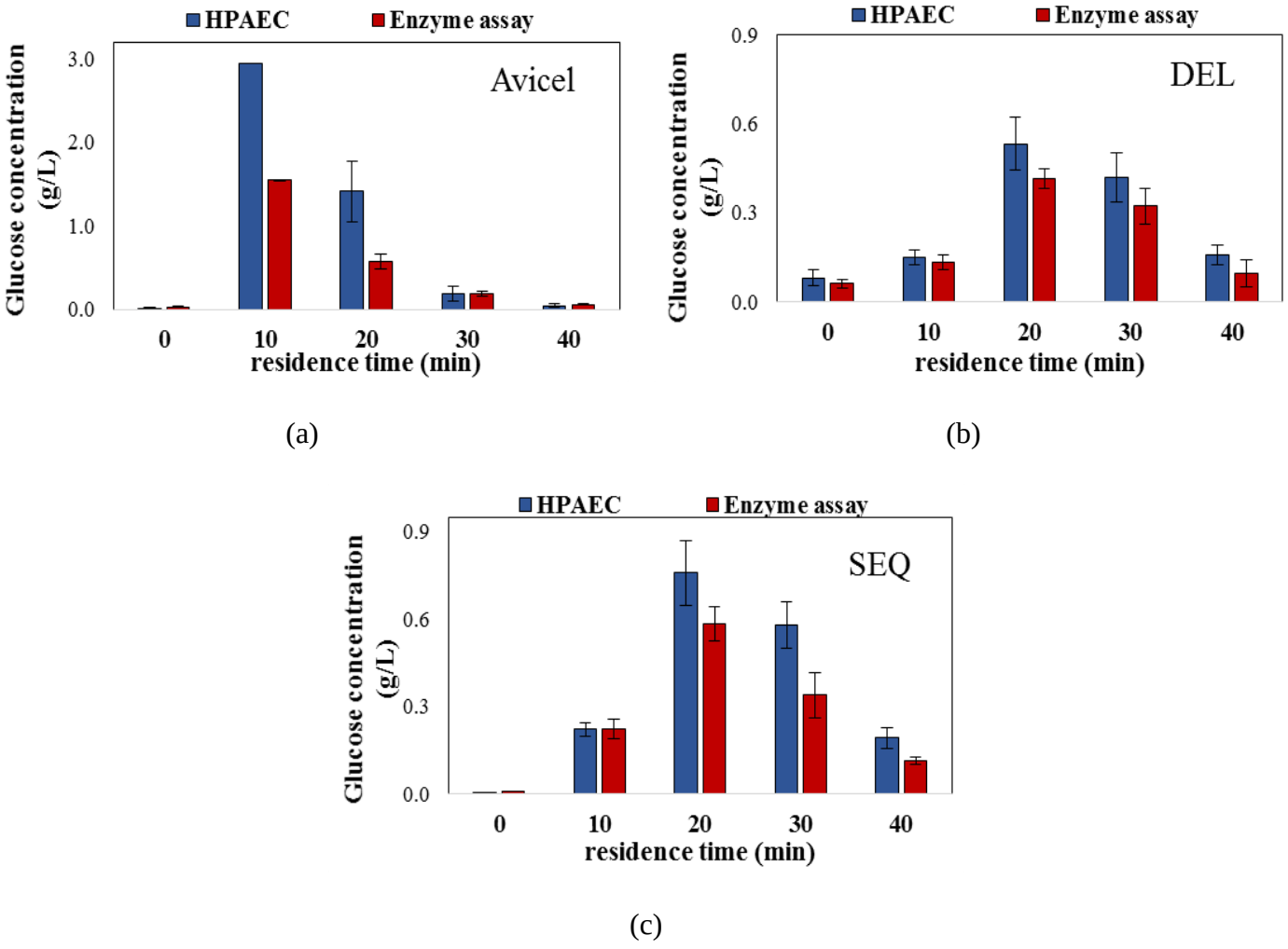

Figure 4-2 - Glucose determined by HPAEC and enzyme assay after SBW hydrolysis of Avicel (a), DEL (b) and SEQ fibres (c) at 250ºC, 1% load and residence times from 0-40min.

Coloured samples and acidic samples could interfere with the enzymes (Megazyme International, 2013). Samples from high residence times (=>30min) were dark brownish and highly acidic (pH<2.5), which could account for some interference. However, looking at results for residence time = 40min, which presented the darkest colour among the residence times from 0-40min, there is no significant difference between the methods. Therefore, it can be concluded that the colour did not greatly interfere with the results.

Acidic samples could also interfere in the analysis. Although samples generated from SBW hydrolysis were in the pH range from 2.1-4.7 (see APPENDIX A), after adding the buffer used during the assay, samples were neutralised (pH=7). Therefore, it was concluded that the pH was not an issue in the results.

Megazyme also suggests that interference by substances that might affect the enzymes is a possibility, however, a list of these substances is not available (Megazyme International, 2013).

Although enzyme assay is not among the common methods used for glucose determination after lignocellulose hydrolysis, there are few reports describing the use of this technique for this purpose. Gao et al. (2010) used the same enzyme assay to quantify glucose after ammonia fibre expansion pretreatment and enzymatic hydrolysis of corn stover (Gao et al., 2010). Bhattacharya and Pletschke (2015) also used the same enzyme assay to quantify glucose in lime-pretreated sugar cane bagasse and corn stover after enzymatic hydrolysis (Bhattacharya and Pletschke, 2015). However, as no other method was used for results comparison, there is no way to know if the results presented in these studies were or not affected by potential inhibitory substances.

Bondar and Mead (1974) studied the possibility of inhibition by some compounds including sugars that are present in the samples of this work, such as fructose. They reported that fructose could account for over-estimation of glucose as fructose can compete as a substrate for the enzymes. However, when fructose was presented in higher concentration, fructose acted as an inhibitor of HK/G-6-PDH enzymes (Bondar and Mead, 1974).

Moreover, Hristozova et al. (2006) studied the effect of furfural in the metabolism of oxidative and fermentative yeasts. They reported that the presence of furfural at low

concentration (0.04%) negatively affected fermentative yeast by inhibiting G-6-PDH (Hristozova et al., 2006).

Therefore, there is a possibility that one or more substances present in the samples had an inhibitory effect in one or both of the enzymes used for glucose quantification. Therefore, the enzyme assay was not suitable for this complex mixture of samples generated in SBW hydrolysis and it was decided to evaluate all the samples using only the results obtained from HPAEC.

4.3.3. Scoping experiments

Although there were other products generated during the SBW hydrolysis such as cello-oligosaccharides (COS), furfural, xylose, etc., the scoping study was focused only on glucose, fructose and HMF, as these were the compounds generated in higher concentration during the conditions evaluated. Moreover, these are the compounds of most interest in this work.

The focus of this section is to evaluate how these three compounds are generated (and decomposed) according to the SBW conditions applied. Therefore, the reactions patterns and other compounds generated during this process are further discussed in section 4.3.6.

Figure 4-3 present a very simplified possible reaction route (Kabyemela et al., 1999), (Jing and Lü, 2008), intended for a brief understanding about the relation among glucose, fructose and HMF during SBW hydrolysis of cellulose.

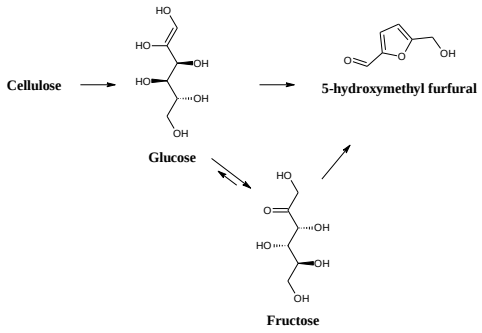

Figure 4-3 - Simplified possible path of cellulose hydrolysis and generation of glucose, fructose and HMF.

Figure 4-3 shows that after glucose is released from cellulose, it can be converted to fructose through isomerization. Then, both glucose and fructose might undergo dehydration to HMF (Jing and Lü, 2008, Kabyemela et al., 1999).

4.3.3.1. Scoping: residence time

Figure 4-4 shows the concentration of glucose, fructose and HMF after SBW hydrolysis of Avicel (a), DEL (b) and SEQ (c) fibres. During the temperature study, the temperature and biomass load were fixed at 250^{o}C and 1%.

From Figure 4-4, it is clear that residence time is, as expected, a major parameter in SBW hydrolysis affecting the products generation. For all biomasses, glucose concentration follows the same path: an increase until a maximum, then a decrease as residence time increases. This concentration increase followed by a decrease along residence time is a common pattern as glucose undergoes further decomposition after being generated (Zhao et al., 2009c).

In addition, the highest glucose concentration is achieved for shorter residence times for Avicel when compared to DEL and SEQ fibres. Moreover, higher amounts of glucose were produced from Avicel. That is an indication that pure cellulose is still easier to hydrolyse compared to cellulose from lignocellulosic matrix, even after the fibres processing.

The same pattern noticed for glucose can also be observed for HMF, i.e., an increase until a maximum concentration, and a decrease for higher residence times due to further decomposition of HMF (Asghari and Yoshida, 2007).

Fructose, on the other hand, seems to be more stable during SBW hydrolysis at these conditions as its concentration only increases during the range of residence time being studied which is the opposite of cases described in the literature. Asghari and Yoshida (2010) evaluated SBW hydrolysis of cellulose from Japanese red pine wood. They described a significant amount

of fructose being generated at 270ºC from 0-15min using a batch reactor and 0.1M phosphate buffer to maintain the pH=2. In their study, fructose was generated in the beginning of the reaction (2min) and it was almost completely decomposed by 7min (Asghari and Yoshida, 2010).

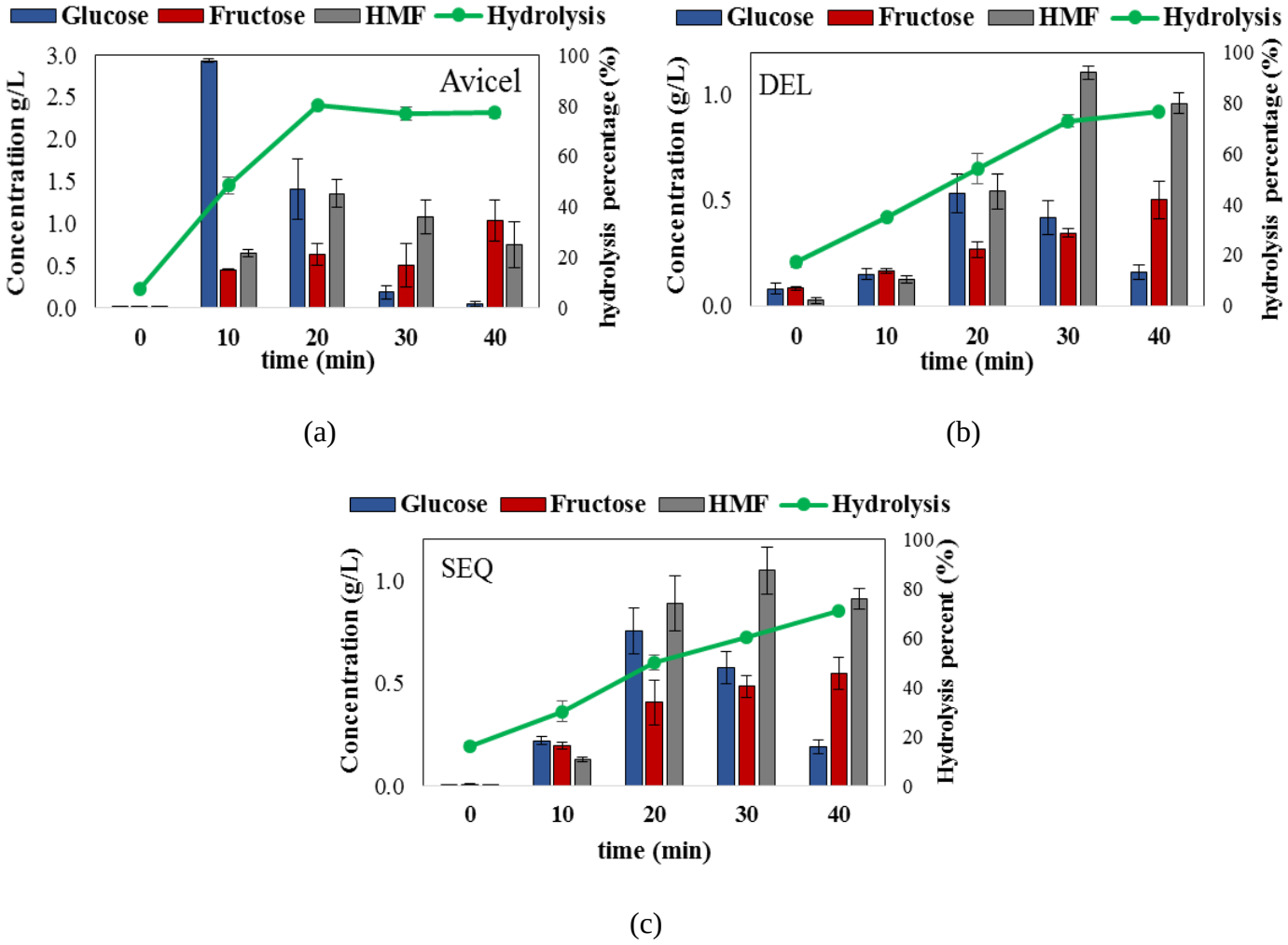

Figure 4-4 - Glucose, fructose and HMF concentrations by HPAEC and hydrolysis percentage (%) after SBW hydrolysis at residence times from 0 to 40min, at 250ºC and 1% biomass load for: (a) Avicel, (b) DEL, and (c) SEQ fibres (n=3).

Usuki et al. (2007) also described glucose isomerisation into fructose in SBW using a flow reactor at 220ºC, loadings from 0.5-5% and residence times from 0-5min. They reported fructose decomposition for residence times from 1min and higher (Usuki et al., 2007).

Nevertheless, residence times used in this scoping were most likely not enough to observe fructose start decomposing.

Comparing the three starting cellulose fibres, all the three compounds analysed, glucose, fructose and HMF, achieved a higher concentration for Avicel compared to SEQ and DEL fibres. Moreover, comparing the cellulose fibres from *Miscanthus*, SEQ fibres resulted in slightly higher glucose and fructose when compared to DEL fibres for most of conditions evaluated at this point. This is a further confirmation of the results suggested after PCA analysis: although very similar in terms of composition, DEL and SEQ fibres present different structure resultant from the two different treatment routes and, therefore, behave differently during hydrolysis process. Moreover, higher glucose production obtained for SEQ fibres compared to DEL is an indication that cellulose is more accessible in SEQ than in DEL fibres.

Figure 4-4 also shows the hydrolysis percentage, i.e., the percentage of solid biomass that was solubilised, along the increase of residence time. In the case of Avicel, high hydrolysis rate is seen in the first 20min of reaction. However, an increase in residence time after 20min did not promote further hydrolysis. This means that harsher conditions, for instance, an increase in temperature, are needed to hydrolyse the remaining solids. Moreover, the higher hydrolysis rate in the lower residence times also confirms that Avicel is easier to hydrolyse than fibres from *Miscanthus*. For DEL and SEQ fibres, the hydrolysis percentage increases almost linearly with increase in residence time in the range evaluated.

Therefore, although an increase in time might lead to higher hydrolysis percentage particularly for DEL and SEQ, it was chosen to maintain 40min as the maximum residence time to be evaluated in the DoE as long residence times resulted in an increase in glucose decomposition.

4.3.3.2. Scoping: temperature

Temperature was evaluated ranging from 220-280ºC using biomass load fixed at 1% for all cases. As the preliminary results showed that glucose concentration was still increasing at 280ºC for SEQ and DEL fibres, 310ºC was included in the study of temperature only for *Miscanthus* fibres.

Exclusively during the scoping experiments to study the effect of temperature of the scoping experiments, residence time accounted for the total time the reactor was inside the oven i.e. heating time + reaction time. Therefore, for all cases the total time was 20min. Table 4-6 shows the heating time and the reaction time for each target temperature from 220 to 310ºC.

Table 4-6 - Average heating and reaction times for each temperature evaluated in the scoping set of experiments.

T (ºC)	220	250	280	310
heating (min)	7	10	14	20
reaction (min)	13	10	6	0

Figure 4-5 shows glucose, fructose and HMF concentrations for Avicel (a), DEL (b) and SEQ fibres (c) after SBW hydrolysis at different temperatures, 1% biomass and 20min total time.

Glucose and HMF show the same pattern presented during residence time evaluation when SBW temperature ranged from mild to high: an increase in production followed by a decrease in these compounds due to their decomposition (Cheng et al., 2009).

In this range of temperature, the highest glucose concentration is seen at 250ºC for Avicel and 280ºC for DEL and SEQ fibres, and, whereas glucose is almost entirely decomposed by 280ºC for Avicel, total glucose decomposition is observed only at 310ºC for DEL and SEQ fibres. These results confirm that cellulose hydrolysis occurs faster for pure cellulose than for both of *Miscanthus* fibres.

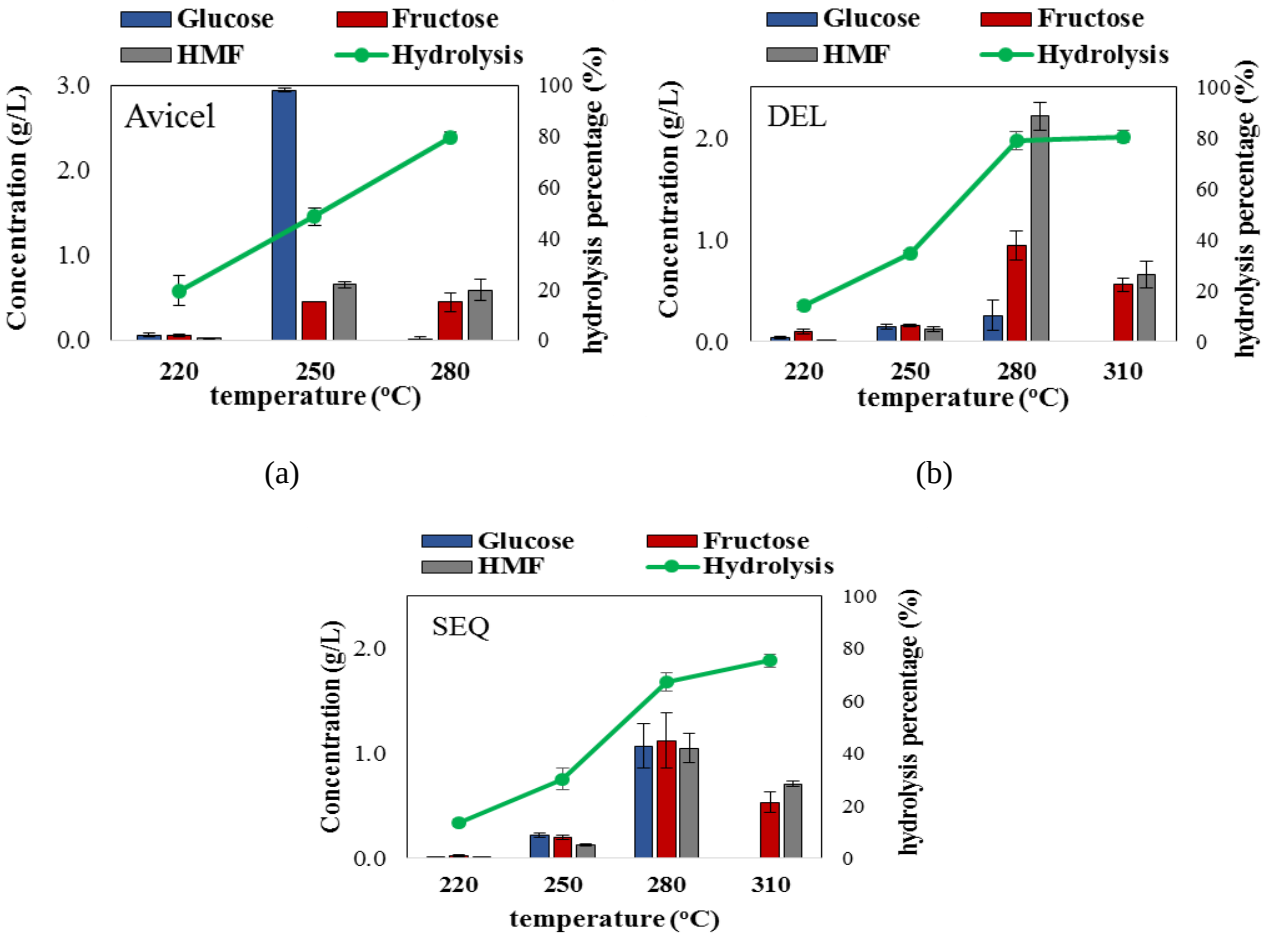

Figure 4-5 - Glucose, fructose and HMF concentrations (g/L) by HPAEC and hydrolysis percentage (%) after SBW hydrolysis at temperatures from 220 to 310°C during 20min (heating + reaction time) and 1% biomass load for: (a) Avicel, (b) DEL, and (c) SEQ fibres (n=3).

HMF decomposition appear to be more significant at high temperatures (Cheng et al., 2009). Even for Avicel, which resulted in decomposition of glucose at lower temperatures, there is no sign of significant HMF decomposition from 250 to 280°C. Cheng et al. (2009) used a batch reactor to hydrolyse switchgrass using SBW. At 250°C and times from 0-300s, they did not observe any HMF decomposition (Cheng et al., 2009). Chuntanapum et al. (2008) also suggested that HMF resisted decomposition in SBW at temperatures up to 250°C using a continuous reactor. For higher temperatures, HMF was rapidly converted into liquid products

(acids) and then, to gases (CO, CO_2) in supercritical conditions (450ºC) (Chuntanapum et al., 2008).

In terms of fructose generation/decomposition, Figure 4-5 shows different results from the ones showed in Figure 4-4. At residence times ranging from 0-40min, fructose concentration did not show any decrease. During temperature study, on the other hand, fructose showed evidence of decomposition under high temperatures (310ºC) as reported in literature (Asghari and Yoshida, 2010).

Hydrolysis percentage was greatly affected by temperature. Mild temperature (220ºC) promoted very little hydrolysis even for Avicel, whereas the highest temperature (310ºC) did not result in a significant increase in hydrolysis compared to 280ºC.

According to Figure 4-5, optimal glucose concentration is in between 250ºC and 310ºC for both SEQ and DEL. Moreover, in the case of Avicel, this optimal is in in between 220ºC and 280ºC. In order to perform the same DoE conditions for all three cellulose fibres, temperature range was decided to be from 220ºC-310ºC for all three biomasses.

4.3.3.3. Scoping: biomass load

Biomass load was the last parameter evaluated after SBW hydrolysis. In this case, hydrolysis was performed using loads from 1-5% at 250ºC and 10min of residence time. Figure 4-6 shows glucose, fructose and HMF concentration and hydrolysis percentage after SBW hydrolysis for different load percentage.

Working with high biomass loads is potentially economically advantageous as higher glucose concentration solution can be produced, which reduce costs with product separation (Kumar et al., 2009). However, high solid-liquid ratios might decrease efficiency of the process due to problems with mixing and mass transfer in heterogeneous reactions (Goh et al., 2010).

Higher load percentages than shown in Figure 4-6 (up to 10%) were tested for the three biomasses. The 10% loading mixture resulted from high biomass loads was a sludge more than a suspension. Moreover, with the exception of Avicel, the other fibres burned inside the reactor due to reactor constrains such as lack of mixing. Therefore, 5% was the limit stablished for load evaluation.

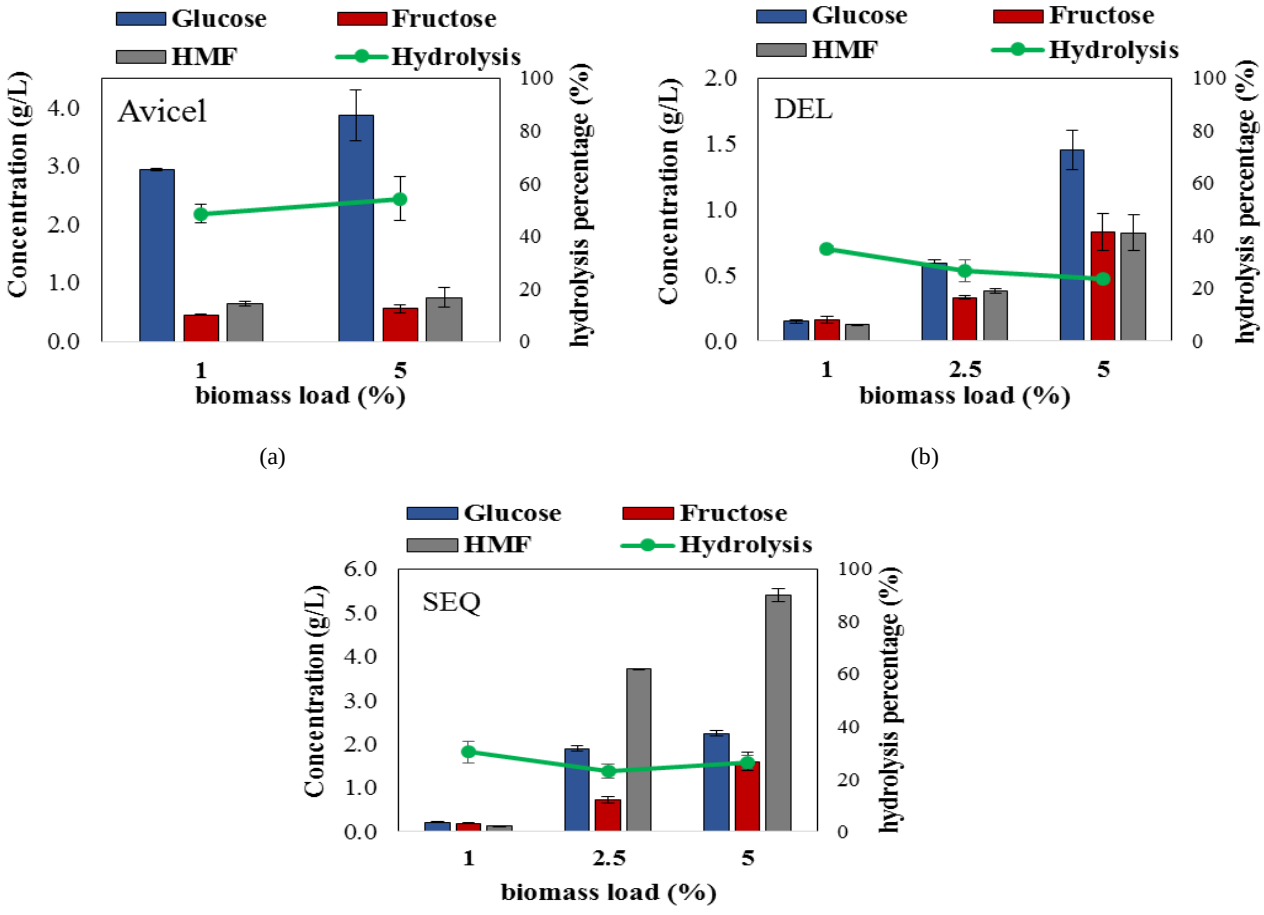

Figure 4-6 - Glucose, fructose and HMF concentrations (g/L) by HPAEC and hydrolysis percentage (%) after SBW hydrolysis at biomass load from 1 to 5% during 10min at 250 ºC for: (a) Avicel, (b) DEL, and (c) SEQ fibres (n=3).

Although the hydrolysis percentage was not significantly affected by the biomass load in the range evaluated, the generation of glucose, fructose and HMF was not linear with the increase of load. Zhao et al. (2009) studied the load effect in supercritical water hydrolysis of

corn stalks and wheat straw and suggested that although higher biomass load increased generation of hexoses, it also caused a decreased in COS yield. Their hypothesis was that hydrolysis of lignocellulose occurs only at the surface of the biomass, therefore, an increase in load will not substantially increase the release of COS (Zhao et al., 2009c).

Moreover, even though load demonstrated to be less influential than temperature and residence time, it remained as one of the three factors to be evaluated in the DoE in the range from 1-5%.

4.3.4. DoE

4.3.4.1. Design of experiments analysis using Response Surface Methodology

Response surface methods (RSM) are particularly useful to describe how the responses varies according to the interaction of process parameters and thereby assist in identifying optimal combination of parameters (Montgomery, 2000). In CCD, experimental repetitions of each run are not needed because the pure error is estimated by the repetitions of the centre points (Oehlert, 2000).

Asymmetric data can be hard to model; therefore, response transformation such as logarithm and square root can be used to assist the analysis (Oehlert, 2000). The Design Expert software suggests by default that when the ratio between maximum and minimum response values ($R_{max/min}$) is higher than 10, a transformation is needed. Avicel, DEL and SEQ fibres presented $R_{max/min}$ of 53, 13 and 16, respectively for glucose (g/L) and 16, 12 and 15 for hydrolysis percentage (%). Therefore, the logarithm transformation (suggested by the software) was applied for all responses.

Common ways of evaluating the accuracy/predictability of the model include the analysis of variance (ANOVA) and R-squared. Table 4-7 shows the ANOVA and the R-squared

and adjusted/predicted R-squared for glucose concentration for the three biomass. Data for hydrolysis is shown in the 0.

Table 4-7 - ANOVA for glucose concentration (g/L) after SBW for 3-factor CCD for (a) Avicel, (b) DEL and (c) SEQ fibres after excluding non-significant terms from the model.

(a)

Source	Sum of Squares	df	Mean Square	F value	p-value
Model	1068.60	5	213.72	55.59	< 0.0001
A-Temperature	167.38	1	167.38	43.53	< 0.0001
B-Residence time	192.70	1	192.70	50.12	< 0.0001
AB	389.16	1	389.16	101.21	< 0.0001
A^2	43.32	1	43.32	11.27	0.0047
B^2	136.71	1	136.71	35.56	< 0.0001
Residual	53.83	14	3.84		
Lack of Fit	52.73	9	5.86	26.77	0.0010
Pure Error	1.09	5	0.22		
Cor Total	1122.43	19			
R-Squared	0.95				
Adj R-Squared	0.93				
Pred R-Squared	0.78				

(b)

Source	Sum of Squares	df	Mean Square	F value	p-value
Model	1333.84	5	266.77	32.28	< 0.0001
A-Temperature	476.21	1	476.21	57.63	< 0.0001
B-Residence time	121.69	1	121.69	14.73	0.0018
AB	234.33	1	234.33	28.36	0.0001
A^2	245.87	1	245.87	29.75	< 0.0001
B^2	196.19	1	196.19	23.74	0.0002
Residual	115.69	14	8.26		
Lack of Fit	115.56	9	12.84	515.32	< 0.0001
Pure Error	0.12	5	0.03		
Cor Total	1449.53	19			
R-Squared	0.92				
Adj R-Squared	0.89				
Pred R-Squared	0.77				

(c)

Source	Sum of Squares	df	Mean Square	F value	p-value
Model	208.28	4	52.07	38.82	< 0.0001
A-Temperature	90.96	1	90.96	67.81	< 0.0001
B-Residence time	24.59	1	24.59	18.33	0.0007
AB	59.26	1	59.26	44.18	< 0.0001
A^2	67.81	1	67.81	50.56	< 0.0001
Residual	20.12	15	1.34		
Lack of Fit	20.11	10	2.01	1393.23	< 0.0001
Pure Error	0.01	5	0.00		
Cor Total	228.40	19			
R-Squared	0.91				
Adj R-Squared	0.89				
Pred R-Squared	0.79				

The analysis of variables significance was made through the variables (and their squared and interaction terms) p-values and 95% confidence interval was used. Hence, if $p>0.05$ the hypothesis that the term is insignificant is true. After analysing which terms were significant in

the model proposed, the terms considered non-significant were excluded and the model was calculated once again (Dejaegher and Vander Heyden, 2011).

The first-order model was unsuitable to represent the data probably due to a curvature in responses at the analysed range (Oehlert, 2000), thus it was not analysed. Therefore, only the second-order model, which contains all the terms of the first-order model plus the quadratic terms (Oehlert, 2000), will be discussed.

Table 4-7 shows the ANOVA and the regression parameters calculated by the Design Expert® Software in which it is possible to see some similarities when comparing the models significant terms for the three biomasses. For instance, significant terms of the second-order equation were: temperature (A); residence time (B); the interaction between temperature and residence time (AB); the square of temperature (A^2); and the square of residence time (B^2). The latest is an exception only for SEQ fibres, which presented B^2 as insignificant. Furthermore, the significance of squared terms (A^2 and B^2) as well as the interaction term (AB) is a confirmation that a first-order model would not be suitable for the analysed data (Bradley, 2007).

R-squared (R^2) is a measure of how much of the data variance is explained by the independent variables (Baş and Boyacı, 2007). The adjusted-R^2 (Adj R-squared) is an adjustment of the R^2 calculated according to the number of model parameters and the number of runs (Kraber, 2013). The predicted R^2 (Pred R-squared) is a measure of the capability of prediction of the model and its value should not have a difference higher than 0.2 compared to the adjusted-R^2 (Richard and Norbert, 2007).

R^2 values of the models are above 0.90 for all cases. Moreover, the comparison between adjusted and predicted R^2 is lower than 0.2 for the three biomasses. However, high R^2 values do not always represent a good regression model, hence, models with high R^2 can still fail to predict data (Baş and Boyacı, 2007). Moreover, although the close values of adjusted and

predicted R^2 is an indication of good model predictability, it is still not enough to consider a model predictable without analysing the model significance and the lack of fit (Richard and Norbert, 2007).

Nevertheless, although the logarithmic transformation provided improvement to the model significance compared to the raw data (data not shown) in all cases (three biomasses and the two responses), significant lack of fit ($p>0.05$) was still obtained for both responses (glucose concentration and hydrolysis percentage) in all biomasses.

The lack of fit is a test calculated by the centre point repetitions and compared to the factorial points mean (Bradley, 2007). Significant lack of fit means that the model is not capable of representing the mean structure (Oehlert, 2000). Moreover, although the model was considered significant (p-values <0.0001) and, therefore, a RSM was generated, its evaluation is not useful if the model presents lack of fit, thus, does not predict new responses.

Although a representative model was not satisfactory obtained, the data generated by the runs in the DoE is liable for interpretation of SBW hydrolysis of cellulose fibres.

Table 4-10 shows the concentration of glucose, fructose, and HMF (g/L) as well as hydrolysis percentage (%) for each of the 20 runs of DoE for Avicel, DEL and SEQ fibres.

Highest glucose yield (Y_{glu}) were achieved for different conditions for each biomass: Avicel have its maximum Y_{glu} (8.7-9.7%) for low temperatures and long residence times (220ºC and 40min); DEL showed highest Y_{glu} (2.2-2.5%) in the centre point (265ºC, 20min, 3% biomass); and SEQ presented maximum Y_{glu} (2-2.5%) for both the centre point and the low temperature/long residence time (220ºC, 40min).

Looking at the centre point, it can be seen that glucose concentration for Avicel is lower than for DEL and SEQ fibres. As the results of the scoping experiments suggested, Avicel have the glucose concentration maximum peak before the *Miscanthus* fibres, this result is an

indication that at the centre point, glucose concentration is already depleting due to further decomposition for Avicel and possible even for DEL and SEQ fibres as well.

Fructose was produced in higher quantities (proportionally to initial mass, Fru/m_i) for high temperatures (310^{o}C) for Avicel, high temperatures (310^{o}C) and centre point for DEL and high temperatures/long residence time (310^{o}C, 40min and 317^{o}C, 20min) and also in the centre point for SEQ. The fact that significant amounts of fructose is being generated already in the centre point for *Miscanthus* fibres is another indication that glucose maximum peak has already been passed at this condition and, thus, glucose previously released was decomposed into fructose.

HMF is being produced in high amounts (proportionally to fibres initial mass, HMF/m_i) at high temperature/short residence time (310^{o}C, 0min) for Avicel, at the centre point for DEL and at high temperature/short residence time and at the centre point for SEQ.

As expected, harsher conditions (high temperatures or long residence times) led to higher hydrolysis percentages. However, comparing hydrolysis percentage for temperatures at 310^{o}C and residence times of 0-40min, it can be seen that longer residence times seems to decrease hydrolysis at high temperatures. The same effect is not observed for 280^{o}C.

This effect of an apparent decreasing in biomass hydrolysis at high temperatures has being reported previously as the result of the formation of precipitates (Carapetudo Antas, 2015). Hashaiken et al. (2007) evaluated hydrolysis of willow in SBW (200-320^{o}C) using both batch and continuous reactor. They observed that temperatures higher than 300^{o}C did not increase hydrolysis percentage. On the contrary, at high temperatures, hydrolysis was lower than at temperatures below 300^{o}C for both reactors configuration. They attributed this decreasing in hydrolysis to an increase in the rate of re-condensation reactions that generate precipitates (Hashaikeh et al., 2007).

Table 4-8 - Results of SBW hydrolysis of cellulose fibres (Avicel, DEL and SEQ) for glucose, fructose and HMF concentration analysed by HPAEC, and calculated hydrolysis percentage and glucose yield (%) for 20 runs of the DoE.

DoE-1				AVICEL							DEL							SEQ						
Run	**T (^oC)**	**Res. time (min)**	**Load (%)**	**Hydrolysis (%)**	**Glu (g/L)**	**Yield Glu (%)**	**Fru (g/L)**	***Fru/m_i (%)**	**HMF (g/L)**	****HMF/m_i (%)**	**Hydrolysis (%)**	**Glu (g/L)**	**Yield Glu (%)**	**Fru (g/L)**	**Fru (g/L)**	**HMF (g/L)**	**HMF/m_i (%)**	**Hydrolysis (%)**	**Glu (g/L)**	**Yield Glu (%)**	**Fru (g/L)**	**Fru (g/L)**	**HMF (g/L)**	**HMF/m_i (%)**
1	265	20	6.4	64.4	0.28	0.39	1.11	1.59	2.32	3.32	60.2	1.37	1.97	0.87	1.25	4.43	6.34	59.9	1.61	2.30	1.54	2.21	4.48	6.42
2	310	0	1.0	78.8	0.09	0.85	0.38	3.46	0.74	6.75	87.3	0.00	0.00	0.00	0.01	0.37	3.38	83.8	0.01	0.10	0.30	2.68	0.69	6.25
3	265	20	3.0	68.3	0.12	0.38	0.58	1.77	0.94	2.86	66.9	0.54	1.64	0.61	1.85	2.65	8.03	65.2	0.83	2.53	0.68	2.06	2.75	8.32
4	310	0	5.0	67.2	0.23	0.41	1.24	2.25	2.31	4.19	72.8	0.01	0.01	1.21	2.20	1.99	3.62	64.2	0.05	0.09	1.12	2.04	3.37	6.13
5	265	20	3.0	67.6	0.07	0.22	0.55	1.66	0.93	2.82	66.8	0.82	2.49	0.76	2.29	2.61	7.92	65.1	0.75	2.28	0.99	2.99	2.28	6.90
6	220	0	5.0	7.8	0.01	0.01	0.01	0.02	0.02	0.04	7.3	0.00	0.00	0.01	0.01	0.01	0.02	5.6	0.00	0.01	0.00	0.01	0.00	0.00
7	220	40	5.0	23.5	5.31	9.65	0.46	0.83	1.42	2.58	19.0	0.57	1.04	0.21	0.37	0.79	1.44	19.9	1.23	2.24	0.23	0.42	1.16	2.10
8	310	40	5.0	61.6	0.00	0.00	2.01	3.65	0.00	0.00	69.6	0.00	0.00	1.12	2.04	0.01	0.02	60.3	0.00	0.00	1.65	3.00	0.00	0.00
9	220	40	1.0	27.5	0.96	8.73	0.11	0.97	0.32	2.92	22.9	0.06	0.54	0.04	0.37	0.10	0.90	21.9	0.27	2.45	0.04	0.34	0.54	4.95
10	265	20	0.5	92.5	0.04	0.79	0.18	3.24	0.30	5.54	84.7	0.02	0.29	0.08	1.44	0.34	6.24	80.1	0.01	0.26	0.18	3.32	0.41	7.37
11	265	0	3.0	14.1	0.67	2.02	0.11	0.32	0.09	0.28	19.2	0.08	0.25	0.25	0.75	0.05	0.16	17.2	0.17	0.50	0.24	0.73	0.06	0.18
12	265	20	3.0	62.7	0.05	0.16	0.55	1.65	0.98	2.97	73.2	0.73	2.22	0.92	2.79	2.68	8.11	72.4	0.84	2.55	1.37	4.15	2.44	7.39
13	265	54	3.0	55.3	0.00	0.00	0.50	1.52	0.02	0.06	61.6	0.00	0.00	0.68	2.07	0.14	0.42	63.8	0.00	0.00	1.05	3.20	0.04	0.11
14	265	20	3.0	61.1	0.04	0.11	0.52	1.58	0.76	2.29	68.0	0.77	2.32	0.80	2.42	2.59	7.85	64.8	0.75	2.28	0.86	2.62	2.15	6.50
15	190	20	3.0	5.8	0.01	0.02	0.00	0.01	0.00	0.00	11.0	0.02	0.07	0.01	0.03	0.01	0.02	9.7	0.01	0.04	0.01	0.02	0.01	0.02
16	317	20	3.0	60.4	0.00	0.00	0.26	0.80	0.17	0.53	71.9	0.00	0.00	0.95	2.89	0.03	0.10	65.3	0.00	0.00	1.40	4.25	0.01	0.04
17	265	20	3.0	62.2	0.05	0.16	0.68	2.07	0.89	2.69	71.6	0.69	2.09	0.74	2.25	2.24	6.78	69.5	0.71	2.16	0.74	2.23	2.21	6.71
18	310	40	1.0	70.4	0.00	0.00	0.44	4.01	0.00	0.00	78.5	0.00	0.00	0.48	4.36	0.02	0.14	76.5	0.00	0.00	0.79	7.21	0.00	0.00
19	265	20	3.0	61.4	0.04	0.11	0.83	2.52	0.76	2.30	65.4	0.83	2.52	0.62	1.88	2.95	8.94	65.7	0.67	2.04	0.91	2.75	2.37	7.17
20	220	0	1.0	11.1	0.00	0.01	0.00	0.02	0.00	0.01	8.7	0.00	0.00	0.00	0.01	0.00	0.04	8.4	0.00	0.01	0.00	0.01	0.00	0.01

*Fru/m_i = fructose generated (g/L) divided by available cellulose ($\frac{Fru}{m_i} = \frac{fructose}{1.1*f*cellulose} * 100\%$), in which f is the fraction of cellulose in each biomass, i.e, f=1, 0.80 and 0.79 for Avicel, DEL and SEQ, respectively.

**HMF/m_i = HMF generated (g/L) divided by available cellulose ($\frac{HMF}{m_i} = \frac{HMF}{1.1*f*cellulose} 100\%$).

These precipitates compounds culminate in accounting as residual solid biomass after SBW hydrolysis resulting in an underestimation of hydrolysed biomass and, thus, decreasing hydrolysis percentage.

At this point, the objective of DoE was to optimize glucose production/yield and possible reactions paths during SBW hydrolysis are discussed in section 4.3.6. The results of glucose, fructose and HMF concentrations obtained by this DoE are an insight that the highest glucose concentration peak is in the range studied, however, the model was not able to represent the reaction and software optimization was not possible. Moreover, glucose yields obtained in this DoE were rather low. As higher glucose yields were achieved during the scoping experiments, it is clear that further glucose yield optimization by SBW hydrolysis is possible.

In order to try to optimize the process, it was necessary to understand the reason why the current DoE was not able to create a predicted model for the SBW hydrolysis process. As the same result was obtained for all three biomasses, it suggests that the problem was related to the reaction modelling more than with the acquired data. In addition, it is improbable that a second order equation is capable of modelling the entire range of independent variables (Montgomery, 2000). Moreover, the persistent lack of fit might indicate that the level of the parameters chosen could have been too broad and, therefore, the modelling of the entire region evaluated by the RSM was not possible (Baş and Boyacı, 2007, Oehlert, 2000). Therefore, in order to try to optimize the reaction, a second DoE was performed aiming to evaluate a smaller region, which could possible allow the obtainment of an accurate new model.

4.3.4.2. DoE-2

As temperature showed to have the greatest effect among the parameters, which was indicated by the lower p-value compared to residence time, DoE-2 was made by limiting the

temperature range from 220-280ºC. The other two parameters, residence time and loading, were kept at the same levels. It was chosen not to decrease residence time levels as DoE results showed high glucose yields for long residence times at low temperatures. Moreover, although biomass loading had no significant effect in the first DoE, it could be the result of the wide range used. Thus, loading was kept as one of the parameters for DoE-2.

Table 4-9 shows the ANOVA and the regression parameters calculated by the Design Expert® software for glucose concentration after SBW hydrolysis for DoE-2 using Avicel (a), DEL (b) and SEQ fibres (c). In DoE-2, HMF concentration (g/L) was also analysed as one response with the aim of finding a parameters range in which not only glucose is maximized, but HMF formation is minimized as well. Results for hydrolysis percentage and HMF concentration can be found in 0.

Table 4-9 shows that, although the models are significant (p-value<0.05) for all three biomasses, all of them presented lack of fit once again. Comparing the models resulted from DoE (Table 4-7) and DoE-2, it is possible to see that SEQ and DEL fibres have very similar results in terms of significant variables. Temperature (A), residence time (B), the interaction between temperature and residence time (AB) and squared of temperature (A^2) are significant terms for both DEL and SEQ in DoE-2 as it occurred for DoE. In the case of DEL fibres, DoE showed B^2 as a significant term, which did not happened in the DoE-2.

Particularly for Avicel, one of the runs was excluded when calculating the parameters shown in Table 4-9-a: run 20 (300ºC, 20min, 3% biomass load) performed as a significant outlier, and no model was achieved when using this run for calculation. Therefore, run 20 was excluded solely for Avicel. That might be the reason why Avicel results in the DoE-2 behaved differently both from previous DoE and from SEQ/DEL fibres in terms of significant terms of the model. Model for Avicel in DoE-2 suggests loading (C) and its squared term (C^2) as

significant, which did not occur in any other results both from glucose concentration of hydrolysis percentage. Moreover, the fact that loading was not considered significant in most of the cases is most likely because of the small range used in the evaluation.

Table 4-9 - ANOVA for glucose concentration (g/L) after SBW for DoE-2using a 3-factor CCD for (a) Avicel, (b) DEL and (c) SEQ fibres after excluding non-significant terms from the model.

(a)

Source	Sum of Squares	df	Mean Square	F value	p-value
Model	117.29	7	16.76	188.50	< 0.0001
A-Temperature	3.14	1	3.14	35.36	< 0.0001
B-Residence time	0.11	1	0.11	1.25	0.2874
AB	9.77	1	9.77	109.93	< 0.0001
C - Loading	67.74	1	67.74	762.04	< 0.0001
A^2	2.84	1	2.84	31.92	0.0001
B^2	24.42	1	24.42	274.78	< 0.0001
C^2	1.21	1	1.21	13.57	0.0036
Residual	0.98	11	0.09		
Lack of Fit	0.90	6	0.15	10.03	0.0115
Pure Error	0.08	5	0.02		
Cor Total	118.27	18			
R-Squared	0.99				
Adj R-Squared	0.99				
Pred R-Squared	0.96				

(b)

Source	Sum of Squares	df	Mean Square	F value	p-value
Model	1133.63	4	283.41	42.56	< 0.0001
A-Temperature	654.07	1	654.07	98.22	< 0.0001
B-Residence time	363.12	1	363.12	54.53	< 0.0001
AB	384.39	1	384.39	57.72	< 0.0001
A^2	345.21	1	345.21	51.84	< 0.0001
Residual	99.89	15	6.66		
Lack of Fit	99.85	10	9.99	1522.56	< 0.0001
Pure Error	0.03	5	0.01		
Cor Total	1233.52	19			
R-Squared	0.92				
Adj R-Squared	0.90				
Pred R-Squared	0.80				

(c)

Source	Sum of Squares	df	Mean Square	F value	p-value
Model	1238.89	4	309.72	44.13	< 0.0001
A-Temperature	690.22	1	690.22	98.33	< 0.0001
B-Residence time	418.07	1	418.07	59.56	< 0.0001
AB	422.34	1	422.34	60.17	< 0.0001
A^2	435.54	1	435.54	62.05	< 0.0001
Residual	105.29	15	7.02		
Lack of Fit	105.26	10	10.53	1810.47	< 0.0001
Pure Error	0.03	5	0.01		
Cor Total	1344.18	19			
R-Squared	0.92				
Adj R-Squared	0.90				
Pred R-Squared	0.83				

When more than one response is analysed at the same time, firstly a model for each responses should be created. Then, the models should be overlapped and conditions that optimize all the responses should be found. In practice, this is not easy to achieve and, therefore,

one of the response should be prioritized for optimization while the other conditions should be aimed to a desired range (Montgomery, 2000). For instance, considering as responses hydrolysis percentage and glucose/HMF concentration, glucose should be prioritized for maximization. Moreover, hydrolysis should not be less than a 60-70% for example; and HMF concentration should not be higher than a toxic amount for a particular yeast during further fermentation. However, as the model is not capable of predicting new data, the combined evaluation of several variables at the same time in order to optimize them was not possible.

Although RSM is an useful tool to understand chemical/biological systems, not all systems/reactions can be predicted by a second-order model (Baş and Boyacı, 2007). Moreover, the tests performed for the DoE analysis in this work were based on the ANOVA and the regression parameter, which have some assumptions such as that the data is normally distributed and have constant variance (Montgomery, 2000). These assumptions are not always true in the real-world problems, however, low degrees of these irregularities might be fixed by some tools (Oehlert, 2000).

For instance, a common approach to handle non-normally distributed data is to apply a response transformation and try to re-analyse the data through RSM (Johnson and Montgomery, 2009, Oehlert, 2000). However, even after applying response-transformation using logarithm, the lack of fit persisted for all responses models both for DoE and for DoE-2. The impossibility of generating a predict model might suggest that response could have a non-normal distribution and, therefore, the analysis of tools such as ANOVA might not be possible or have been affected by the non-normality of the data (Oehlert, 2000).

The Normal Plot of Residuals created by the Design Expert® can be used to diagnose normal distribution and confirm/deny data non-normality. Figure 4-7 shows the Normal Plot of

Residuals (after logarithm-transformation of the data) for glucose concentration (g/L) after SBW hydrolysis for DoE-2 for Avicel (a), DEL (b) and SEQ (c) fibres.

In the case that the response follows a normal distribution, the Normal Plot of Residuals shows the residuals of runs following a straight line (Kraber, 2013). Figure 4-7 shows clearly that none of the plot for the three fibres present a straight line. The same result was found for the first DoE in all the responses: glucose/HMF concentration (g/L) and hydrolysis percentage (%), for all biomasses (data not shown). Therefore, it can be concluded that all the data for both DoEs are non-normally distributed.

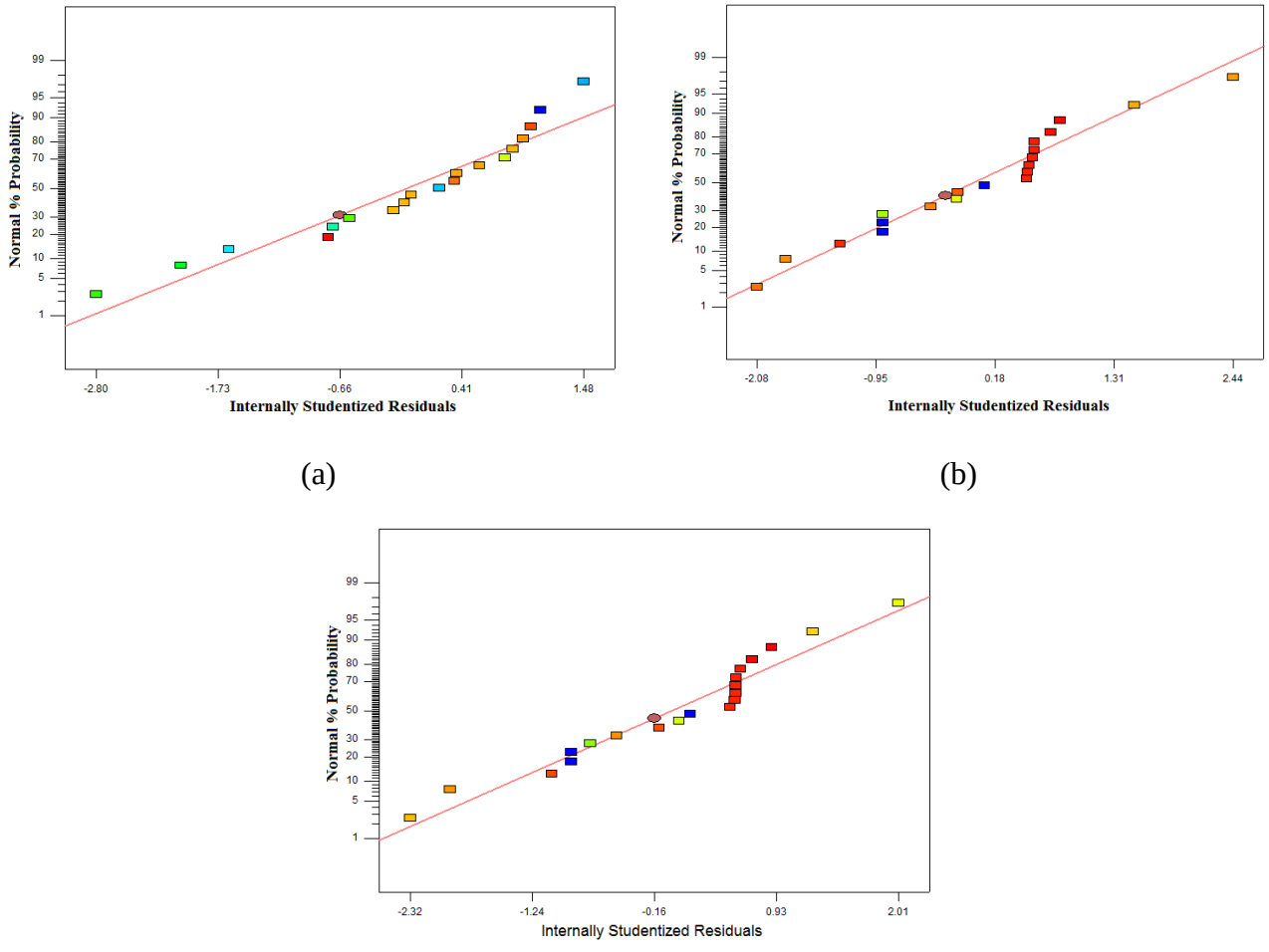

Figure 4-7 - Normal Plot of Residuals obtained by Design Expert® for glucose concentration (g/L) after SBW hydrolysis in DoE-2 for Avicel (a), Del (b) and SEQ fibres (c).

There are cases in which non-normal distributions can still be analysed by ANOVA and it depends on how much the data is far from normality, which is very difficult to determine (Oehlert, 2000). However, even though the ANOVA results could have been compromised by the non-normality of the data, some conclusions can still be suggested. For instance, the results of p-values are thought to be less affected by non-normality (Oehlert, 2000). Moreover, as the significance of variables analysed by the p-values was reasonably similar in the two DoEs and for both of the responses (glucose and hydrolysis percentage), the parameters that most affect the responses analysed for SBW could still be suggested even when the data fails the normality assumption. These parameters would be the temperature, residence time, the interaction between these two and the squared of temperature.

The difficulty of getting a model that predicts the process could also be related to the changes made in the axial levels (see section 4.2.3). The axial points performed in a CCD are the conditions used for estimation of the quadratic terms (Bradley, 2007). Therefore, the modification of these parameters values might have resulted in the impossibility of getting a predictable model and contributed significantly for the lack of fit obtained for all conditions and biomass analysed.

Optimization of SBW hydrolysis of lignocellulosic biomass conversion using RSM and design of experiments have been reported in literature. Mazaheri et al. (2010) investigated the performance of SBW hydrolysis of oil palm in a batch reactor through RSM using a central composite rotatable design and 5 parameters: temperature (220-320^{o}C), residence time (7.5-82.5min), particle size (<250μm and between 710-1000μm), biomass loading (3.75-16.25g in 100mL of water) and percentage of NaOH used as an additive (0-10wt.%). They used only one response, liquid products percentage and they reported have obtained a significant model that present high R^2 (0.94) and adj-R^2 (0.93) and insignificant lack of fit (Mazaheri et al., 2010).

The fact that they used a 5-factors CCD and, therefore, performed a much larger number of experiments (42 against 20 runs performed in DoE and DoE-2) might have been an advantage in terms of statistical analysis. ANOVA, in some cases, might provide a fair analysis even for non-normally distributed samples particularly for high number of runs (Oehlert, 2000).

Xin and Saka (2008) used RSM to optimize hydrolysis of Japanese beech in a 5mL batch reactor. They evaluated only two parameters, temperature and residence time, in a small range, 170-220^{o}C and 3-15min using a full factorial experimental design. They obtained a good model prediction and high regression parameters (R^2 and adj-R^2) and were able to statistically optimize the process for sugars release (Saka, 2008). Although they did not present values for the lack of fit of the models or comparison between predicted and actual results of the optimal point, their design of experiments was simpler than the one performed in this work and in a narrower range, which could have contributed to the successful result in their modelling.

In conclusion, it is still not clear whether the non-normality of data and/or the manipulation of the levels of axial points in the CCD affected the overall results of the analysis, or if the range evaluated was still too broad even after shortening it for DoE-2. However, even though the model is not significant and cannot be used for future predictions, it still can be used to find best conditions that leads to target responses (Dejaegher and Vander Heyden, 2011). Moreover, results of DoE-2 are liable to be analysed and conclusions could be made from them.

Table 4-10 shows DoE-2 results for several compounds concentration in g/L (glucose, xylose, fructose, HMF and furfural) as well as for hydrolysis percentage (%).

Initially, comparing the results obtained from DoE (Table 4-8) and DoE-2 (Table 4-10), it is possible to see that higher glucose yields were achieved using the conditions of DoE-2. For instance, maximum Y_{glu} obtained in DoE-2 were 20.0, 3.3 and 11.2% for Avicel, DEL and SEQ, respectively, whereas in DoE the maximum Y_{glu} were 9.7, 2.5 and 2.6%, respectively.

For Avicel, high temperature and low residence time (280°C, 0min) resulted in the highest hydrolysis percentage and Y_{glu}. However, at these conditions, high amounts of fructose, HMF and furfural were also identified. Significant amounts of these decomposition/isomerization products indicates that released glucose is already undergoing further reaction even during the heating time. This is a constraint of the reactor type, as batch reactor usually requires significantly higher heating times than it is needed in flow reactors, for example (Yu et al., 2007). Therefore, glucose being generated during the heating time will be further decomposed if not separated as soon as it is released (Jørgensen et al., 2007), which is not feasible in the current reactor configuration.

DEL fibres showed very small improvement in terms of glucose production compared to results from the first DoE. Maximum Y_{glu} were obtained both in the centre point (250°C, 20min) and high temperature/low residence times (280°C, 0min). Loading did not demonstrated a significant influence in Y_{glu}, as predicted by the model. An exception was for the lowest biomass load (0.5%) in run 17, which resulted in much lower Y_{glu} compared to same temperature/residence time conditions with other loads (3 and 6.4%). As cellulose hydrolysis is believed to be a superficial reaction (Zhao et al., 2009c), it is possible that hydrolysis occur very fast when the loading is very low, therefore, glucose is decomposed faster when compared to higher loadings.

Maximum Y_{glu} for SEQ fibres were achieved at the same conditions as for DEL fibres (250°C/20min and 280°C/0min), however, in considerably higher values. Moreover, as it happened for Avicel, the conditions used in the DoE-2 significantly improved Y_{glu} from SEQ fibres.

Comparing DEL and SEQ fibres it is possible to see significant differences in terms of concentration of soluble products. As these fibres showed a very similar composition

Table 4-10 - Results of SBW hydrolysis of cellulose fibres(Avicel, DEL and SEQ) for glucose, fructose, HMF concentration (g/L) analysed by HPAEC; furfural concentration analysed by HPLC; and calculated hydrolysis percentage and glucose yield (%) for 20 runs of the DoE-2.

DoE-2				AVICEL									DEL										SEQ									
Run	T (°C)	Res. time (min)	Load (%)	Hydrol. (%)	Glu (g/L)	YGlu (%)	Fru (g/L)	* Fru/ m_i (%)	HMF (g/L)	** HMF/ m_i (%)	Furfural (g/L)	*** Furfural /m_i (%)	Hydrol. (%)	Glu (g/L)	YGlu (%)	Xyl (g/L)	**** Xyl/ m_i (%)	Fru (g/L)	* Fru/ m_i (%)	HMF (g/L)	** HMF /m_i (%)	Furfural (g/L)	*** Furfural/ m_i (%)	Hydrol. (%)	YGlu (%)	YGlu (%)	Xyl (g/L)	**** Xyl/ m_i (%)	Fru (g/L)	* Fru/ m_i (%)	HMF (g/L)	** HMF /m_i (%)	Furfural (g/L)	*** Furfural/ m_i (%)
1	220	40	5.0	22.7	5.43	9.8	0.78	1.4	1.42	2.6	0.77	1.4	19.0	0.64	1.4	0.05	1.1	0.28	0.6	0.92	2.1	0.53	1.1	21.9	1.01	2.3	0.17	6.3	0.48	1.1	1.14	2.6	0.52	1.1
2	280	0	5.0	83.2	10.01	18.0	3.54	6.4	4.03	7.3	1.53	2.8	31.3	1.24	2.8	0.00	0.0	1.87	4.2	0.90	2.0	0.59	1.2	54.8	4.91	11.2	0.00	0.0	3.88	8.9	3.37	7.7	1.05	2.3
3	220	0	1.0	9.6	0.00	0.0	0.00	0.0	0.00	0.0	0.00	0.0	9.3	0.00	0.0	<0.01	0.2	0.00	0.0	0.00	0.0	0.01	0.1	9.3	0.00	0.0	<0.01	0.4	0.00	0.0	0.00	0.0	0.00	0.0
4	250	20	3.0	74.8	2.46	7.4	1.64	5.0	3.54	10.7	1.10	3.3	46.9	0.84	3.2	0.00	0.0	1.29	4.9	2.11	7.9	0.56	1.9	51.5	2.14	8.2	0.00	0.0	1.52	5.8	2.34	8.9	0.71	2.5
5	250	20	3.0	70.9	2.88	8.6	1.74	5.3	3.04	9.2	0.91	2.8	36.6	0.87	3.3	0.00	0.0	1.44	5.4	2.25	8.5	0.61	2.1	53.0	2.38	9.1	0.00	0.0	1.53	5.8	3.14	11.9	0.75	2.7
6	250	54	3.0	63.8	0.02	0.0	2.36	7.1	0.14	0.4	0.47	1.4	68.2	0.03	0.1	0.00	0.0	0.43	1.6	0.85	3.2	0.73	2.5	64.4	0.03	0.1	0.00	0.0	3.10	11.8	1.19	4.5	0.57	2.0
7	220	40	1.0	31.0	0.82	7.4	0.13	1.2	0.49	4.4	0.17	1.5	23.9	0.12	1.4	0.01	1.6	0.05	0.6	0.11	1.2	0.14	1.5	21.9	0.15	1.7	0.04	8.3	0.10	1.2	0.13	1.5	0.10	1.1
8	250	0	3.0	9.3	0.32	0.9	0.00	0.0	0.06	0.2	0.03	0.1	15.5	0.07	0.2	0.12	4.9	0.37	1.4	0.04	0.1	0.12	0.4	13.1	0.06	0.2	0.20	12.2	0.26	1.0	0.03	0.1	0.11	0.4
9	280	0	1.0	94.1	2.22	20.0	0.78	7.1	0.85	7.7	0.36	3.3	24.0	0.20	2.2	0.00	0.0	0.25	2.9	0.04	0.5	0.09	0.9	22.9	0.84	9.6	0.00	0.0	0.61	6.9	0.40	4.6	0.17	1.9
10	250	20	3.0	73.5	2.59	7.8	1.84	5.6	3.45	10.4	0.99	3.0	43.6	0.87	3.3	0.00	0.0	1.44	5.4	2.25	8.5	0.60	2.1	60.2	2.44	9.3	0.00	0.0	1.74	6.6	3.30	12.5	0.87	3.1
11	250	20	3.0	67.3	2.11	6.3	1.71	5.2	3.21	9.7	1.14	3.5	44.6	0.72	2.7	0.00	0.0	1.09	4.1	2.00	7.5	0.70	2.4	59.3	2.46	9.3	0.00	0.0	1.75	6.7	3.41	13.0	0.88	3.2
12	200	20	3.0	7.3	0.11	0.3	0.08	0.2	0.06	0.2	0.03	0.1	3.5	0.05	0.2	2.15	87.0	0.13	0.5	0.02	0.1	0.17	0.6	12.7	0.01	0.0	1.54	96.4	0.00	0.0	0.00	0.0	0.08	0.3
13	250	20	3.0	73.7	2.20	6.6	1.92	5.8	3.66	11.1	1.09	3.3	50.0	0.77	2.9	0.00	0.0	1.16	4.4	2.03	7.6	0.63	2.2	61.0	2.44	9.3	0.00	0.0	1.72	6.5	3.43	13.1	0.93	3.3
14	250	20	3.0	68.2	2.16	6.5	1.90	5.8	3.29	10.0	0.96	2.9	42.4	0.74	2.8	0.00	0.0	1.25	4.7	1.91	7.2	0.66	2.3	53.6	2.72	10.4	0.00	0.0	1.81	6.9	3.39	12.9	0.81	2.9
15	250	20	6.4	61.0	3.97	5.6	3.92	5.6	3.09	4.4	1.58	2.3	48.9	1.60	2.8	0.00	0.0	2.25	4.0	4.67	8.3	1.48	2.4	57.1	5.46	9.8	0.00	0.0	2.75	5.0	7.73	13.9	1.75	3.0
16	220	0	5.0	6.2	0.01	0.0	0.00	0.0	0.02	0.0	0.01	0.0	7.3	0.00	0.0	0.02	0.4	0.01	0.0	0.01	0.0	0.03	0.1	6.5	0.00	0.0	0.01	0.6	0.01	0.0	0.00	0.0	0.00	0.0
17	250	20	0.5	83.2	0.22	3.9	0.36	6.6	0.70	12.8	0.17	3.1	47.5	0.08	1.7	0.00	0.0	0.10	2.4	0.13	2.9	0.04	0.8	71.2	0.17	3.8	0.00	0.0	0.43	9.7	0.47	10.6	0.16	3.5
18	280	40	5.0	58.2	0.04	0.1	5.22	9.5	0.00	0.0	0.33	0.6	63.3	0.00	0.0	0.00	0.0	2.03	4.6	0.07	0.2	0.20	0.4	67.3	0.00	0.0	0.00	0.0	3.10	7.1	0.04	0.1	0.30	0.7
19	280	40	1.0	69.3	0.01	0.1	0.93	8.5	0.00	0.0	0.08	0.7	68.4	0.00	0.0	0.00	0.0	0.66	7.4	0.08	0.9	0.04	0.5	75.1	0.00	0.0	0.00	0.0	1.07	12.2	0.02	0.2	0.06	0.6
20	300	20	3.0	73.9	0.00	0.0	2.04	6.2	0.32	1.0	0.40	1.2	65.1	0.00	0.0	0.00	0.0	1.71	6.4	0.03	0.1	0.39	1.3	68.5	0.00	0.0	0.00	0.0	3.83	14.6	0.09	0.3	0.41	1.5

*Fru/m_i = fructose generated divided by available cellulose (g/L): $\frac{Fru}{m_i} = \frac{fructose}{1.1*f*cellulose} * 100\%$, in which f is the fraction of cellulose in each biomass, i.e, f=1, 0.80 and 0.79 for Avicel, DEL and SEQ, respectively.

**HMF/m_i = HMF generated divided by available cellulose (g/L): $\frac{Fru}{m_i} = \frac{HMF}{1.1*f*cellulose} * 100\%$; ***Furfural/$m_i$ = Furfural generated divided by available cellulose + hemicellulose (g/L): $\frac{furfural}{m_i} = \frac{HMF}{1.1*f*hemi+cellulose} * 100\%$.

****Xyl/m_i = xylose generated divided by available hemicellulose (g/L): $\frac{Xyl}{m_i} = \frac{xylose}{1.1*f*hemicellulose} * 100\%$, in which f is the fraction of hemicellulose in each biomass, i.e, 0.072 and 0.048 for DEL and SEQ, respectively.

(section 3.3.6.2), it is clear that the difference presented by these two fibres during SBW hydrolysis is due to structural differences. The result is a strong suggestion that the hypothesis placed in the previous chapter was accurate about the sequential extraction not only selectively extracting target compounds but also modify the remaining fibres structure.

The comparison of the results in both DoEs for Avicel, DEL and SEQ fibres confirmed that pure cellulose led to significant higher glucose yields and hydrolysis percentage. The higher efficiency of hydrolysing Avicel compared to lignocellulose fibres is most likely due to structural differences. Even after the direct/sequential processing, cellulose fibres obtained from lignocellulosic biomass are still bonded at some extent to lignin, which probably makes it more difficult to access cellulose bonds than in a pure cellulose material. Moreover, the significant difference between the particle size of Avicel and the fibres generated from processing of MxG might have affected cellulose hydrolysis. Avicel is a fine dust, whereas DEL and SEQ fibres are a much larger fibre of about 8-10 times Avicel particle size (see Figure 3-19). Large particle size could lead to both heat transfer problems and difficult the accessibility of bonds and also to problems related to surface overcooking and incomplete hydrolysis of internal portions (Ruiz et al., 2013).

Fructose and HMF showed the concentration same pattern presented in the first DoE for all three biomasses: very little of these compounds is being generated for mild conditions (temperatures up to 250^{o}C and residence times up to 20min). Then, an increase in process severity increase their formation until a maximum, followed by a decreasing due to their decomposition.

Xylose was only detected at mild temperatures (200-220^{o}C) and at 250^{o}C/0min for both DEL and SEQ. It is even possible that xylose might have been generated in higher amounts than detected in DoE-2 samples, because at these temperatures xylose is not stable and it will

rapidly undergo decomposition (Chen et al., 2008). In fact, Jing and Lü (2007 and 2008) evaluated both xylose and glucose decomposition in SBW using a batch reactor and described that glucose achieved 96% decomposition at 220^{o}C after 90min (Jing and Lü, 2008), while the same percentage of xylose decomposition was achieved after only 50min at the same temperature (Chen et al., 2008). Their findings suggest that not only xylose will be released from hemicellulose faster than glucose from cellulose, due to already discussed structural reasons, but also xylose will be faster decomposed compared to glucose and, therefore, more difficult to detect in the hydrolysis extract. Moreover, as expected, no xylose was detected for Avicel samples.

Hydrolysis percentage achieved values up to 94% for Avicel, however, both DEL and SEQ fibres showed maximum hydrolysis of about 68-75%. As values as high as 87% were obtained in the first DoE, it can be concluded that DEL and SEQ can be further hydrolysed, however, they need harsher conditions than those performed in the DoE-2.

Furfural was not among the compounds to be investigated during SBW hydrolysis at first because it is widely accepted that this compound is a result of C-5 dehydration (Chen et al., 2008). Moreover, as the xylose is the only C-5 sugar in SEQ and DEL fibres and it is presented in small percentage (4.8 and 7.2% in SEQ and DEL fibres, respectively), it was considered that furfural would be produced in insignificant conditions. However, while analysing the HPAEC chromatograms from DoE-2, it was observed that a reasonable amount of xylose was being produced in mild temperatures (200 and 220^{o}C). Moreover, as xylose decomposes into furfural, which is thought to be very toxic for yeasts during fermentation (Palmqvist and Hahn-Hägerdal, 2000b), it was decided to run all samples of DoE-2 in HPLC for furfural quantification.

Table 4-10 shows that, on the contrary of what was expected, furfural is produced in most of the runs performed in the DoE-2. Unexpectedly, furfural is produced in significant quantities even for Avicel, which does not contain C-5 sugars. The presence of furfural in most of the DoE-2 conditions, and particularly in Avicel samples, is a confirmation that furfural is not produced exclusively from C-5 sugars. Furthermore, it is likely that a mechanism of furfural generation from glucose is possible even though it is not well addressed in the literature. Furfural generation is further discussed in next sections.

4.3.5. Mass balance after SBW hydrolysis

In order to estimate the losses during the SBW hydrolysis, a mass balance was calculated only for DoE-2. Table 4-11 shows the mass balance after SBW hydrolysis in which the initial mass (m_i), the mass left in the reactor after SBW hydrolysis (m_f) and the mass obtained by drying the liquid fraction after the hydrolysis (DW) can be seen for Avicel, SEQ and DEL fibres.

As it can be seen in Table 4-11, mass balance values are quite far from the ideally expected 100%. Moreover, some of the DoE-2 conditions have lower values for all three biomasses, for instance, run 20 presents the lowest mass balance values for all fibres, which suggest that the run conditions is affecting the mass recovery.

Two phenomenon could be associated with the apparent ‘loss’ of mass: 1) evaporation of other compounds than only water, for instance HMF, furfural and organic acids (acetic, formic), during the drying step performed to calculate DW; and 2) formation of a gas fraction (gasification) during the SBW hydrolysis.

In order to quantify how much HMF would evaporate in the conditions used for drying the samples (65^{o}C until samples were completely dried), HMF samples were dried using the

same protocols used for the samples (section 4.2.1.2.3). In these conditions, 27 ± 2% of HMF was evaporated during the drying step. Therefore, it can be concluded that part of the HMF contents of the samples was also evaporated during samples drying stage, which can account for some of the mass loss presented by the mass balance.

Table 4-11 - Mass balance after SBW hydrolysis for Avicel, DEL and SEQ fibres.

DoE-2				AVICEL			DEL			SEQ		
Run	**T (°C)**	**Res. time (min)**	**m_i (g)**	**m_f (g)**	**DW (g)**	**Mass balance (%)**	**m_f (g)**	**DW (g)**	**Mass balance (%)**	**m_f (g)**	**DW (g)**	**Mass balance (%)**
1	220	40	0.75	0.58	0.10	90.73	0.61	0.06	88.37	0.59	0.08	89.33
2	280	0	0.75	0.13	0.52	86.64	0.52	0.10	81.65	0.34	0.31	86.62
3	220	0	0.15	0.14	0.01	94.44	0.14	0.00	92.07	0.14	0.00	92.67
4	250	20	0.45	0.11	0.20	68.62	0.24	0.06	67.45	0.25	0.07	72.37
5	250	20	0.45	0.13	0.14	60.64	0.29	0.05	74.35	0.21	0.10	69.75
6	250	54	0.45	0.16	0.14	67.17	0.14	0.12	59.21	0.16	0.11	60.22
7	220	40	0.15	0.10	0.03	88.69	0.11	0.01	80.81	0.12	0.01	87.08
8	250	0	0.45	0.41	0.01	93.60	0.38	0.03	90.41	0.39	0.02	91.72
9	280	0	0.15	0.01	0.11	81.57	0.11	0.00	78.33	0.12	0.03	94.75
10	250	20	0.45	0.12	0.20	71.57	0.25	0.07	72.81	0.18	0.15	72.51
11	250	20	0.45	0.15	0.13	62.27	0.25	0.08	73.45	0.18	0.13	68.57
12	200	20	0.45	0.42	0.00	93.74	0.43	0.01	98.53	0.37	0.03	89.62
13	250	20	0.45	0.12	0.17	63.34	0.22	0.08	67.63	0.18	0.14	69.31
14	250	20	0.45	0.14	0.18	70.99	0.26	0.08	74.81	0.21	0.13	75.20
15	250	20	0.95	0.37	0.26	66.51	0.49	0.19	71.37	0.41	0.30	74.43
16	220	0	0.75	0.70	0.01	94.53	0.69	0.01	93.66	0.71	0.01	95.97
17	250	20	0.08	0.01	0.04	68.16	0.04	0.01	69.79	0.02	0.03	70.80
18	280	40	0.75	0.31	0.18	66.00	0.28	0.15	57.03	0.29	0.18	62.60
19	280	40	0.15	0.05	0.05	62.40	0.05	0.04	54.98	0.04	0.05	58.23
20	300	20	0.45	0.12	0.14	56.24	0.16	0.06	47.46	0.14	0.11	56.17

Moreover, other volatile components such as small organic acids such as formic and levulinic acids generated from furfural (Jing and Lü, 2007) and HMF (Toor et al., 2011) decomposition are also likely to have evaporated in this step.

Even less volatile compounds than HMF as furfural might be evaporated during the drying stage to some extent. Converti et al. (2000) hydrolysed sulphuric acid pretreated milled wood samples using steam explosion. Afterwards, they heated the hydrolysed extracts to 100°C for 160min in order to evaporate acetic acid and furfural prior to fermentation. They suggested

that 96.8% of acetic acid and 58.3% of furfural were successfully removed from the extracts (Converti et al., 2000). Therefore, the furfural present in the samples could also have been partially evaporated at the conditions used to dry the samples.

Although gasification of lignocellulose is preferred at temperatures close to supercritical conditions (T>374ºC) (Toor et al., 2011), there are reports about gasification in low extents (<10%) occurring at temperatures as low as 235ºC (Kumar and Gupta, 2009). Cheng et al. (2009) evaluated the formation of gas during SBW hydrolysis of switchgrass. They reported that gas yield increased from 17 to 49% (wt%) when temperature increased from 250 to 350ºC. Moreover, they analysed the gas produced and revealed that it was mainly composed of CO and CO_2, with trace amounts of H_2 and CH_4 (Cheng et al., 2009). Mazaheri et al (2010) utilized a batch reactor to hydrolyse oil palm fruit fibre using SBW at temperatures ranging from 210-330ºC for 90min using 10% biomass load. They observed that gas contents was increased from 10 to almost 40% (wt%) with the increase in temperature (Mazaheri et al., 2010).

In addition, the generation of gaseous products during SBW hydrolysis seems to be closely related to temperature. The data presented in Table 4-11 also suggested the same as higher temperatures (280 and 300ºC) showed significant mass losses for all three biomasses. Moreover, mass balance results also suggest that residence time could be similarly related to gas production as higher residence times (40min and higher) also presented low values of mass balance.

Furthermore, harsher conditions (high temperatures and long residence times) also resulted in higher amounts of decomposed products, which possibly increase the amount of mass losses due to evaporation in the sample-drying step.

Moreover, in order to confirm the hypotheses of evaporation during drying step and gasification during SBW hydrolysis, it would be necessary to perform some extra analysis. For

instance, gaseous products would need to be collected for quantification and, therefore, gases could be accounted for in the mass balance; and samples should be analysed for organic acids in an attempt to quantify all possible volatile products before sample-drying step. As these analyses were not performed in this work, the reasons for the material losses presented in Table 4-11 and suggested in this discussion remain as hypotheses.

Additionally, as a result of mass losses due to the probable evaporation of some compounds as well as gasification, it is difficult to calculate processing losses. Nevertheless, material loss could be estimated using one of DoE-2 conditions that most likely minimize the undesirable evaporation of volatiles and gasification processes. Therefore, run 3 (220^{o}C, 0min, 1% biomass) was chosen as at these conditions, due to low temperature and short residence time, it is expected that only trace amounts of decomposition products (HMF, organic acids) were generated and gasification is unlikely to have occurred in significant amounts. Consequently, considering run 3, material loss during SBW hydrolysis vary from 6-8%.

4.3.6. Reactions and products in the SBW hydrolysis of cellulose fibres

Biomass undergoes to a variety of complex chemical reactions under hydrothermal conditions that are dependent on parameters conditions (temperature, residence time) and also on biomass composition (Toor et al., 2011).

Most of the attempts reported in literature to understand mechanism/kinetics reactions in SBW use pure cellulose and pure glucose to comprehend these compounds decomposition in SBW (Matsumura et al., 2006). This simplification is usually not accurate for lignocellulose biomass due to the structural and chemical differences compared to pure cellulose. Moreover, results showed in previous sections confirmed that pure cellulose was easier hydrolysed compared to cellulose fibres from *Miscanthus*. However, in this work this simplification will

be considered close to the truth, as both DEL and SEQ are ~80% cellulose by composition. In addition, the role of residual lignin and xylan during SBW was also be discussed.

4.3.6.1. Main products generated from cellulose during SBW hydrolysis

The reactions involving cellulose under hydrothermal conditions can be classified in five major groups: depolymerisation, isomerisation, dehydration, fragmentation and condensation (Antal Jr et al., 1990).

The first step of hydrolysis is thought to be depolymerisation, i.e., the cleavage of cellulose into COS of different DPs. It is not clear whether the position where these cleavages occur are random or if there are more susceptible regions, caused perhaps by different degrees of crystallinity.

Subsequent to their release, COS are broken into smaller molecules such as glucose and released. Sugar release from oligomers are believed to be from the termini, i.e., not from the internal glycosidic bonds (Kimura et al., 2012). Therefore, according to this theory, once the oligosaccharide is cleaved from the polymeric structure, it will mainly release monomeric sugars, and not COS with lower DP.

Finally, reactions both from glucose and products generated from glucose start taking place, such as isomerisation, fragmentation, dehydration and condensation (Antal Jr et al., 1990).

In the conditions performed in this work, COS can only be seen in mild conditions (low temperature/short residence time). Figure 4-8 shows the chromatogram obtained by HPAEC for SEQ fibres after SBW hydrolysis at 220^{o}C, for 0min using 5% biomass.

Figure 4-8 is an insight of what happens in the beginning of the hydrolysis, as this sample was collected as soon as temperature achieved 220^{o}C, which took about 7min. In this

figure, it is possible to see a wide range of cello-oligosaccharides with DPs as high as 20. The identified COS in this figure (cellobiose, cellotetraose and cellohexaose) were compared to standards. From theses identified COS, the others can be deduced by their position in the chromatogram.

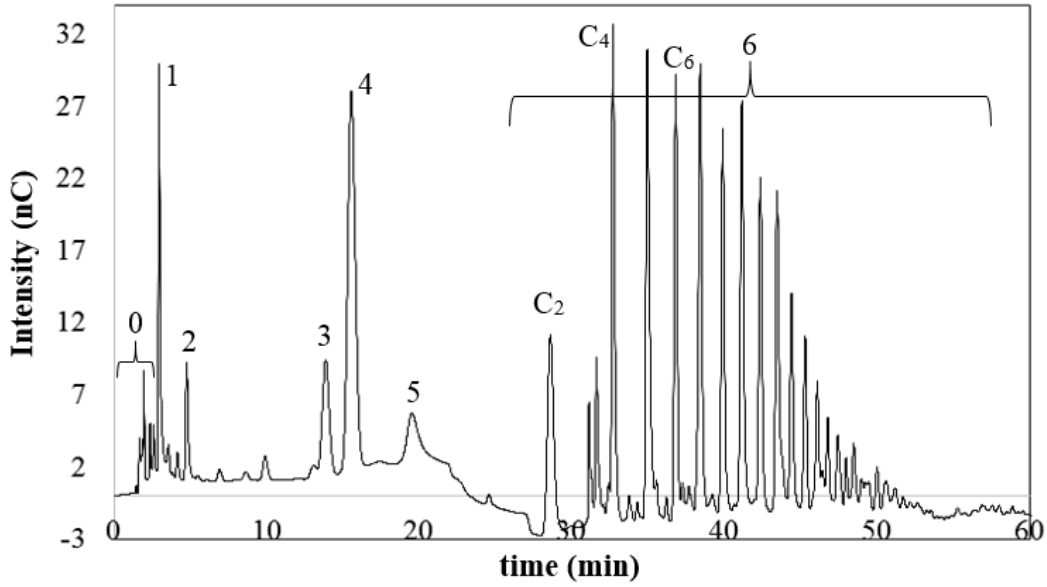

Figure 4-8 - Chromatogram obtained by HPAEC for SEQ fibres after SBW hydrolysis at 220ºC for 0min and using 5% biomass load (DoE-2,run 16). Compounds: 0- 'washed compounds'; 1- unknown; 2- HMF; 3- glucose; 4- xylose; 5- fructose, and 6- COS (C2-cellobiose, C4-cellotrataose, C6- cellohexaose).

The main compound in this sample is xylose (peak 4, 0.01g/L), which is expected, as remaining hemicellulose fraction will be rapidly hydrolysed at this temperature. Glucose (3), fructose (5) and HMF (2) are also present but in very small amounts: 0.004, 0.01 and 0.002g/L, respectively.

The HPAEC-PAD system is an important tool capable of detecting a large quantity of compounds generated during SBW hydrolysis even in very small concentrations (Yu and Wu, 2011). However, several of these compounds are still unknown both because of the lack of available standards and because of the complexity of the SBW reactions that is still not fully

understood. Moreover, the effort in terms of compound characterization were aimed at the major compounds generated.

Compounds indicated by peak 0 are most likely compounds that do not have strong interaction with the solvent/column and are washed out from the column in less than 2min. These compounds were not analysed. Small peaks in between 2 and 3 appeared only in mild conditions and at very low intensity, suggesting they are sample impurities and/or other residual fractions of the biomass. Moreover, as their concentration are insignificant, these compounds were not evaluated. The compound 2 is unknown, however, as it appears in several other samples, there is an attempt to suggest its nature further in the discussion.

Figure 4-9 shows the chromatogram obtained by HPAEC after SBW hydrolysis of SEQ fibres at 280ºC, 0min and 5% biomass. This sample has been diluted 50 times, therefore, that needs to be taken into consideration when comparing Figure 4-9 with Figure 4-8 in terms of peak intensity. Glucose (3) and HMF (2) were the main compounds of SBW hydrolysis at these conditions (4.9 and 3.4g/L, respectively). Fructose (4) is also present in considerable amounts (1g/L). In smaller amounts, the previously called unknown compound and COS are also visible.

Figure 4-9 can be seen as a continuation of the reaction presented by Figure 4-8, i.e., after passing by the point of 220ºC, the reaction in this sample was left to continue until 280ºC was achieved. Therefore, this chromatogram suggests that after COS are formed in the beginning of the reaction (as shown in Figure 4-8), they are decomposed into smaller molecules, and the concentration of COS becomes insignificant. This result means that depolymerisation into COS was almost exclusively in the beginning of the reaction, which was confirmed as significant amounts of COS were not observed in any sample with residence times higher than 0min. However, hydrolysis percentage continued to increase with residence time. That could be a result of glucose being released from the termini of COS with high DP. Therefore, the

results in this work suggests that depolymerisation, i.e., the attack of internal glycoside bonds that generates COS, happens in the beginning of the hydrolysis; then this mechanism is replaced by release of only terminal glucoses in the surface of the biomass during the course of the reaction.

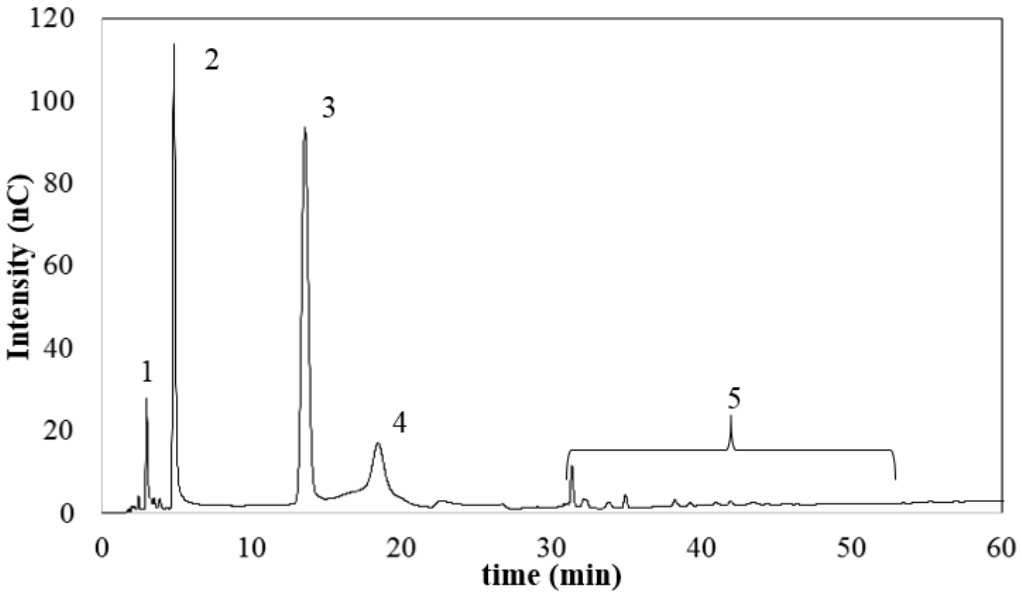

Figure 4-9 - Chromatogram obtained by HPAEC for SEQ fibres after SBW hydrolysis at 280ºC for 0min and 5% biomass load (DoE-2,run 2). Compounds: 1-unknown; 2- HMF; 3- glucose; 4- fructose; 5- region of COS.

Figure 4-10 shows the 'continuation' of Figure 4-9, in which samples were taken when the reaction was at 300ºC for 20min. Fructose (2) is the dominant compound at this conditions, which is one of the harshest condition performed in the DoE-2. It can be seen that glucose and COS are absent and HMF is present in small quantity. As a result of the complete absence of glucose, it can be suggested that this harsh condition favoured the glucose to fructose isomerisation at such a level that glucose was converted as soon as it was released, and therefore was not detected in the media.

In order to try to suggest the nature of the unknown compound that appeared just before HMF in the chromatograms shown in Figure 4-8 and Figure 4-9 (and in several other

chromatogram not shown), it was necessary to compare the chromatograms obtained in this work with similar chromatogram reported in literature.

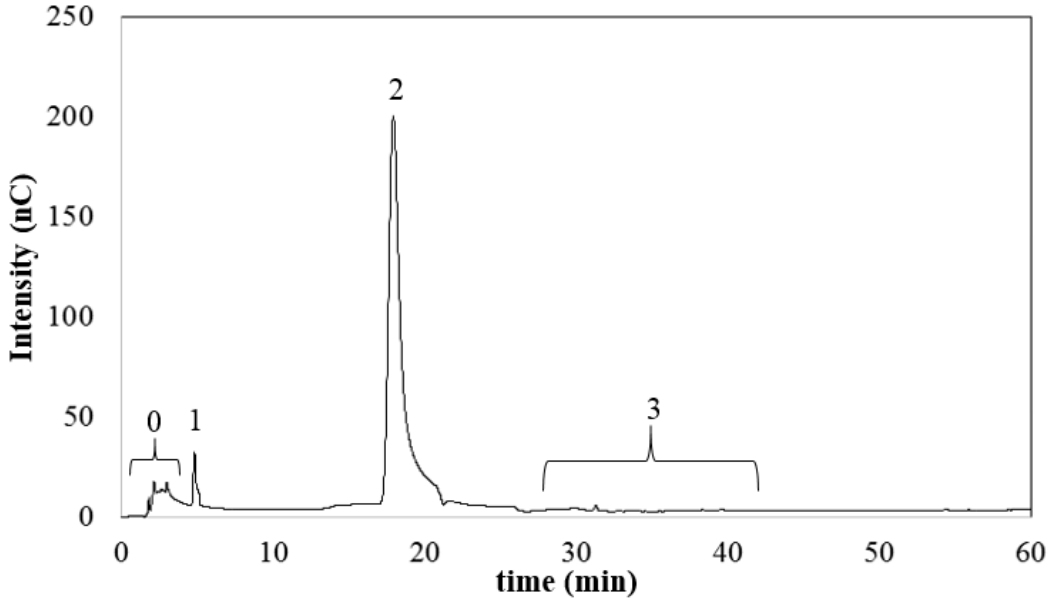

Figure 4-10 - Chromatogram obtained by HPAEC for SEQ fibres after SBW hydrolysis at 300ºC for 20min and 3% biomass load (DoE-2,run 20). Compounds: 0- 'washed out'; 1- HMF; 2- fructose; 3- region of COS.

Yu and Wu (2011) studied the decomposition of glucose in hydrothermal conditions. They used a continuous reactor and temperatures varying from 175-275ºC. Apart from HMF, they observed the formation of fructose, erythrose, glycolaldehyde, glyceraldehyde and 1,6-anyhydroglucose as decomposition products (Yu and Wu, 2011). For their analysis, they used a HPAEC system and a CarboPac PA20 column, which is a column optimized for mono- and disaccharides, very similar to the CarboPac PA1 used in this work (optimized for monosaccharides). In addition, a very similar elution method was also performed using an isocratic concentration of NaOH. In their study, a peak appears before HMF and the authors suggest it to be either glycolaldehyde or glyceraldehyde, as these two compounds could not be separated using their method. In a similar study, Yu et al. (2013) used a continuous reactor to study decomposition of cellobiose in water at temperatures from 225-275ºC. The same

analytical equipment used in the previous work was used once again, however, the elution method was slightly different as a very small NaOH concentration (5mM) was applied in the first 10min (where the peak of interest is), which might have facilitated peak separation. No glyceraldehyde was mentioned this time and the peak before HMF was attributed to glycolaldehyde (Yu et al., 2013).

Therefore, comparisons about elution order can be made between the chromatograms presented in these two publications and this work. Moreover, considering these studies performed in similar method conditions compared to this work, it is plausible that the unknown peak presented in Figure 4-8 and Figure 4-9 is either glycolaldehyde or glyceraldehyde.

In addition, as it was mentioned in the methodology section (see 2.6), for the separation method used in the HPAEC, the sequence of compound elution is dependent on their pK_a. The higher the pK_a of the compound, the faster its elution, as it will interact less with the column. HMF, glyceraldehyde and glycolaldehyde have pK_as of 12.6, 12.8 and 14.2, respectively. Hence, both glyceraldehyde and glycolaldehyde would elute before HMF, which is another evidence that the unknown compound could be either of these two suggestions. At this time, this educated suggestion is offered as an attempt of identification; however, for a positive verification of the nature of the unknown compound, a standard needs to be used.

4.3.6.2. Mechanism of cellulose hydrolysis in SBW

Although there have been some attempts to characterize reaction pathways/mechanism of reaction in hydrothermal conditions (Kabyemela et al., 1997, Kimura et al., 2012, Sasaki et al., 1998), it is still not fully understood (Peterson et al., 2008).

Glucose decomposition path is strongly dependent on the temperature, for instance, gases are mainly produced under supercritical/near water critical conditions as the existent free

radical favours gases production. On the other hand, under SBW temperatures, the ionic conditions, i.e., high H^+ and OH^- concentration, dehydration products are the main pathway for glucose decomposition (Chuntanapum et al., 2008).

Glucose and fructose can be found in three forms when dissolved in water: open chain, and pyranose and furanose rings, which are rings with 6 and 5 carbons, respectively, as shown in Figure 4-11 (Peterson et al., 2008). In non-catalysed hydrothermal conditions, the molar fraction of pyranose ring, furanose ring and open chain forms are 98, 1.5 and 0.04% for glucose and 52, 44 and 5% for fructose, respectively (Kimura et al., 2012).

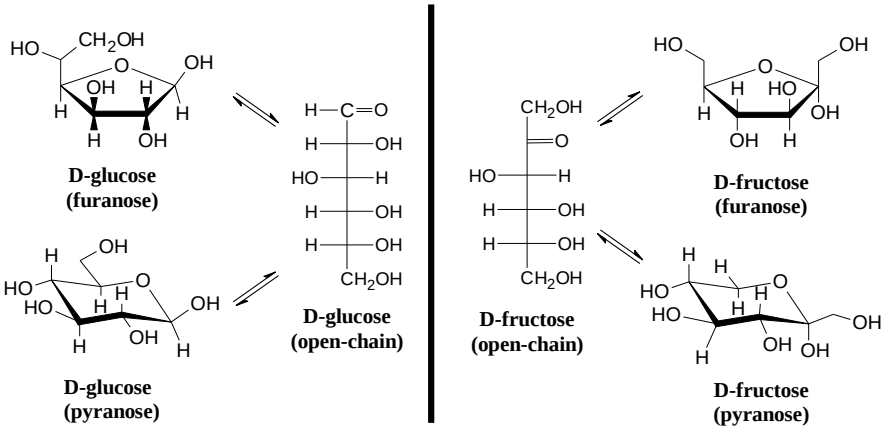

Figure 4-11 - Glucose and fructose existents forms when dissolved in water: open chain, pyranose ring and furanose ring.

Data resulted from DoE and DoE-2 showed a significant amount of fructose generated during SBW hydrolysis. Glucose isomerization into fructose under super- and subcritical water hydrolysis is well documented in literature (Kabyemela et al., 1999, Usuki et al., 2007). Moreover, glucose isomerization into mannose in SBW has also being reported (Srokol et al., 2004, Yu et al., 2013). Nevertheless, mannose was not detected in any sample during this work.

It is well accepted that glucose undergoes isomerization into fructose through a mechanism called Lobry de Bruyn Alberda van Ekenstein (LBAE) transformation (Antal Jr et al., 1990). LBAE mechanism consists of glucose transforming into three intermediates: an

aldehyde, an enediol (alkenes containing OH in both sides of a C=C bond), and a ketone, before its conversion into fructose, as shown in Figure 4-12 (Kabyemela et al., 1999).

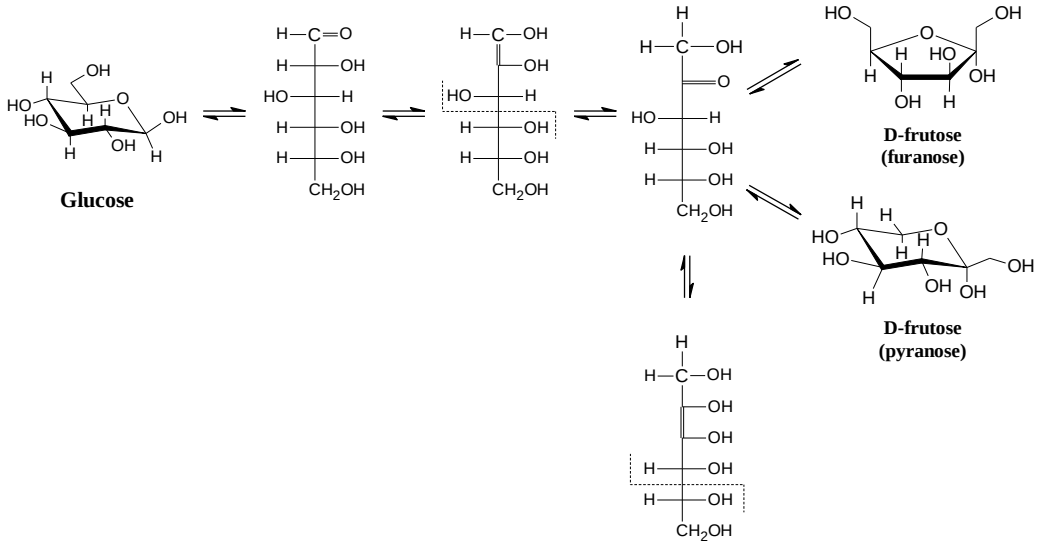

Figure 4-12 - Glucose isomerization into fructose by Lobry de Bruyn Alberda van Ekenstein (LBAE) transformation through aldehyde, enediol, and ketone intermediates. Source: adapted from (Kabyemela et al., 1999).

Moreover, Kimura et al. (2012) proposed a mechanism in which glucose is converted into fructose even before the hydrolysis of the glucose unit from the oligosaccharide. In this mechanism, the last glucose unit of a linear chain (oligosaccharide) has an anomeric carbon free to react in the terminal unit on the right side. They proposed that this terminal glucose unit undergoes reversible isomerisation via the enediol intermediate and it is converted into fructose even before being released from the chain. Once this termini fructose is hydrolysed, the succeeding termini glucoses can be released before turning into fructose. Furthermore, this same mechanism does not occur in the glucose unit at the left side as its anomeric carbon is obstructed by the glycosidic bond (Kimura et al., 2012). It is still unclear at what conditions this path would prevail, however, their findings are important to be considered, as the occurrence of this mechanism could prevent glucose of ever becoming available in the media.

Although glucose and fructose are isomers and can follow the same path in hydrothermal reactions, they present different reactivity (Peterson et al., 2008). Fructose is thought to be more reactive than glucose, which results in a significantly higher rate of glucose isomerisation into fructose than the opposite path (Kabyemela et al., 1997). Moreover, the acidic conditions provided by SBW favours fructose formation during the LBAE isomerisation equilibrium (Speck Jr, 1958). This fact might explain the absence of glucose whereas high levels of fructose were observed under harsh conditions in SBW hydrolysis (Figure 4-10): the acidity of the media could have favoured the LBAE equilibrium towards fructose in a level that glucose was isomerised as soon as released.

In addition, while pyranose rings are the most predominant form of glucose in hydrothermal conditions, fructose has greater amounts of furanose and open-chain forms presented under SBW conditions (Srokol et al., 2004), which also accounts for differences in reactivity as each anomeric form reacts differently (Rosatella et al., 2011).

HMF was generated in significant amounts in the conditions analysed in this work. HMF can be generated from both glucose and fructose (Kabyemela et al., 1999, van Putten et al., 2013). A general path of HMF formation and decomposition in hydrothermal (acid) conditions is shown in Figure 4-13 (Lewkowski, 2001).

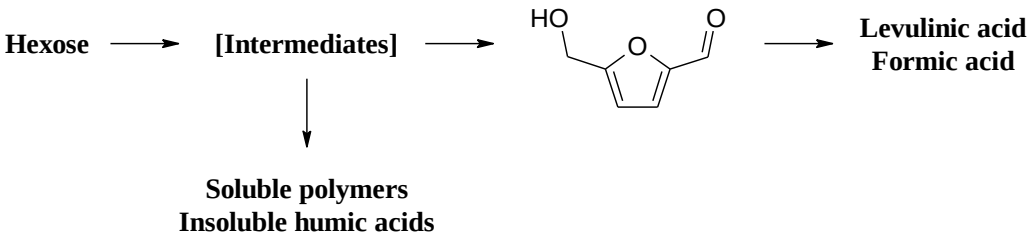

Figure 4-13 - Generation of HMF from hexoses and further decomposition into organic acids and soluble/insoluble products.

Source: modified from (Lewkowski, 2001).

There is no consensus for the path of HMF formation during SBW hydrolysis of cellulose and two main mechanisms have been proposed: acyclic and cyclic routes (van Putten et al., 2013).

Fructose conversion into HMF is thought to be a cyclic route through the formation of a highly reactive intermediate named fructofuranosyl (Kabyemela et al., 1999) as shown in Figure 4-14.

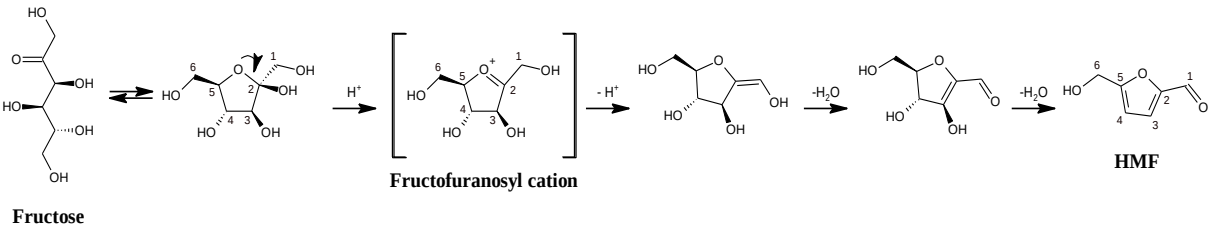

Figure 4-14 - Mechanism of fructose conversion into HMF via fructofuranosyl intermediate. Source: modified from (Perez Locas and Yaylayan, 2008).

Glucose conversion into HMF, on the other hand, requires an open ring reaction, followed by the formation of an intermediate named 3-deoxy-glucosone, which then cycleses to HMF, as shown in Figure 4-15 (Perez Locas and Yaylayan, 2008). Moreover, fructose could also generate 3-deoxy-glucosone, and subsequently, HMF via an open ring route (van Putten et al., 2013).

Nevertheless, because of the higher complexity of breaking and cyclising the glucose/fructose rings, conversion of HMF through cyclic route via fructose is more likely to be the main path for this reaction (Perez Locas and Yaylayan, 2008, van Putten et al., 2013).

HMF itself undergoes further reactions when not separated from the SBW media. HMF rehydration in acidic media leads to the generation of levulinic and formic acids by the cleavage of the furan ring (Lewkowski, 2001). The mechanism of levulinic acid formation from HMF was proposed by Hovart et al. (1985) and it is shown in Figure 4-16 (Horvat et al., 1985).

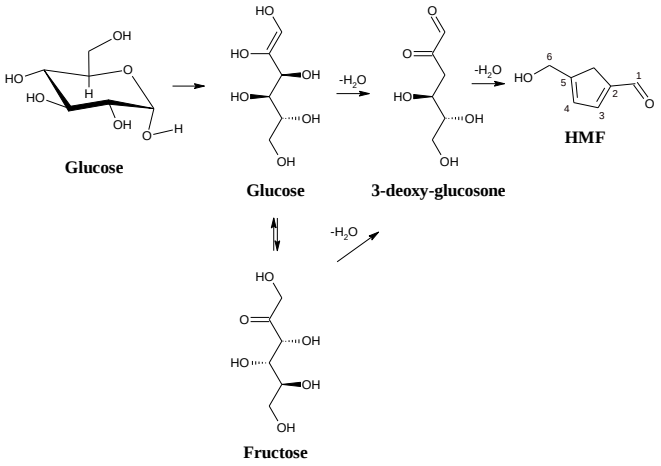

Figure 4-15 - Scheme of glucose conversion into HMF via open ring and 3-deoxy-glucosone intermediate. Source: modified from (Perez Locas and Yaylayan, 2008) and (van Putten et al., 2013).

On the other hand, at higher temperatures (>280ºC) a compound named 1,2,4-benzenetriol was observed as the main product of HMF decomposition. Luijkx et al. (1993) investigated the HMF reactions in SBW using a flow reactor and temperatures from 290-380ºC. They observed that the major product formed was 1,2,4-benzenetriol (Luijkx et al., 1993). Skorol et al. (2004) also investigated HMF decomposition in SBW in a flow-type reactor at 340ºC and residence times ranging from 25-200s. They reported the primary product as being 1,2,4-benzenetriol (Srokol et al., 2004).

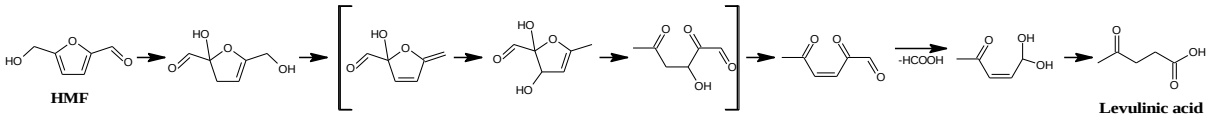

Figure 4-16 - HMF rehydration into levulinic acid during hydrolysis. Source: modified from (Rosatella et al., 2011).

Moreover, the formation of other furan compounds from HMF is also possible, particularly in super- and near critical water conditions (Chuntanapum et al., 2008). The polymerisation of HMF is also described as a possible route when the media is not acidic enough to favour HMF rehydration (Asghari and Yoshida, 2010).

Humin, a dark-coloured solid, can be formed from HMF in hydrothermal treatment and acid-catalysed conditions (Patil and Lund, 2011). The mechanism of humin generation could be a reaction between HMF and glucose/fructose (Rosatella et al., 2011) or between HMF and its intermediates produced during HMF decomposition (Rasmussen et al., 2014).

Although all the routes mentioned are possible, at the temperatures used in this work, it is more likely that HMF have been decomposed into levulinic and formic acid. Moreover, the low pH of samples under harsh conditions (high temperature/longer residence times) indicate the generation of acids compounds, which is in agreement with HMF decomposition into organic acids.

It is widely spread in literature that HMF comes exclusively from C-6 sugars, while furfural is a dehydration product solely from C-5 sugars (Agbor et al., 2011, Rasmussen et al., 2014, Rogalinski et al., 2008). However, after the results obtained in the DoE-2 that shows significant amounts of furfural in samples from SBW hydrolysis of Avicel, it was clear that furfural could be formed also from C-6 sugars.

Ashaghari and Yoshida (2007) described the formation of furfural during acid-catalysed fructose decomposition in SBW in a continuous reactor. They evaluated temperatures in the range from 210-270^{o}C, pressures from 4-15MPa, residence times from 0-300s, and using HCl as catalyst. Moreover, they performed the same reaction using HMF as start material and did not detect furfural among the products. Therefore, they suggested that furfural was most likely generated direct from fructose in subcritical water conditions (Asghari and Yoshida, 2007).

Luijkx et al. (1992) also observed the possibility of furfural formation from HMF in supercritical conditions. They detected furfural at high temperatures (380^{o}C) and suggested that HMF to furfural path is favoured by high temperatures (Luijkx et al., 1993). These results suggest that the formation of furfural from HMF is possible, but it is more likely to happen in

near critical/supercritical water conditions (Jin and Enomoto, 2011). Therefore, in the range of temperature used in this work, it is more likely that furfural was formed from fructose.

The use of high temperatures (>280°C) usually favours glucose decomposition through retro-aldol condensation reactions because of the decrease in water density (Kumar and Gupta, 2008). Sasaki et al. (2000) showed that after cellulose hydrolysis under near critical and supercritical water conditions, HMF was not the main product. They used a flow-type reactor and pure cellulose to evaluate the products in temperatures ranging from 320-400°C and residence times from 0.05-10s. Glyceraldehyde, glycolaldehyde, dihydroxyacetone, erythrose, 1,6-anyhydroglucose, pyruvaldehyde, HMF, furfural and acids were produced in these conditions. Figure 4-17 shows a scheme of generation of some of these products from glucose. Moreover, all the products can also be generated from fructose, apart from 1,6-anyhydroglucose, which was only observed from glucose (Kabyemela et al., 1999).

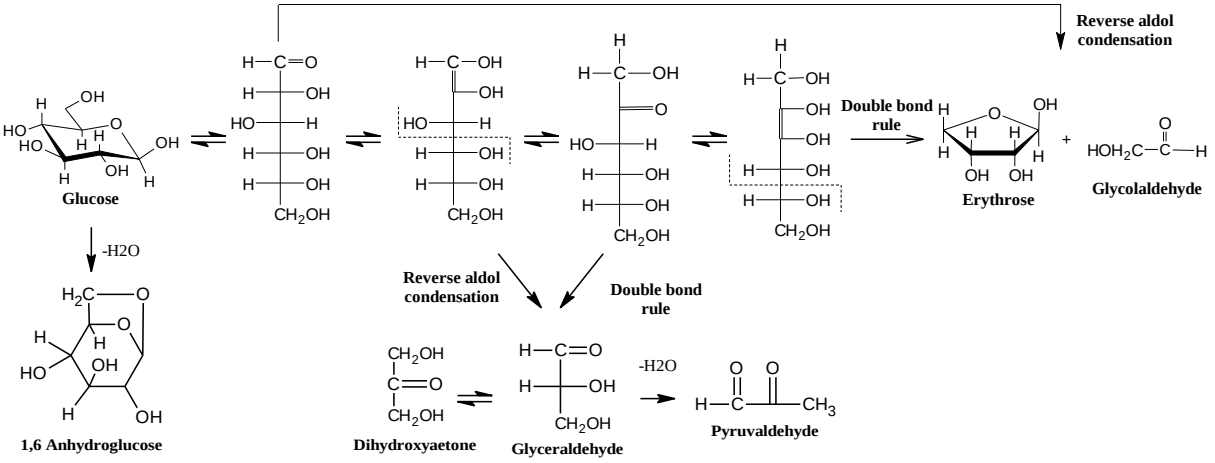

Figure 4-17 - Possible path for the formation of 1,6-anyhydroglucose, erythrose, glycolaldehyde, glyceraldehyde and pyruvaldehyde in hydrothermal conditions. Source: modified from (Kabyemela et al., 1999).

Although retro-aldol products are usually minor products in SBW (Ehara and Saka, 2005), considering that the unknown peak shown in Figure 4-8 and Figure 4-9 is in fact either glycolaldehyde or glyceraldehyde as previously suggested, that might be an indication that the

retro-aldol path was also presented during SBW hydrolysis of cellulose at some extent. Nevertheless, dehydration path is most likely the main route of glucose/fructose decomposition in the conditions performed in this work (indicated by the higher amounts of HMF compared to the unknown peak).

Lignin present in biomass will also react during SBW hydrolysis. Apart from the re-polymerisation already discussed (see section 3.3.5.5), lignin will also undergo hydrolysis and generate compounds that could cause inhibition during fermentation (Palmqvist and Hahn-Hägerdal, 2000b). Moreover, one of the reasons for delignification prior to SBW hydrolysis is to avoid the formation of phenols and methoxy-phenols caused mainly by the cleavage of ether bonds in lignin (Toor et al., 2011). Figure 4-18 shows a simplified scheme of lignin hydrolysis under hydrothermal conditions.

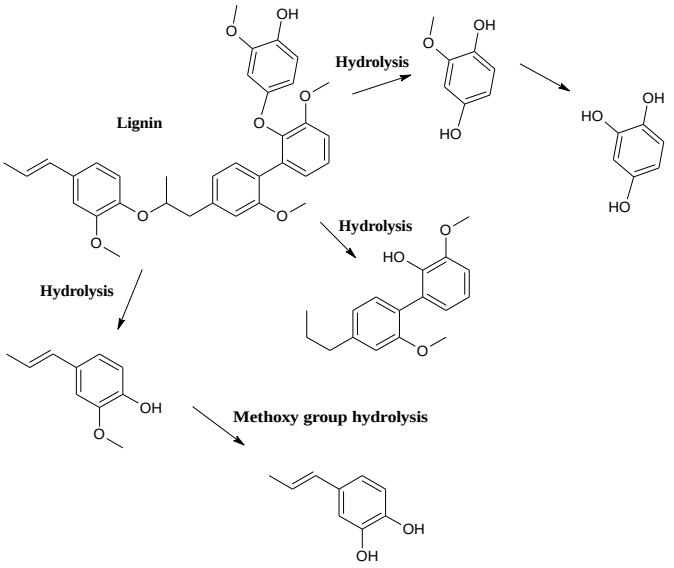

Figure 4-18 - Simplified scheme of lignin hydrolysis. Source: modified from (Toor et al., 2011).

In addition to hydrolysis decomposition, lignin present in biomass might also react with soluble products generated during SBW hydrolysis and originate insoluble compounds, decreasing sugar recovery (Rogalinski et al., 2008). Moreover, it is also possible that lignin

precipitates during SBW hydrolysis. Kumar and Gupta (2009) reported that a precipitate was formed in the liquid fraction after SBW of switchgrass at temperatures ranging from 235-260ºC. After analysing this precipitate, they concluded that sugars were only a minimal percentage of this precipitate and lignin was the major component of it (Kumar and Gupta, 2009).

4.3.7. SBW for hydrolysis of Miscanthus fibres for glucose production

Miscanthus is widely studied as a promising lignocellulosic source for bioethanol production (Brosse et al., 2012, Chou, 2009). The common processing approach applied to this energy crop is to perform a pretreatment to expose cellulose fibres, followed by an enzymatic hydrolysis (Boakye-Boaten et al., 2015, Xiao et al., 2011).

Subcritical water used as a pretreatment in *Miscanthus* has often been reported as a promising technology to disarrange lignocellulosic matrix by hydrolysing hemicellulose into soluble products and break cellulose-lignin linkages. Therefore, biomass surface area is increased, facilitating enzymatic hydrolysis (Mosier et al., 2005b), as well as the SBW hydrolysis performed in this work.

Lignocellulosic biomass composition is thought to play an important role in hydrolysis, for instance, higher lignin contents is believed to be a drawback due to the possibility of formation of phenolic compounds (Palmqvist and Hahn-Hägerdal, 2000b). However, the results from SBW, particular from DOE-2, shows SEQ fibres as easier hydrolysable fibres compared to DEL even though SEQ fibres have higher lignin content (16.3 against 12.8% from DEL fibres). Therefore, it could be inferred that fibres structure and accessibility were more important than the composition in this work. Therefore, in this work, the SBW extractions and the modified organosolv method successfully modified the lignocellulosic biomass structure,

as indicated in the principal component analysis done in the FTIR spectra, and it seems that it has driven to major differences in hydrolysis under SBW condition.

The sequential extraction route using SBW hydrolysis followed by the modified organosolv method proposed in chapter 3 had the objective of not only selectively extracting lignocellulosic components through processing, but also changing cellulose fibres structure in order to make it more accessible to hydrolysis. Therefore, it seems to have been achieved as SEQ fibres demonstrated a better potential of cellulose conversion into glucose than DEL fibres during SBW hydrolysis.

SBW hydrolysis of pure cellulose into glucose has been broadly investigated and considered a promising clean technology (Kumar and Gupta, 2008, Moller et al., 2013, Sasaki et al., 2000, Yu and Wu, 2010). However, the use of SBW in lignocellulose biomass is more challenging due to structural reasons (Zhao et al., 2009b) and has not being widely explored. Moreover, to date, the use of SBW for cellulose hydrolysis using *Miscanthus x giganteus* has not being reported. Nevertheless, other lignocellulosic biomass were evaluated for monomeric sugars production using SBW hydrolysis. Cheng et al. (2009) utilized SBW to hydrolyse switchgrass using a batch reactor and evaluated temperatures from 250-350^{o}C and very low residence times (1-300s). They achieved hydrolysis percentages as high as 90% and glucose yields (from total available glucan) of 19.4% at 300^{o}C and 15s (Cheng et al., 2009). Lü and Saka (2010) analysed the hydrolysis of milled Japanese beech in SBW using both batch and flow-type reactors. They observed that the optimal temperature for glucose production was lower for batch reactor (230^{o}C) compared to the flow reactor (270^{o}C) for the same 15min reaction. They reported glucose yields of 4.6 and 35.5% (wt.) for batch and flow reactor, respectively (Lü and Saka, 2010).

In summary, although glucose yields presented in this work (up to 11% wt.) might be increased by changes in operational parameters (such as reactor type, heating time, continuous separations of produced glucose, temperature, residence time, etc.), the use of non-catalysed SBW for glucose production from pre-processed MxG fibres was demonstrated to be possible. Moreover, the biorefinery concept applied on sequential extraction of MxG assessed the feasibility of an integrated process in which purified streams of biomass extractives, hemicellulose, and lignin can be produced, and at the same time as making cellulose more accessible in an environment-friendly process.

In a next step, some of the glucose extracts obtained by SBW were used as carbon source in fermentation for bioethanol production and it will be discussed in the next chapter.

4.3.8. Structural changes after SBW hydrolysis

Although it is believed that SBW affects even the cellulose structure that remains solid during the reactions, it is not clear what the effect of SBW in the fibres is. For instance, it is established that DP gradually decreases with SBW hydrolysis. On the other hand, the crystallinity of cellulose is not significantly changed after hydrothermal reactions (Tolonen et al., 2011). In order to analyse if there was any significant changes in structure of cellulose fibres that remained solid after SBW hydrolysis, FTIR and PCA were performed.

4.3.8.1. FTIR

After SBW hydrolysis of cellulose fibres, the remaining solids were dried and analysed by FTIR. Figure 4-19 shows FTIR spectra for Avicel (a) DEL (b) and SEQ fibres (c) before and after SBW hydrolysis at mild condition: low temperature and short residence times (220^{o}C, 0min).

Figure 4-19 shows that there is almost no visible change in the FTIR spectra of samples after SBW hydrolysis at mild conditions when compared to the samples before SBW process (see Figure 3-21). Therefore, it indicates that mild conditions are not enough to promote structural changes that can be detected by the FTIR spectra.

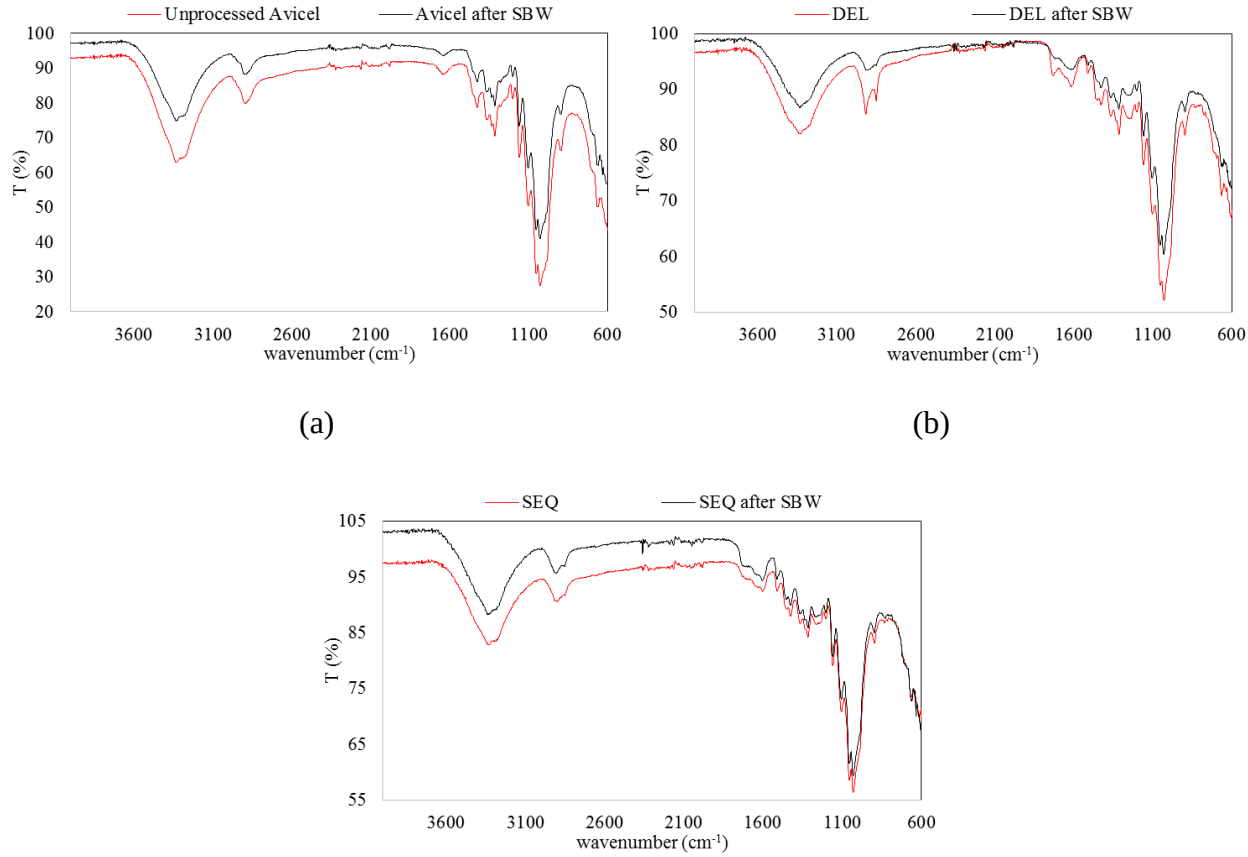

Figure 4-19 - FTIR spectra of (a) Avicel, (b) DEL and (c) SEQ fibres before and after SBW hydrolysis at 220°C, 0min, and 1% biomass load (DoE-2, run 7)

Figure 4-20 shows FTIR spectra for Avicel DEL and SEQ fibres for SBW at harsh condition: high temperature and long residence times (280°C, 40min). Harsh conditions resulted in substantially modified spectra as it can be seen in Figure 4-20. Changes in peak shape and intensity can be seen in the region from 2800-2900cm^{-1} and from 3000-4000cm^{-1}, which are attributed to C-H/C-H$_2$ and to hydrogen bonds, respectively (Adel et al., 2010, Bessadok et al.,

2007, Lan et al., 2011). Moreover, drastic changes are observed in the wavenumbers from 850-1700cm^{-1} in which cellulose, lignin and hemicellulose have several characteristic peaks (the description of these peaks can be seen in section 3.3.7.2).

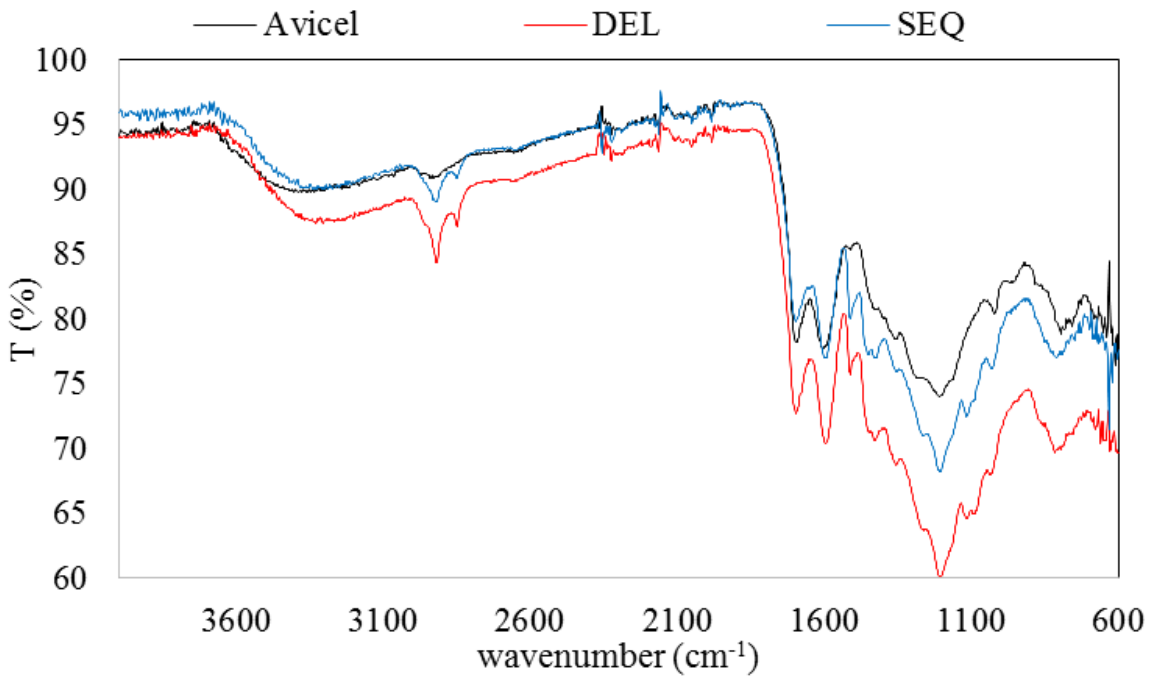

Figure 4-20 - FTIR spectra of Avicel, DEL and SEQ fibres after SBW hydrolysis at 280ºC, 40min and 1% biomass load (DoE-2, run 19).

The changes observed in the spectra is a confirmation of structural changes caused by SBW hydrolysis on the remained cellulose fibres. Moreover, in order to try to identify modification patterns, PCA was performed on the FTIR spectra for all 20 DoE runs for the three fibres.

4.3.8.2. PCA for DoE-2 data

Principal Component Analysis was successful in demonstrating structural changes during MxG processing in the previous chapter. Therefore, this analysis was applied once again

in order to try to identify the patterns of changes during SBW hydrolysis according to the conditions applied.

The FTIR data used for this PCA were the same five biological replicates of each fibre used in the previous analysis: DEL, SEQ and Avicel (Av). Moreover, all 20 DoE-2 runs for the three fibres were used.

Data manipulation on FTIR data was applied prior the PCA. Although all 4 data manipulations tested previously (see Table 3-4) were applied in the DoE-2 data, the M4 (smoothing, 2nd-derivative, normalisation) was again the one which showed the clearest results and it is the only manipulation that will be discussed.

4.3.8.2.1. Scores Plot

Figure 4-21, Figure 4-22 and Figure 4-23 show the scores plot for fibres and DoE-2 runs for Avicel, DEL and SEQ, respectively. In these Figures, the DoE-2 runs were identified by the following label: 'X_Y_Z', in which X is the temperature (^{o}C), Y is the residence time (min) and Z is the biomass load (%). Moreover, C_n refers to the replicate n (1-6) of the central point (250^{o}C, 20min and 3%).

Four clusters could be identified for Avicel, shown in Figure 4-21: 1) Avicel unprocessed samples along with samples submitted to SBW in mild conditions (low temperature and/or short residence time); 2) samples that produced the highest glucose yields; 3) all the samples at 250^{o}C and 20min (different loadings); and 4) samples under harsh conditions (high temperature and/or long residence time).

As it was visually suggested by the FTIR spectra shown in Figure 4-19, samples under mild SBW hydrolysis conditions did not present significant differences compared to Avicel fibres, therefore, they appear in the same cluster as Avicel.

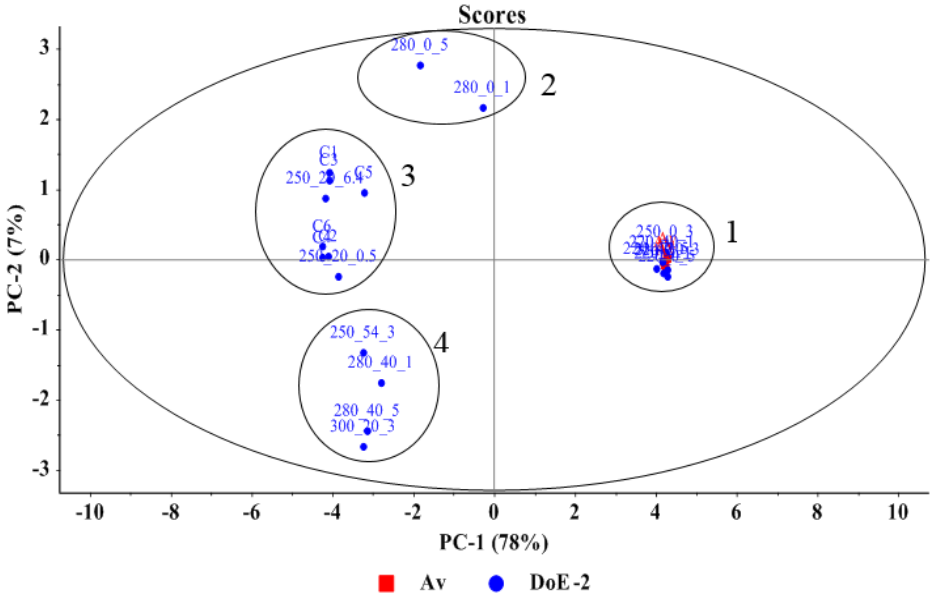

Figure 4-21 - PCA scores plots for FTIR data from Avicel (unprocessed and after SBW hydrolysis (DoE-2)) after smoothing+2nd-derivative+normalisation.

The difference among the samples is essentially how much the process of SBW hydrolysis managed to alter the solid structure of the remaining solid. It is clear that, once there has been a significant transformation, the samples moved along PC1 from positive to negative. Therefore, PC1 for Avicel could be related to the loss of amorphous portion of cellulose, as it is expected that amorphous fraction will react first (Foston and Ragauskas, 2012).

Samples also moved along PC2 from positive to negative, the same direction of the increase of conditions severity. That could suggest that samples under harsh conditions have not only cellulose in the remaining solids, but also other compounds created by the condensation reactions already described to be more presented under severe SBW conditions. Therefore, PC2 could be related to the increase in composition of something different from cellulose. Moreover, experimentally, all these 4 samples were black, in an almost carbonized state after the SBW for all tree fibres, which resulted in them clustering together for all three biomasses.

Contrary to Avicel, which presented a rather logical clustering, DEL fibres presented some 'outside of the logical' samples. For instance, 250_20_0.5 that can be seen in the top of Figure 4-22 would be more logical if presented with other samples at the same temperature and residence time, on cluster 2. Moreover, according to the FTIR spectra shown in Figure 4-19, samples 220_0_1 and 220_0_5 were not modified compared to DEL fibres. Therefore, it would be expected to see them along with DEL in cluster 1.

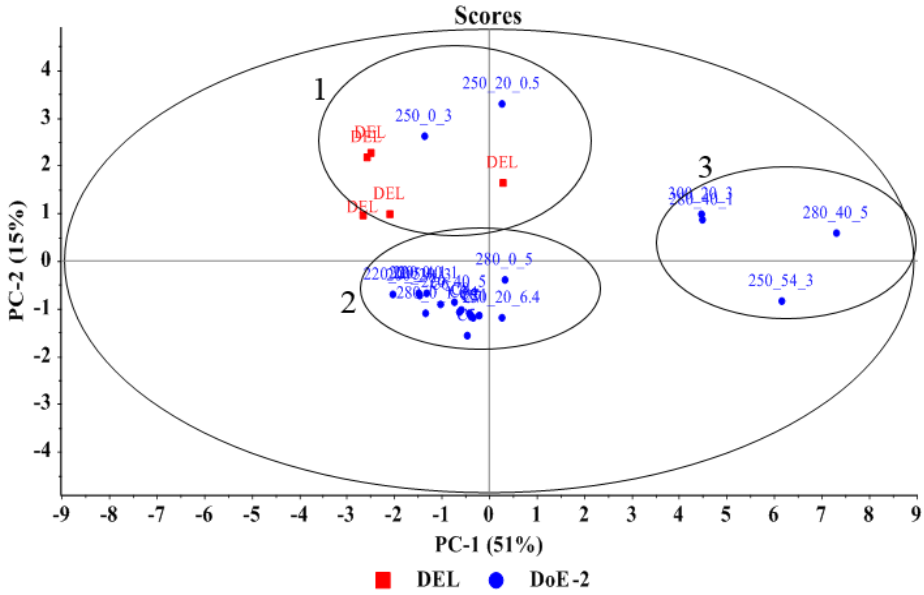

Figure 4-22 - PCA scores plots for FTIR data from DEL fibres (DEL fibres before and after SBW hydrolysis (DoE-2)) after smoothing+2nd-derivative+normalisation.

Although there are samples whose position is not well understood, it could be suggested that PC2 explains small changes in the FTIR spectra. For instance, DEL fibres are first moving down from PC2 positive to negative, without significant changes in PC1. On the other hand, there is a large transition along PC1 from negative to positive for samples under harsh SBW conditions (high temperature and/or long residence time), shown by cluster 3. This is the same pattern presented by Avicel samples: first, samples move along one of the PCs for small changes in severity; then, samples move along the other PC for harsh conditions. Therefore, the PCs in

DEL analysis could very well be related to the same features described for Avicel but for the opposite PC, i.e., the loss of amorphous fraction along PC2 and the structural change due to partial carbonization and the increase of non-soluble polymers due to condensation reactions in PC1.

Figure 4-23 shows that SEQ fibres presented a similar cluster as Avicel with one difference: samples 280_0_1 and 280_0_5 are not in a separated cluster, as it happened for Avicel. Looking at the results of DoE in terms of compounds (glucose, HMF, etc.) in Table 4-10, it can be seen that differently from Avicel, SEQ fibres did not show a significant difference between the samples 280_0_1/5 and the centre point. Therefore, it is logical that as the composition in the extracts is similar, the remained fibres will also be similar and will appear in the same cluster, as it can be seen in this figure.

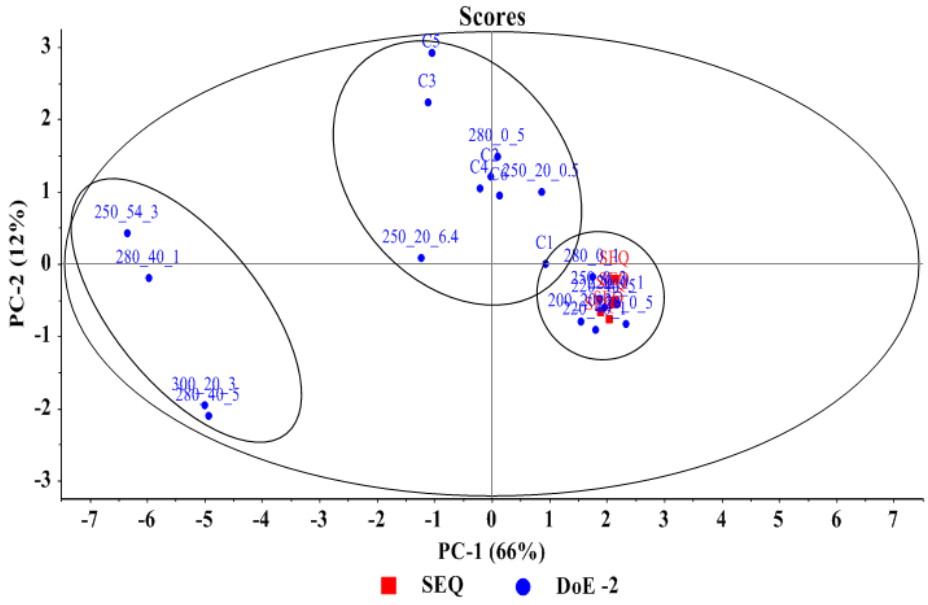

Figure 4-23 - PCA scores plots for FTIR data from SEQ fibres (SEQ fibres before and after SBW hydrolysis (DoE-2)) after smoothing+2nd-derivative+normalisation.

Once again, the pattern among the PCs is repeated: small changes from mild conditions to the centre point are described by PC2 from negative to positive; whereas more significant structural/compositional change was described by PC1 from positive to negative.

The differentiation of fibres structure caused by different treatment conditions has been reported before. Ryden et al. (2014) investigated the effect of severity of steam explosion treatment by analysing FTIR spectra by PCA. They were able to obtain a visible distinction among the samples according to their treatment severity and the PCs obtained were clearly severity related (Ryden et al., 2014). An increase in CI after cellulose hydrolysis was hypothesised to be the result of decreasing in cellulosic amorphous portion due to the preferential conversion of amorphous and I_α fractions (Sannigrahi et al., 2010).

4.3.8.2.2. Loadings Plot

Figure 4-24-a-c shows the loadings plots for (a) Avicel, (b) DEL and (c) SEQ fibres. It can be seen that the three biomasses show very similar loadings plots and wavenumber at 1050-1055cm^{-1} and at 1080 cm^{-1} were the bands that influenced the most the data variability. These bands were also very influential in the previous PCA performed using MxG, 120ºC, 180ºC, DEL, SEQ and Avicel fibres and they are attributed to C-C bonds and pyranose rings, respectively (Garside and Wyeth, 2003, Morán et al., 2008).

In summary, although it is not clear what PC1 or PC2 physically describe, it is certain that they can differentiate the samples according to SBW conditions through the FTIR data. It is very difficult to make a more complete analysis about PC1 and PC2 without more information about the DoE samples such as composition, crystallinity, etc. However, the objective of this PCA analysis was to confirm that SBW promotes not only the depolymerisation and further reaction on the fibres, but also alters the structure of the remained fibres. This objective seems

to have been achieved as the scores plots in this section clearly show the differences among the samples and some inferences according to the SBW conditions could be made.

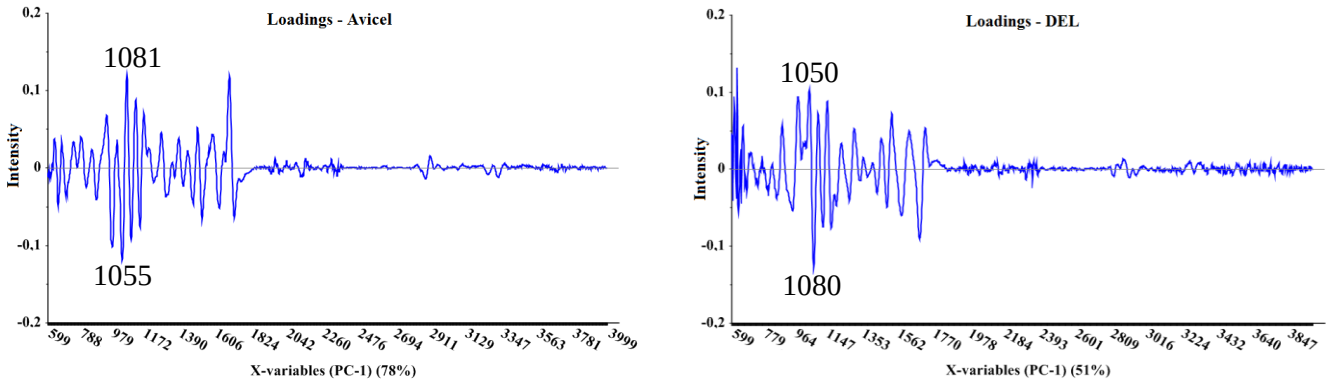

(a) (b)

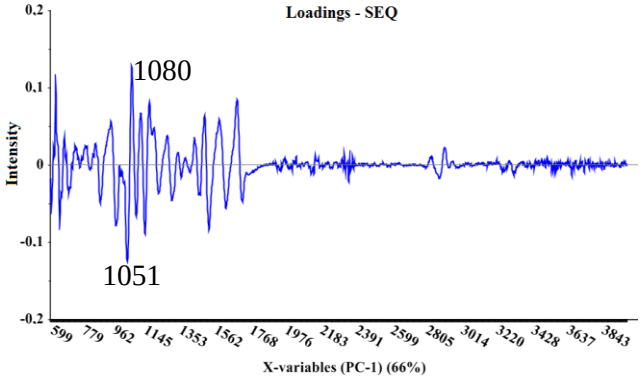

(c)

Figure 4-24 - Loading plot for FTIR data after applying smoothing, 2nd-derivative and normalisation for (a) Avicel, (b) DEL and (c) SEQ fibres for PC1

4.4. Conclusion

The use of subcritical water for cellulose hydrolysis for glucose production was evaluated for fibres obtained from MxG direct and sequential processing (DEL and SEQ), and compared to pure cellulose fibres (Avicel).

SBW hydrolysis was investigated through a scoping of experiments followed by a design of experiments. The scoping showed that parameters such as temperature and residence

time play the main role in glucose production as well as its further decomposition and in and the overall hydrolysis percentage. Moreover, biomass load did not significantly affect the process in the range evaluated.

The design of experiments performed, CCD, did not describe the responses (compounds concentration and hydrolysis percentage) in a significant way. Therefore, the application and evaluation of RSM was not possible. This result could have been due to a wide range of parameters evaluated as well as due to modifications applied in the design. Nevertheless, the analysis of the DoE data allowed an understanding of the SBW hydrolysis process and its reactions.

Non-catalysed SBW hydrolysis was able to depolymerise cellulose fibres and release glucose monomers. Best conditions for glucose production were achieved for high temperatures and short residence times (280^{o}C, 0min). Although significant amounts of glucose were produced, indicated by high hydrolysis percentage, the majority of this sugar was further decomposed into fructose, HMF, furfural and other organic acids. Moreover, this decomposition is mainly due to reactor configuration, which required a significant amount of time to achieve optimal temperatures and did not allowed glucose separation as soon as it was being produced.

DEL and SEQ fibres obtained from MxG by different processing routes were evaluated for glucose production. Even though both *Miscanthus* fibres presented a very similar composition in terms of cellulose, lignin and hemicellulose, SEQ fibres demonstrated to be the best option for glucose production, probably due to more accessible cellulose fibres as a result of the sequential treatment applied in these fibres. Nevertheless, higher amounts of fermentation inhibitors such as HMF and furfural were also found in SEQ fibres compared to DEL. Comparing both *Miscanthus* fibres with pure cellulose it could be confirmed that cellulose from

lignocellulosic structure still presented higher difficulty to hydrolysis even after the pretreatments performed. Glucose yields, as well as inhibitors formation, were higher for Avicel, suggesting that pure cellulose has more accessible fibres than SEQ and DEL fibres.

FTIR and PCA were used to evaluate the effect of SBW hydrolysis in the remained cellulose fibres and demonstrated that severity of the hydrolysis conditions affects not only the soluble products (glucose, HMF, etc.) but also the non-hydrolysed fibres by changing its structure and/or composition.

The results presented in this chapter are an indication that it is possible to apply an integrated process in order to generate purified streams of the main lignocellulosic components at the same time as making cellulose fibres accessible for SBW hydrolysis and glucose production. Furthermore, SBW was revealed to be a potential interesting alternative to the common acid/enzymatic hydrolysis processes. Although improvements are needed to increase efficiency in each step, the integrated process demonstrated in this work suggests that biorefinery is a promising concept to approach 2nd-generation bioethanol production.

Glucose extracts generated by the SBW hydrolysis of Avicel, DEL and SEQ fibres were used as carbon source for fermentation in order to produce bioethanol and this process is discussed in Chapter 5.

CHAPTER 5

FERMENTATION OF GLUCOSE OBTAINED BY SBW HYDROLYSIS OF *Miscanthus x giganteus* CELLULOSE FIBRES

5.1. Introduction

The biorefinery approach allows a wide variety of possible products derived from biomass such as fuels, power, and an extensive platform of chemicals including organic acids and alcohols (Kamm et al., 2000). Among the products, bioethanol is of particular significance as a suitable replacer for fossil fuels (Cherubini, 2010, Sánchez and Cardona, 2008). Moreover, ethanol is also an important solvent and largely used in the production of chemical compounds such as ethane, polyethylene and polyvinyl acetate (Kamm and Kamm, 2004). Therefore, 2nd-generation bioethanol holds an important role in a bio-based economy (Demirbas, 2009a).

After obtaining glucose from cellulose fraction in lignocellulosic matrix (discussed in previous chapters), glucose can be biologically converted into bioethanol through fermentation. Although fermentation of lignocellulosic extracts is theoretically similar to the fermentation process performed for 1st-generation bioethanol, it faces challenges such as large fraction of non-fermentable compounds (C-5 sugars, lignin), low glucose concentration extracts, and the presence of fermentation inhibitors, which are reported to decrease fermentation efficiency (Wang and Sun, 2010). These drawbacks need to be overcome in order to make the process

cost-effective. Lignocellulosic bioethanol yields are highly affected by the microorganism and the glucose extracts composition (Hamelinck et al., 2005). Therefore, an industrial *S. cerevisiae* (strain 3233) largely used in commercial bioethanol production was chosen for its high adaptability to new environments (Basso et al., 2008) and its high potential of biomass and ethanol yields even in the presence of inhibitors (Pereira et al., 2014).

The aim of this chapter was using extracts obtained from SBW hydrolysis as carbon source in preliminary studies of fermentative ethanol production. Yeast growth and bioethanol yields were used for fermentation evaluation in a variety of conditions. In addition, fermentation using extracts obtained by SBW had not previously been reported and the comparison between SBW extracts from the two routes of MxG processing (DEL and SEQ fibres) provided an insight about the potential of the integrated processing discussed throughout this work.

5.2. Material and Methods

5.2.1. Yeast growth in agar plate

The yeast used for the alcoholic fermentation was *Saccharomyces cerevisiae* strain 3233 purchased from the National Collection of Yeast Cultures (NCYC). According to the NCYC, this strain was obtained from fermentation process during ethanol production in Brazil and it is also called PE-02 (or PE-2).

The yeast was delivered in a agar slope and was stored at 4^{o}C during the work. In order to grow the yeast, an agar plate was prepared using Yeast Mold (YM) broth (Difco^{TM}), mixed with distilled water to produce a final composition (w/v) of 0.3% of yeast extract, 0.3% of malt extract, 0.5% of peptone, and 1% of glucose. Agar (Sigma) was also added to this medium at 1.5% (w/v). The medium was autoclaved for 15min at 121^{o}C and left to cool to ~40^{o}Cbefore filling plastic petri dishes.

After the medium was solidified, *S. cerevisiae* was transferred from the agar slope and spread on the plate to generate single colonies. The plates were then incubated at 30ºC for about 20h.

After the incubation, a colony was collected for microscopy observation to ensure there was no contamination with other species such as bacteria (Figure 5-1). The equipment used was an Olympus BX50.

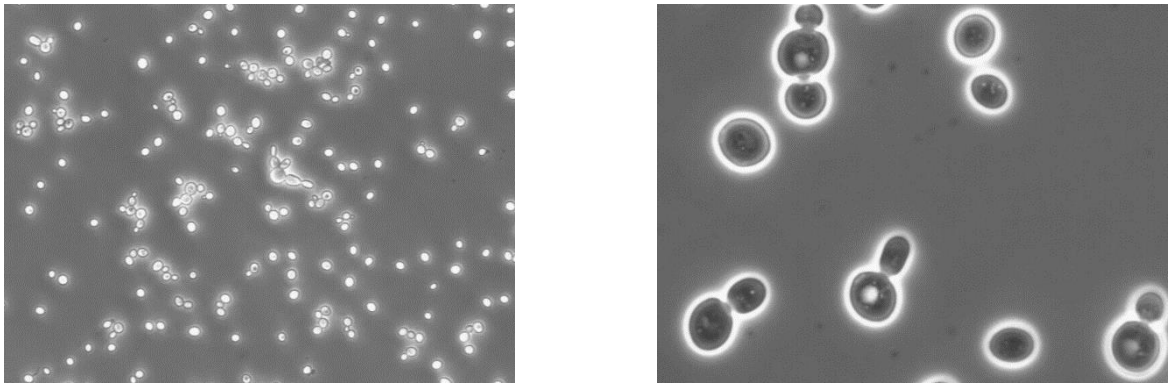

(a) (b)

Figure 5-1 - Microscopic image of *Saccharomyces cerevisiae* strain 3233(NCYC) amplified (a) 20x and (b) 100x.

The absence of smaller bacterial cells suggests that there was no contamination. Moreover, yeast cell division process by budding can be observed in the larger magnification.

5.2.2. Overnight culture

The yeast was incubated overnight before fermentation runs. This overnight culture (OV) was made using the YM broth. The natural pH of YM broth is around 6, therefore, in order to prepare the yeast for the acidic condition of the extracts, the pH of YM broth was decreased to about 4.4 using HCl solution (5M). 10mL of pH corrected medium was placed in 25mL flasks and autoclaved for 15min at 121ºC, and then it was left to cool.

A single colony of yeast was transferred from the agar plate to 25mL flask and the flask was covered with foam. The flask was incubated at 30ºC and 150rpm for 18h. At the end of 18h, samples from the OV (1mL) were analysed in a spectrophotometer (Cecil Aquarius CE 7500) at 600nm for optical density (OD) analysis. On average, an OD of 7-8 was achieved. The overnight culture was used to inoculate the fermentation media as soon as it reached 18h. New yeast growth in agar plates and overnight cultures were performed for each fermentation run.

5.2.3. Fermentation

Each fermentation condition was performed 2 times using 3 flasks each time. Therefore, the results were an average of 6 flasks performed in two independent replicates.

YM broth was used as a standard medium and compared to the fermentation made using glucose extracts obtained by SBW hydrolysis of Avicel, DEL and SEQ fibres.

10mL of fermentation medium (YM/ glucose extracts) was placed in 25mL flasks. When Avicel/DEL/SEQ glucose extracts were used, yeast and malt extract and peptone were added at the same concentration as the YM broth. Flasks were autoclaved for 15min at 121ºC prior to fermentation runs.

100μL of the overnight culture was added to each flasks (1% v/v). The flasks were incubated at 30ºC with no agitation to induce the anaerobic process. Fermentation runs lasted for 48h and samples were taken (50μL) and diluted using phosphate-buffered saline (PBS, Oxoid) at the following times: 0, 1, 2, 3, 4, 5, 6, 8, 10, 12, 24, 30, 36 and 48h.

5.2.3.1. pH study

From the previous chapter it was revealed that glucose extracts were generated with low pH (values depending on SBW conditions). In order to evaluate *S. cerevisiae* growth according

to pH, 3 pH values were tested: 2.6, 4.4 and 6 using citrate/phosphate buffer (Table 5-1) and YM broth.

Table 5-1 - Fraction of citric acid and Na_2HPO_4 for buffers preparation at different pH. Source: (Sigma Aldrich).

pH	0.1M citric acid (%)	0.2M Na_2HPO_4 (%)
2.6	89.1	10.9
4.4	55.9	44.1
6.0	36.1	63.2

5.2.3.2. HMF toxicity study

In order to evaluate the yeast growth when in the presence of HMF, a run was performed using the YM media containing 1g/L of HMF.

5.2.4. Analysis by flow cytometry

The volume of the fermentation runs (10mL) is impractical for analysis of cell number by OD as a significant volume (500-1000μL) is needed for this analysis. Therefore, flow cytometry was used to measure yeast population during growth, as well as determine cell viability.

5.2.4.1. Background

Flow cytometry (FC) is a powerful technique that rapidly analyse cells using light scattering and fluorescence (Díaz et al., 2010).

The way light scatters in the cells due to its membrane, topography and internal components, allows cells differentiation. The side-scattered light (SSC) is proportional to the cell internal granules. Therefore, cells with high granularity will have high SSC; on the other hand, the forward-scattered light (FSC) is proportional to cell size, thus, large cells have high

FSC (BD Biosciences, 2000). The plot of SSC versus FSC can differentiate cell population as shown in the scheme in Figure 5-2.

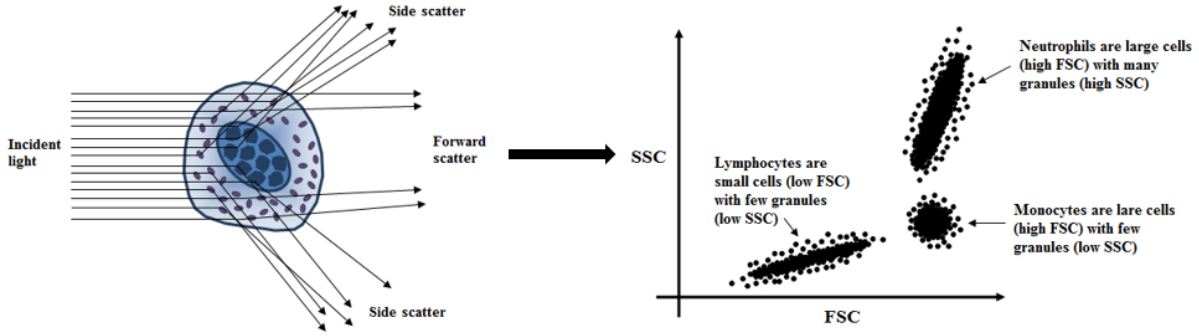

Figure 5-2 - Scheme of light scatter in a flow cytometer and cells differentiation by the plot of SSC and FSC. Source: modified from (UQ)

Even though optical density analysis is widely used, it gives no information about the viability of the cells (Díaz et al., 2010). Flow cytometry is also able to measure cell viability. Live yeast cells have a plasma membrane that is impermeable to dyes such as Propidium iodide (PI). Therefore, such dyes can be used to evaluate membrane integrity (Hewitt and Nebe-Von-Caron, 2001).

The use of a combination of stains improves the precision of the analysis (Díaz et al., 2010). In this work, a combination of permeable/impermeable stains was used. PI is a dye that does not cross the cytoplasmic membrane when the cell is healthy. Moreover, this dye binds to cellular DNA and emits red fluorescence when cell integrity is compromised, therefore, it can be used to distinguish live/dead cells (Hewitt and Nebe-Von-Caron, 2001). On the other hand, Syto 9 is membrane-permeable and stains all cells green. Using these two stains together, cells with intact membrane fluoresce green and damaged cells fluoresce red, therefore, live/dead cells can be quantified (Díaz et al., 2010).

5.2.4.2. Method

Although FC has been used for fermentation evaluation (Herrero et al., 2006, Mannazzu et al., 2008), it has not been applied to lignocellulosic fermentation. The equipment used was a BD Accuri™ C6 flow cytometer using the BD Accuri C6 Analysis Software.

Samples diluted in PBS were analysed in the FC for cells counting as soon as they were collected. Then, samples were stained with 10μL of PI (200μL/mL) and 5μL of Syto 9 (200μL/mL) and left to stain for 5min. Stained samples were analysed in the FC once again for analysis of cells viability.

In order to both ensure that the quantity of stain used was enough to the samples being analysed and to find the position of the dead cells in the fluorescence graphs, a sample of cells in the standard fermentation run was killed and evaluated. The cells were killed by heating up the sample to 100ºC for 15min. After cooling the sample, it was stained and analysed by FC.

5.2.4.3. Limitation

There is the potential of yeast cells flocculating into a 'ball' of cell. This case could result in underestimation of cells numbers as each 'ball' would account as one event (Boyd et al., 2003). This problem is minimized by diluting the sample and analysing it in the FC as soon as it is collected.

5.2.5. Ethanol analysis

5.2.5.1. Enzyme essay for ethanol determination

5.2.5.1.1. Background

Ethanol is commonly quantified by HPLC using a refractive index detector. However, the size of fermentation samples used in this work (μL) make it unfeasible for HPLC analysis.

Therefore, an enzymatic assay from Megazyme (Ethanol Assay) was used to determine ethanol concentration in fermented samples.

According to Megazyme (2014), the ethanol reacts with NAD^+ (catalysed by alcohol dehydrogenase) to produce acetaldehyde, which is further reacted to acetic acid and NADH in the presence of aldehyde dehydrogenase, as shown in Equation 5-1 and Equation 5-2 (Megazyme, 2014).

$$Ethanol + NAD^+ \xrightarrow{ADH} acetaldehyde + NADH + H^+ \qquad \text{Equation 5-1}$$

$$Acetaldehyde + NAD^+ + H_2O \xrightarrow{Al-DH} acetic\ acid + NADH + H^+ \qquad \text{Equation 5-2}$$

The production of NADH can be measured by an increase in absorbance and it is proportional to twice the amount of ethanol in the sample (Megazyme, 2014).

5.2.5.1.2. Limitation

The assay is linear for ethanol contents from 0.25-12μg per assay. Moreover, interferences may occur when alcohol is present in the distilled water used and/or in the air (Megazyme, 2014).

5.2.5.1.3. Materials and Method

Ethanol assay was purchased from Megazyme containing five bottles: 1) buffer (pH 9); 2) NAD^+; 3)Al-DH; 4) ADH; and 5) ethanol standard (5g/L).

Spectrophotometer used was a Tecan Spectrophotometer Infinite® 200Pro set at 340nm. Three classes of solutions (blank, samples and standard solutions) were prepared in plastic micro-plates.

Blank was prepared using 0.21mL of distilled water and adding the buffer and NAD^+ (0.02mL of each) and 0.005mL of Al-DH. Samples were prepared using 0.20mL of distilled water and 0.01mL of sample, buffer and NAD^+ (0.02mL of each) plus 0.005mL of Al-DH.

Standards were prepared using the same volumes as in samples solution, replacing the sample volume by standard solutions.

After preparing all three classes of solutions, plates were closed using a plastic cover and agitated gently. Although the assay protocol states the reaction takes up to 5min, it was observed that samples from these work required a considerable longer time to stabilize the absorbance. Therefore, instead of 5 min, 20min of reaction was applied. All the solutions were read in spectrophotometer and absorbance were recorded (A_1).

After reading A_1, 2µL of ADH was added to each well in the plate. Plates were once again closed and stirred. After 20min, the second absorbance of each well was recorded (A_2).

Ethanol absorbance (ΔA_{EtOH}) was calculate as described in Equation 5-3

$$\Delta A_{EtOH} = (A_2 - A_1)_{sample/standard} - (A_2 - A_1)_{blank} \qquad \text{Equation 5-3}$$

Figure 5-3 shows ethanol calibration curve made using ethanol standard provided in the enzyme kit and diluting it to the following concentrations: 2.5, 1.25, 0.625, and 0.1mg/L. Slope and R^2, 358.1 and 0.97 respectively, were calculated using Excel.

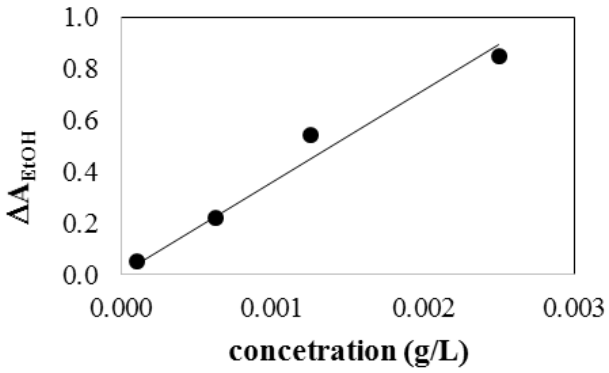

Figure 5-3 - Ethanol calibration curve by glucose enzymatic assay.

5.2.5.2. Calculation of ethanol yield (Y_{etOH})

In alcoholic fermentation, each glucose mol consumed generates two ethanol and two carbon dioxide molecules, as shown in Equation 5-4:

$$C_6H_{12}O_6 \rightarrow 2\ C_2H_5OH + 2CO_2$$ Equation 5-4

Considering the molar masses of glucose and ethanol, 180 and 46 g/mol, respectively; 1mol of glucose (180g) produces 2mols of ethanol (92g). Therefore, the theoretical mass yield of ethanol in fermentation is shown in Equation 5-5.

$$Theoretical\ EtOH\ (g/L) = \ initial\ glucose\ (\frac{g}{L}) * 0.511$$ Equation 5-5

Therefore, Y_{etOH} was calculated as the ratio between the ethanol concentration of a sample and the theoretical ethanol concentration, which varies with initial glucose concentration.

5.2.6. Analysis by HPAEC

Some fermented samples were analysed for contents of glucose as well as HMF. This analysis was performed by HPAEC and the method is described in section 2.6.

Prior to the HPAEC analysis, fermented samples were filtrated using 13mm syringe filters (Acrodic® LC, 0.45μm, PVDF membrane) to ensure no cells were injected in the HPAEC equipment.

5.3. Results and discussion

5.3.1. Standard fermentation

The yeast chosen for fermentation evaluation (NCYC-3233) is an industrial strain that is largely used in bioethanol production in Brazil (Basso et al., 2008). This strain presented higher ethanol and biomass yields and less glycerol production when compared to Baker yeast, a commonly used strain in research field (Basso et al., 2008). Moreover, it has already been evaluated for ethanol production from lignocellulosic extracts with promising results (Pereira et al., 2014).

The YM broth was used as a standard condition. Therefore, fermentation runs using glucose extracts obtained from SBW hydrolysis as well as the evaluation of pH and HMF toxicity were compared to the standard condition.

5.3.1.1. Flow cytometer

FC analysis generates counts of particles (cells) per unit of volume as well as light scattering and fluorescence. Figure 5-4 shows the side/forward scatter graph (SSC vs FSC: a) as well as the red versus green fluorescence plot before (b) and after (c) staining the cells for the standard *S. cerevisiae* fermentation using YM broth at the beginning of the process (0h).

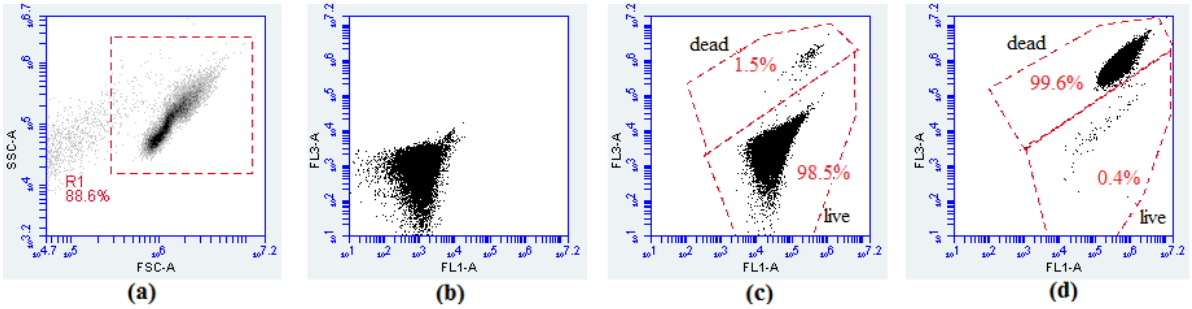

Figure 5-4 - Graphs obtained by FC analysis: (a) light scattering of yeast cells in the standard fermentation (0h); (b) fluorescence graph before staining (0h); (c) fluorescence graph after cell staining using PI and Syto 9 (0h); (d) fluorescence graph of dead yeast cells after staining using PI and Syto 9 (t=48h). *FL1-A: green fluorescence (Syto 9); FL3-A: red fluorescence (PI)

Figure 5-4-a shows that, although there are other particles present in the sample, yeast cells can be easily identified by their high forward and side scatter. Figure 5-4-b shows the fluorescence before staining, which is the yeast cell autoflorescence. Figure 5-4-c was obtained after staining the cells with Syto9 and PI, in which two populations can be distinguished. To ensure which was the dead population, dead yeast cells were killed by heat; their fluorescence (after staining) is shown in Figure 5-4-d. Therefore, FC is a powerful tool to evaluate

fermentation that allows not only evaluate yeast growth but also to evaluate cells integrity and quantify live/dead cells during the fermentation runs.

Most of the discussion of yeast growth curves was made using live cells counting (unless otherwise stated). The approach of evaluating fermentation using direct counts of live cells is not well explored and it opens the possibility of a new method to evaluate fermentation of lignocellulosic extracts fermentation for ethanol production.

5.3.1.2. Yeast growth

Figure 5-5 shows the numbers of live and dead yeast cells analysed by FC during fermentation. It can be seen that the yeast growth has its lag phase between 0-4h and the exponential phase between 4-12h.

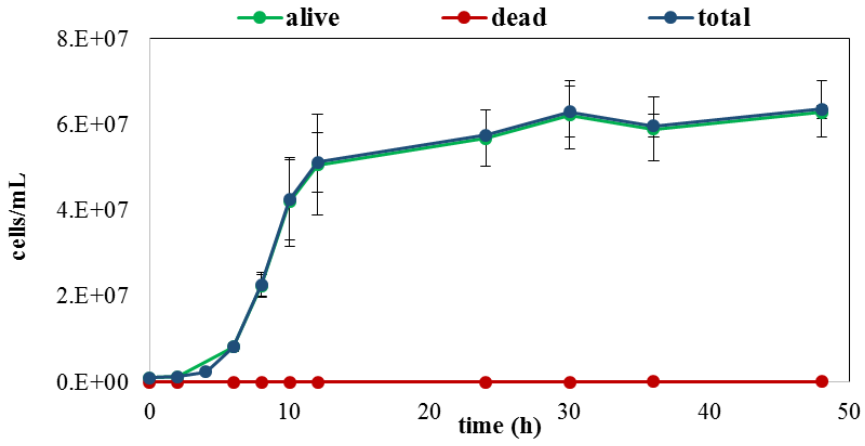

Figure 5-5 - *S. cerevisiae* growth and cells viability (alive/dead) analysed by FC during anaerobic fermentation in YM media at pH 4.4, 30ºC for 48h (n=6).

When available glucose has been depleted, *S. cerevisiae* can consume ethanol in an oxidative pathway. Moreover, this change in carbon source causes a behaviour in the yeast growth curve called diauxic growth, in which the cell number increases, however, in a smaller

rate than during the exponential phase (Jones and Kompala, 1999). According to Figure 5-1, it is possible to suggest a diauxic behaviour between 12-30h.

After 30h, the growth entered its stationary phase. No significant number of dead cells is seen even at 48h, which is not unexpected as yeast cells can adapt to remain alive in the stationary phase for an unknown period (Werner-Washburne et al., 1996).

5.3.2. Evaluation of pH and HMF toxicity

5.3.2.1. Evaluation of pH

In an attempt to evaluate yeast viability in different pH values, buffer solutions of pH 2.6, 4.4 and 6 were prepared using citric acid and Na_2HPO_4 and used in combination with YM broth.

Figure 5-6 shows the total number of yeast cells plus number of live/dead under these pH values in which it is possible to see that the yeast growth was supressed for all pH values. Moreover, while there is only a small difference between the growth at pH 4.4 and 6, the yeast does not survive at the lowest pH (2.6).

The difference between the run at pH 4.4 presented in Figure 5-6 and the standard fermentation shown in Figure 5-1 is that in the latter the pH was adjusted using HCl, instead of the citric acid/ Na_2HPO_4 buffer used here. Therefore, the suppression of growth is most likely related to the use of the chosen buffer, even though citrate/phosphate buffer is commonly used in microbiological cultures (Siegumfeldt et al., 2000, Valli et al., 2006).

Citric acid is an important specie in yeast metabolism. Moreover, the significant decrease of cells multiplication shown in Figure 5-6 as a consequence of the use of buffering could be related to the excess of citrate in the media. High availability of citrate ions causes an inhibitory effect of ATP and in activity of phosphofructokinase-1 (enzyme that regulates

glycolysis), which leads to a reducing in the flow of glucose in the glycolysis path (Nelson and Cox, 2004).

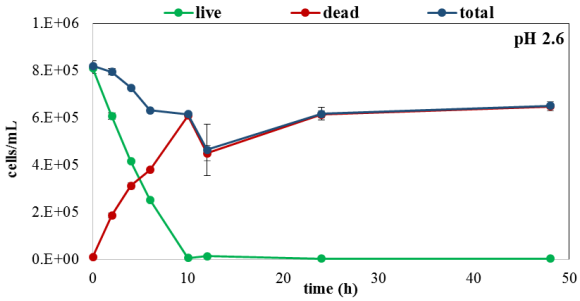

(a)

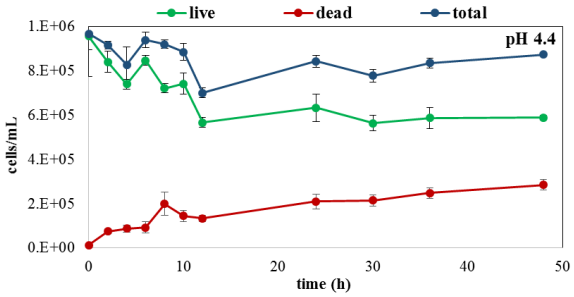

(b)

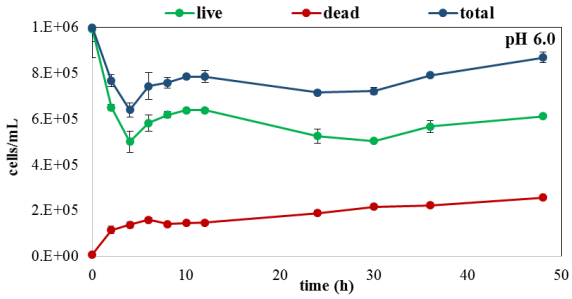

(c)

Figure 5-6 - *S. cerevisiae* cell number (total/alive/dead) analysed by FC during anaerobic fermentation in YM media at 30ºC for 48h using citric acid/Na_2HPO_4 buffer at pH: 2.6 (a), 4.4 (b) and 6 (c) (n=6).

In addition, the high concentration of salts resulted from the addition of the buffer might have created an osmotic stress in the yeast cells. High osmolarity caused by high salt concentration might lead to severe cell dehydration and affect ionic equilibrium in the plasma membrane and nutrients uptake, which can result in cells death (Mager and Varela, 1993).

As the buffer used did not lead to results in terms of yeast tolerance regarding to pH, it was decided to maintain the use of pH 4.4 adjusted by HCl and in the standard condition.

5.3.2.2. HMF toxicity test

The level of toxicity of HMF is highly dependent on the microorganism and strain (Martín and Jönsson, 2003). Therefore, in order to evaluate if the strain 3233 would tolerate HMF at a medium concentration, a fermentation run using 1g/L of HMF was performed. Figure 5-7 shows the comparison between the standard fermentation run and the YM medium containing HMF.

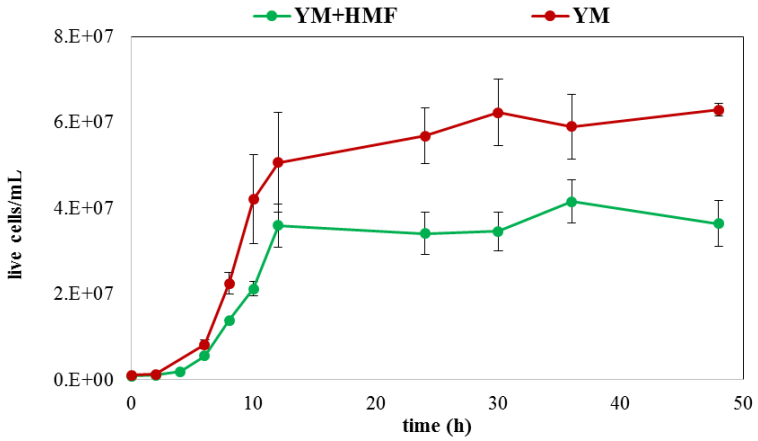

Figure 5-7 - Comparison of yeast growth curve of standard fermentation and fermentation using YM media containing 1g/L of HMF.

As it can be seen in Figure 5-7, the presence of HMF did not totally supress yeast growth, however, compared to the standard media, it is clear that HMF had some inhibitory effect that could potentially increase with the increase in HMF concentration.

Rosatella et al. (2011) presented a comparison among strains of *S. cerevisiae* and its tolerance and effects caused by HMF. They reported strains of yeasts that were able to produce ethanol and no growth decrease with HMF concentrations as high as 4g/L. On the other hand, less tolerant strains were observed for which 2.5g/L of HMF resulted in significant decrease of growth (Rosatella et al., 2011).

The inhibitory effect of HMF in yeast cell metabolism is not well understood, but it is believed that HMF is consumed by *S. cerevisiae* at the same time as glucose is being consumed. Moreover, 5-hydroxymethylfurfurylalcohol has been detected from yeast consumption of HMF (Taherzadeh et al., 2000).

To confirm if HMF was in fact consumed by the yeast cells during fermentation, samples at time 0 and 48h were analysed by HPAEC. According the HPAEC chromatograms (not shown), both HMF and glucose were completely consumed by 48h.

Figure 5-8 shows the ethanol concentration determined by ethanol enzyme assay during fermentation for YM broth and YM+HMF media. As it can be seen, ethanol concentration was mostly affected in the beginning of fermentation. However, the values obtained at the end (48h) are similar with and without HMF addition. Therefore, although the presence of HMF affected the yeast growth, the ethanol production seems to have been less affected by this compound.

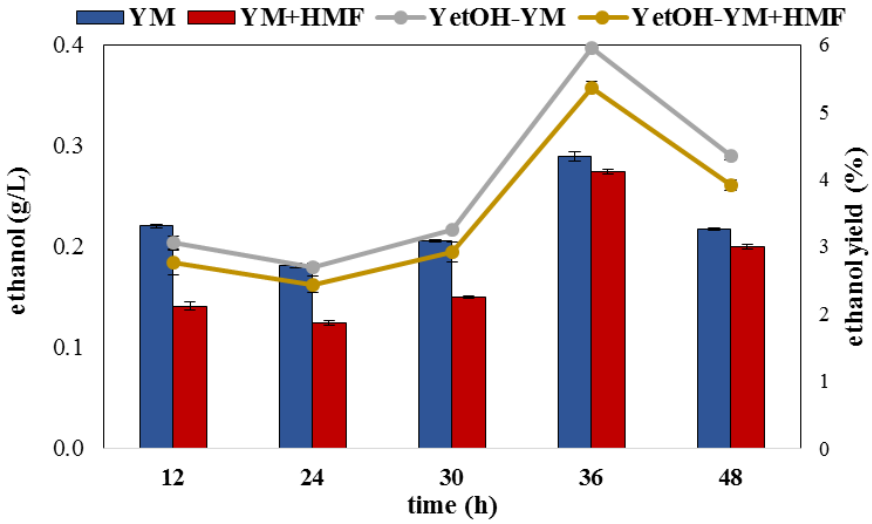

Figure 5-8 - Ethanol concentration (g/L) determined by ethanol enzyme assay for fermentation using YM broth and YM+HMF (1g/L).

The consumption of HMF is believed to reduce availability of ATP and NAD(P)H required for HMF reduction into HMF-alcohol (Almeida et al., 2007). Moreover, furans

(furfural and HMF) have a strong inhibitory effect to respiratory pathway through enzymes such as alcohol dehydrogenase (ADH), pyruvate dehydrogenase (PDH), and aldehyde dehydrogenase (ALDH). On the other hand, pyruvate to ethanol path is less affected by furans (Modig et al., 2002), which explains why yeast growth is more affected by these compounds than ethanol production (Martín and Jönsson, 2003, Palmqvist and Hahn-Hägerdal, 2000b).

The ethanol yields obtained by both standard fermentation and YM+HMF were unexpectedly low, which could be a result of the non-optimized parameters used in this work. High glucose concentration might have an inhibitory effect in the fermentation due to an increase in osmotic stress (Pereira et al., 2010). However, the strain used in this work was previously reported to perform fermentation at glucose concentrations as high as 300g/L, which is much higher than the 10g/L used when using YM broth.

Parameters such as temperature and pH also have an important effect in the generated products during fermentation, e.g., the conditions used could be leading to the formation of glycerol instead of ethanol. Nevertheless, more experiments such as glycerol quantification would be required in order to understand what is in fact inhibiting ethanol production and/or optimize the fermentation.

5.3.3. Fermentation using SBW hydrolysed extracts

5.3.3.1. Glucose extract media without addition of yeast nutrients

From an industrial point of view, the ideal fermentation process would utilized lignocellulosic extracts with no added nutrients such as peptone, which would contribute to lower the overall process cost. Therefore, in order to evaluate if it was possible to use glucose extracts only, no additional nutrients were used in this fermentation run. Table 5-2 shows glucose and HMF initial composition analysed by HPAEC for extracts obtained from Avicel,

DEL and SEQ fibres after SBW hydrolysis at 250ºC, 10min and 1% biomass load. The pH of the extracts measured at the beginning of fermentation is also shown and it was not corrected for the run.

Table 5-2 - Initial glucose and HMF concentration analysed by HPAEC for the extracts obtained from SBW hydrolysis of three biomass at 250ºC, 10min and 1% load.

Fibre	Glucose (g/L)	HMF (g/L)	pH
Avicel	2.69	0.44	2.66
DEL	0.04	0.11	3.32
SEQ	0.50	0.39	2.89

Figure 5-9 shows the growth curve (alive, dead and total cells) for fermentation performed without addition of nutrients using extracts from Avicel, DEL and SEQ fibres hydrolysis. It can be seen that no growth was possible.

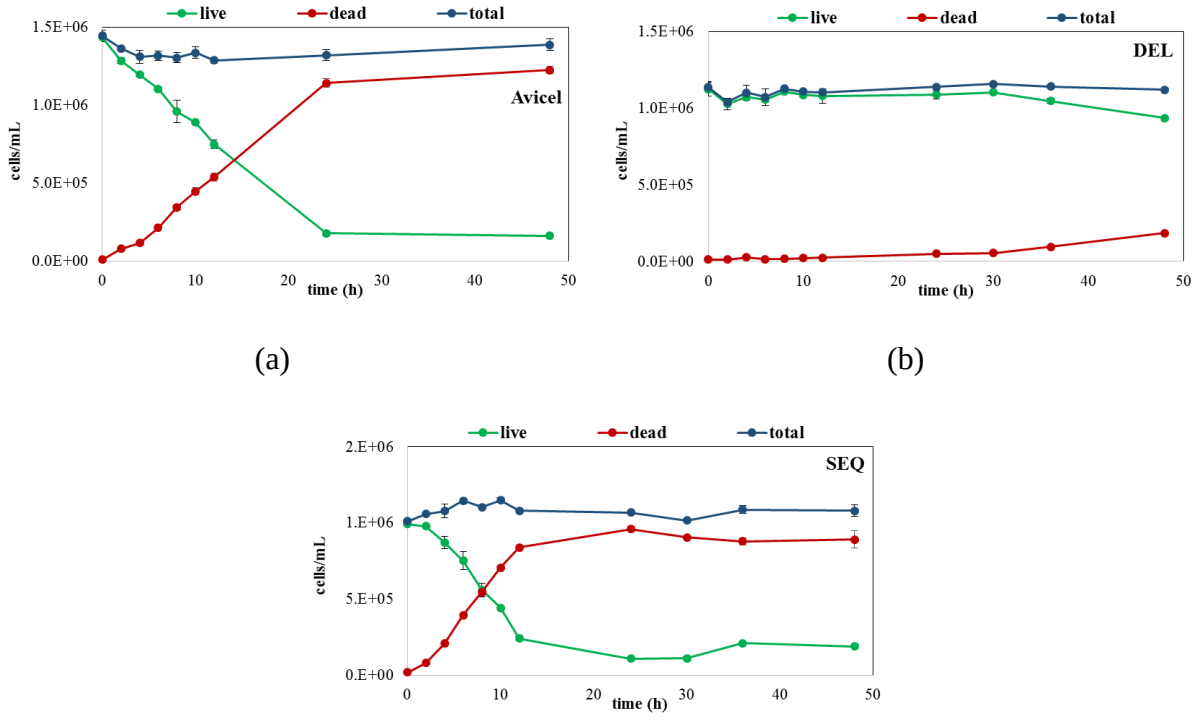

(a) (b)

(c)

Figure 5-9 - *S. cerevisiae* cell numbers (total/live/dead) for fermentation using glucose extracts media obtained from Avicel (a), DEL (b) and SEQ (c) fibres after SBW hydrolysis at 250ºC, 10min and 1% load.

Comparing the extracts from the three biomasses, Avicel and SEQ led to significant number of dead cells in about 24h. On the other hand, the yeast kept alive until the end of fermentation when media was the extract from DEL. Moreover, at the end of 48h glucose was only consumed in DEL extracts and at very small quantity (0.007g/L). This result indicate that Avicel and SEQ extracts were more toxic than, most likely because of higher concentrations of inhibitors and low pH compared to DEL extracts. Moreover, although DEL extracts were not toxic, it did not support yeast growth.

5.3.3.2. Glucose extract media with addition of yeast nutrients

5.3.3.2.1. Low initial glucose contents

This time, fermentation was performed using fibres extracts after SBW hydrolysis plus yeast and malt extract as well as peptone as nutrients at the same concentration as in YM broth.

The Avicel sample used was similar to the previous section to provide comparison between addition or not of nutrients. This time, however, it was decided to use SEQ and DEL extracts with similar contents of glucose, to allow a direct comparison between these fibres. Table 5-3 shows the initial glucose and HMF concentration of the extracts used in the fermentation. Values of pH are not shown because after the addition of nutrients, the pH of the extracts were increased to 5.4-5.8 for all biomasses.

Table 5-3 - Glucose and HMF initial composition analysed by HPAEC for the extracts obtained from SBW hydrolysis of Avicel, DEL and SEQ fibres.

Fibre	Glucose (g/L)	HMF (g/L)
Avicel	2.880	0.518
DEL	0.081	0.080
SEQ	0.084	0.067

Figure 5-10 shows the yeast growth curve (live cells) for the three biomasses extracts as well as for YM broth for comparison. The diauxic pattern discussed for the YM curve (see section 5.3.1.2) can be seen in all of the curves. Moreover, no significant number of dead cells was observed in any of the media at 48h.

YM broth resulted in significant higher yeast growth compared to the SBW hydrolysed extracts. This result was expected as the presence of compounds such as furans, phenols and organic acids have an inhibitory effect on the yeast. Nevertheless, the growth of each media was not proportional to the glucose contents. For instance, although YM have 100 times more glucose than DEL and SEQ extracts, the growth of YM media was only about 10 times higher. That is a further suggestion that something inhibited the growth in YM broth, which resulted in the low ethanol yields discussed previously.

The presence of inhibitors did not prevent yeast growth, even though the growth was most likely affected by the presence of them, as indicated in the evaluation of HMF in YM broth. Moreover, the effect of several inhibitory compounds was found to have a synergism that affects yeast metabolism in a stronger way than the presence of the same compounds separately (Palmqvist and Hahn-Hägerdal, 2000b).

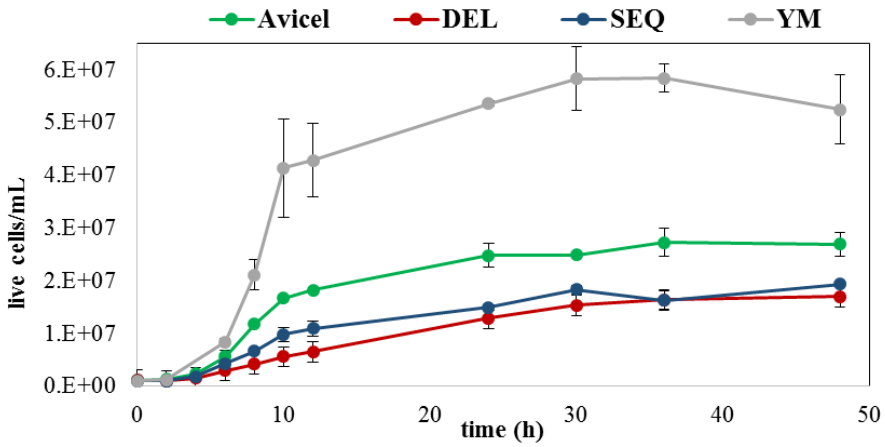

Figure 5-10 - *S. cerevisiae* growth curve (alive cells) for fermentation using YM broth and glucose extracts media obtained from Avicel, DEL and SEQ fibres after SBW hydrolysis with addition of nutrients.

Yeast growth in these media might be improved by the prior extracts detoxification. Detoxification includes biological, physical and chemical processes such as treatments with enzymes, roto-evaporation, liquid-liquid extraction and treatment using compounds such as alkaline and sulphite (Palmqvist and Hahn-Hägerdal, 2000a). However, the addition of a step prior to fermentation would increase costs. Therefore, the decision of extracts detoxification would require a more detail investigation of the gain in yeast growth/ethanol yields and the cost of the inclusion of an extra process step.

Figure 5-11 shows the Y_{etOH} for fermentation of DEL and SEQ extracts, which can be compared as their initial glucose concentration was similar.

The yeast strain used in this work (3233-NCYC) was reported to be very efficient in ethanol production of sugar cane juice achieving yields as high as 92% (Basso et al., 2008). Compared to sugar cane extracts, it is expected that ethanol yields will be lower when using lignocellulosic extracts due to the presence of inhibitory substances.

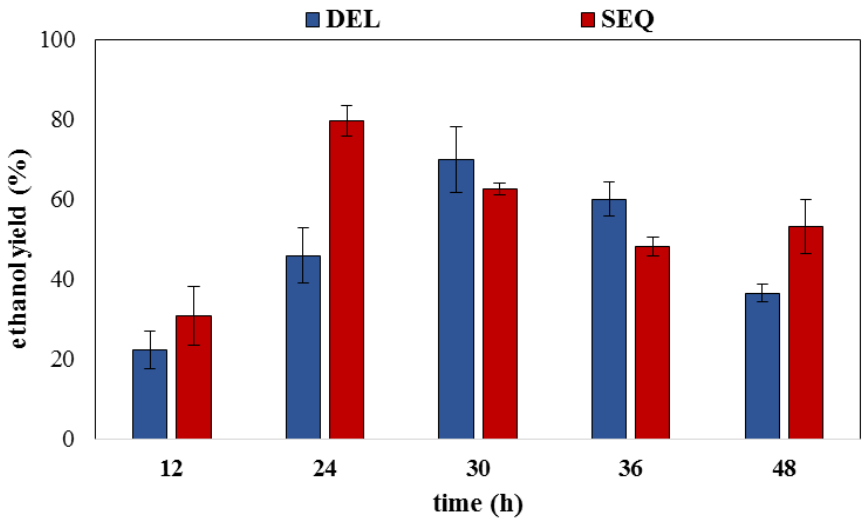

Figure 5-11 - Ethanol yields (Y_{etOH}) determined by ethanol enzyme assay for fermentation using extracts from DEL and SEQ fibres.

Y_{etOH} achieved 80% for SEQ extracts at 24h, while DEL extracts maximum Y_{etOH} was 70% at 30h. After the maximum value, ethanol concentration started decreasing due to its consumption by the yeast (Jones and Kompala, 1999). Therefore, even for a similar initial composition, SEQ fibres presented slightly better maximum Y_{etOH}, probably due to the lower contents of inhibitors that were not quantified such as furfural, acetic acid, etc.

At low glucose concentrations (<50mg/L), *S. cerevisiae* can metabolize glucose in an oxidative pathway, which does not produce ethanol (Jones and Kompala, 1999). However, considering the alcohol yields observed in this fermentation, it is unlikely that this path has occurred in significant extent.

Considering both the yeast growth curve for YM and SBW hydrolytes and the Y_{etOH} for these media, it is important to notice that although YM have significant higher initial glucose (10g/L) which is 100 times higher than the extracts. Moreover it was not reflected at the same proportion either in terms of yeast growth or ethanol production. This is an evidence that something is inhibiting not only ethanol production (as discussed in section 5.3.2.2) but also yeast growth in the YM broth fermentation.

5.3.3.2.2. High initial glucose contents

High sugar concentration is preferable for fermentation process because it will generate higher product concentration, and therefore, facilitate its recovery (Jørgensen et al., 2007). However, high concentrated hydrolysis extracts potentially also contains a high concentration of fermentation inhibitors, as it happened in this work, which will probably result in significant decrease of productivity (Jørgensen et al., 2007). Table 5-4 shows the initial glucose and HMF concentration in each extract after SBW hydrolysis at 280^{o}C, 0min and 5% load.

Figure 5-12 shows the growth curve for *S. cerevisiae* using extracts containing maximum glucose concentration obtained in the DoE-2 plus nutrients. In this Figure, only a

slight cell numbers increase can be seen in the first hours of fermentation. After 6h of fermentation, yeast cells started dying in a very fast rate.

Table 5-4 - Glucose and HMF initial composition analysed by HPAEC for the extracts obtained from SBW hydrolysis of Avicel, DEL and SEQ fibres at 280ºC, 0min and 5% biomass load.

Fibre	Glucose (g/L)	HMF (g/L)
Avicel	10.05	3.44
DEL	0.79	0.83
SEQ	4.56	2.48

Very small quantities of glucose were consumed by the end of fermentation (up to 20%) and no HMF was consumed. The results show that although the concentration of glucose was high, the concentration of inhibitors was highly toxic and resulted in affecting glucose metabolism and led to yeast dead.

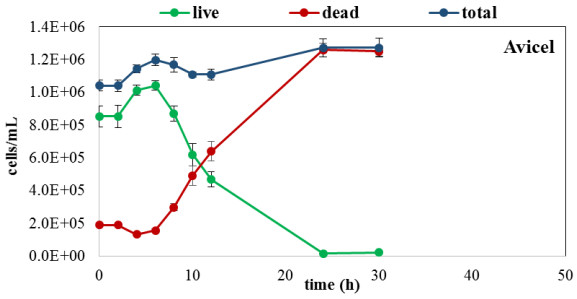

(a)

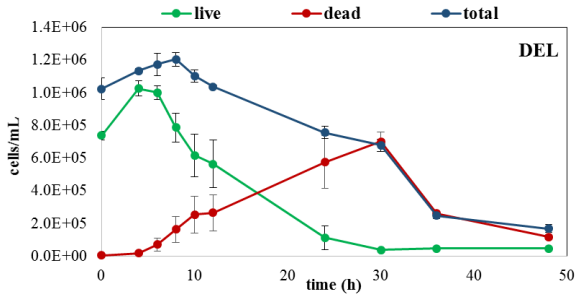

(b)

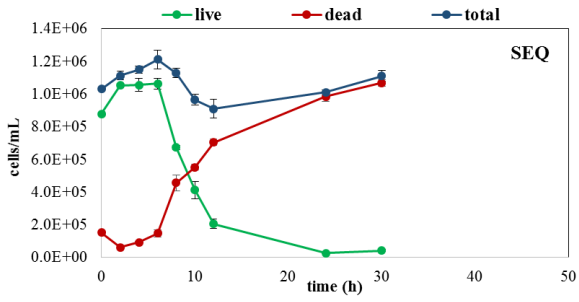

(c)

Figure 5-12 - *S. cerevisiae* growth curve (live, dead and total cells) for fermentation using glucose extracts media obtained from Avicel, DEL and SEQ fibres after SBW hydrolysis at optimal glucose condition (DoE-2) with addition of nutrients.

In summary, the overall preliminary results indicate the potential of using extracts obtained from SBW hydrolysis of lignocellulosic biomass for production of 2nd-generation ethanol. However, it is clear that the fermentation process of these extracts is extremely challenging and several aspects require a deeper evaluation including other potential yeast strains, limit level of inhibitors, optimization of fermentation parameters, etc., in order to make this process conceivable.

5.4. Conclusion

Fermentation of hydrolysed extracts obtained from lignocellulosic biomass is a challenge for 2nd-generation bioethanol production mostly because of the low glucose concentration extracts as well as the presence of inhibitory substances. This chapter evaluated the feasibility of alcoholic fermentation of SBW hydrolysed extracts using a well-known industrial yeast. Moreover, an innovative method of cells analysis was also applied using flow cytometry.

Analysis of cells using a flow cytometer provided an understanding of cells viability and allowed an efficient discussion based on live/dead cell numbers. Therefore, FC could easily replace common optical density analysis as a powerful technique for fermentation evaluation.

The preliminary results showed that the standard fermentation using YM broth is being inhibit and requires optimization as ethanol yield as well as biomass production were low.

The presence of HMF during fermentation was tested and it seemed to affect yeast growth more than ethanol production. However, the use of SBW extracts containing high concentration of glucose and inhibitors prevented ethanol production, yeast growth and led to yeast death.

On the other hand, fermentation using lower concentrate extracts obtained from SBW hydrolysis of DEL and SEQ fibres achieved high ethanol yields up to 80% of theoretical. Moreover, although the use of extracts from both fibres led to similar results, the use of SEQ fibres is still preferred in a biorefinery point of view as it leads to a more sustainable processing route without any drawbacks when compared to DEL fibres.

CHAPTER 6

CONCLUSIONS AND FUTURE WORK

6.1. Conclusions

The economic viability of 2nd-generation bioethanol could be achieved by increasing the overall value of the feedstock throughout more efficient processes and the co-production of high valued components from the different fractions of the lignocellulosic biomass. In this work, biomass fractionation was investigated using 'green' technologies in a biorefinery approach, in which the cellulose fraction was processed to generate bioethanol and the extracted hemicellulose and lignin fractions have the potential to be used in high valuable compounds.

In the approach utilised in this work, cellulose fibres from MxG were purified using direct and sequential extractions, and these processes were compared in terms of the fibres and the other streams (lignin and hemicellulose) obtained. The direct removal of extractives, hemicellulose and lignin performed in one-step using a modified organosolv method resulted in the complete removal of extracts, partial removal of hemicellulose (which was rapidly dehydrated into decomposed products) and in 71.7% removal of the lignin presented in the raw MxG. On the other hand, extraction in 3-steps achieved the complete removal of extractives (1st-step); 71.4% of hemicellulose extraction (2nd-step); and 60.9% removal of lignin (3rd-step). Higher percentage of lignin extraction were obtained in the direct extraction most likely due to the higher incidence of undesirable side reactions (e.g. condensation) in the pre-processed fibres during the organosolv step. Therefore, evaluation of new operations parameters for the 3rd-step of the sequential process could improve lignin extraction. Moreover, although less efficient in

terms of lignin removal, the sequential extraction process showed the potential to produce purified streams of biomass fractions that could lead to high value products, which is highly desirable in 2nd-generation bioethanol processes.

Composition of cellulose-enriched fibres did not vary significantly comparing the two extraction routes: direct route led to fibres (DEL) containing 7.2%, 12.9% and 79.9% of hemicellulose, lignin and cellulose, respectively; while fibres obtained from the sequential treatment (SEQ) presented 4.8%, 16.3% and 78.9% of hemicellulose, lignin and cellulose, respectively. On the other hand, physical analysis (SEM, FTIR, PCA) demonstrated that although similar in composition, cellulose fibres obtained by different processing routes were structurally different.

Cellulose-enriched fibres obtained from MxG were hydrolysed using subcritical water (SBW) as a 'green' solvent/media for glucose production. Temperature (190-320ºC), residence time (0-54min) and biomass loading (0.5-6.4%) were evaluated using a 3 factors Central Composite Design of experiments (DoE). The use of DoE for glucose production optimization demonstrated to be unsuitable due to the complexity of the system resulted from SBW hydrolysis of lignocellulosic biomass. However, from the results obtained in two sets of DoE data, it was possible to infer that temperature and residence time showed great effect in the production of glucose as well as in glucose decomposition, while biomass loading did not show significant effect in the range evaluated. The process used for cellulose purification (direct vs sequential extractions) had a great effect on subsequent glucose production by SBW hydrolysis. Moreover, sequential extraction process demonstrated to produce more accessible cellulose fibres, which resulted in higher glucose production compared to the direct extraction of biomass components. Glucose yields obtained from SEQ fibres achieved 11.2%, whereas glucose yields from DEL fibres achieved only 3.3%. Moreover, commercial cellulose (Avicel) was used as a

standard pure cellulose and it proved to be easier hydrolysable compared to MxG cellulose fibres: Avicel glucose yields achieved 20%. The use of a batch reactor led to low efficiencies (glucose yields) due to constrains intrinsic to the reactor configuration such as long heating time and high inhibitors formations due to the impossibility of removing glucose as soon as it is formed. Reactions during SBW hydrolysis were evaluated according to products observed and it was recognised that, although other paths are also possible, at the conditions evaluated dehydration is the predominant reaction path for the monosaccharides decomposition. The structure of remaining fibres after SBW hydrolysis were evaluated using FTIR and PCA and they showed structural modification in different degrees, depending on process parameters.

Preliminary fermentation studies were performed to assess the production of ethanol from glucose produced using SBW of cellulose fibres obtained from MxG. An industrial *Saccharomyces Cerevisiae* strain was used to evaluate the fermentation of glucose into bioethanol. Although process parameters were not optimized, a range of fermentation using different glucose extracts produced by commercial cellulose (Avicel) and MxG fibres (DEL and SEQ) as well as standard conditions using pure glucose were performed and compared. The effect of the presence of inhibitory substances during fermentation on both ethanol production and yeast growth was more or less pronounced according to their concentrations. Moreover, fermentation results showed that, although parameters optimization is mandatory for the process success, ethanol yields achieved 70% and 80% for DEL and SEQ fibres, respectively. Therefore, fermentation results showed the possibility of producing bioethanol after lignocellulosic biomass pretreatment and hydrolysis using a combination of environment-friendly processes.

6.2. Future work

The sequential extractions proposed in this work showed potential for glucose generation using environment-friendly processes. Future work should be focused on optimization of the processing steps.

The use of sequential extractions to purify cellulose fibres showed promising results, however this step could be optimized in order to achieve high extraction of lignocellulosic biomass fractions as well as allow the recovery of each fraction for further processing. During the preparation of cellulose-enriched fibres, removal of extractives and extraction of hemicellulose were effective. Moreover, optimization in order to pursue a specific desirable product, e.g. XOS, could be achieved through change of operational conditions. Extraction of lignin using a modified organosolv method requires optimization as the conditions used (optimized for MxG raw fibres) demonstrated to be too aggressive for the pre-processed fibres. Therefore, there is opportunity to optimize lignin extraction from the cellulosic fibres after removal of extractives and hemicellulose by changing operational parameters such as temperature and residence time. Moreover, efficient ways to recover and/or concentrate each fraction requires evaluation as well as studies in their application possibilities.

Cellulose hydrolysis using SBW demonstrated that it is possible to use this method for glucose production. However, low glucose yields were obtained, hence, process optimization is needed. Moreover, an important next step is to evaluate the use of other reactor configurations such as flow-types or membrane reactors in which operational parameters (flow rate, temperature, and residence time) will need to be investigated and the possibility of glucose removal during the process could be pursued. In this way, glucose decomposition, which was the main reason for the low glucose yield obtained in this work, could be avoided, thus making the process significantly more efficient.

Fermentation presented only preliminary studies in order to evaluate the feasibility of using glucose produced by SBW hydrolysis. Therefore, a significant amount of optimization could be performed in order to make the process economically feasible. These optimizations include fermentation parameters (temperature, time, used of other yeast/strain) as well as fermentation configuration (continuous and fed-batch). Moreover, the evaluation of suitability of detoxification methods could also be significant.

REFERENCES

Abdullah, R., Ueda, K. and Saka, S. (2014) Hydrothermal decomposition of various crystalline celluloses as treated by semi-flow hot-compressed water. **Journal of Wood Science**, 60: (4): 278-286.

Adel, A.M., El–Wahab, Z.H.A., Ibrahim, A.A., et al. (2010) Characterization of microcrystalline cellulose prepared from lignocellulosic materials. Part I. Acid catalyzed hydrolysis. **Bioresource Technology**, 101: (12): 4446-4455.

Agblevor, F.A., Hames, B.R., Schell, D., et al. (2007) Analysis of biomass sugars using a novel HPLC method. **Applied Biochemistry and Biotechnology**, 136: (3): 309-326.

Agbor, V.B., Cicek, N., Sparling, R., et al. (2011) Biomass pretreatment: Fundamentals toward application. **Biotechnology Advances**, 29: (6): 675-685.

Ahmad, T., Kenne, L., Olsson, K., et al. (1995) The formation of 2-furaldehyde and formic acid from pentoses in slightly acidic deuterium oxide studied by 1H NMR spectroscopy. **Carbohydrate Research**, 276: (2): 309-320.

Aida, T.M., Shiraishi, N., Kubo, M., et al. (2010) Reaction kinetics of d-xylose in sub- and supercritical water. **The Journal of Supercritical Fluids**, 55: (1): 208-216.

Almeida, J.R.M., Modig, T., Petersson, A., et al. (2007) Increased tolerance and conversion of inhibitors in lignocellulosic hydrolysates by Saccharomyces cerevisiae. **Journal of Chemical Technology & Biotechnology**, 82: (4): 340-349.

Antal Jr, M.J., Mok, W.S.L. and Richards, G.N. (1990) Mechanism of formation of 5-(hydroxymethyl)-2-furaldehyde from d-fructose and sucrose. **Carbohydrate Research**, 199: (1): 91-109.

Arato, C., Pye, E.K. and Gjennestad, G. (2005) "The Lignol Approach to Biorefining of Woody Biomass to Produce Ethanol and Chemicals". In Davison, B.;Evans, B.;Finkelstein, M. & McMillan, J. (Eds.) **Twenty-Sixth Symposium on Biotechnology for Fuels and Chemicals**. Humana Press 871-882.

Asghari, F.S. and Yoshida, H. (2007) Kinetics of the Decomposition of Fructose Catalyzed by Hydrochloric Acid in Subcritical Water: Formation of 5-Hydroxymethylfurfural, Levulinic, and Formic Acids. **Industrial & Engineering Chemistry Research**, 46: (23): 7703-7710.

Asghari, F.S. and Yoshida, H. (2010) Conversion of Japanese red pine wood (Pinus densiflora) into valuable chemicals under subcritical water conditions. **Carbohydrate Research**, 345: (1): 124-131.

Balakshin, M., Capanema, E., Gracz, H., et al. (2011) Quantification of lignin–carbohydrate linkages with high-resolution NMR spectroscopy. **Planta**, 233: (6): 1097-1110.

Balat, M., Balat, H. and Öz, C. (2008) Progress in bioethanol processing. **Progress in Energy and Combustion Science**, 34: (5): 551-573.

Barnette, A.L., Lee, C., Bradley, L.C., et al. (2012) Quantification of crystalline cellulose in lignocellulosic biomass using sum frequency generation (SFG) vibration spectroscopy and comparison with other analytical methods. **Carbohydrate Polymers**, 89: (3): 802-809.

Baş, D. and Boyacı, İ.H. (2007) Modeling and optimization I: Usability of response surface methodology. **Journal of Food Engineering**, 78: (3): 836-845.

Basso, L.C., de Amorim, H.V., de Oliveira, A.J., et al. (2008) **Yeast selection for fuel ethanol production in Brazil**.

BD Biosciences (2000) "Introduction to Flow Cytometry: A learning guide". **Manual Part Number: 11-11032-01**.

Beale, C.V., Bint, D.A. and Long, S.P. (1996) Leaf photosynthesis in the C4-grass Miscanthus x giganteus, growing in the cool temperate climate of southern England. **Journal of Experimental Botany**, 47: (2): 267-273.

Berndes, G., Azar, C., Kåberger, T., et al. (2001) The feasibility of large-scale lignocellulose-based bioenergy production. **Biomass and Bioenergy**, 20: (5): 371-383.

Bessadok, A., Marais, S., Gouanvé, F., et al. (2007) Effect of chemical treatments of Alfa (Stipa tenacissima) fibres on water-sorption properties. **Composites Science and Technology**, 67: (3–4): 685-697.

Bhattacharya, A. and Pletschke, B.I. (2015) Strategic optimization of xylanase–mannanase combi-CLEAs for synergistic and efficient hydrolysis of complex lignocellulosic substrates. **Journal of Molecular Catalysis B: Enzymatic**, 115: 140-150.

Boakye-Boaten, N.A., Xiu, S., Shahbazi, A., et al. (2015) Liquid hot water pretreatment of Miscanthus x giganteus for the sustainable production of bioethanol. **Bioresources**, 10: (3): 5890-5905.

Bondar, R.J.L. and Mead, D.C. (1974) Evaluation of Glucose-6-Phosphate Dehydrogenase from Leuconostoc mesenteroides in the Hexokinase Method for Determining Glucose in Serum. **Clinical Chemistry**, 20: (5): 586-590.

Botello, J.I., Gilarranz, M.A., RodrÍGuez, F., et al. (1999) Recovery of Solvent and By-Products from Organosolv Black Liquor. **Separation Science and Technology**, 34: (12): 2431-2445.

Boyd, A.R., Gunasekera, T.S., Attfield, P.V., et al. (2003) A flow-cytometric method for determination of yeast viability and cell number in a brewery. **FEMS Yeast Research**, 3: (1): 11-16.

Bradley, N. (2007) **The Response Surface Methodology**. Master of Science, Indiana University South Bend.

Bröll, D., Kaul, C., Krämer, A., et al. (1999) Chemistry in Supercritical Water. **Angewandte Chemie International Edition**, 38: (20): 2998-3014.

Brosse, N., Dufour, A., Meng, X., et al. (2012) Miscanthus: a fast-growing crop for biofuels and chemicals production. **Biofuels, Bioproducts and Biorefining**, 6: (5): 580-598.

Brosse, N., Sannigrahi, P. and Ragauskas, A. (2009) Pretreatment of Miscanthus x giganteus Using the Ethanol Organosolv Process for Ethanol Production. **Industrial & Engineering Chemistry Research**, 48: (18): 8328-8334.

Carapetudo Antas, F.T. (2015) **An assessment of the utility of subcritical water to recover bioactive compounds from cider lees**. University of Birmingham.

Carpita, N.C. and Gibeaut, D.M. (1993) Structural models of primary cell walls in flowering plants: consistency of molecular structure with the physical properties of the walls during growth. **The Plant Journal**, 3: (1): 1-30.

Carvalheiro, F., Duarte, L.C. and Gírio, F.M. (2008) Hemicellulose biorefineries: a review on biomass pretreatments. **Journal of Scientific and Industrial Research**, 67: 849-864.

Cataldi, T.R.I., Campa, C. and De Benedetto, G.E. (2000) Carbohydrate analysis by high-performance anion-exchange chromatography with pulsed amperometric detection: The potential is still growing. **Fresenius' Journal of Analytical Chemistry**, 368: (8): 739-758.

Chandra, R.P., Bura, R., Mabee, W.E., et al. (2007) "Substrate Pretreatment: The Key to Effective Enzymatic Hydrolysis of Lignocellulosics?". In Olsson, L. (Ed.) **Biofuels**. Springer Berlin Heidelberg 67-93.

Chen, M.-H., Bowman, M.J., Cotta, M.A., et al. (2016) Miscanthus × giganteus xylooligosaccharides: Purification and fermentation. **Carbohydrate Polymers**, 140: 96-103.

Chen, M.-H., Bowman, M.J., Dien, B.S., et al. (2014) Autohydrolysis of Miscanthus x giganteus for the production of xylooligosaccharides (XOS): Kinetics, characterization and recovery. **Bioresource Technology**, 155: 359-365.

Chen, M., Zhao, J. and Xia, L. (2008) Enzymatic hydrolysis of maize straw polysaccharides for the production of reducing sugars. **Carbohydrate Polymers**, 71: (3): 411-415.

Chen, Z., Hu, T.Q., Jang, H.F., et al. (2015) Modification of xylan in alkaline treated bleached hardwood kraft pulps as classified by attenuated total-internal-reflection (ATR) FTIR spectroscopy. **Carbohydrate Polymers**, 127: 418-426.

Cheng, L., Ye, X.P., He, R., et al. (2009) Investigation of rapid conversion of switchgrass in subcritical water. **Fuel Processing Technology**, 90: (2): 301-311.

Cherubini, F. (2010) The biorefinery concept: Using biomass instead of oil for producing energy and chemicals. **Energy Conversion and Management**, 51: (7): 1412-1421.

Chiaramonti, D., Prussi, M., Ferrero, S., et al. (2012) Review of pretreatment processes for lignocellulosic ethanol production, and development of an innovative method. **Biomass and Bioenergy**, 46: (0): 25-35.

Chou, C.-H. (2009) Miscanthus plants used as an alternative biofuel material: The basic studies on ecology and molecular evolution. **Renewable Energy**, 34: (8): 1908-1912.

Chuntanapum, A., Yong, T.L.-K., Miyake, S., et al. (2008) Behavior of 5-HMF in Subcritical and Supercritical Water. **Industrial & Engineering Chemistry Research**, 47: (9): 2956-2962.

Clifton-Brown, J.C., Breuer, J. and Jones, M.B. (2007) Carbon mitigation by the energy crop, Miscanthus. **Global Change Biology**, 13: (11): 2296-2307.

Clifton-Brown, J.C. and Lewandowski, I. (2000) Overwintering problems of newly established Miscanthus plantations can be overcome by identifying genotypes with improved rhizome cold tolerance. **New Phytologist**, 148: (2): 287-294.

Converti, A., Domínguez, J.M., Perego, P., et al. (2000) Wood Hydrolysis and Hydrolyzate Detoxification for Subsequent Xylitol Production. **Chemical Engineering & Technology**, 23: (11): 1013-1020.

Corradini, C., Cavazza, A. and Bignardi, C. (2012) High-Performance Anion-Exchange Chromatography Coupled with Pulsed Electrochemical Detection as a Powerful Tool to Evaluate Carbohydrates of Food Interest: Principles and Applications. **International Journal of Carbohydrate Chemistry**, 2012: 13.

Corradini, D. (2010) **Handbook of HPLC**. Second Edition.USA: Taylor & Francis Group.

Damaso, M.C.T., Machado, C.M.M., Rodrigues, D.d.S., et al. (2014) Bioprocesses for biofuels: an overview of the Brazilian case. **Chemical and Biological Technologies in Agriculture**, 1: (1): 1-8.

Dejaegher, B. and Vander Heyden, Y. (2011) Experimental designs and their recent advances in set-up, data interpretation, and analytical applications. **Journal of Pharmaceutical and Biomedical Analysis**, 56: (2): 141-158.

Demirbas, A. (2009a) Biorefineries: Current activities and future developments. **Energy Conversion and Management**, 50: (11): 2782-2801.

Demirbas, M.F. (2009b) Biorefineries for biofuel upgrading: A critical review. **Applied Energy**, 86, Supplement 1: (0): S151-S161.

Dence, C.W. (1992) "The determination of Lignin". **Methods in Lignin Chemistry**. Germany, Springer-Verlag.

Díaz, M., Herrero, M., García, L.A., et al. (2010) Application of flow cytometry to industrial microbial bioprocesses. **Biochemical Engineering Journal**, 48: (3): 385-407.

Dionex (2004) "Analysis of Carbohydrates by High-Performance Anion-Exchange Chromatography with Pulsed Amperometric Detection (HPAE-PAD)". **Thermo Fisher Scientific - Technical Note 20**. USA.

Dionex (2013) "Eluent Preparation for High-Performance Anion-Exchange Chromatography with Pulsed Amperometric Detection". In Rohrer, J. (Ed.) **Thermo Fisher Scientific - Dionex Technical Note 71**. USA.

Domon, J.-M., Baldwin, L., Acket, S., et al. (2013) Cell wall compositional modifications of Miscanthus ecotypes in response to cold acclimation. **Phytochemistry**, 85: (0): 51-61.

Donohoe, B.S., Decker, S.R., Tucker, M.P., et al. (2008) Visualizing lignin coalescence and migration through maize cell walls following thermochemical pretreatment. **Biotechnology and Bioengineering**, 101: (5): 913-925.

Doyle, C. and Dorsey, J. (1998) "Reversed-Phase HPLC: Preparation and Characterization of Reversed-Phase Stationary Phases". In Katz, E.;Eksteen, R. & Miller, P.S.N. (Eds.) **Handbook of HPLC**. USA, Marcel Dekker.

Duff, S.J.B. and Murray, W.D. (1996) Bioconversion of forest products industry waste cellulosics to fuel ethanol: A review. **Bioresource Technology**, 55: (1): 1-33.

Ebringerová, A. (2005) Structural Diversity and Application Potential of Hemicelluloses. **Macromolecular Symposia**, 232: (1): 1-12.

Ehara, K. and Saka, S. (2005) Decomposition behavior of cellulose in supercritical water, subcritical water, and their combined treatments. **Journal of Wood Science**, 51: (2): 148-153.

El Hage, R., Brosse, N., Chrusciel, L., et al. (2009) Characterization of milled wood lignin and ethanol organosolv lignin from miscanthus. **Polymer Degradation and Stability**, 94: (10): 1632-1638.

El Hage, R., Brosse, N., Sannigrahi, P., et al. (2010a) Effects of process severity on the chemical structure of Miscanthus ethanol organosolv lignin. **Polymer Degradation and Stability**, 95: (6): 997-1003.

El Hage, R., Chrusciel, L., Desharnais, L., et al. (2010b) Effect of autohydrolysis of Miscanthus x giganteus on lignin structure and organosolv delignification. **Bioresource Technology**, 101: (23): 9321-9329.

El Rassi, Z. (2002) "Reversed-phase and hydrophobic interaction chromatography of carbohydrates and glycoconjugates". In Ziad El, R. (Ed.) **Carbohydrate Analysis by Modern Chromatography and Electrophoresis**. Elsevier 41-102.

Esbensen, K.H. (2002) **Multivariate Data Analysis - in Practice: An introduction to multivariate data analysis and experimental design.** 5th Edition.CAMO Process AS.

Escobar, J.C., Lora, E.S., Venturini, O.J., et al. (2009) Biofuels: Environment, technology and food security. **Renewable and Sustainable Energy Reviews**, 13: (6-7): 1275-1287.

European Commission (2011) "Bio-based economy for Europe: state of play and future potential. Part 1". **Report on the European Commission's Public on-line consultation**.

Faulon, J.-L., Carlson, G.A. and Hatcher, P.G. (1994) A three-dimensional model for lignocellulose from gymnospermous wood. **Organic Geochemistry**, 21: (12): 1169-1179.

Fitzpatrick, M., Champagne, P., Cunningham, M.F., et al. (2010) A biorefinery processing perspective: Treatment of lignocellulosic materials for the production of value-added products. **Bioresource Technology**, 101: (23): 8915-8922.

Food and Agriculture Organization of the United Nations (2008) "Opportunities and challenges of biofuel production for food security and the environment in Latin America and the Caribbean". **Document prepared for the 30th Session of the FAO Regional Conference for Latin America and the Caribbean, held in Brasilia, Brazil**.

Foston, M. and Ragauskas, A.J. (2012) Biomass Characterization: Recent Progress in Understanding Biomass Recalcitrance. **Industrial Biotechnology**, 8: (4): 191-208.

Frias, J.A.d. and Feng, H. (2013) Switchable butadiene sulfone pretreatment of Miscanthus in the presence of water. **Green Chemistry**, 15: (4): 1067-1078.

Gao, D., Chundawat, S.P.S., Krishnan, C., et al. (2010) Mixture optimization of six core glycosyl hydrolases for maximizing saccharification of ammonia fiber expansion (AFEX) pretreated corn stover. **Bioresource Technology**, 101: (8): 2770-2781.

García-Aparicio, M., Ballesteros, I., González, A., et al. (2006) Effect of inhibitors released during steam-explosion pretreatment of barley straw on enzymatic hydrolysis. **Applied Biochemistry and Biotechnology**, 129: (1-3): 278-288.

Garrote, G., Domínguez, H. and Parajó, C.J. (2001) Study on the deacetylation of hemicelluloses during the hydrothermal processing of Eucalyptus wood. **Holz als Roh- und Werkstoff**, 59: (1): 53-59.

Garrote, G., Domínguez, H. and Parajó, J.C. (1999) Mild autohydrolysis: an environmentally friendly technology for xylooligosaccharide production from wood. **Journal of Chemical Technology & Biotechnology**, 74: (11): 1101-1109.

Garside, P. and Wyeth, P. (2003) Identification of Cellulosic Fibres by FTIR Spectroscopy: Thread and Single Fibre Analysis by Attenuated Total Reflectance. **Studies in Conservation**, 48: (4): 269-275.

Gírio, F.M., Fonseca, C., Carvalheiro, F., et al. (2010) Hemicelluloses for fuel ethanol: A review. **Bioresource Technology**, 101: (13): 4775-4800.

Goh, C.S., Lee, K.T. and Bhatia, S. (2010) Hot compressed water pretreatment of oil palm fronds to enhance glucose recovery for production of second generation bio-ethanol. **Bioresource Technology**, 101: (19): 7362-7367.

González-Muñoz, M.J., Alvarez, R., Santos, V., et al. (2012) Production of hemicellulosic sugars from Pinus pinaster wood by sequential steps of aqueous extraction and acid hydrolysis. **Wood Science and Technology**, 46: (1): 271-285.

Gullón, P., Romaní, A., Vila, C., et al. (2012) Potential of hydrothermal treatments in lignocellulose biorefineries. **Biofuels, Bioproducts and Biorefining**, 6: (2): 219-232.

Hamelinck, C.N., Hooijdonk, G.v. and Faaij, A.P.C. (2005) Ethanol from lignocellulosic biomass: techno-economic performance in short-, middle- and long-term. **Biomass and Bioenergy**, 28: (4): 384-410.

Harmsen, P., Huijgen, W., Bermudez, L., et al. (2010) **Literature review of physical and chemical pretreatment processes for lignocellulosic biomass**. Wageningen: Wageningen UR, Food & Biobased Research.

Hashaikeh, R., Fang, Z., Butler, I.S., et al. (2007) Hydrothermal dissolution of willow in hot compressed water as a model for biomass conversion. **Fuel**, 86: (10–11): 1614-1622.

Hatfield, R. and Fukushima, R.S. (2005) Can Lignin Be Accurately Measured? **Crop Science**, 45: (3): 832-839.

Hatfield, R., Jung, H.J.G., Ralph, J., et al. (1994) A comparison of the insoluble residues produced by the Klason lignin and acid detergent lignin procedures. **Journal of the Science of Food and Agriculture**, 65: 51-58.

Haverty, D., Dussan, K., Piterina, A.V., et al. (2012) Autothermal, single-stage, performic acid pretreatment of Miscanthus x giganteus for the rapid fractionation of its biomass components into a lignin/hemicellulose-rich liquor and a cellulase-digestible pulp. **Bioresource Technology**, 109: 173-177.

Hendriks, A.T.W.M. and Zeeman, G. (2009) Pretreatments to enhance the digestibility of lignocellulosic biomass. **Bioresource Technology**, 100: (1): 10-18.

Herrero, M., Quirós, C., García, L.A., et al. (2006) Use of Flow Cytometry To Follow the Physiological States of Microorganisms in Cider Fermentation Processes. **Applied and environmental microbiology**, 72: (10): 6725-6733.

Hewitt, C.J. and Nebe-Von-Caron, G. (2001) An industrial application of multiparameter flow cytometry: Assessment of cell physiological state and its application to the study of microbial fermentations. **Cytometry**, 44: (3): 179-187.

Himmel, M.E., Ding, S.-Y., Johnson, D.K., et al. (2007) Biomass Recalcitrance: Engineering Plants and Enzymes for Biofuels Production. **Science**, 315: (5813): 804-807.

Hori, R. and Sugiyama, J. (2003) A combined FT-IR microscopy and principal component analysis on softwood cell walls. **Carbohydrate Polymers**, 52: (4): 449-453.

Horvat, J., Klaić, B., Metelko, B., et al. (1985) Mechanism of levulinic acid formation. **Tetrahedron Letters**, 26: (17): 2111-2114.

Hristozova, T., Angelov, A., Tzvetkova, B., et al. (2006) Effect of furfural on carbon metabolism key enzymes of lactose-assimilating yeasts. **Enzyme and Microbial Technology**, 39: (5): 1108-1112.

Hu, F. and Ragauskas, A. (2012) Pretreatment and Lignocellulosic Chemistry. **BioEnergy Research**, 5: (4): 1043-1066.

Hu, F. and Ragauskas, A. (2014) Suppression of pseudo-lignin formation under dilute acid pretreatment conditions. **RSC Advances**, 4: (9): 4317-4323.

Huang, H.-J., Ramaswamy, S., Tschirner, U.W., et al. (2008) A review of separation technologies in current and future biorefineries. **Separation and Purification Technology**, 62: (1): 1-21.

Huber, G.W., Iborra, S. and Corma, A. (2006) Synthesis of Transportation Fuels from Biomass: Chemistry, Catalysts, and Engineering. **Chemical Reviews**, 106: (9): 4044-4098.

Huijgen, W.J.J., Smit, A.T., de Wild, P.J., et al. (2012) Fractionation of wheat straw by prehydrolysis, organosolv delignification and enzymatic hydrolysis for production of sugars and lignin. **Bioresource Technology**, 114: (0): 389-398.

Hulleman, S.H.D., van Hazendonk, J.M. and van Dam, J.E.G. (1994) Determination of crystallinity in native cellulose from higher plants with diffuse reflectance Fourier transform infrared spectroscopy. **Carbohydrate Research**, 261: (1): 163-172.

Ingram, T., Wörmeyer, K., Lima, J.C.I., et al. (2011) Comparison of different pretreatment methods for lignocellulosic materials. Part I: Conversion of rye straw to valuable products. **Bioresource Technology**, 102: (8): 5221-5228.

Jin, F. and Enomoto, H. (2011) Rapid and highly selective conversion of biomass into value-added products in hydrothermal conditions: chemistry of acid/base-catalysed and oxidation reactions. **Energy & Environmental Science**, 4: (2): 382-397.

Jing, Q. and Lü, X. (2007) Kinetics of Non-catalyzed Decomposition of D-xylose in High Temperature Liquid Water. **Chinese Journal of Chemical Engineering**, 15: (5): 666-669.

Jing, Q. and Lü, X. (2008) Kinetics of Non-catalyzed Decomposition of Glucose in High-temperature Liquid Water. **Chinese Journal of Chemical Engineering**, 16: (6): 890-894.

Johnson, R.T. and Montgomery, D.C. (2009) Choice of second-order response surface designs for logistic and Poisson regression models. **International Journal of Experimental Design and Process Optimisation**, 1: (1): 2-23.

Jones, K.D. and Kompala, D.S. (1999) Cybernetic model of the growth dynamics of Saccharomyces cerevisiae in batch and continuous cultures. **Journal of Biotechnology**, 71: (1–3): 105-131.

Jørgensen, H., Kristensen, J.B. and Felby, C. (2007) Enzymatic conversion of lignocellulose into fermentable sugars: challenges and opportunities. **Biofuels, Bioproducts and Biorefining**, 1: (2): 119-134.

Kabyemela, B.M., Adschiri, T., Malaluan, R.M., et al. (1997) Kinetics of Glucose Epimerization and Decomposition in Subcritical and Supercritical Water. **Industrial & Engineering Chemistry Research**, 36: (5): 1552-1558.

Kabyemela, B.M., Adschiri, T., Malaluan, R.M., et al. (1999) Glucose and Fructose Decomposition in Subcritical and Supercritical Water: Detailed Reaction Pathway, Mechanisms, and Kinetics. **Industrial & Engineering Chemistry Research**, 38: (8): 2888-2895.

Kačuráková, M., Capek, P., Sasinková, V., et al. (2000) FT-IR study of plant cell wall model compounds: pectic polysaccharides and hemicelluloses. **Carbohydrate Polymers**, 43: (2): 195-203.

Kamm, B., Gruber, P.R. and Kamm, M. (2000) "Biorefineries – Industrial Processes and Products". **Ullmann's Encyclopedia of Industrial Chemistry**. Wiley-VCH Verlag GmbH & Co. KGaA.

Kamm, B. and Kamm, M. (2004) Principles of biorefineries. **Applied Microbiology and Biotechnology**, 64: (2): 137-145.

Kataoka, Y. and Kondo, T. (1998) FT-IR Microscopic Analysis of Changing Cellulose Crystalline Structure during Wood Cell Wall Formation. **Macromolecules**, 31: (3): 760-764.

Kaylen, M., Van Dyne, D.L., Choi, Y.-S., et al. (2000) Economic feasibility of producing ethanol from lignocellulosic feedstocks. **Bioresource Technology**, 72: (1): 19-32.

Kim, K.H. and Hong, J. (2001) Supercritical CO2 pretreatment of lignocellulose enhances enzymatic cellulose hydrolysis. **Bioresource Technology**, 77: (2): 139-144.

Kim, S. and Holtzapple, M.T. (2006) Effect of structural features on enzyme digestibility of corn stover. **Bioresource Technology**, 97: (4): 583-591.

Kim, S., Lee, C. and Kafle, K. (2013) Characterization of crystalline cellulose in biomass: Basic principles, applications, and limitations of XRD, NMR, IR, Raman, and SFG. **Korean Journal of Chemical Engineering**, 30: (12): 2127-2141.

Kimura, H., Nakahara, M. and Matubayasi, N. (2012) Noncatalytic Hydrothermal Elimination of the Terminal d-Glucose Unit from Malto- and Cello-Oligosaccharides through Transformation to d-Fructose. **The Journal of Physical Chemistry A**, 116: (41): 10039-10049.

Klemm, D., Heublein, B., Fink, H.-P., et al. (2005) Cellulose: Fascinating Biopolymer and Sustainable Raw Material. **Angewandte Chemie International Edition**, 44: (22): 3358-3393.

Kline, L.M., Hayes, G.D., Alvin, R.W., et al. (2010) Simplified determination of lignin content in hard and soft woods via UV-spectrophotometric analysis of biomass dissolved in ionic liquids. **Bioresources**, 5: (3): 1366-1383.

Kok, W.T. (1998) "Principles of Detection". In Katz, E.;Eksteen, R. & Miller, P.S.N. (Eds.) **Handbook of HPLC**. USA, Marcel Dekker.

Kondo, T., Mizuno, K. and Kato, T. (1987) Some characteristics of forage plant lignin. **Japan Agricultural Research Quarterly**, 21: (1): 47-52.

Kraber, S. (2013) "How to Get Started with Design-Expert® Software". Minneapolis, MN, Stat-Ease, Inc.

Kruse, A. and Dinjus, E. (2007) Hot compressed water as reaction medium and reactant: Properties and synthesis reactions. **The Journal of Supercritical Fluids**, 39: (3): 362-380.

Kumar, P., Barrett, D.M., Delwiche, M.J., et al. (2009) Methods for Pretreatment of Lignocellulosic Biomass for Efficient Hydrolysis and Biofuel Production. **Industrial & Engineering Chemistry Research**, 48: (8): 3713-3729.

Kumar, R., Hu, F., Sannigrahi, P., et al. (2013) Carbohydrate derived-pseudo-lignin can retard cellulose biological conversion. **Biotechnology and Bioengineering**, 110: (3): 737-753.

Kumar, S. and Gupta, R.B. (2008) Hydrolysis of Microcrystalline Cellulose in Subcritical and Supercritical Water in a Continuous Flow Reactor. **Industrial & Engineering Chemistry Research**, 47: (23): 9321-9329.

Kumar, S. and Gupta, R.B. (2009) Biocrude Production from Switchgrass Using Subcritical Water. **Energy Fuels**, 23: 5151-5159.

Lan, W., Liu, C.-F. and Sun, R.-C. (2011) Fractionation of Bagasse into Cellulose, Hemicelluloses, and Lignin with Ionic Liquid Treatment Followed by Alkaline Extraction. **Journal of Agricultural and Food Chemistry**, 59: (16): 8691-8701.

Langeveld, J.W.A., Dixon, J. and Jaworski, J.F. (2010) Development Perspectives Of The Biobased Economy: A Review. **Crop Science**, 50: (Supplement_1).

Larson, E.D. (2008) Biofuel production technologies: status, prospects and implications for trade and development. **United Nations Conference on Trade and Development (UNCTAD)**, (Available from: http://www.unctad.org/en/docs/ditcted200710_en.pdf (accessed 04-08-13)).

Le Ngoc Huyen, T., Rémond, C., Dheilly, R.M., et al. (2010) Effect of harvesting date on the composition and saccharification of Miscanthus x giganteus. **Bioresource Technology**, 101: (21): 8224-8231.

Lenihan, P., Orozco, A., O'Neill, E., et al. (2010) Dilute acid hydrolysis of lignocellulosic biomass. **Chemical Engineering Journal**, 156: (2): 395-403.

Leskinen, T., Kelley, S.S. and Argyropoulos, D.S. (2015) Refining of Ethanol Biorefinery Residues to Isolate Value Added Lignins. **ACS Sustainable Chemistry & Engineering**, 3: (7): 1632-1641.

Levy, I., Shani, Z. and Shoseyov, O. (2002) Modification of polysaccharides and plant cell wall by endo-1,4-β-glucanase and cellulose-binding domains. **Biomolecular Engineering**, 19: (1): 17-30.

Lewandowski, I., Clifton-Brown, J.C., Scurlock, J.M.O., et al. (2000) Miscanthus: European experience with a novel energy crop. **Biomass and Bioenergy**, 19: (4): 209-227.

Lewandowski, I. and Heinz, A. (2003) Delayed harvest of miscanthus—influences on biomass quantity and quality and environmental impacts of energy production. **European Journal of Agronomy**, 19: (1): 45-63.

Lewkowski, J. (2001) Synthesis, chemistry and applications of 5-hydroxymethyl-furfural and its derivatives. **Arkivoc**, 2: 17-54.

Li, J., Henriksson, G. and Gellerstedt, G. (2007) Lignin depolymerization/repolymerization and its critical role for delignification of aspen wood by steam explosion. **Bioresource Technology**, 98: (16): 3061-3068.

Ligero, P., Kolk, J.C.v.d., Vega, A.d., et al. (2011) Production of xylo-oligosaccharides from Miscanthus × giganteus by autohydrolysis. **Bioresources**, 6: (4): 4417-4429.

Limayem, A. and Ricke, S.C. (2012) Lignocellulosic biomass for bioethanol production: Current perspectives, potential issues and future prospects. **Progress in Energy and Combustion Science**, 38: (4): 449-467.

Lin, Y. and Tanaka, S. (2006) Ethanol fermentation from biomass resources: current state and prospects. **Applied Microbiology and Biotechnology**, 69: (6): 627-642.

Liu, C.-F. and Sun, R.-C. (2010) "Cellulose". **Cereal Straw as a Resource for Sustainable Biomaterials and Biofuels**. Amsterdam, Elsevier 131-167.

Liu, C.-Z., Wang, F., Stiles, A.R., et al. (2012) Ionic liquids for biofuel production: Opportunities and challenges. **Applied Energy**, 92: (0): 406-414.

Liu, L. and Chen, H. (2006) Enzymatic hydrolysis of cellulose materials treated with ionic liquid [BMIM] Cl. **Chinese Science Bulletin**, 51: (20): 2432-2436.

Lowry, J.B., Conlan, L.L., Schlink, A.C., et al. (1994) Acid Detergent Dispersible Lignin in Tropical Grasses. **Journal of the Science of Food and Agriculture**, 65: 41-49.

Lu, F. and Ralph, J. (2010) "Chapter 6 - Lignin". **Cereal Straw as a Resource for Sustainable Biomaterials and Biofuels**. Amsterdam, Elsevier 169-207.

Lü, H., Ren, M., Zhang, M., et al. (2013) Pretreatment of Corn Stover Using Supercritical CO2 with Water-Ethanol as Co-solvent. **Chinese Journal of Chemical Engineering**, 21: (5): 551-557.

Lü, X. and Saka, S. (2010) Hydrolysis of Japanese beech by batch and semi-flow water under subcritical temperatures and pressures. **Biomass and Bioenergy**, 34: (8): 1089-1097.

Luijkx, G.C.A., van Rantwijk, F. and van Bekkum, H. (1993) Hydrothermal formation of 1,2,4-benzenetriol from 5-hydroxymethyl-2-furaldehyde and d-fructose. **Carbohydrate Research**, 242: 131-139.

Lygin, A.V., Upton, J., Dohleman, F.G., et al. (2011) Composition of cell wall phenolics and polysaccharides of the potential bioenergy crop –Miscanthus. **GCB Bioenergy**, 3: (4): 333-345.

Mager, W.H. and Varela, J.C.S. (1993) Osmostress response of the yeast Saccharomyces. **Molecular Microbiology**, 10: (2): 253-258.

Mannazzu, I., Angelozzi, D., Belviso, S., et al. (2008) Behaviour of Saccharomyces cerevisiae wine strains during adaptation to unfavourable conditions of fermentation on synthetic medium: Cell lipid composition, membrane integrity, viability and fermentative activity. **International Journal of Food Microbiology**, 121: (1): 84-91.

Mansouri, N.-E.E. and Salvadó, J. (2006) Structural characterization of technical lignins for the production of adhesives: Application to lignosulfonate, kraft, soda-anthraquinone, organosolv and ethanol process lignins. **Industrial Crops and Products**, 24: (1): 8-16.

Maris, A.A., Abbott, D., Bellissimi, E., et al. (2006) Alcoholic fermentation of carbon sources in biomass hydrolysates by Saccharomyces cerevisiae: current status. **Antonie van Leeuwenhoek**, 90: (4): 391-418.

Martín, C. and Jönsson, L.J. (2003) Comparison of the resistance of industrial and laboratory strains of Saccharomyces and Zygosaccharomyces to lignocellulose-derived fermentation inhibitors. **Enzyme and Microbial Technology**, 32: (3–4): 386-395.

Matsumura, Y., Yanachi, S. and Yoshida, T. (2006) Glucose Decomposition Kinetics in Water at 25 MPa in the Temperature Range of 448−673 K. **Industrial & Engineering Chemistry Research**, 45: (6): 1875-1879.

Matsunaga, M., Matsui, H., Otsuka, Y., et al. (2008) Chemical conversion of wood by treatment in a semi-batch reactor with subcritical water. **The Journal of Supercritical Fluids**, 44: (3): 364-369.

Mazaheri, H., Lee, K.T., Bhatia, S., et al. (2010) Subcritical water liquefaction of oil palm fruit press fiber for the production of bio-oil: Effect of catalysts. **Bioresource Technology**, 101: (2): 745-751.

McDonough, T.J. (1992) "The chemistry of organosolv delignification". **TAPPI Solvent Pulping Seminar**. Boston, Massachusetts, Georgia Institute of Technology.

Megazyme (2014) "Ethanol Assay Procedure". Megazyme International Ireland.

Megazyme International (2013) "D-Glucose- HK Assay Procedure". Ireland.

Menon, V. and Rao, M. (2012) Trends in bioconversion of lignocellulose: Biofuels, platform chemicals & biorefinery concept. **Progress in Energy and Combustion Science**, 38: (4): 522-550.

Michell, A.J. (1990) Second-derivative F.t.-i.r. spectra of native celluloses. **Carbohydrate Research**, 197: 53-60.

Modig, T., Liden, G. and Taherzadeh, M.J. (2002) Inhibition effects of furfural on alcohol dehydrogenase, aldehyde dehydrogenase and pyruvate dehydrogenase. **Biochemical Journal**, 363: (3): 769-776.

Mohsen-Nia, M., Amiri, H. and Jazi, B. (2010) Dielectric Constants of Water, Methanol, Ethanol, Butanol and Acetone: Measurement and Computational Study. **Journal of Solution Chemistry**, 39: (5): 701-708.

Moller, M., Harnisch, F. and Schroder, U. (2013) Hydrothermal liquefaction of cellulose in subcritical water-the role of crystallinity on the cellulose reactivity. **RSC Advances**, 3: (27): 11035-11044.

Monrroy, M., Garcia, J.R., Troncoso, E., et al. (2015) Fourier transformed near infrared (FT-NIR) spectroscopy for the estimation of parameters in pretreated lignocellulosic materials for bioethanol production. **Journal of Chemical Technology & Biotechnology**, 90: (7): 1281-1289.

Montgomery, D.C. (2000) **Design and Analysis of Experiments**. 5th Edition.USA: John Wiley & Sons.

Moon, R.J., Martini, A., Nairn, J., et al. (2011) Cellulose nanomaterials review: structure, properties and nanocomposites. **Chemical Society Reviews**, 40: (7): 3941-3994.

Morán, J., Alvarez, V., Cyras, V., et al. (2008) Extraction of cellulose and preparation of nanocellulose from sisal fibers. **Cellulose**, 15: (1): 149-159.

Mosier, N., Wyman, C., Dale, B., et al. (2005a) Features of promising technologies for pretreatment of lignocellulosic biomass. **Bioresource Technology**, 96: (6): 673-686.

Mosier, N.S., Hendrickson, R., Brewer, M., et al. (2005b) Industrial scale-up of pH-controlled liquid hot water pretreatment of corn fiber for fuel ethanol production. **Applied Biochemistry and Biotechnology**, 125: (2): 77-97.

Moure, A., Gullón, P., Domínguez, H., et al. (2006) Advances in the manufacture, purification and applications of xylo-oligosaccharides as food additives and nutraceuticals. **Process Biochemistry**, 41: (9): 1913-1923.

Nabarlatz, D., Farriol, X. and Montané, D. (2004) Kinetic Modeling of the Autohydrolysis of Lignocellulosic Biomass for the Production of Hemicellulose-Derived Oligosaccharides. **Industrial & Engineering Chemistry Research**, 43: (15): 4124-4131.

Naidu, S.L., Moose, S.P., Al-Shoaibi, A.K., et al. (2003) Cold Tolerance of C4 photosynthesis in Miscanthus x giganteus: Adaptation in Amounts and Sequence of C4 Photosynthetic Enzymes. **Annu Rev Plant Physiol**, 132: (3): 1688-1697.

Naik, S.N., Goud, V.V., Rout, P.K., et al. (2010) Production of first and second generation biofuels: A comprehensive review. **Renewable and Sustainable Energy Reviews**, 14: (2): 578-597.

NASA (2013) **Global Climate Change** [online]. [Accessed Available from : http://climate.nasa.gov, accessed 04-09-2013

Nelson, D.L. and Cox, M.M. (2004) **Lehninger Principles of Biochemistry**. Fourth Edition.Macmillan Higher Education.

Nelson, M.L. and O'Connor, R.T. (1964) Relation of certain infrared bands to cellulose crystallinity and crystal lattice type. Part II. A new infrared ratio for estimation of crystallinity in celluloses I and II. **Journal of Applied Polymer Science**, 8: (3): 1325-1341.

O'Sullivan, A. (1997) Cellulose: the structure slowly unravels. **Cellulose**, 4: (3): 173-207.

Oehlert, G.W. (2000) **A First Course in Design and Analysis of Experiments**. New York: W. H. Freeman.

Oh, S.Y., Yoo, D.I., Shin, Y., et al. (2005) Crystalline structure analysis of cellulose treated with sodium hydroxide and carbon dioxide by means of X-ray diffraction and FTIR spectroscopy. **Carbohydrate Research**, 340: (15): 2376-2391.

Oliet, M., Rodríguez, F., Santos, A., et al. (2000) Organosolv Delignification of Eucalyptus globulus: Kinetic Study of Autocatalyzed Ethanol Pulping. **Industrial & Engineering Chemistry Research**, 39: (1): 34-39.

Olsson, C. and Westman, G. (2013) "Direct dissolution of cellulose: Background, Means and Applications". In van de Ven, T. & Godbout, L. (Eds.) **Cellulose - Fundamental Aspects**. InTech 153.

Ostergaard, S., Olsson, L. and Nielsen, J. (2000) Metabolic Engineering of Saccharomyces cerevisiae. **Microbiology and Molecular Biology Reviews**, 64: (1): 34-50.

Otieno, D.O. and Ahring, B.K. (2012) The potential for oligosaccharide production from the hemicellulose fraction of biomasses through pretreatment processes: xylooligosaccharides (XOS), arabinooligosaccharides (AOS), and mannooligosaccharides (MOS). **Carbohydrate Research**, 360: 84-92.

Paksung, N. and Matsumura, Y. (2015) Decomposition of Xylose in Sub- and Supercritical Water. **Industrial & Engineering Chemistry Research**, 54: (31): 7604-7613.

Palmqvist, E. and Hahn-Hägerdal, B. (2000a) Fermentation of lignocellulosic hydrolysates. I: inhibition and detoxification. **Bioresource Technology**, 74: (1): 17-24.

Palmqvist, E. and Hahn-Hägerdal, B. (2000b) Fermentation of lignocellulosic hydrolysates. II: inhibitors and mechanisms of inhibition. **Bioresource Technology**, 74: (1): 25-33.

Pan, X., Arato, C., Gilkes, N., et al. (2005) Biorefining of softwoods using ethanol organosolv pulping: Preliminary evaluation of process streams for manufacture of fuel-grade ethanol and co-products. **Biotechnology and Bioengineering**, 90: (4): 473-481.

Pan, X., Kadla, J.F., Ehara, K., et al. (2006) Organosolv Ethanol Lignin from Hybrid Poplar as a Radical Scavenger: Relationship between Lignin Structure, Extraction Conditions, and Antioxidant Activity. **Journal of Agricultural and Food Chemistry**, 54: (16): 5806-5813.

Panagiotopoulos, C. and Sempéré, R. (2005) The molecular distribution of combined aldoses in sinking particles in various oceanic conditions. **Marine Chemistry**, 95: (1–2): 31-49.

Pandey, M.P. and Kim, C.S. (2011) Lignin Depolymerization and Conversion: A Review of Thermochemical Methods. **Chemical Engineering & Technology**, 34: (1): 29-41.

Parajo, J.C., Alonso, J.L. and Santos, V. (1995) Kinetics of Catalyzed Organosolv Processing of Pine Wood. **Industrial & Engineering Chemistry Research**, 34: (12): 4333-4342.

Park, S., Baker, J., Himmel, M., et al. (2010) Cellulose crystallinity index: measurement techniques and their impact on interpreting cellulase performance. **Biotechnology for Biofuels**, 3: (1): 10.

Parliament of the United Kingdom (2008) "Climate Change Act 2008". **Her Majesty´s Stationary Office**. London.

Pasquini, D., Pimenta, M.T.B., Ferreira, L.H., et al. (2005) Extraction of lignin from sugar cane bagasse and Pinus taeda wood chips using ethanol–water mixtures and carbon dioxide at high pressures. **The Journal of Supercritical Fluids**, 36: (1): 31-39.

Patil, S.K.R. and Lund, C.R.F. (2011) Formation and Growth of Humins via Aldol Addition and Condensation during Acid-Catalyzed Conversion of 5-Hydroxymethylfurfural. **Energy & Fuels**, 25: (10): 4745-4755.

Pauly, M. and Keegstra, K. (2008) Cell-wall carbohydrates and their modification as a resource for biofuels. **The Plant Journal**, 54: (4): 559-568.

Peng, F., Ren, J.-L., Xu, F., et al. (2009) Comparative Study of Hemicelluloses Obtained by Graded Ethanol Precipitation from Sugarcane Bagasse. **Journal of Agricultural and Food Chemistry**, 57: (14): 6305-6317.

Pereira, F.B., Guimarães, P.M.R., Teixeira, J.A., et al. (2010) Optimization of low-cost medium for very high gravity ethanol fermentations by Saccharomyces cerevisiae using statistical experimental designs. **Bioresource Technology**, 101: (20): 7856-7863.

Pereira, F.B., Romaní, A., Ruiz, H.A., et al. (2014) Industrial robust yeast isolates with great potential for fermentation of lignocellulosic biomass. **Bioresource Technology**, 161: (0): 192-199.

Perez Locas, C. and Yaylayan, V.A. (2008) Isotope Labeling Studies on the Formation of 5-(Hydroxymethyl)-2-furaldehyde (HMF) from Sucrose by Pyrolysis-GC/MS. **Journal of Agricultural and Food Chemistry**, 56: (15): 6717-6723.

Peterson, A.A., Vogel, F., Lachance, R.P., et al. (2008) Thermochemical biofuel production in hydrothermal media: A review of sub- and supercritical water technologies. **Energy & Environmental Science**, 1: (1): 32-65.

Plácido, J. and Capareda, S. (2014) Analysis of alkali ultrasonication pretreatment in bioethanol production from cotton gin trash using FT-IR spectroscopy and principal component analysis. **Bioresources and Bioprocessing**, 1: (1): 1-9.

Poletto, M., Pistor, V. and Zattera, A.J. (2013) "Structural Characteristics and Thermal Properties of Native Cellulose". In Ven, T.G.M.V.D. (Ed.) **Cellulose - Fundamental Aspects**.

Prado, J.M., Follegatti-Romero, L.A., Forster-Carneiro, T., et al. (2014) Hydrolysis of sugarcane bagasse in subcritical water. **The Journal of Supercritical Fluids**, 86: (0): 15-22.

Purdy, S.J., Cunniff, J., Maddison, A.L., et al. (2014) Seasonal Carbohydrate Dynamics and Climatic Regulation of Senescence in the Perennial Grass, Miscanthus. **BioEnergy Research**, 8: (1): 28-41.

Raessler, M. (2011) Sample preparation and current applications of liquid chromatography for the determination of non-structural carbohydrates in plants. **TrAC Trends in Analytical Chemistry**, 30: (11): 1833-1843.

Ragauskas, A.J., Williams, C.K., Davison, B.H., et al. (2006) The Path Forward for Biofuels and Biomaterials. **Science**, 311: (5760): 484-489.

Rasmussen, H., Sørensen, H.R. and Meyer, A.S. (2014) Formation of degradation compounds from lignocellulosic biomass in the biorefinery: sugar reaction mechanisms. **Carbohydrate Research**, 385: 45-57.

Ren, J.-L. and Sun, R.-C. (2010) "Hemicelluloses". **Cereal Straw as a Resource for Sustainable Biomaterials and Biofuels**. Amsterdam, Elsevier 73-130.

(2007) **45th AIAA Aerospace Sciences Meeting and Exhibit** United States American Institute of Aeronautics and Astronautics.Aerospace Sciences Meetings

Rogalinski, T., Ingram, T. and Brunner, G. (2008) Hydrolysis of lignocellulosic biomass in water under elevated temperatures and pressures. **The Journal of Supercritical Fluids**, 47: (1): 54-63.

Rohrer, J.S., Basumallick, L. and Hurum, D. (2013) High-performance anion-exchange chromatography with pulsed amperometric detection for carbohydrate analysis of glycoproteins. **Biochemistry (Moscow)**, 78: (7): 697-709.

Roque, R.M.N. (2013) **Hydrolysis of lignocellulosic biomass by a modified organosolv method on a biorefinery prespective: example of *Miscanthus x Giganteus***. Doctor of Philosophy, University of Birmingham.

Rosatella, A.A., Simeonov, S.P., Frade, R.F.M., et al. (2011) 5-Hydroxymethylfurfural (HMF) as a building block platform: Biological properties, synthesis and synthetic applications. **Green Chemistry**, 13: (4): 754-793.

Rousset, P., Aguiar, C., Labbé, N., et al. (2011) Enhancing the combustible properties of bamboo by torrefaction. **Bioresource Technology**, 102: (17): 8225-8231.

Rubin, E.M. (2008) Genomics of cellulosic biofuels. **Nature**, 454: (7206): 841-845.

Ruiz, H.A., Rodríguez-Jasso, R.M., Fernandes, B.D., et al. (2013) Hydrothermal processing, as an alternative for upgrading agriculture residues and marine biomass according to the biorefinery concept: A review. **Renewable and Sustainable Energy Reviews**, 21: (0): 35-51.

Ryden, P., Gautier, A., Wellner, N., et al. (2014) Changes in the composition of the main polysaccharide groups of oil seed rape straw following steam explosion and saccharification. **Biomass and Bioenergy**, 61: 121-130.

Saake, B. and Lehnen, R. (2000) "Lignin". **Ullmann's Encyclopedia of Industrial Chemistry**. Wiley-VCH Verlag GmbH & Co. KGaA.

Saka, L.X.S. (2008) Optimization of Japanese beech hydrolysis treated with batch hot-compressed water by response surface methodology. **International Journal of Agricultural and Biological Engineering**, 1: (2): 39-45.

Sánchez, Ó.J. and Cardona, C.A. (2008) Trends in biotechnological production of fuel ethanol from different feedstocks. **Bioresource Technology**, 99: (13): 5270-5295.

Sannigrahi, P., Kim, D.H., Jung, S., et al. (2011) Pseudo-lignin and pretreatment chemistry. **Energy & Environmental Science**, 4: (4): 1306-1310.

Sannigrahi, P., Miller, S.J. and Ragauskas, A.J. (2010) Effects of organosolv pretreatment and enzymatic hydrolysis on cellulose structure and crystallinity in Loblolly pine. **Carbohydrate Research**, 345: (7): 965-970.

Sannigrahi, P. and Ragauskas, A.J. (2013) "Fundamentals of Biomass Pretreatment by Fractionation". In Wyman, C.E. (Ed.) **Aqueous Pretreatment of Plant Biomass for Biological and Chemical Conversion to Fuels and Chemicals**. John Wiley & Sons, Incorporated.

Santos, R.B., Hart, P., Jameel, H., et al. (2013) **Wood Based Lignin Reactions Important to the Biorefinery and Pulp and Paper Industries**.

Sasaki, M., Adschiri, T. and Arai, K. (2003a) Production of Cellulose II from Native Cellulose by Near- and Supercritical Water Solubilization. **Journal of Agricultural and Food Chemistry**, 51: (18): 5376-5381.

Sasaki, M., Fang, Z., Fukushima, Y., et al. (2000) Dissolution and Hydrolysis of Cellulose in Subcritical and Supercritical Water. **Industrial & Engineering Chemistry Research**, 39: (8): 2883-2890.

Sasaki, M., Hayakawa, T., Arai, K., et al. (2003b) Measurement of the Rate of RetroAldol Condensation of d-Xylose in Subcritical and Supercritical Water. **World Scientific**, 169-176.

Sasaki, M., Kabyemela, B., Malaluan, R., et al. (1998) Cellulose hydrolysis in subcritical and supercritical water. **The Journal of Supercritical Fluids**, 13: (1–3): 261-268.

Scheller, H.V. and Ulvskov, P. (2010) Hemicelluloses. **Annual Review of Plant Biology**, 61: (1): 263-289.

Shatalov, A.A. and Pereira, H. (2005) Kinetics of organosolv delignification of fibre crop Arundo donax L. **Industrial Crops and Products**, 21: (2): 203-210.

Siegumfeldt, H., Björn Rechinger, K. and Jakobsen, M. (2000) Dynamic Changes of Intracellular pH in Individual Lactic Acid Bacterium Cells in Response to a Rapid Drop in Extracellular pH. **Applied and environmental microbiology**, 66: (6): 2330-2335.

Sigma Aldrich **Buffer Reference Center** [online]. http://www.sigmaaldrich.com/life-science/core-bioreagents/biological-buffers/learning-center/buffer-reference-center.html#citric [Accessed 22nd of June 2015]

Sills, D.L. and Gossett, J.M. (2012) Using FTIR to predict saccharification from enzymatic hydrolysis of alkali-pretreated biomasses. **Biotechnology and Bioengineering**, 109: (2): 353-362.

Sim, S.F., Mohamed, M., Lu, N.A.L.M.I., et al. (2012) Computer-assisted analysis of Fourier Transform Infrared (FTIR) spectra for characterization of various treated and untreated agriculture biomass. **Bioresources**, 7: (4): 5367-5380.

Simon, J., Müller, H.P., Koch, R., et al. (1998) Thermoplastic and biodegradable polymers of cellulose. **Polymer Degradation and Stability**, 59: (1–3): 107-115.

Sluiter, A., Hames, B., Ruiz, R., et al. (2008) Determination of Structural Carbohydrates and Lignin in Biomass. **NREL Laboratory of Analytical Procedure**.

Sluiter, A., Ruiz, R., Scarlata, C., et al. (2005) Determination of Extractives in Biomass. **NREL Laboratory of Analytical Procedure**.

Sluiter, J.B., Ruiz, R.O., Scarlata, C.J., et al. (2010) Compositional Analysis of Lignocellulosic Feedstocks. 1. Review and Description of Methods. **Journal of Agricultural and Food Chemistry**, 58: (16): 9043-9053.

Soccol, C.R., Faraco, C., Karp, S., et al. (2011) "Lignocellulosic bioethanol: Current status and future perspectives". In Ashok, P. (Ed.) **Biofuels: Alternative feedstock and conversion processes**. Elsevier.

Spatari, S., Bagley, D.M. and MacLean, H.L. (2010) Life cycle evaluation of emerging lignocellulosic ethanol conversion technologies. **Bioresource Technology**, 101: (2): 654-667.

Speck Jr, J.C. (1958) "The Lobry De Bruyn-Alberda Van Ekenstein Transformation". In Melville, L.W. (Ed.) **Advances in Carbohydrate Chemistry**. Academic Press 63-103.

Srokol, Z., Bouche, A.-G., van Estrik, A., et al. (2004) Hydrothermal upgrading of biomass to biofuel; studies on some monosaccharide model compounds. **Carbohydrate Research**, 339: (10): 1717-1726.

Stevulova, N., Cigasova, J., Estokova, A., et al. (2014) Properties Characterization of Chemically Modified Hemp Hurds. **Materials**, 7: (12): 8131-8150.

Sun, Y. and Cheng, J. (2002) Hydrolysis of lignocellulosic materials for ethanol production: a review. **Bioresource Technology**, 83: (1): 1-11.

Sun, Y., Lin, L., Pang, C., et al. (2007) Hydrolysis of Cotton Fiber Cellulose in Formic Acid. **Energy & Fuels**, 21: (4): 2386-2389.

Taherzadeh, M.J., Gustafsson, L., Niklasson, C., et al. (2000) Physiological effects of 5-hydroxymethylfurfural on Saccharomyces cerevisiae. **Applied Microbiology and Biotechnology**, 53: (6): 701-708.

Taherzadeh, M.J. and Karimi, K. (2008) Pretreatment of Lignocellulosic Wastes to Improve Ethanol and Biogas Production: A Review. **International Journal of Molecular Sciences**, 9: (9).

Taherzadeh, M.J. and Karimi, K. (2011) "Fermentation Inhibitors in ethanol processes and different strategies to reduce their effects". **Biofuels: Alternative feedstocks and conversion processes**. Academic Press.

Tan, H.T., Lee, K.T. and Mohamed, A.R. (2011) Pretreatment of lignocellulosic palm biomass using a solvent-ionic liquid [BMIM]Cl for glucose recovery: An optimisation study using response surface methodology. **Carbohydrate Polymers**, 83: (4): 1862-1868.

Thielemans, W., Can, E., Morye, S.S., et al. (2002) Novel applications of lignin in composite materials. **Journal of Applied Polymer Science**, 83: (2): 323-331.

Timilsena, Y.P., Abeywickrama, C.J., Rakshit, S.K., et al. (2013) Effect of different pretreatments on delignification pattern and enzymatic hydrolysability of miscanthus, oil palm biomass and typha grass. **Bioresource Technology**, 135: 82-88.

Tolonen, L.K., Zuckerstätter, G., Penttilä, P.A., et al. (2011) Structural Changes in Microcrystalline Cellulose in Subcritical Water Treatment. **Biomacromolecules**, 12: (7): 2544-2551.

Toor, S.S., Rosendahl, L. and Rudolf, A. (2011) Hydrothermal liquefaction of biomass: A review of subcritical water technologies. **Energy**, 36: (5): 2328-2342.

Tuomela, M., Vikman, M., Hatakka, A., et al. (2000) Biodegradation of lignin in a compost environment: a review. **Bioresource Technology**, 72: (2): 169-183.

UQ **Fluorescence Assisted Cell Sorting** [online]. http://www.di.uq.edu.au/sparqfacs The University of Queensland - Australia [Accessed 6th May 2016]

Usuki, C., Kimura, Y. and Adachi, S. (2007) Isomerization of Hexoses in Subcritical Water. **Food Science and Technology Research**, 13: (3): 205-209.

Valli, M., Sauer, M., Branduardi, P., et al. (2006) Improvement of Lactic Acid Production in Saccharomyces cerevisiae by Cell Sorting for High Intracellular pH. **Applied and environmental microbiology**, 72: (8): 5492-5499.

Van Dyk, J.S. and Pletschke, B.I. (2012) A review of lignocellulose bioconversion using enzymatic hydrolysis and synergistic cooperation between enzymes—Factors affecting enzymes, conversion and synergy. **Biotechnology Advances**, 30: (6): 1458-1480.

Van Dyne, D.L., Blase, M.G. and Clements, L.D. (1999) "A strategy for returning agriculture and rural America to long-term full employment using biomass refineries.". In Janick, J. (Ed.) **Perspectives on New Crops and New Uses**. Alexandria, ASHS Press.

van Putten, R.-J., van der Waal, J.C., de Jong, E., et al. (2013) Hydroxymethylfurfural, A Versatile Platform Chemical Made from Renewable Resources. **Chemical Reviews**, 113: (3): 1499-1597.

Van Soest, P.J. and Wine, R.H. (1967) Use of detergents in the analysis of fibrous feeds. IV. Determination of plant cell-wall constituents. **J. Ass. Offic. Agr. Chem**, 50: 50-55.

van Walsum, G.P. (2001) Severity function describing the hydrolysis of xylan using carbonic acid. **Applied Biochemistry and Biotechnology**, 91: (1): 317-329.

van Walsum, G.P. and Shi, H. (2004) Carbonic acid enhancement of hydrolysis in aqueous pretreatment of corn stover. **Bioresource Technology**, 93: (3): 217-226.

Vandenbrink, J.P., Hilten, R.N., Das, K.C., et al. (2011) Analysis of Crystallinity Index and Hydrolysis Rates in the Bioenergy Crop Sorghum bicolor. **BioEnergy Research**, 5: (2): 387-397.

Vanderghem, C., Brostaux, Y., Jacquet, N., et al. (2012) Optimization of formic/acetic acid delignification of Miscanthus x giganteus for enzymatic hydrolysis using response surface methodology. **Industrial Crops and Products**, 35: (1): 280-286.

Vanholme, B., Desmet, T., Ronsse, F., et al. (2013) Towards a carbon-negative sustainable bio-based economy. **Frontiers in Plant Science**, 4: 174.

Vassilev, S.V., Baxter, D., Andersen, L.K., et al. (2012) An overview of the organic and inorganic phase composition of biomass. **Fuel**, 94: (0): 1-33.

Vázquez, G., Antorrena, G., González, J., et al. (1997) Acetosolv pulping of pine wood. Kinetic modelling of lignin solubilization and condensation. **Bioresource Technology**, 59: (2–3): 121-127.

Vázquez, M.J., Alonso, J.L., Domínguez, H., et al. (2000) Xylooligosaccharides: manufacture and applications. **Trends in Food Science & Technology**, 11: (11): 387-393.

Vázquez, M.J., Garrote, G., Alonso, J.L., et al. (2005) Refining of autohydrolysis liquors for manufacturing xylooligosaccharides: evaluation of operational strategies. **Bioresource Technology**, 96: (8): 889-896.

Viikari, L., Vehmaanperä, J. and Koivula, A. (2012) Lignocellulosic ethanol: From science to industry. **Biomass and Bioenergy**, 46: (0): 13-24.

Villaverde, J.J., Li, J., Ek, M., et al. (2009) Native Lignin Structure of Miscanthus x giganteus and Its Changes during Acetic and Formic Acid Fractionation. **Journal of Agricultural and Food Chemistry**, 57: (14): 6262-6270.

Visser, P., Pignatelli, V., Jorgensen, U., et al. (2001) "Utilisation of Miscanthus". In 2000 (Ed.) **Miscanthus for Energy and Fibre**. London, Earthscan.

Wang, K. and Sun, R.-C. (2010) "Biorefinery Straw for Bioethanol". **Cereal Straw as a Resource for Sustainable Biomaterials and Biofuels**. Amsterdam, Elsevier 267-287.

Werner-Washburne, M., Braun, E., Crawford, M.E., et al. (1996) Stationary phase in the yeast Saccharomyces cerevisiae. **Molecular Microbiology**, 19: (6): 1159-1166.

Williams, D.L. and Dunlop, A.P. (1948) Kinetics of Furfural Destruction in Acidic Aqueous Media. **Industrial & Engineering Chemistry**, 40: (2): 239-241.

Wyman, C. (1996) **Handbook on Bioethanol: Production and Utilization**. Taylor & Francis.

Wyman, C.E., Decker, S.R., Himmel, M.E., et al. (2004) "Hydrolysis of Cellulose and Hemicellulose". **Polysaccharides**. CRC Press.

Xiao, L.P., Sun, Z.-J., Shi, Z.-J., et al. (2011) Impact of hot compressed water pretreatment on the structural changes of wood biomass for bioethanol production. **Bioresources**, 6: (2): 1576-1598.

Xu, F., Shi, Y.-C. and Wang, D. (2012) Enhanced production of glucose and xylose with partial dissolution of corn stover in ionic liquid, 1-Ethyl-3-methylimidazolium acetate. **Bioresource Technology**, 114: (0): 720-724.

Xu, F., Yu, J., Tesso, T., et al. (2013a) Qualitative and quantitative analysis of lignocellulosic biomass using infrared techniques: A mini-review. **Applied Energy**, 104: 801-809.

Xu, Y., Fan, L., Wang, X., et al. (2013b) **Simultaneous Separation and Quantification of Linear Xylo- and Cello-Oligosaccharides Mixtures in Lignocellulosics Processing Products on High-Performance Anion-Exchange Chromatography Coupled with Pulsed Amperometric Detection**.

Xu, Y., Li, K. and Zhang, M. (2007) Lignin precipitation on the pulp fibers in the ethanol-based organosolv pulping. **Colloids and Surfaces A: Physicochemical and Engineering Aspects**, 301: (1–3): 255-263.

Yang, B. and Wyman, C.E. (2008) Pretreatment: the key to unlocking low-cost cellulosic ethanol. **Biofuels, Bioproducts and Biorefining**, 2: (1): 26-40.

Yinghuai, Z., Yuanting, K.T. and Hosmane, N.S. (2013) **Applications of Ionic Liquids in Lignin Chemistry**.

Yu, Q., Zhuang, X., Wang, Q., et al. (2012) Hydrolysis of sweet sorghum bagasse and eucalyptus wood chips with liquid hot water. **Bioresource Technology**, 116: 220-225.

Yu, Y., Lou, X. and Wu, H. (2007) Some Recent Advances in Hydrolysis of Biomass in Hot-Compressed Water and Its Comparisons with Other Hydrolysis Methods†. **Energy & Fuels**, 22: (1): 46-60.

Yu, Y., Shafie, Z.M. and Wu, H. (2013) Cellobiose Decomposition in Hot-Compressed Water: Importance of Isomerization Reactions. **Industrial & Engineering Chemistry Research**, 52: (47): 17006-17014.

Yu, Y. and Wu, H. (2009) Characteristics and Precipitation of Glucose Oligomers in the Fresh Liquid Products Obtained from the Hydrolysis of Cellulose in Hot-Compressed Water. **Industrial & Engineering Chemistry Research**, 48: (23): 10682-10690.

Yu, Y. and Wu, H. (2010) Significant Differences in the Hydrolysis Behavior of Amorphous and Crystalline Portions within Microcrystalline Cellulose in Hot-Compressed Water. **Industrial & Engineering Chemistry Research**, 49: (8): 3902-3909.

Yu, Y. and Wu, H. (2011) Kinetics and Mechanism of Glucose Decomposition in Hot-Compressed Water: Effect of Initial Glucose Concentration. **Industrial & Engineering Chemistry Research**, 50: (18): 10500-10508.

Yuan, J.S., Tiller, K.H., Al-Ahmad, H., et al. (2008) Plants to power: bioenergy to fuel the future. **Trends in Plant Science**, 13: (8): 421-429.

Zhang, M., Xu, Y. and Li, K. (2007) Removal of residual lignin of ethanol-based organosolv pulp by an alkali extraction process. **Journal of Applied Polymer Science**, 106: (1): 630-636.

Zhang, T., Wyman, C.E., Jakob, K., et al. (2012a) Rapid selection and identification of Miscanthus genotypes with enhanced glucan and xylan yields from hydrothermal pretreatment followed by enzymatic hydrolysis. **Biotechnology for Biofuels**, 5: (1): 1-14.

Zhang, Y.-H.P. (2008) Reviving the carbohydrate economy via multi-product lignocellulose biorefineries. **Journal of Industrial Microbiology & Biotechnology**, 35: (5): 367-375.

Zhang, Y. and Lee, Y.C. (2002) "High-performance anion-exchange chromatography of carbohydrates on pellicular resin columns". In Ziad El, R. (Ed.) **Carbohydrate Analysis by Modern Chromatography and Electrophoresis**. Elsevier 207-250.

Zhang, Z., Khan, N.M., Nunez, K.M., et al. (2012b) Complete Monosaccharide Analysis by High-Performance Anion-Exchange Chromatography with Pulsed Amperometric Detection. **Analytical Chemistry**, 84: (9): 4104-4110.

Zhao, H., Baker, G.A. and Cowins, J.V. (2010) Fast enzymatic saccharification of switchgrass after pretreatment with ionic liquids. **Biotechnology Progress**, 26: (1): 127-133.

Zhao, H., Kwak, J.H., Conrad Zhang, Z., et al. (2007) Studying cellulose fiber structure by SEM, XRD, NMR and acid hydrolysis. **Carbohydrate Polymers**, 68: (2): 235-241.

Zhao, H., Kwak, J.H., Wang, Y., et al. (2006) Effects of Crystallinity on Dilute Acid Hydrolysis of Cellulose by Cellulose Ball-Milling Study. **Energy & Fuels**, 20: (2): 807-811.

Zhao, X., Cheng, K. and Liu, D. (2009a) Organosolv pretreatment of lignocellulosic biomass for enzymatic hydrolysis. **Applied Microbiology and Biotechnology**, 82: (5): 815-827.

Zhao, X., Zhang, L. and Liu, D. (2012) Biomass recalcitrance. Part I: the chemical compositions and physical structures affecting the enzymatic hydrolysis of lignocellulose. **Biofuels, Bioproducts and Biorefining**, 6: (4): 465-482.

Zhao, Y., Lu, W.-J. and Wang, H.-T. (2009b) Supercritical hydrolysis of cellulose for oligosaccharide production in combined technology. **Chemical Engineering Journal**, 150: (2–3): 411-417.

Zhao, Y., Lu, W.-J., Wang, H.-T., et al. (2009c) Fermentable hexose production from corn stalks and wheat straw with combined supercritical and subcritical hydrothermal technology. **Bioresource Technology**, 100: (23): 5884-5889.

ABBREVIATIONS

GHG – greenhouse gases

MxG - raw *Miscanthus x giganteus*

SBW - subcritical water

CI – crystallinity index

NREL - National Renewable Energy Laboratory

IR - infrared spectroscopy

NMR - nuclear magnetic resonance

AIL - acid insoluble lignin

ADL - acid detergent lignin

HPLC - high performance liquid chromatograph

ODW - oven dry weight

ASL - acid soluble lignin

FTIR - Fourier-transform infrared spectroscopy

PCA - Principal Component Analysis

SEM - Scanning electron microscopy

HPAEC - High-performance anion-exchange chromatography

PAD - pulsed amperometric detection

DP - degree of polymerisation

GC - gas chromatography

RI - refractive index

FID - flame ionization detector

MS - mass spectrometry

ICS - Ion Chromatography System

RPC - Reversed-phase liquid chromatography

DEL fibres - cellulose-enriched fibres resultant from direct delignification

SEQ fibres - cellulose-enriched fibres resultant from sequential extraction

120ºC fibres - solid fraction after 1st-step extraction using SBW at 120ºC

180ºC fibres - solid fraction after 2nd-step extraction using SBW at 120ºC and 180ºC

XOS - xylo-oligosaccharides

COS - cello-oligosaccharides

HMF - 5- hydroxymethylfurfural

RSM - response surface methodology

CCD - central composite design

DoE - Design of experiments

LBAE - Lobry de Bruyn Alberda van Ekenstein (transformation)

NCYC - National Collection of Yeast Cultures

YM - yeast mold

S. cerevisiae - *Saccharomyces cerevisiae*

OD - optical density

FC - flow cytometry

SSC - side-scattered light

FSC - forward -scattered light

PI - propidium iodide

$\mathbf{Y_{etOH}}$ - ethanol yield

$\mathbf{Y_{glu}}$ - glucose yield

APPENDICES

APPENDIX A

Table A1 – pH values after (a) DoE-1 and (b) DoE-2 runs for Avicel, DEL andSEQ fibres.

(a)

DoE-1				pH		
Run	**T (°C)**	**Res. time (min)**	**Load (%)**	**Avicel**	**DEL**	**SEQ**
1	265	20	6.4	2.4	2.3	2.4
2	310	0	1.0	2.6	2.6	2.5
3	265	20	3.0	2.4	2.5	2.4
4	310	0	5.0	2.1	2.3	2.3
5	265	20	3.0	2.4	2.5	2.4
6	220	0	5.0	4.3	4.5	4.0
7	220	40	5.0	2.9	3.2	3.0
8	310	40	5.0	2.8	2.8	2.8
9	220	40	1.0	3.3	3.4	3.1
10	265	20	0.5	2.8	2.9	2.8
11	265	0	3.0	3.3	3.1	3.1
12	265	20	3.0	2.6	2.6	2.4
13	265	54	3.0	2.7	2.7	2.7
14	265	20	3.0	2.7	2.7	2.4
15	190	20	3.0	4.1	3.8	3.6
16	317	20	3.0	2.8	2.8	2.5
17	265	20	3.0	2.7	2.7	2.6
18	310	40	1.0	2.9	3.0	2.5
19	265	20	3.0	2.7	2.9	2.7
20	220	0	1.0	4.0	4.6	4.4

(b)

DoE-2				pH		
Run	**T (°C)**	**Res. time (min)**	**Load (%)**	**Avicel**	**DEL**	**SEQ**
1	220	40	5.0	2.9	3.2	3.0
2	280	0	5.0	2.4	2.8	2.5
3	220	0	1.0	4.5	4.3	4.2
4	250	20	3.0	2.4	2.7	2.7
5	250	20	3.0	2.4	2.8	2.6
6	250	54	3.0	2.5	2.6	2.5
7	220	40	1.0	3.1	3.5	3.4
8	250	0	3.0	3.3	3.7	3.4
9	280	0	1.0	2.5	3.1	2.9
10	250	20	3.0	2.4	2.7	2.7
11	250	20	3.0	2.5	2.7	2.6
12	200	20	3.0	3.5	3.5	3.3
13	250	20	3.0	2.4	2.7	2.5
14	250	20	3.0	2.4	2.8	2.6
15	250	20	6.4	2.3	2.6	2.4
16	220	0	5.0	4.4	4.5	4.7
17	250	20	0.5	2.8	3.2	2.9
18	280	40	5.0	2.5	2.6	2.5
19	280	40	1.0	2.8	2.8	2.7
20	300	20	3.0	2.7	2.7	2.4

APPENDIX B

Table B1 – ANOVA for hydrolysis percentage after SBW in the DoE using 3-factor CCD for (a) Avicel, (b) DEL and (c) SEQ fibres after excluding non-significant terms from the model.

(a)

Source	Sum of Squares	df	Mean Square	F value	p-value
Model	12.06	5	2.41	26.95	< 0.0001
A-Temperature	5.77	1	5.77	64.52	< 0.0001
B-Residence time	1.35	1	1.35	15.10	0.0016
AB	0.61	1	0.61	6.82	0.0205
A^2	1.63	1	1.63	18.16	0.0008
B^2	0.79	1	0.79	8.79	0.0102
Residual	1.25	14	0.09		
Lack of Fit	1.24	9	0.14	56.12	0.0002
Pure Error	0.01	5	0.00		
Cor Total	13.31	19			
R-Squared	0.91				
Adj R-Squared	0.87				
Pred R-Squared	0.80				

(b)

Source	Sum of Squares	df	Mean Square	F value	p-value
Model	11.77	5	2.35	29.65	< 0.0001
A-Temperature	6.61	1	6.61	83.21	< 0.0001
B-Residence time	1.35	1	1.35	17.01	0.0010
AB	0.53	1	0.53	6.73	0.0212
A^2	0.85	1	0.85	10.76	0.0055
B^2	1.07	1	1.07	13.42	0.0026
Residual	1.11	14	0.08		
Lack of Fit	1.10	9	0.12	62.64	0.0001
Pure Error	0.01	5	0.00		
Cor Total	12.89	19			
R-Squared	0.91				
Adj R-Squared	0.88				
Pred R-Squared	0.67				

(c)

Source	Sum of Squares	df	Mean Square	F value	p-value
Model	12.69	5	2.54	28.05	< 0.0001
A-Temperature	6.52	1	6.52	72.02	< 0.0001
B-Residence time	1.72	1	1.72	19.02	0.0007
AB	0.71	1	0.71	7.89	0.0139
A^2	1.10	1	1.10	12.20	0.0036
B^2	1.13	1	1.13	12.52	0.0033
Residual	1.27	14	0.09		
Lack of Fit	1.26	9	0.14	67.29	0.0001
Pure Error	0.01	5	0.00		
Cor Total	13.96	19			
R-Squared	0.91				
Adj R-Squared	0.88				
Pred R-Squared	0.66				

Table B-2 – ANOVA for hydrolysis percentage after SBW in the DoE-2 using 3-factor CCD for (a) Avicel, (b) DEL and (c) SEQ fibres after excluding non-significant terms from the model.

(a)

Source	Sum of Squares	df	Mean Square	F value	p-valu
Model	13.84	5	2.77	18.36	< 0.000
A-Temperature	8.12	1	8.12	53.90	< 0.000
B-Residence time	2.02	1	2.02	13.37	0.002
AB	1.23	1	1.23	8.17	0.012
A^2	1.82	1	1.82	12.06	0.003
B^2	1.27	1	1.27	8.43	0.011
Residual	2.11	14	0.15		
Lack of Fit	2.10	9	0.23	120.66	< 0.000
Pure Error	0.01	5	0.00		
Cor Total	15.95	19			
R-Squared	0.87				
Adj R-Squared	0.82				
Pred R-Squared	0.70				

(b)

Source	Sum of Squares	df	Mean Square	F value	p-value
Model	12.03	5	2.41	54.99	< 0.0001
A-Temperature	0.68	1	0.68	15.57	0.0015
B-Residence time	2.13	1	2.13	48.66	< 0.0001
AB	0.00	1	0.00	0.06	0.8081
A^2	2.17	1	2.17	49.63	< 0.0001
B^2	0.38	1	0.38	8.79	0.0102
Residual	0.61	14	0.04		
Lack of Fit	0.56	9	0.06	5.58	0.0364
Pure Error	0.06	5	0.01		
Cor Total	12.65	19			
R-Squared	0.95				
Adj R-Squared	0.93				
Pred R-Squared	0.83				

(c)

Source	Sum of Squares	df	Mean Square	F value	p-value
Model	9.22	4	2.31	22.80	< 0.0001
A-Temperature	0.84	1	0.84	8.30	0.0114
B-Residence time	3.56	1	3.56	35.17	< 0.0001
A^2	0.67	1	0.67	6.59	0.0215
B^2	1.73	1	1.73	17.09	0.0009
Residual	1.52	15	0.10		
Lack of Fit	1.49	10	0.15	27.03	0.0010
Pure Error	0.03	5	0.01		
Cor Total	10.74	19			
R-Squared	0.86				
Adj R-Squared	0.82				
Pred R-Squared	0.55				

Table B-3 – ANOVA for HMF concentration after SBW in the DoE-2 using 3-factor CCD for (a) Avicel, (b) DEL and (c) SEQ fibres after excluding non-significant terms from the model.

(a)

Source	Sum of Squares	df	Mean Square	F value	p-valu
Model	10.24	7	1.46	32.53	< 0.000
A-Temperature	0.14	1	0.14	3.18	0.1021
B-Residence time	0.19	1	0.19	4.19	0.065
C-Loading	0.95	1	0.95	21.18	0.000
AB	2.70	1	2.70	60.02	< 0.000
A^2	3.55	1	3.55	78.84	< 0.000
B^2	1.51	1	1.51	33.54	0.0001
C^2	0.57	1	0.57	12.72	0.004
Residual	0.49	11	0.04		
Lack of Fit	0.48	6	0.08	20.77	0.002
Pure Error	0.02	5	0.00		
Cor Total	10.74	18			
R-Squared	0.95				
Adj R-Squared	0.92				
Pred R-Squared	0.81				

(b)

Source	Sum of Squares	df	Mean Square	F value	p-value
Model	76.22	6	12.70	14.79	< 0.0001
A-Temperature	9.92	1	9.92	11.55	0.0048
B-Residence time	2.10	1	2.10	2.44	0.1423
C-Loading	10.22	1	10.22	11.90	0.0043
AB	11.06	1	11.06	12.88	0.0033
A^2	32.51	1	32.51	37.86	< 0.0001
B^2	11.20	1	11.20	13.04	0.0032
Residual	11.16	13	0.86		
Lack of Fit	11.14	8	1.39	318.64	< 0.0001
Pure Error	0.02	5	0.00		
Cor Total	87.38	19			
R-Squared	0.87				
Adj R-Squared	0.81				
Pred R-Squared	0.59				

(c)

Source	Sum of Squares	df	Mean Square	F value	p-value
Model	120.09	6	20.01	16.82	< 0.0001
A-Temperature	5.22	1	5.22	4.39	0.0564
B-Residence time	0.05	1	0.05	0.04	0.8379
C-Loading	9.07	1	9.07	7.62	0.0162
AB	42.21	1	42.21	35.46	< 0.0001
A^2	35.02	1	35.02	29.42	0.0001
B^2	19.44	1	19.44	16.34	0.0014
Residual	15.47	13	1.19		
Lack of Fit	15.36	8	1.92	87.97	< 0.0001
Pure Error	0.11	5	0.02		
Cor Total	135.56	19			
R-Squared	0.89				
Adj R-Squared	0.83				
Pred R-Squared	0.52				